MINERAL FACIES IN PELITIC ROCKS WITH PARTICULAR REFERENCE TO THE BUCHAN TYPE METAMORPHISM OF NORTH-EASTERN SCOTLAND.

NEIL F.C. HUDSON

DOCTOR OF PHILOSOPHY

UNIVERSITY OF EDINBURGH

1975

ABSTRACT

The Dalradian rocks of Aberdeenshire and Banffshire have been affected by a regional metamorphism giving rise to andalusite, cordierite, staurolite and garnet in pelitic rocks (Buchan Type Metamorphism).

Four zones are recognised in which the following assemblages (with muscovite and quartz) first appear: Biotite Zone (chlorite-biotite, B.1); Cordierite Zone (cordierite-chlorite-biotite, C.1); Andalusite Zone (andalusite-cordierite-biotite, A.1); Staurolite Zone (staurolite-andalusite-biotite, S.4). The biotite zone separates two N.E.-S.W. trending sets of higher grade zones. The staurolite zone is absent from the eastern set. Both sequences pass into sillimanite bearing rocks at higher grade.

The above distribution of assemblages along with the trend of upgrade Mg enrichment indicated by analyses of coexisting cordierite-biotite (in A.1) and staurolite-biotite (in S.4) suggest the following isograd forming reactions:

Cordierite Isograd:	chlorite + muscovite ⇌ cordierite + biotite	1
Andalusite Isograd:	cordierite + muscovite ⇌ andalusite + biotite	2
Staurolite Isograd:	andalusite + biotite ⇌ staurolite + muscovite	3

These reactions are di- or multi- variant in nature and isograds in the field mark lines where the reactions occur for the most Fe rich bulk compositions present. Mineral analyses suggest that this is close to $100MgO/MgO+FeO = 40$, whilst bulk rock analyses suggest M/FM of 38.

The above reactions are examined in the model system Al_2O_3-K_2O-FeO-MgO-SiO_2-H_2O (AKFMSH) in which they are divariant. Reaction 3 has a medium positive dP/dT and is crossed from the high to low entropy sides, indicating that the P,T gradient was strongly pressure controlled near the staurolite isograd. Parageneses involving garnet (which is always Mn rich), and those lacking muscovite (including some gedrite bearing assemblages) are considered with reference to the systems AKFMSH-MnO and AFMSH respectively, for which theoretically determined petrogenetic grids are advanced. PT grids are also advanced to show relationships between uni- di- and multi- variant equilibria in the above systems. The Buchan sequence is compared with published sequences from other terrains and variations are interpreted in terms of the grids.

A possible mechanism for reaction 2 (above) is advanced on textural evidence.

Declaration

Except where reference is made to published work or personal communications, the work presented in this thesis is original and has not previously been submitted for a degree or any other qualification at this or any other university.

N J Hudson.

Acknowledgements

I would like to express my gratitude to Dr. K. R. Gill and Mr. P. Cooper for invaluable assistance with photography and to Dr. K.R. Gill for assistance in the identification of opaque minerals. Dr. J.R. Ashworth kindly gave permission for the use of his unpublished data on specimens 15462, 15463 and 15464, and Dr. D.J. Fettes made available some of his personal slides. Thanks is due in particular to all those persons who took valuable time and trouble to instruct me in the operation of analytical equipment and to Dr. Ben Harte for his enthusiastic and stimulating supervision throughout the project.

Financial support during the period 1970-1973 was provided by a N.E.R.C. research studentship which is gratefully acknowledged. Mrs. Sheila Otter typed the manuscript.

CONTENTS PAGE

Erratum: pages 62 and 64 are reversed.

KEY TO FIGURE LOCATIONS

LIST OF TABLES

LIST OF MAPS

1.1. Introduction

Within the Earth's Crust, orogenic belts form complex major tectonic and petrological provinces, of which an understanding is essential in the interpretation of crustal processes. The Scottish Dalradian is amongst the best studied of orogenic belts and the nature and variety of its regional metamorphism, established initially through the work of Barrow (1893,1912); Read (1923, 1952); Bailey (1923); Tilley (1925); Harker (1932) and Wiseman (1934) has formed a standard for comparison with other orogenic belts throughout the world.

On the basis of work carried out on the metamorphism of the pelitic rocks, the Dalradian has been divided into two major areas:

a) a region of lower pressure cordierite and andalusite bearing rocks comprising an area of some 1200 square miles in Aberdeenshire and Banffshire (Map 1) where the metamorphsm is said to be of the 'Buchan Type';

b) a much larger region of higher pressure kyanite, staurolite and almandine bearing rocks comprising the rest of the Dalradian where the metamorphism is said to be of the 'Barrovian Type'.

Whereas the classical regions of Barrovian Type Metamorphism have received considerable detailed chemical, mineralogical and petrolgical investigation over the last twenty years (e.g. Chinner, 1960, 1961, 1965, 1967; Atherton 1964,1968; Mather 1970; Atherton and Brotherton 1972) the region of Buchan Type Metamorphism has received relatively little attention with the work of Ashworth (1972,1975) on the sillimanite bearing rocks and migmatites of the Huntly-Portsoy area standing alone. Detailed textural studies (e.g. Rast 1958; Sturt and Harris 1961; Johnson 1962,1963; Fettes 1968, 1971; Harte and Johnson 1969 etc) have established detailed structural time scales and related these to the growth of metamorphic minerals in both areas. Broad discussions of the relationships between the two areas have been given by Chinner (1966) Fettes (1968) and Porteous (1973). The present study is intended to present information on mineral assemblages and compositions and the range of bulk compositions present in metapelites at grades below the sillimanite isograd in the Buchan region.

1.2. Outline of the Geology of the Buchan Area

The area generally known as Buchan, comprises the low lying parts of the counties of Aberdeenshire and Banffshire, North-East Scotland. It is a rich arable farming area and as such inland exposures are scarce and generally restricted to quarries and stream sections. The coastal sections, however, afford virtually continuous exposure.

The geology of the area, as mapped by members of the Geological Survey of Scotland, is represented on sheet 9 ($\frac{1}{4}$" series) and

sheets 86, 87, 96 and 97 (1" series). Memoirs are available for all sheets (Wilson 1882,1886, Read 1923).

The geology consists of deformed Dalradian metasediments which have been intruded by a large discontinuous sheet like gabbroic body and later by a series of late Caledonian granites. Parts of the area are unconformably overlaid by sediments of Old Red Sandstone Age (Map 1).

Table 1.2 gives a synopsis of events in N.E. Scotland during the Caledonian orogenic phase in relation to time as defined by palaeontological (Downie et al 1971) and radiometric (Pankhurst 1970, 1974) evidence.

Stratigraphy of the Dalradian metasediments

The present outcrop pattern of the metasediments is controlled by a major synclinal structure known as the Turriff (Read 1923) or Boyndie (Sutton and Watson 1956) Syncline. This fold has a N.E. - S.W. (Caledonoid) trending axis which plunges gently to the north, crossing the coast of the Moray Firth near Banff (Map 1).

With regard to the Dalradian as a whole, Johnson (1965) has pointed out that although individual horizons may be traced for considerable distances along the Caledonoid trend, this is seldom possible for any great distance across it. This is partially true even within the restricted area of Buchan, so that variations exist in the local stratigraphic successions as determined in the east and west limbs of the Boyndie Syncline.

MAP 1

The major geological features of north-east Scotland.

Modified from Sheet 9 ($\frac{1}{4}$ inch series) geological survey of Scotland.

Boundary between S.Highlands/Argyll groups after Read and Farquhar 1956; Fettes 1968; Ashworth 1972; is in large part approximate.
Huntly-Portsoy Gabbro outcrop after Munro 1970; Ashworth 1972.
Fold axial traces after Johnson and Stewart 1961.

= = - shear zones (after Ashworth 1972)

● - black slate outcrops in Macduff Slates

BS = Boyndie Syncline

BA = Buchan Anticline

HTA = Huntly-Tarves Antiform

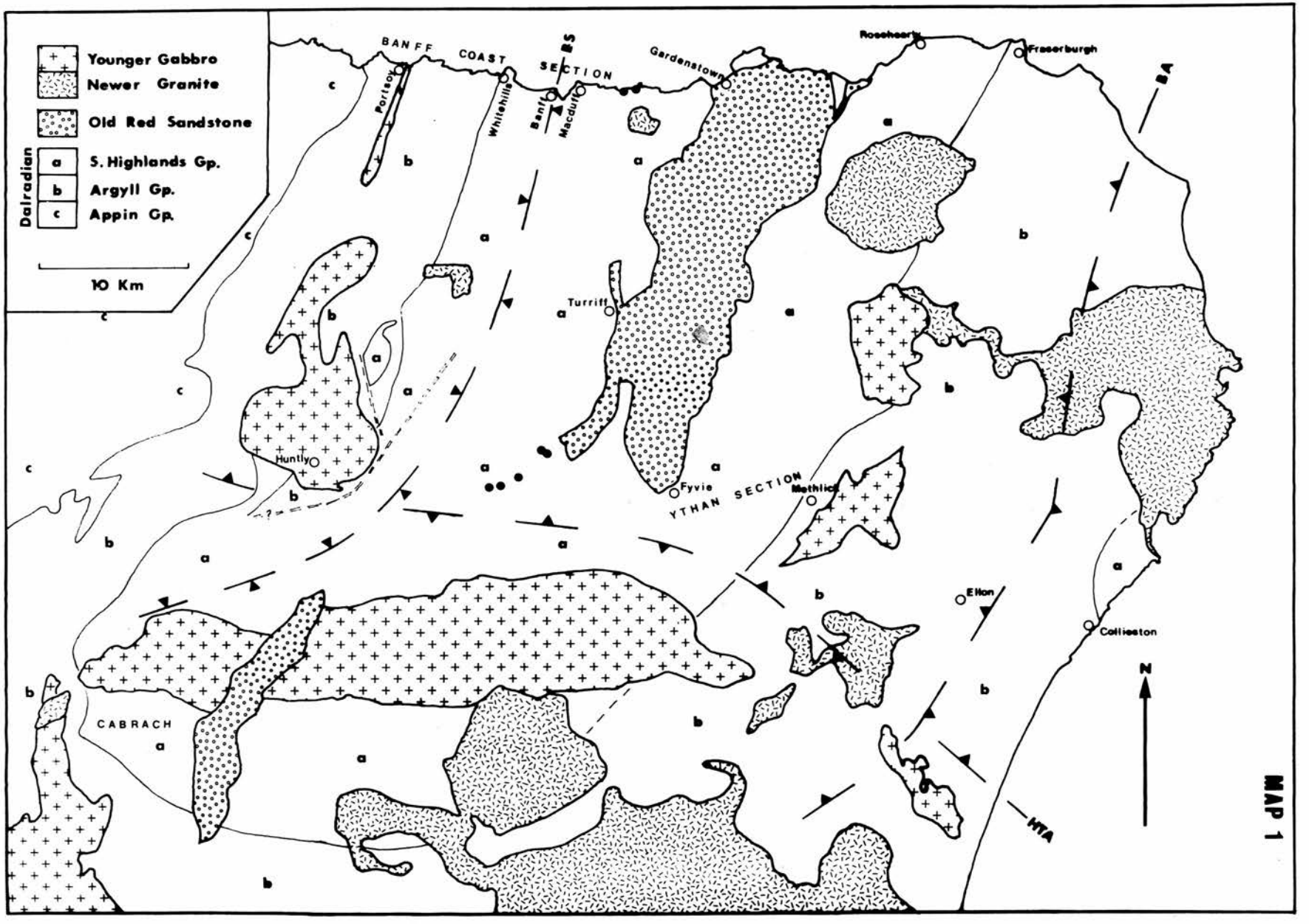
Younger Gabbro
Newer Granite
Old Red Sandstone
Dalradian
a S. Highlands Gp.
b Argyll Gp.
c Appin Gp.
10 Km
BANFF COAST SECTION
Portsoy
Whitehills
Banff
Macduff
Gardenstown
Rosehearty
Fraserburgh
BS
BA
Turriff
Huntly
Fyvie
Methlick
YTHAN SECTION
Ellon
Collieston
CABRACH
N
MTA
MAP 1

The local stratigraphy of the Banff-Portsoy-Huntly area has been worked out by Read (1923, 1936, 1955), Sutton and Watson (1955) and Ashworth (1972) and in the Rosehearty-Fyvie-Collieston area by Wilson (1882, 1886), Read (1952), Read and Farquhar (1956) and Fettes (1968). The results of these workers are summarised in Map 1 and in Table 1.1 (after Harris and Pitcher 1975). To some extent these subdivisions are dependent on metamorphic grade, which is further discussed below.

Read (1923) suggested that a major stratigraphic division could be placed above the Boyne Limestone giving rise to an upper Banff Division and a Lower Keith Division. He postulated that the boundary of the Banff and Keith Divisions represented a major tectonic slide, known as the Boyne Lag, along which a number of litho-stratigraphic units were cut out. Ashworth (1972) has remapped the litho-stratigraphy in a critical area to the east and south of Portsoy and has shown that variations in litho-stratigraphy may be more easily explained in terms of sedimentary facies variation than tectonic elimination, a view originally advocated by Horne (in Read 1923) and supported by Fettes (1968). In this case the evidence for the Boyne Lag seems ill founded.

Following the correlation of the Loch Tay-Deeside-Boyne limestones by Read (1927, 1955) several other major correlation schemes have been advanced (e.g. Anderson 1948; Rast 1963; Johnson 1965; Harris and Pitcher 1975). Recent microfossil evidence (Downie et al 1971) has suggested that the rocks of the Macduff Slate Group (see

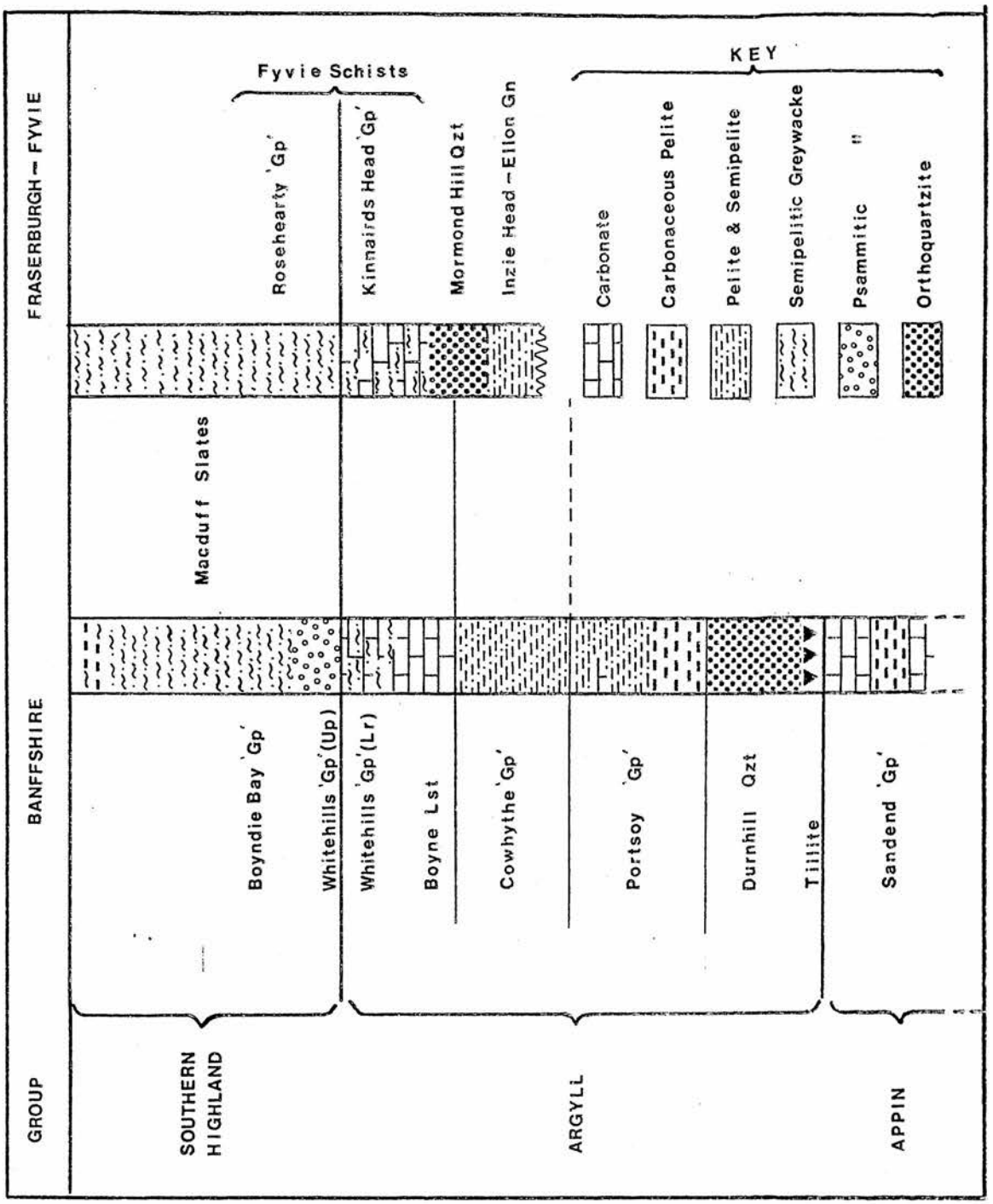

Table 1.1 : Stratigraphy of Dalradian rocks in N.E. Scotland after Harris and Pitcher (1975).

Table 1.1) are Arenig in age and may be correlated with the fault bound Arenig rocks of the Highland Boundary Fault zone known as the Highland Border Series. Table 1.1. shows the Buchan Dalradian stratigraphy in relation to the general correlation scheme and time scale advanced by Harris and Pitcher (1975).

Structural History of the Metasediments

The structure of the Dalradian as a whole has been summarised by Johnson (1965) whilst discussions of more local aspects in Buchan have been given by Read (1923, 1955) Read and Farquhar (1956) Sutton and Watson (1956) Johnson (1962) Fettes (1968, 1971) and Ashworth (1972).

The major structure of the area is considered to be a large nappe, termed the 'Banff Nappe' by Read (1955) which represents a north eastwards extension of the 'Tay Nappe' of the Central Highland area, (e.g. Bailey 1925; Shackleton 1958; Sturt 1961). This nappe is thought to close to the south east. In the central highland area a plunge culmination occurs and here the nappe is eroded down to its lower limb forming a belt of inverted strata from Kintyre to Stonehaven, whilst in Buchan the upper (right way up) limb is preserved in a plunge depression.

The upper limb of the Banff Nappe has been modified by two major folds known as the Boyndie Syncline (Read 1923; Sutton and Watson 1956) and the Buchan Anticline (Read and Farquhar 1956), which are thought to be third generation structures (Johnson 1962). Near

the Moray First coast, these folds have N.E.-S.W. trending axial traces but further south they swing westwards around a late open structure known as the Huntly-Tarves Antiform (Johnson and Stewart 1961) (see Map 1).

Table 1.2 gives a summary of events in the Buchan area in relation to those recorded in the Barrovian area. (Terminology of movement phases after Harte and Johnson (1969) and Johnson (1962)). Detailed studies of fold episodes in various other parts of the Barrovian area are given by King and Rast (1956), Rast (1958), Sturt (1961) Sturt and Harris (1961), Harris (1962) and Treagus (1964). Harte and Johnson (1969) note five deformation phases in Angus (excluding late brittle structures) and suggest that these show reasonable agreement with the sequence of events in other areas. Discrepancies do, however, exist and some deformational episoides may be absent in some areas e.g. Rast (1958), Sturt (1961) in the Schichallion-Loch Tummel area do not record structures equivalent to Harte and Johnson's D_3 whilst Fettes (1968) in some parts of Buchan does not record D_2 equivalent structures. Sturt and Harris (1961) record a period of dolerite intrusion prior to their F_3 structures, and this may be represented in Buchan by a sill complex in the lower Whitehills Group. These have been metamorphosed to amphibolites and folded by the F_3? movements (Sutton and Watson 1955) but are not foliated and retain a relict igneous fabric.

Metamorphic mineral growth in relation to structural history

Johnson (1962), Harte and Johnson (1969) and others have shown that there is a general correlation in time of growth of the major

Event	Barrovian Region	Buchan Region	
1 Deposition of:	Highland Border Series	Macduff Slates	Arenig 520-510 my
2 1st Generation structures	D_1 Tay Nappe (primary regional cleavage)	F_1 Banff Nappe	
3 2nd Generation structures	D_2 usually minor folds (+ mineral lineation)	F_2	
4 Dolerite Intrusion	present	?	
5 Main Period of porphyroblast growth	st; ky; gt.	some gt. st; cord; andal.	
6 Gabbro Intrusion	absent	Huntly Insch etc related mig + sill growth in Cowhythe Gneiss	501 + 17 my
7 3rd Generation structures	D_3 Major	F_3 Folds	
8	period of matrix coarsening followed by sill. growth	matrix coarsening	
9 4th and 5th Generation structures	D_4 & D_5 Locally absent mainly retrogressive metamorphism	F_4 & F_5 ?	
10 Brittle structures			
11 Major Granite Intrusion			~460 my

Table 1.2 : Synopsis of events occurring in the Dalradian during the Caledonian orogeny.

porphyroblast forming minerals (kyanite, staurolite, andalusite and cordierite) in both the Barrovian and Buchan areas during a single static phase between the second and third movement episodes, (see Table 1.2) though in Buchan there is some evidence to suggest continued growth during F_3. In some areas garnet growth has coincided with that of the above phases (e.g. Angus see Harte and Johnson 1969) whilst in some other areas garnet shows evidence of poly phase growth. At lower structural levels (Barrovian part) of the Banffshire Coast and in the Cowhythe Gneiss Johnson (1962) records garnets of;

a) syn to post F_2 and pre F_3

b) post F_1 and pre F_2

suggesting that the metamorphic grade during the early structural history of this area may have been higher than in Angus. No inclusion trails have been recorded in garnets from the Boyndie Bay and Whitehills groups (true Buchan region) but inclusion relationships (see Chapter 2, section 5) suggest that garnet growth was pre- or simultaneous with that of the other porphyroblasts.

Harte and Johnson (1969) record a period of 'general matrix coarsening', involving recrystallisation of quartz, plagioclase, biotite and muscovite occurring between their D_3 and D_4 movements. Johnson (1962) records that included quartz in early formed garnet (b-above) is of smaller size than that in post F_2 garnet which is in turn smaller in size than groundmass quartz. This indicates a progressive coarsening of the matrix with time in the lower structural levels of the Banffshire Dalradian. In the

Boyndie Bay and Whitehills groups (see Chapter 2 section 5), matrix quartz and feldspar is generally coarser than included material even that near the edge of andalusite porphyroblasts which have grown in part during the F_3 movements indicating that in Buchan a post F_3 period of matrix coarsening occurred.

The age of sillimanite growth in Buchan has been shown by Ashworth (1972) to be later than the main period of porphyroblast growth in the Huntly-Portsoy area where it is thought to be related to intrusion of the Younger Gabbros and Fettes (1970) has shown that sillimanite hornfelses associated with the Insch Gabbro have destroyed S_1 cleavage but been disrupted by S_3 cleavage. This indicates that sillimanite growth in these areas predated the F_3 movements and therefore predated the period of matrix coarsening, a result which is at odds with that of Harte and Johnson (1969) who suggest that sillimanite growth in Angus post dates the matrix coarsening period and the D_3 movements. There is, however, agreement in general terms with the scheme proposed by Chinner (1966) on regional grounds for a regional andalusite-kyanite metamorphism followed by a later overprint of migmatisation and sillimanite growth.

The 'Younger' basic igneous complexes

A general account of the 'Younger' basic igneous complexes has been given by Mercy (1965). These are the Insch, Huntly, Haddo House, Arnage, Maud and Belhelvie masses and possibly the Morven-Cabrach mass. Many of these intrusions show steeply inclined

igneous banding (e.g. Stewart (1946), Shackleton (1948)), and are thought to have originally formed one large sheet like intrusion which was later deformed and sheared during part of the Caledonian deformation (Shackleton 1956 (in Read and Farquhar 1956), Stewart and Johnson (1961).

Fettes (1970) working on the western end of the Insch mass has shown the development of a contact aureole. Within this aureole porphyroblastic andalusite-cordierite hornfels are developed, destroying the S_1 cleavage whilst prophyroblasts are disrupted by S_3 strain slip cleavages. He concludes that intrusion of the Insch mass is post-F_1 but pre-F_3.

Fettes (1970) has recognised and mapped four isograds within this aureole based on the appearance of spots, andalusite, fibrolite and potash feldspar. To the east of the Rhynie Old Red Sandstone outlier (NJ 500300) only the two lower grade isograds are developed whilst to the west, at deeper structural levels, all four appear and may be traced into the regional isograds. Fettes considers the continuity of contact and regional isograds to be due to the interaction of the regional geothermal gradient with that set up by the intrusion implying that the country rocks were still hot at the time of intrusion.

Ashworth (1972) has carried out a detailed investigation of the high grade gneisses and migmatites in the Portsoy-Huntly area. He showed a definite relationship between the distribution of high

temperature assemblages and migmatites and their proximity to the Huntly gabbro mass. In addition, he mapped sillimanite and potash feldspar isograds which show a marked discordant relationship to the lower grade regional zones, especially near Aberchirder. He suggests that the growth of sillimanite and the production of migmatites was related to the intrusion of the gabbro sheet and was slightly later than the main regional metamorphic climax. Read (1951, 1952) has also illustrated the close relationships between migmatite development and the basic intrusions in the Haddo House-Arnage area.

Radiometric dating (Pankhurst 1970) has been unable to establish any time difference between the intrusion of the basic sheet, the climax of metamorphism and the F_3 fold movements. The time lag between intrusion and subsequent folding must have been sufficient for the consolidation of the intrusions, however, considering the attitude of the igneous banding. Moreover, there is considerable evidence that the sheet underwent massive shearing during the fold movements (Read 1950, 1956; Stewart and Johnson 1961; Fettes 1968).

The period of gabbroic intrusion is shown in relation to other events during the Caledonian orogeny in Table 1.2.

1.3. Review of Ideas on metamorphic zones, facies and reactions with particular reference to Buchan

The first detailed survey of the geology of Buchan was carried out by J.S.G. Wilson (1882, 1886) of the then Geological Survey of Scotland. During his mapping of sheets 87 and 97 (1" series) he

recognised the regional development of the mineral andalusite. Without discussing the origin of the metamorphic rocks, he divided them into four lithological groups:

1 Clay Slates

2 Knotted and Andalusite schists (Knotenschiefer)

3 Quartz Schists with quartzites

4 Gneiss

which are essentially the divisions as they appear on the present geological maps. The division of the rocks into these four groups is based partially on lithological differences and partly on mineralogical and textural differences. The boundary between groups (1) and (2) is essentially based on a mineralogical change in rocks of the same composition and lithology* (i.e. it is of metamorphic origin), whilst the boundary between groups (2) and (3) represents a lithological change from pelites to psammites and quartzites. The boundary between groups 2/3 and group 4 is partly lithological and partly textural. In chosing to divide the rocks in this manner, Wilson had virtually mapped the general scheme of the metamorphic zones, almost by accident, and his boundary between Clay Slates and Knotted Schists remains as the cordierite isograd today. The boundary of his Gneiss group is less clearly related to the metamorphism but would appear to approximate to the potash feldspar isograd.

The general state of the science at this time is clearly illustrated in a paper by Horne (1886) arguing in favour of a metamorphic

* It should be noted that this boundary locally transgresses lithological units (see also Walls,1937).

origin for these rocks as against direct precipitation from a primeval sea.

At about the same time, Barrow was mapping further south in the region of Glen Esk and Glen Clova and published his classic account of 'progressive metamorphic zones' in 1893. This paper put forward the concept of zones based on the appearance of regional 'index minerals' and separated by boundaries termed 'outer limits', later renamed 'isograds' by C.E. Tilley (1924). The zonal sequence described by Barrow was:

0) Zone of clastic mica
1) Zone of digested mica
} Chlorite Zone (Tilley 1925)

2) Biotite Zone

3) Garnet Zone

4) Staurolite Zone

5) Kyanite Zone

6) Sillimanite Zone

in order of increasing grade. Barrow's work was later extended and confirmed by Bailey (1923), Tilley (1925) and Elles and Tilley (1930). Tilley (1925) modified the zonal scheme of Barrow (1893) replacing the two lowest grade zones with a single chlorite zone to give the sequence now generally known as 'Barrow's Zones' or "Barrovian Metamorphism".

Also, in the early 1920s, parts of Buchan originally mapped by Horne, Wilson and Hinxman were remapped by H.H. Read (sheets 86,

96 Geol. Surv. Scot. 1" series). Read (1923) drew attention to the association of andalusite with cordierite and with staurolite and garnet.

Around 1930 the idea that Barrow's Zones represented a normal sequence of events during regional metamorphism had become firmly entrenched (Harker 1928, 1932), although descriptions of anomalous areas, apart from Buchan, had appeared in the literature (Streckeisen 1928, Suzuki 1930). The acceptance of this 'normal metamorphism' doctrine was illustrated in 1931 by Elles attempt to apply Barrow's Zones to some of the andalusite bearing rocks of the Banffshire coast.

Harker (1932) briefly discusses the metamorphism in the Buchan area attributing the anomalous mineral assemblages to defficient shearing stress. He suggests that an upgrade sequence of assemblages is; andalusite-biotite schist; andalusite-garnet schist; andalusite-staurolite schist; cordierite-sillimanite-potash feldspar gneiss, attributing the formation of andalusite to a sort of retrogressive process caused by relaxing shearing stress whilst the temperature remained high.

Read (1952) gave a more detailed account of the rocks occurring in the Ythan Valley near Fyvie Aberdeenshire. He recognised six divisions which were interpreted as a sequence of increasing grade.

a) "Slate Grade"; comprising sericite-chlorite-biotite-quartz slates $\pm$ opaques $\pm$ tourmaline.

b) "Knotted Phyllite Grade"; comprising 'slaty phyllites' with groundmass sericite-biotite-quartz-opaques and

carrying small 'knots' of andalusite and cordierite and unoriented plates of chlorite. Read observed that cordierite knots carrying inclusions of all groundmass minerals appeared at a lower grade than andalusite knots which include only quarts.

c) "Andalusite-Cordierite Schist Grade"; comprising three sub groups. (i) A lower grade group with groundmass biotite-muscovite-quartz and large porphyroblasts of cordierite and andalusite. (ii) A higher grade group with the same mineralogy as (i) but carrying plagioclase and rare staurolite in addition. Large irregular plates of muscovite also occur. (iii) Coarser grained schists of similar mineralogy but carrying sillimanite in addition. The sillimanite occurs both as stout prisms and as fibrolite associated with biotite.

d) "Cordierite-Sillimanite Gneiss Grade" with quartz, cordierite biotite, muscovite, plagioclase, sillimanite and in some cases potash feldspar.

e) "Permeation Gneisses"; comprising cordierite and garnet gneisses with typical mineralogy quartz-oligoclase-biotite-muscovite-cordierite-garnet-orthoclase-sillimanite, in some cases with andalusite.

f) "Migmatitic Gneisses"; with typical assemblages cordierite-spinel-garnet-biotite-plagioclase $\pm$ sillimanite quartz-biotite-plagioclase $\pm$ garnet $\pm$ cordierite $\pm$ hypersthene hornblende-quartz-

plagioclase ± ortho pyroxene ± clinopyroxene

quartz-plagioclase-potash feldspar-biotite ± garnet ± cordierite ± spinel.

Read pointed out that this was a progressive sequence entirely different in character from the Barrovian sequence and coined the new term 'Buchan Type Metamorphism' to emphasise this. He considered that this type of sequence represented a situation where temperature was overwhelmingly dominant over shearing stress, calling it regional thermal metamorphism to distinguish it from 'normal' regional metamorphism (i.e. Barrovian). He pointed out that there was also a difference in attitude of the isograd surfaces. These appeared to be steep in the Barrovian area, but the large displacement of the boundary between Buchan grades (a) and (b) by a normal fault near Fyvie (NJ 763377) showed that this surface had a low angle of dip. Read considered that the whole sequence (a) to (f) was the result of one single metamorphic event though he did point out that there was some evidence to suggest that the migmatisation was slightly later since it involved some of the lower grade rocks.

Developments in the field of structural geology had, by the early 1960s reached a point where metamorphic mineral growth could be dated in relation to structural events by the use of minor structures and microtextures. The work of Rast (1958) Sturt and Harris (1961) and Johnson (1962) showed that the structural and metamorphic histories of both the Barrovian and Buchan regions showed striking

similarities with the major period of porphyroblast growth (involving staurolite, cordierite, kyanite and andalusite) occurring essentially coevally after the F_2 fold movements and prior to or during the F_3 movements. The two types of metamorphism were thus clearly related and Johnson (1962, 1965), suggested that the assemblages of the Buchan region had formed at higher structural levels than those of the Barrovian region. The sillimanite metamorphism and associated gneiss development and migmatisation occurred slightly later than this (Chinner 1966; Harte and Johnson 1969; Ashworth 1972, 1975). During the 1950s and early 1960s the development of experimental petrology showed that the effect of shearing stress on the stability fields of minerals was negligible, whilst the influences of hydrostatic pressure were considerable. At the same time, investigations of other metamorphic terrains showed that sequences involving andalusite and cordierite were equally as common as Barrow's Zones (e.g. Joplin 1942, 1943; James 1955; Zwart 1958; Chevenoy 1958; Miyashiro 1958).

These advances left the way clear for ideas based on the ground work of Goldschmidt (e.g. 1915, 1921) and Eskola (e.g. 1915, 1920) who had been striving to interpret metamorphic rocks in terms of their chemical equilibria (see Miyashiro 1973, p. 434). Eskola's concepts of 'metamorphic facies' and 'mineral facies' implied that mineral assemblages in metamorphic rocks were indicative of their conditions of formation. Eskola (1939) set out eight Facies, each being considered to indicate different ranges of pressure and temperature. Diagnostic mineral assemblages thus allowed the allocation of a rock to a specific facies and implied a range of P,T conditions of formation.

It has, however, proved difficult to define boundaries between metamorphic facies because of the diversity of assemblages associated with such a wide range of bulk compositions as is found in metamorphic rocks. The concept has thus become the centre of many arguments. This has resulted in a series of different suggested definitions with considerable disagreement over the validity of some facies and the number of recognised facies and subfacies (e.g. Fyfe, Turner and Verhoogen 1958, Lambert 1965, Winkler 1967, Turner 1968). This has lead some workers to suggest their total abandonment (Winkler 1970, 1974).

Bowen (1940) suggested that a sequence of experimentally determined univariant reactions for a given chemical system could be plotted on a P,T diagram. Since some of the reactions are likely to intersect, this would give rise to a 'petrogenetic grid' in which univariant reaction curves separate P,T regions, each of which is characterised by a specific set of stable joins. Such P,T pigeon holes were later termed 'mineral facies' as distinct from 'metamorphic facies' by Thompson (1955) and 'facies types' by Albee (1965).

Although related to the 'metamorphic facies' concept, the 'petrogenetic grid/mineral facies' concept differs from it by considering at any one time only a limited compositional range, within a defined chemical system.

Miyashiro (1961) pointed out that any progressive metamorphic sequence must show a 'metamorphic facies series'. He used a

combination of the metamorphic facies classification along with a very simple petrogenetic grid, involving only the Al_2SiO_5 inversion curves and the reaction jadeite + qz ⇌ albite, to estimate the pressure and temperature regimes. From this basis he suggested that metamorphic belts indicated three principal facies series, which differed mainly on the operating total pressure, in order of decreasing pressure as follows:

1) Jadeite - Glaucophane Type (no staurolite or cordierite)
2) Kyanite - Sillimanite Type (+ staur + garnet)
3) Andalusite - Sillimanite Type (+ cordierite $\pm$ garnet)

He also pointed out that minor variations occurred and that on a world basis, the three types were transitional via intermediate groups, citing the classic Buchan Type as typical of the low pressure intermediate group on account of the association staurolite + cordierite.

Other workers attempted to refine this idea, based largely on the metamorphic facies concept (e.g. Troger 1963, Hietanen 1967) and succeeded in showing that the variations between areas were complex. Hietanen suggests nine facies series, whilst Troger suggests thirteen.

It became clear that a more rigorous approach was required in order to sort out the P and T relationships of these series. Bowen's petrogenetic grid concept held a possible answer provided only one

group of rocks was considered. Even with the restricted compositional range implied in the concept, it was clear that any individual group of rocks (e.g. pelites) still represented a highly complex chemical system and though the stability ranges of many metamorphic minerals were being investigated it was obvious that it would take many years if not decades, before the system could be experimentally defined.

In 1965 Albee put forward the first comprehensive theoretically determined petrogenetic grid for pelitic rocks. This was based on the groundwork of many previous workers, amongst whom Schreinemakers (publications between 1915 and 1925, republished 1965) and Thompson (1955, 1957, 1961) must be singled out. This work was later followed by Hoschek (1969), Kepezhinskhas (1973) and Hess (1969) who produced similar grids.

As previously mentioned, Chinner (1966) considered the distribution of sillimanite in the Dalradian to be overprinted on the andalusite/kyanite distribution. Neglecting sillimanite, he produced a map of the regional distribution of andalusite and kyanite and applied a simple petrogenetic grid to it. In this way, he succeeded in contouring the whole of the east Dalradian with fossil isotherms and isobars although the actual values of these contours remain unknown. This showed a very interesting feature. The isotherms and isobars were parallel on the Banffshire coast, but perpendicular in the Highland border region. This might, in fact, have been foreseen as it is fully in accord with the attitude of the isograd surfaces in the two regions. Read (1952)

had previously pointed out that isograds showed a low angle of dip in Buchan, and had as a result, proposed that the metamorphism was largely depth controlled.

Chinner explained the non parallelism of contours in the Highland border region in terms of syn-metamorphic folding. Richardson (1970) however, indicated that this might be an inherent property of any metamorphic belt. He discussed the relationship between a facies series and the fossil geothermal gradient, indicating that any facies series is more directly related to the present erosion surface which will show an arbitrary section through the thermal structure of the belt. He speculated on such thermal structures in some detail, pointing out that 'normal' geothermal gradients may give rise to Miyashiro's Kyanite-Sillimanite facies series, but that the others require an anomalous thermal distribution in the crust. The lower pressure facies series require a higher geothermal gradient and thus any such belt developed on or adjacent to the continental crust, must show a dome or anticlinal thermal structure as the high geothermal gradients grade into more normal gradients. If the pressure surfaces are largely depth controlled this would give rise to a non parallel situation near the edge of the thermal anticline at deeper structural levels, whilst at high levels near the axis of the anticline the P and T surfaces would be essentially parallel. A thermal anticline of this nature had previously been proposed for the Caledonides by W.Q. Kennedy (1948) based on the regional distribution of the metamorphic zones.

The definition of more detailed facies series in the Dalradian

involving the index minerals chloritoid, garnet, staurolite and cordierite, has been attempted by Porteous (1973) whilst a more detailed approach using key mineral assemblages has been given by Harte (in press).

As discussed above, several recent attempts have been made to interpret metamorphic sequences in terms of petrogenetic grids derived for model pelite systems (e.g. Albee 1965c; Hess 1969). This work has achieved at least a partial success. Detailed investigations of isograds in the field have shown, however, that isograd forming reactions are not, in general, directly comparable with univariant reactions as shown on published petrogenetic grids (e.g. Chinner 1965; Evans and Guidotti 1966). This is due to the complexity of natural systems which introduce extra variables causing reactions to become di- or multi- variant. Recently Hensen (1971) and Hensen and Green (1971, 1972, 1973) have outlined the manner in which such reactions may be examined and used for two common Granulite Facies assemblages. It is one of the intentions of this study to show how isograd reactions in Buchan are related to petrogenetic grids for model pelite systems.

1.4. Outline of Thesis

The ultimate objective of the present study was to define a facies series for the classical 'Buchan Type' metamorphic terrain of N.E. Scotland and to erect model systems which could be used to explain it and relate it to facies series described from elsewhere as a means to a better understanding of the P,T conditions realised in metamorphic belts.

The following individual aims may be set out.

1) To establish mineral assemblages and their variation with metamorphic grade.
2) To obtain chemical data to establish the presence or absence of grade related variations in mineral compositions.
3) To determine isograd reactions.
4) To relate isograd reactions (a) to one another, to other possible reactions and (b) to those occurring in other terrains.
5) To obtain estimates of temperature and pressure conditions prevailing during the metamorphism.
6) To assess the influence of bulk rock compositions on assemblages and reactions.
7) To elucidate, where possible, the mechanisms of reactions occurring in the rocks.

Mineral assemblages were established by means of a field and petrographic investigation, the results of which are discussed in Chapter 2 (assemblages are given in Appendix I). Four zones have been recognised at grades below the sillimanite isograd and characterised by the first appearance of mineral assemblages (+ muscovite and quartz) as follows: Biotite Zone (chlorite-biotite, B.1); Cordierite Zone (chlorite - cordierite - biotite, C.1); Andalusite Zone (andalusite - cordierite - biotite, A.1); Staurolite Zone (andalusite - staurolite - biotite $\pm$ garnet, S.4).

Mineral analyses, carried out by electron microprobe, are listed in Appendix III. Mineralogical notes are given in Chapter 3 whilst the analyses are discussed in relation to mineral assemblages in Chapter 5. These analyses indicate a trend of upgrade Mg enrichment in cordierite and biotite (in A.1) and in staurolite and biotite (in S.4) which, taken in conjunction with the assemblage distribution suggest isograd reactions (Chapter 6 sections 2 and 3):

Cordierite Isograd: chlorite + muscovite $\rightleftharpoons$ cordierite + biotite 1

Andalusite Isograd: cordierite + muscovite $\rightleftharpoons$ cordierite + biotite 2

Staurolite Isograd: andalusite + biotite $\rightleftharpoons$ staurolite + muscovite 3

The above reactions, which are for rocks with muscovite and no garnet, were related to each other by means of the model system Al_2O_3-K_2O-FeO-MgO-SiO_2-H_2O (AKFMSH) whilst garnet bearing and muscovite free (including some gedrite bearing) assemblages were treated in the systems AKFMSH-Mn and AFMSH respectively. Petrogenetic grids for the above systems showing the topology for both univariant and multivariant equilibria are presented in Chapter 6 sections 4 to 6. The Buchan sequences are compared with those of other terrains in Chapter 6 section 7. Accurate P,T values cannot be given, however, the grids suggest that the P,T path on the Banffshire coast passed between 2 & 4 Kb in the range 520 - 570°C at the cordierite isograd and then became strongly pressure controlled, crossing reaction 3 above (or its Mn-bearing equivalent) from the high to low entropy sides, on entry into the staurolite

zone. At higher grades the P,T path must have passed close to the Al_2SiO_5 triple point and thence into the kyanite stability field, realising the kyanite bearing schists near Portsoy.

Bulk rock analyses (Appendix II) were carried out by XRF and are discussed in Chapter 4. The rocks are similar to other Dalradian metapelites and greywacke siltstones though compositions suitable for the development of highly aluminous biotite free assemblages are absent. Reactions 1, 2 and 3 above are di- or multi-variant in nature, and isograds in the field mark lines where the reactions run for the most Fe rich bulk compositions present. Mineral analyses suggest that the critical M/FM(100MgO/MgO+FeO) is near 40 whilst bulk rock data indicates 38.

A possible mechanism for reaction 2 above, is discussed in Chapter 7.

CHAPTER 2

Petrography

2.1. Upgrade Sequences, Terminology and Spatial Distribution of the Metamorphic Zones.

The outcrop pattern of the Dalradian metamorphic rocks of Buchan is controlled by the major Boyndie Syncline (see Chapter 1, page 7) so that the lowest grade (Biotite Zone) rocks occupy its core. To both east and west of the Biotite Zone, the metamorphic grade of the rocks increases and the upgrade sequences may be most easily dealt with by reference to those sections which offer the best exposure. These are:

(a) The Banffshire Coast Section with respect to the western set of zones (see Map 4).

(b) The Ythan Valley Section with respect to the western set of zones (see Map 5).

(a) Upgrade Sequence on the Banffshire Coast.

In an east to west traverse from Head of Garness (NJ 745650) to Whyntie Head (NJ 630660) one passes from a series of chlorite and biotite bearing slates and greywackes of low metamorphic grade into a sequence of middle grade rocks characterised by the occurrence of 'spots', cordierite or andalusite at Banff (NJ 688648). One mile further west near Boyndie Bay (NJ 670648) the rocks are characterised by the occurrence of staurolite. Such rocks persist as far west as Whyntie Head where the rocks begin to develop sillimanite (Ashworth 1972, 1975).

(b) Upgrade Sequence in the Valley of the River Ythan.

In a west to east traverse from Fyvie (NJ 763377) to Methlick (NJ 857376) one passes from chlorite and biotite bearing rocks similar to those on the Banffshire coast into higher grade rocks characterised by 'spots' cordierite or andalusite at (NJ 784366). These rocks persist as far east as Chapelhaugh (NJ 843393) where sillimanite begins to develop. Staurolite is lacking.

Some confusion has arisen as a result of the stratigraphic importance which has been attached to some metamorphic boundaries in Buchan, particularly that boundary involving the appearance of 'spots'. For this reason the grade terminology used by Read (1923, 1952) will be abandoned in preference for a more standard approach based on the zonal terminology of Barrow (1893, 1912). Each zone is given an index mineral name based on the mineral appearing at its low grade boundary. Despite the fact that some of the zonal boundaries are likely to be due to continuous (di- or multi-variant) reactions (Thompson 1955, 1957) and thus dependent on bulk rockchemistry as well as external variables i.e. P, T, etc. the term 'isograd' (Tilley 1924) will be retained in preference to Barrow's term 'outer limit' because of its widespread use in the literature. It should be stressed that this term is used in the widest sense, without implying anything about the nature of reactions giving rise to isograds in the field and is here defined after Miyashiro (1973) as the line of outcrops along which a mineral assemblage begins to appear.

The general disposition of the metamorphic zones and isograds in the field is shown in Map 2.

The rocks of the Biotite Zone are slates and greywackes of the Macduff Group which outcrop over a strip of ground some twelve miles wide by twenty five miles long from Banff (NJ 688648) to Gardenstown (NJ 793645) and southwards as far as the Insch gabbro. The zone is in part unconformably overlaid by unmetamorphosed sediments of Old Red Sandstone age. The diagnostic assemblage of the biotite zone is:
white mica - chlorite - biotite - quartz (assemblage B.2)
and this assemblage occurs throughout its outcrop. The zone is, however, symmetrical about a low grade axis marked by a tract of rocks some one to two miles in width which can be located near Head of Garness (NJ 745650) and near Nether Lenshie (NJ 683406). These areas are characterised by the presence of some rocks lacking biotite which show the assemblage
white mica - chlorite - quartz (B.1)
in association with rocks showing assemblage B.2. These rocks are referred to the Lower Biotite Zone.

The petrography and mineral compatibility of biotite zone rocks are discussed in Chapter 2 section 2 and Chapter 5 section 2 respectively.

The metamorphic grade of the rocks increases to both east and west of the Biotite Zone so that the Cordierite Zone and subsequent

MAP 2

The major metamorphic features of the Dalradian of North East Scotland.

Based on data of Read and Farquhar 1956; Chinner 1966; Fettes 1968,1970; Ashworth 1972; present study and sheet 9 ($\frac{1}{4}$" series) Geological Survey of Scotland.

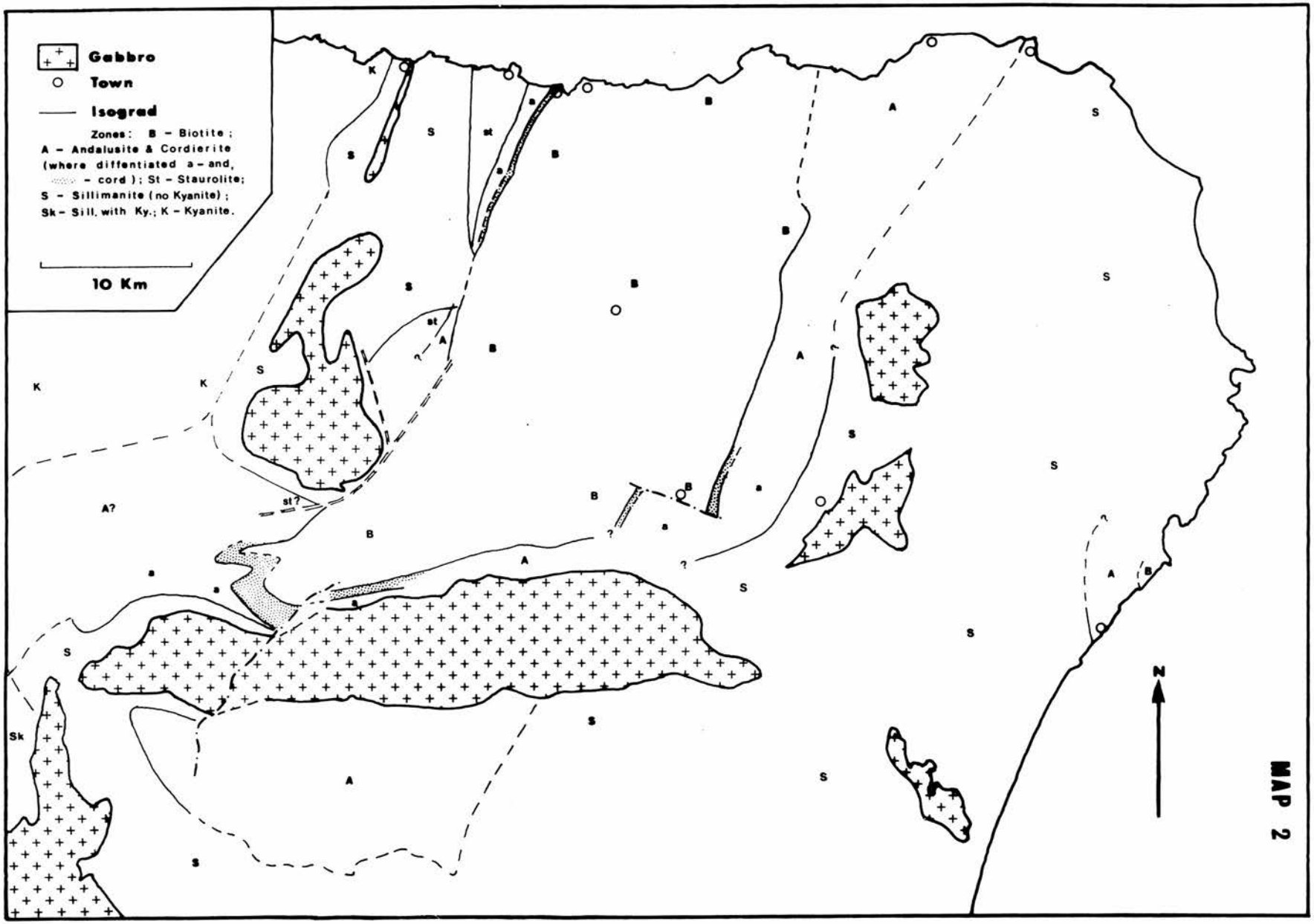
Gabbro
Town
Isograd
Zones: B – Biotite ;
A – Andalusite & Cordierite
(where diffentiated a – and,
– cord); St – Staurolite;
S – Sillimanite (no Kyanite) ;
Sk – Sill. with Ky.; K – Kyanite.
10 Km
N
MAP 2

Andalusite Zone occur symmetrically about it, forming two parallel belts which close to the south of the Insch Gabbro.

The Cordierite Zone is always narrow approximately $\frac{1}{4}$ mile in width and comprises part of those stratigraphic units mapped by officers of the Geological Survey as the Boyndie Bay Group and Fyvie Schists. The lower boundary of this zone is the Cordierite Isograd (see Chapter 2 section 3, Chapter 5 section 2 and Chapter 6). This isograd is defined by the appearance of cordierite 'spots' in the rocks, the assemblages being
white mica - biotite - cordierite - quartz (assemblage C.2) commonly
white mica - biotite - chlorite - cordierite - quartz (assemblage C.1) rarely

The Andalusite Zone is in turn symmetrically disposed around the cordierite zone. Its lower boundary is the Andalusite Isograd marked by the appearance of andalusite in the assemblage
muscovite - biotite - cordierite - andalusite - quartz.
The rocks of this zone again comprise parts of the Boyndie Bay Group and Fyvie Schists. The lower boundary of the zone is extremely poorly exposed so that the orientation of the isograd can only rarely be determined. It is mapable over one mile only in the eastern set of zones (Map 5), whilst it can be positioned roughly over a distance of some four miles within the western set of zones (Map 4). On the Banffshire Coast the zone has a width of around half a mile although the position of its upper boundary is uncertain. In contrast the andalusite zone has a width of almost two miles in the Ythan Valley and this may be in part related to the

lower regional dip of the rocks. The petrography and mineral compability of this zone are discussed in Chapter 2 section 3 and Chapter 5 section 3.

Unlike the cordierite and andalusite zones which are symmetrically developed to the east and west of the biotite zone, the Staurolite Zone is confined to the west. Reports of occurrences of staurolite in the Ythan Valley (Read 1952) were not confirmed whilst staurolite localities published by Porteous (1973) for the same area fallwithin the sillimanite zone of the present study. The width of the staurolite zone is a maximum of $2\frac{3}{4}$ miles on the Banffshire coast (Map 4) whilst, to the south, its width decreases as the sillimanite zone encroaches upon it (Ashworth 1972, 1975). The lower boundary of the zone is the staurolite isograd commonly marked by the appearance of the assemblage

andalusite - staurolite - biotite - muscovite - quartz (S4)

The appearance of staurolite is commonly accompanied by garnet, (For more detailed accounts of the petrography and mineral assemblages see Chapter 2 section 4 and Chapter 5 sections 4 and 5). This zone is comprised of rocks falling within the Whitehills Group and part of the Boyndie Bay Group.

The mineralogy of rocks occurring on the Banffshire Coast is summarised and shown in relation to some recent metamorphic facies schemes (Winkler 1967; Turner 1968; Miyashiro 1973) in Table 2.1. The presence of cordierite and andalusite in many of the rocks, clearly places them in the low pressure parts of the

Zone	Biotite		Cordierite	Andalusite	Staurolite
Common assemblages in pelites and greywacke siltstones	ser-chl-bi ser-chl	ser-chl-bi ser-bi	ser-chl-bi-co ser-bi-co ser-bi	ms-bi-and-co ms-bi-co (ms-bi-and)	ms-bi-and-st-co ms-bi-and-st ms-bi-and-co and-co-bi-st ms-bi-st ms-bi-co ms-bi-and and-bi-st
Other Minerals generally present	← quartz →				
	← Albite →	?← plagioclase →			
	← ilmenite →				
Sometimes present	← sulphide →				
	← epidote? →	→			← spessartite → gedrite ← →
Metamorphic Facies	GREENSCHIST		- - - - - - - -	AMPHIBOLITE	

SILLIMANITE ISOGRAD

Table 2.1: Summary of mineralogy of rocks from the Banffshire Coast

greenschist /amphibolite facies (Winkler 1967, Miyashiro 1973) or hornfels facies (Turner 1968). Leaving aside disagreements over facies nomenclature, the most important problem with regard to the Buchan rocks arises from definitions quoted for the green schist/amphibolite facies boundary in the low pressure region. Winkler (1967) states on page 116 that "the boundary between the greenschist and amphibolite facies.....is marked by the incompatibility of chlorite and quartz....." whilst on page 119 he states "The amphibolite facies commences with the first appearance of cordierite, staurolite, ortho amphibole, diopside and grossular/andradite". The definition of page 116 would place the boundary at the present andalusite isograd whilst page 119 places it at the cordierite isograd. Miyashiro (1973 p.300) suggests that the low pressure amphibolite facies begins with the appearance of andalusite, cordierite or almandine and implies that chlorite and phengitic white mica are simultaneously eliminated. Turner (1968 p. 193) states with respect to his hornblende hornfels facies (in which he includes the regional rocks of Abukuma, the Pyrenees and Buchan) that "muscovite - biotite - quartz is ubiquitous in pelitic rocks" and adds here and on page 223 that andalusite and cordierite appear, staurolite and almandine may occur, whilst "pelitic rocks <u>seldom</u> contain chlorite except as a retrogressive phase." The inclusion of the word seldom implies that chlorite may occasionally occur. Winkler (1967) recognises the occurrence of andalusite - chlorite - quartz assemblages but places them in the green schist facies.

As a result of this controversy it seems most reasonable to treat

andalusite and cordierite bearing assemblages which contain primary chlorite as transitional assemblages and the cordierite zone (containing assemblage C.1) has been shown as a transitional region in Table 2.1. The hornblende hornfels facies of Turner (1968) is considered equivalent to the low pressure amphibolite facies of Winkler (1967) and Miyashiro (1973).

2.2. The Biotite Zone (Banff Coast Section)

In the field these rocks form an alternating series of greywackes grits and pelites of the Macduff Slate Group. Many sedimentary structures are preserved including fine scale cross beds, graded units, sedimentary dykes and loads (Plates 1 and 2a) and (Sutton and Watson 1955). The sedimentary facies are varied. Mud flake conglomerates are common and lensoid masses of coarse sandstone occur amongst graded units.

The pelitic rocks in hand specimen are grey, grey-green or occasionally black and are generally extremely fine grained. Some types occasionally show trails of larger quartz grains and some show small brown pits as a result of weathering feldspars. Sulphides are often visible sometimes concentrated in pods. Biotite is recognisable, in hand specimen, only in the higher grade parts of the zone near Macduff (NJ 715650).

The only rocks which lack biotite occur in the lowest grade part of the zone near Garness Head (NJ 745650) and Old Haven (NJ 733646) of which specimen 43849 (Plate 2b) is typical. It contains very

fine grained chlorite and white mica aligned in a prominent cleavage along with quartz, plagioclase and a considerable amount of carbonaceous material. Along with these rocks biotite bearing slates occur; specimen 43852 is a typical example in which biotite forms small sparse porphyroblasts. Chlorite lenses are also present along with a very fine grained greenish sericite occurring in felts and larger flakes of white mica.

Specimen 43860 (Plate 3a) is typical of the higher grade slates near Macduff in which fine white mica flakes define a prominent penetrative cleavage. Chlorite occurs as fine flakes and lensoid masses also aligned in this direction whilst biotite occurs as numerous small porphyroblasts seldom showing any preferred orientation. At any locality biotite tends to be more abundant in rocks of a semi pelitic nature, a relationship previously noted with respect to the biotite isograd in the Aberfoyle Area (Mather 1970).

Quartz and plagioclase, occasionally twinned, are ubiquitous. In some cases lenses rich in these minerals occur parallel to the original bedding direction. At lowest grade twinned plagioclase has RI $<$ balsam and is near to albite in composition. It often appears clouded and sometimes contains tiny blebs of a high relief material (possibly epidote?) (Specimen 43845). Within the higher grades near Macduff plagioclase becomes crisp and inclusion free and has RI $>$ balsam, indicating that it now contains more of the anorthite molecule.

Potash feldspar has not been identified from any of the pelitic or semi pelitic rocks though it does occur in coarse grit horizons.

A brown slightly pleochroic mineral is present in the groundmass of some of the lowest grade slates. This material has low birefringence and does not exhibit the typical speckled extinction of biotite. It is rarely seen to interfinger with chlorite. Because of its fine grain size and scarcity separation of this mineral is impossible. It is probably a mineral similar to that described by Chaterjee (1966) which he considered to be an alteration product of chlorite.

Biotite can be seen in all stages of alteration to chlorite. In other cases it alters in a different manner its colour being leached whilst the grain becomes crowded with fine opaque needles, often arranged parallel to the cleavage traces, and forming a criss-cross arrangement when viewed parallel to the basal plane. These may be leucoxene or rutile as suggested by Schwartz (1958).

Of the five polished sections studied all contain ilmenite in various stages of alteration to rutile. Some rocks are rich in sulphide. Magnetite is absent.

Accessories include tourmaline which is common, rare apatite and occasionally a very fine grained high relief material which may be epidote. Calcite and pyrite occur as late crack infillings or veinlets.

Since biotite bearing rocks occur throughout this zone, all rocks are considered as belonging to the Biotite Zone. Minor variations in the assemblages allow the subdivision of this zone into lower and higher grade parts and although a definite isograd cannot be accurately placed between them, they may be indicated as follows:

a) Lower Biotite Zone (Garness Head - Old Haven)

The following assemblages coexist with quartz, albite and opaques.

chlorite - biotite - white mica

chlorite - white mica

b) Upper Biotite Zone (Old Haven - Banff)

The following assemblages coexist with quartz, plagioclase and opaques.

chlorite - biotite - white mica

biotite - white mica

Near the high grade margin of the zone, chlorite becomes rare as the rocks tend to become more siliceous.

Throughout the sequence a slight increase in grainsize occurs along with a considerable increase in the amount and size of biotite porphyroblasts.

2.3. The Cordierite and Andalusite Zones (Banff Coast Section)

The original sedimentary rock types occurring in these zones are essentially similar to those described for the biotite zone, section 2.2 though falling within the Read's (1923) Boyndie Bay Group.

The cordierite isograd is marked in the field by the first appearance of small dark 'spots' in hand specimen (Plates 3b and 4a). These are very sparse and small to begin with, about 1mm across but increase rapidly in abundance and size to 4 or 5 mm within 20 yards of the isograd. Individual 'spots' often overgrow several fine laminations. (Plate 4b). Although they occur in rocks of both pelitic and semi pelitic composition they are more abundant in the former. 'Spots' may be entirely absent from the pelitic portions of mudflake conglomerates but when present they are always smaller than those developed in adjacent continuous beds, suggesting that their growth has been restricted in some way.

Green chlorite is clearly visible in hand specimen in some rocks and when present may be very abundant. The nature of such chlorite and 'spots' are considered in sub sections 2.3(a) and 2.3(b).

Specimen 43867 is typical of the rocks near the isograd at Banff (NJ 688648). It contains biotite porphyroblasts in a ground mass of quartz, plagioclase and weakly aligned white mica. 'Spots' occur sporadically distributed through the rock so that they may not be represented within a random thin section plane. Specimen 43865 is a rock lacking 'spots' altogether whilst specimen 43870 carries fine primary chlorite flakes aligned in the schistosity in addition to white mica, biotite and 'spots'.

Some 150 yards west of the appearance of 'spots' large partly

fresh cordierite porphyroblasts occur up to 1 cm in diameter (Plate 6a). They are generally spherical to elliptical in shape and are crowded with inclusions of quartz, biotite, white mica and opaques. Their edges are virtually always altered to a pale yellow isotropic pinite whilst their actual margins tend to be diffuse when observed under a high power objective. They commonly exhibit sector twinning (Plate 6b). Large chlorite and white mica laths which sometimes occur within them are thought to be retrogressive. These porphyroblasts occur in a ground mass of quartz, plagioclase and fine grained white mica, which generally forms selvages around them, whilst biotite occurs as small porphyroblasts occasionally showing a weak alignment. Idiomorphic chlorite porphyroblasts (sometimes poikiloblasts) may occur, generally showing polysynthetic twinning.

Some 50' yards up grade andalusite occurs in low exposures on the beach (specimen 43876) above a small anticline (NJ 6821 6458) marking the beginning of the andalusite zone. It occurs as poikiloblastic grains of variable size along with large cordierite porphyroblasts in a rock very similar to that described before (Plate 7a). In hand specimen it may be distinguished from cordierite by its generally squarish to rectangular shape and lighter colour.

To the west andalusite is again absent from the rocks which are largely semi pelites and its rarity makes the position of an

isograd very tenuous. Since the first rocks to carry large fresh cordierite porphyroblasts are petrographically very similar to those above the appearance of andalusite they may best be treated along with the andalusite zone.

Of five polished sections from both zones, all contain ilmenite, whilst pyrite, pyrrhotite and possibly primary rutile also occur.

The groundmass textures occurring in these rocks are typically complex. Despite the fact that Read (1923) referred to the rocks as phyllites, planar fabrics (either cleavage or schistosity) are commonly poorly developed or lacking entirely, and textures in many rocks may be considered as transitional between those of schists and hornfelses. For example, specimen 43876 (Plate 7a) shows a variety of fabric types. Groundmass biotite shows a weak preferred orientation and where cordierite porphyroblasts occur, they overgrow this structure (Plate 7b). The internal trails are in some cases parallel with the groundmass alignment and in others at an angle to it, swinging into continuity near porphyroblast margins. In the latter cases weak crenulations are usually developed in the adjacent groundmass. Selvages also occasionally occur adjacent to rotated porphyroblasts and where these are present white mica may show a similar alignment to biotite. Through most of the groundmass however, it shows a largely decussate arrangement (Plate 8a).

In rocks which are richer in quartz and feldspar e.g. specimen

43873 these minerals are generally equant, imparting a granoblastic texture to the rock.

In restricted zones, some several yards across, a strong schistosity is developed, marked by alignment of biotite and white mica (Plate 8b). Here the rocks are highly altered with much late chlorite development, and porphyroblasts which are always completely pseudomorphed, may be rodded in the schistosity. Such rodded porphyroblasts are figured by Johnson (1962). The implications of these structures on the relative age of porphyroblast growth are considered in Chapter 2 section 5(d), whilst the mineralogy of the rocks is summarised in Table 2.1.

2.3.(a) 'Spots'

The boundary between the Macduff Slates and the Boyndie Bay Group, although mapped by the Geological Survey (Read 1923) as both a stratigraphic and metamorphic boundary, is essentially of metamorphic origin. It is defined by a mineral reconstitution resulting in the appearance of 'spots' (Plates 3b, 4a, 4b) as an upgrade traverse is made from the Macduff Slates. These 'spots' are seen in the field as small dark circular patches and at any one locality a line between spotted and non spotted rocks can be placed to an accuracy of a few yards.

Under the microscope (Plate 5) the 'spots' typically show a similar mineralogy to the groundmass, though quartz and biotite often display a slightly smaller grain size within the 'spot'.

They always have diffuse boundaries. The area is apparently bound together by a fine web of unidentifiable material which may be isotropic or exhibit very low birefringence, in which case several stringers may be observed to extinguish together, the whole 'spot' giving the impression of extinguishing in a patchy manner. In some cases (still < 100 feet from the isograd), the web appears to be a fine aggregate of sericitic mica showing higher birefringence. These 'spots' commonly show a concentric zonation, with an outer zone of isotropic web and an inner zone of coarser white mica or vice versa. In other cases the 'spots' contain a deep brownish yellow material; or large ragged retrograde chlorites may occur where such chlorites are abundant in the groundmass.

Several of these observations (including shape and the presence of isotropic, brownish yellow and pinitic material) suggest the presence of cordierite or cordierite alteration product within the 'spots'. An origin of the 'spots' by alteration of andalusite (the other porphyroblast occurring immediately upgrade) is not favoured because andalusite, although never seen entirely pseudomorphed, commonly shows square cross sections, the corners and edges of which are well preserved in areas of partial alteration to white mica which exhibits a serpentinous texture. In higher grade rocks, particularly in the Ythan Valley (see Chapter 2 section 6) e.g. specimen 43985 typical 'spots' can often be seen in association with partly altered andalusites and are readily distinguished from them.

X-ray diffraction traces showed the 'spots' to consist largely of 2M muscovite and 14Å chlorite along with quartz and biotite (included material) but failed to show clear positive evidence of the presence of cordierite or any other mineral. A comparison of diffraction traces from 'spots' with those of adjacent groundmass did however suggest the presence of some 1M muscovite in 'spots'. This may be significant in the light of the suggestion by Schreyer and Yoder (1961) that isotropic alteration of cordierite consists of 1M muscovite and 7Å 'chlorite'.

Although the evidence is obviously not clear, and one cannot be sure that all the 'spots' have the same origin it is considered most likely that these 'spots' represent altered cordierite porphyroblasts, and they will be considered as such in the following chapters. This conclusion is supported by Bosma (1967) who noted the presence of cordierite in some'spots' of similar nature in some rocks from the central Pyrenees.

2.3.(b) The Status of Chlorite

Chlorite in some form is invariably present in some rocks at all grades. In the biotite zone it occurs as minute flakes and lenses aligned with the cleavage and is undoubtedly primary in origin. In the staurolite zone it occurs as irregular flakes and radiating clusters often within or near the edges of pseudomorphs, and must be of late stage origin and retrogressive in nature. It is occasionally seen to overgrow crenulations which are demonstrably later than the growth of andalusite or cordierite.

Within the cordierite and andalusite zones, chlorite occurs in several forms a) as small randomly oriented idioblastic sometimes poikiloblastic crystals, b) as radiating ragged flakes in pseudomorphs ('spots') and c) very occasionally as fine flakes aligned with white mica in the ground mass.

The occurrence of (b) in pseudomorphs suggest, as for the staurolite zone chlorite, a late stage retrogressive origin; whilst type (a) chlorite appears similar to that of (b). Type (c) however has all the petrographic characteristics of a primary phase, and has been accepted as such.

2.4. The Staurolite Zone

The original sedimentary rock types are again similar to those described for the lower grade zones as far west as Whitehills (NJ 655657) which marks the transition between the Boyndie Bay and Whitehills groups (Plate 11). West of Whitehills calcareous beds become increasingly dominant whilst pelites and greywackes are restricted to the horizons outcropping at (NJ 644660), (NJ 641659) and (NJ 631659) near Whyntie Head. (Sutton and Watson 1955).

The first exposures of staurolite bearing rocks are to be found near the bottom of the shingle beach on the west side of Boyndie Bay (NJ 667650). In hand specimen the rocks are more apparently schistose than those of the andalusite and cordierite zones (Plate 11b) though groundmass fabrics are equally complex when

examined in detail. Andalusite and staurolite porphyroblasts are prominent on freshly weathered surfaces of some rocks (Plate 12a) occurring amongst a groundmass which is usually pale grey in colour with small specks of dark biotite. In addition many rocks show circular greenish patches rich in chlorite.

The mineralogy of the rocks is summarised in Table 2.1 whilst a more detailed list of assemblages is given in Table 5.3.

The rocks are commonly heterogeneous with respect of porphyroblast development and some thin sections from a single hand specimen may lack a porphyroblast phase which is present in others. The rocks may however be classified for descriptive purposes into five groups based on silicate assemblages with four or more phases plus quartz and on associated textures.

a) Andalusite - biotite - staurolite - muscovite schists.

Specimen 43912 is typical of this group at Boyndie Bay, (Plate 13a). The rock contains porphyroblasts of andalusite and staurolite which occur in a groundmass of quartz, biotite, plagioclase muscovite and opaques. Groundmass quartz and feldspar are granoblastic and essentially fine grained (up to 0.1mm in diameter) though noticeably coarser than that of the lower grade rocks. Smaller muscovite and larger biotite flakes occur within this material and are typically concentrated near andalusite porphyroblasts. In some parts of the slide these micas show

a preferred orientation (particularly near the two lower andalusite crystals in Plate 13a) whilst in other parts it is virtually lacking and biotite may approach a decussate arrangement, particularly between the two upper andalusite crystals (Plate 13a and b). In other parts of the groundmass the texture is transitional between these two extremes.

Andalusite forms porphyroblasts with a tendency towards rectangular sections up to 6 mm long. The included material is commonly quartz and biotite of finer grain size than the groundmass and occasionally staurolite. Opaque material (largely ilmenite) also occurs and is noticeably concentrated in andalusite. Quartz - biotite inclusion trails are not well developed but where present are straight and at an angle to the groundmass alignment over most of the porphyroblast but swing into parallelism near the margins.

Staurolite forms smaller porphyroblasts up to 2mm long carrying less included material than andalusite and is commonly twinned. Inclusions are restricted to quartz and ilmenite again of smaller grain size than the groundmass and showing no regular arrangement.

Limited secondary chlorite development occurs as alteration of biotite and staurolite whilst andalusite may be altered near its edges to a fine silvery material, presumably fine white mica.

Tourmaline and apatite occur as accessories in 43912 whilst garnet also occurs in small amounts in some similar rocks, e.g. 43945 (Plates 14 a and b).

Specimen 43918 is typical of the group at higher grade near Whitehills (Plate 16a). It contains large irregularly shaped andalusite and smaller staurolite poikiloblasts along with small idoblastic garnets which are virtually inclusion free. The groundmass shows a small scale foliation composed of alternate bands of granoblastic quartz and plagioclase, and schistose muscovite and biotite, the whole being crenulated with some associated strain slip cleavage development. It is considerably coarser grained than that of corresponding rocks at Boyndie Bay and is richer in muscovite.

Included quartz/biotite trails in andalusite are continuous with the main schistosity and almost of the same grain size whilst the porphyroblasts themselves are deformed by crenulatious and apparently broken where strain slip cleavages pass through them. (see Johnson 1962). Opaque material again shows a concentration within andalusite.

Included material in staurolite is almost exclusively quartz which is generally arranged in straight trails at an angle to the main schistosity though s-shaped trails and continuous trails also occur.

Specimen 43943 from Kinnairdy (NJ 612501) illustrates a texture

typical of this group very clearly (Plate 15). The rock lies close to the sillimanite isograd, (Ashworth 1972, 1975) where that boundary encroaches furthest onto the regional zonal pattern so that it is less than half a mile above the staurolite isograd.

The rock carries andalusite and staurolite porphyroblasts in a groundmass of granoblastic quartz and feldspar carrying a schistosity of oriented biotite and muscovite.

Andalusite porphyroblasts show a tendency to form large square cross sectioned prisms up to one centimetre across but these commonly show semicircular to arcurate enclaves. They are crowded with inclusions of quartz, biotite and considerable opaque material which is conspicuously absent from the margins of porphyroblasts where they border on such enclaves. These opaque free margins appear to represent overgrowths which are in optical continuity with the main porphyroblast. The material within the enclaves is clean granoblastic-polygonal quartz and plagioclase commonly showing triple junction contacts and biotite which shows no preferred orientation. Traces of pinite are occasionally to be found in the central portions suggesting that the material originally occupying these enclaves was cordierite. Such pseudomorphs are considered to be the result of an increase in grade and are akin to similar textures described in rocks from the Ythan Valley (Chapter 2 section 6).

Staurolite forms small square porphyroblasts crowded with inclusions of opaque material and quartz and is not related to the recrystallized pseudomorphs. Some chlorite occurs as

alteration of biotite. One small pod of fibrolite is present within quartz and adjacent to it the corner of an andalusite porphyroblast has been replaced by plates of muscovite.

Thin dark horizons occurring most notably at Boyndie Bay (specimen 43910) contain andalusite and staurolite porphyroblasts commonly crowded with fine carbonaceous inclusions and apatite in a groundmass which is also rich in these minerals. In these rocks andalusite commonly shows partially developed chiastolite cross structures (Plate 16b).

Occasionally other rocks may lack one of the main porphyroblast phases. Thin horizons at Boyndie Bay 43913 commonly lack andalusite being essentially staurolite-biotite-muscovite schists $\pm$ gt whilst to the West of Whitehills many rocks lack staurolite and are andalusite-biotite-muscovite schists (specimens 43921, 43922) or andalusite-biotite-garnet-muscovite schists (43915).

b) Andalusite - biotite - staurolite - muscovite - cordierite pseudomorph schists

Such rocks are restricted to localities close to the staurolite isograd at Boyndie Bay and Black Law (NJ 638547). Specimen 43904 is typical containing porphyroblasts of andalusite staurolite and biotite in a groundmass of quartz and plagioclase carrying fine white mica flakes and giving rise to the main schistosity, which is weakly crenulated.

Andalusite porphyroblasts are up to 2 cm long, xenoblastic and include quartz, biotite, opaques and occasionally staurolite. Inclusion trails have similar relations to those described for

specimen 43912. They are in part altered to a fine silvery matery.

Staurolite porphyroblasts are idioblastic and included material is mainly quartz. Trails are generally straight and at an angle to the main schistosity though one crystal has been observed which exhibits weakly S-shaped trails which are continuous with the schistosity.

Biotite forms small porphyroblasts containing quartz and exhibits many pleochroic haloes. Garnet is present in some rocks in accessory amounts.

In addition to these porphyroblasts, circular to oval pseudomorphs occur composed mainly of large ragged chlorite and white mica crystals, although quartz, biotite and occasionally staurolite may occur within them. Such biotite is commonly oriented at an angle to the main schistosity and may represent original inclusion trails. In other rocks (specimen 43908) similar pseudomorphs contain pinite centres suggesting that the original material forming the porphyroblast was cordierite. These are considered to be retrogressive pseudomorphs after cordierite and should not be confused with those previously described from specimen 43943 (page 49). They may be seen in contact with both staurolite and andalusite.

c) Andalusite - staurolite - cordierite - biotite rocks.

This group is distinguished from group b) since they lack muscovite. Such rocks occur throughout the staurolite zone and specimen 43942 (Plate 17b) from Maunderlea Quarry

(NJ 633563) is typical. Andalusite staurolite and largely fresh cordierite porphyroblasts sometimes exhibiting a hexagonal outline, occur in a groundmass of granoblastic quartz and plagioclase. Biotite generally shows no preferred orientation through most of the groundmass though it may form selvages around porphyroblasts.

Andalusite forms large porphyroblasts with a tendency to a square outline though they are generally interputed by cordierite porphyroblasts. It includes quartz, opaques and some biotite along with occasional staurolite crystals and partially encloses cordierite, mimicking those enclave textures described from specimen 43943. Opaque inclusions are lacking or greatly reduced in number near to contacts with cordierite. Staurolite porphyroblasts show variable development of crystal shape and twinning.

Cordierite forms circular to oval porphyroblasts up to 6 mm long which include minute crystals of biotite and quartz, and occasionally crystals of staurolite. They sometimes show yellow pleochroic haloes. Edges of porphyroblasts are commonly altered to yellow isotropic pinite though in some cases part of a porphyroblast may be altered completely to an aggregate of large ragged chlorite and muscovite crystals.

All porphyroblasts can be seen in contact with each other. No inclusion trails have been seen in these rocks.

Similar rocks may carry accessory amounts of garnet (43903)

or muscovite (43894) which occurs in the groundmass only in areas well removed from porphyroblasts.

Others lack andalusite and cordierite and are staurolite - biotite - garnet rocks (43940) or biotite - garnet rocks, again lacking muscovite. Plate 18a shows a horizon from specimen 43940 rich in garnet and lacking muscovite.

d) Cordierite - biotite - andalusite - muscovite schists.

Specimen 43901 is typical of this group at Boyndie Bay. The groundmass is composed of alternate bands of granoblastic quartz and plagioclase carrying oriented biotite and white mica, and schistose muscovite and biotite carrying some quartz. Opaque minerals are distributed throughout the groundmass. The muscovite is notably coarser grained than that of staurolite schists from the same locality.

Andalusite occurs as small square prisms entirely altered to the typical fine white mica within muscovite rich folice
Cordierite occurs as circular to oval porphyroblasts partially altered to isotropic pinite set within granulose seams whilst muscovite rich ones sweep around them. It is crowded with small inclusions of quartz, biotite, opaques and fine muscovite which in some porphyroblasts define straight trails at an angle to the schistosity. In other cases the trails curve near the edges of prophyroblasts into parallelism with the schistosity.

Specimen 43919 is a similar rock from Whitehills. It has slightly coarser grain size and is richer in muscovite. Rocks with this mineralogy do not occur west of Whitehills.

Similar rocks occur at Boyndie Bay which lack andalusite being essentially cordierite - biotite - muscovite schists. All stages of alteration of cordierite occur through pinite to coarse chlorite - muscovite pseudomorphs. These rocks occur immediately west of the staurolite isograd (within 250 yards) and do not occur at higher grades.

One instance has been noted at this locality of a highly altered rock which contains large coarse chlorite - muscovite pseudomorphs, probably after cordierite along with one small crystal of staurolite.

2.5. Textural relationships and Mineral Growth

a) The structural time scale

A detailed investigation of fold episodes in the area has not been carried out in this study and as such most of the following section is based on the work of Johnson (1962) and Fettes (1968, 1970, 1971). During the present investigation isoclinal folds have been noted near Whitehills Harbour (NJ 655657). At this locality crenulations (F_3 of Johnson 1962) are seen to fold a schistosity which is axial planar to the isoclinal folds (S_1; F_1 Johnson 1962) and also to deform a biotite lineation which lies at an acute angle to S_1 (S_2 of Johnson 1962). At

virtually all other localities structures are restricted to a main schistosity, which has been considered to represent S_1, and less commonly crenulations and strain slip cleavages which have been considered to represent S_3. As such little can be concluded about relationships between porphyroblast growth and the F_2 deformation episode.

b) The groundmass fabrics

As pointed out in previous sections of this chapter, groundmass fabrics are typically complex and variable. Within the staurolite zone alone fabrics may vary from entirely granoblastic to entirely schistose, with all possible intermediate cases. This appears to be partially dependent on original composition. Greywacke siltstones (Lithology Type II; see Chapter 4 section 2) typically give rise to granoblastic rocks e.g. specimen 43902 whilst true pelites (Lithology Type I Chapter 4 section 2) typically give rise to schistose rocks e.g. specimen 43919. Lithologies which were originally intermediate (Type I/II Lithologies) might thus be expected to have groundmass fabrics which are partially schistose and partially granoblastic (e.g. specimen 43945 Plate 14a). Even in the most schistose rocks, however, groundmass quartz and plagioclase tend to be equant rather than elongate. Quartz inclusion trails in porphyroblasts from these rocks are often composed of small elongate grains of finer grain size than the present groundmass material. This suggests that the groundmass was once finely schistose and has undergone considerable static recrystallisation during or after porphyroblast growth. On the other hand inclusion trails are

never found in porphyroblasts occurring in granoblastic rocks. Here quartz inclusions tend to be equant though still finer grained than the present groundmass. This suggests that the original groundmass was probably finely granoblastic before recrystallisation occurred. Spry (1969 p.259) has suggested a subdivision of regional metamorphic rocks into Low- and High-stress types based not on mineralogical grounds (e.g. Harker 1932) but on textural grounds. He has cited the rocks of Buchan as an example of the former type, but points out that an association of low hydrostatic pressure (occurrence of andalusite or cordierite) with low stress is not universal. The controlling factor would appear to be the timing of the climax of metamorphism i.e. whether the major period of mineral growth takes place during a deformational phase or a static phase.

c) Porphyroblast inclusion relationships

A regular sequence of inclusion relationships exists between porphyroblasts. Garnet occurs as included material in andalusite, cordierite and staurolite. Staurolite occurs as inclusions in andalusite and cordierite whilst cordierite is seen partially enclosed by andalusite. Andalusite never occurs as included material. This may suggest a time sequence garnet growth - staurolite growth - cordierite growth - andalusite growth. However a relationship is also present between size of porphyroblasts and the inclusion sequence as follows:

garnet size	staurolite	cordierite	andalusite

so that with the possible exception of cordierite andalusite relations this is probably a reflection of the rate of porphyroblast growth rather than period of growth.

d) Porphyroblast growth in relation to the structural time scale

Andalusite: Inclusion trails in andalusite, composed of small elongate quartz crystals and sometimes biotite or opaque material, occur quite commonly in the staurolite zone but have not been observed in the andalusite zone. Inclusion trails are always continuous with the main groundmass schistosity (S_1) which they therefore post date. Their relationship to S_3 strain slip cleavages and crenulations is less clear as previously discussed by Johnson (1962 p.50). Trails are generally straight and at an angle to the main groundmass schistosity over most of the porphyroblast but swing rapidly into continuity near the edges (e.g. Plate 12a and b). In many cases the shape of F_3 crenulations appears to be controlled by andalusite porphyroblasts (see also Johnson 1962 p.50) and in many cases crenulations are lacking in the groundmass except immediately adjacent to andalusites. Andalusite crystals, ruptured by S_3 strain slip cleavages are present in specimen 43918. This textural evidence is in agreement with Johnson (1962) that andalusite growth was largely complete before the F_3 movements occurred though curved trails near the edge of porphyroblasts suggests that, in some cases at least, growth continued during the F_3 movements.

Cordierite: Inclusion trails of biotite, which are continuous with the main schistosity occur within cordierite from both the andalusite (e.g. specimen 43876) and staurolite zones (e.g.

specimen 43904). In most cases these trails have a similar relationship to those occurring in andalusite being straight and at an angle to the main schistosity over most of the porphyroblast but swinging into continuity near the edges. In both specimens 43904 and 43876 minor crenulations are developed near porphyroblasts suggesting that they have been controlled by the prior presence of the porphyroblasts. In specimen 43933 strain slip cleavage is seen to bend round and terminate against a cordierite porphyroblast (Plate 18b). These textural relations suggest that cordierite grew post S_1 but pre- and in part during the F_3 movements. The rodded porphyroblasts described by Johnson (1962) from Scotstown (NJ 682646) occur in rocks where a strong schistosity is developed (e.g. 43882 Plate 8b). This is thought to be an S_3 schistosity sporadically developed and associated with considerable retrogression of cordierite. In areas where this is not developed (e.g. specimen 43876) a relict S_1 schistosity is preserved by a weak biotite alignment (Plate 7b). More detailed work is required to finally confirm this point and it is hoped that this may be carried out in the near future.

Staurolite: Despite the common occurrence of trails of elongated quartz crystals inclusion trail relationships within staurolite are extemely complex. Within individual specimens (43904; 43918) straight trails may be seen which are in most cases at an angle to the main schistosity but in some cases continuous with it and apparently undeflected. To further complicate the issue one crystal showing a continuous s-shaped trail has been observed from each specimen. These s-shaped trails may represent

staurolites rolled in the S_1 cleavage or overgrown S_2 crenulations which have been described by Johnson (1962) from Sandend west of Portsoy. No clear picture of staurolite growth emerges from the present discussion but textures are compatible with the post F_2 pre F_3 age advanced by Johnson (1962).

Garnet: No inclusion trails have been found but since this mineral is commonly included in the other porphyroblast phases it must have been in process of formation during or before the growth of the other phases.

For the purpose of following chapters, all porphyroblast growth will be considered to have taken place during an essentially static metamorphism beginning after the F_2 fold movements and finishing before or during the F_3 fold movements.

2.6. Ythan Valley Section

In this traverse the metamorphic grade increases from west to east.

The Biotite Zone rocks are essentially similar to those described previously although they are poorly exposed in this area. Slates lacking biotite occur near Lenshie (NJ 683406) whilst at exposes to both east and west all rocks contain biotite suggesting that the zone is symmetrical about a low grade axis, (see Chapter 2 section 2 also).

The cordierite isograd which is well exposed at (NJ 784366) is again marked by the appearance of 'spots' whilst some half a mile further east andalusite appears in the rocks as small square prisms. These rocks all fall into the knotted Phyllite Grade of Read (1952). At this grade the rocks are similar to those of the cordierite and andalusite zones of the Banffshire Coast. The schistosity is poorly developed but where it is discernable it passes through spots without deflection.

Further upgrade towards Fetterletter (NJ 807388) the rocks become coarser grained and more obviously schistose whilst fresh cordierite and andalusite porphyroblasts become common. These rocks are equivalent to the Andalusite - Cordierite Schist Grade of Read (1952).

Crenulation and strain slip cleavages are first seen near Fetterletter (NJ 807388) becoming more common eastwards and are associated with open monoclinal folds (Fettes 1968). Cordierite porphyroblasts are here rotated with respect to the schistosity which they overgrow and in some cases where crenulations are well developed (specimen 44022) the growth of cordierite is demonstrably earlier, since inclusion trails are straight. These textures suggest that time relations of porphyroblast growth are similar to those of the Banffshire Coast.

2.7. Rocks containing orthorhombic amphibole

Orthorhombic amphibole has not been previously recorded in rocks of sedimentary origin from Buchan. The presence of this mineral was first observed by Dr B. Harte of the University of Edinburgh in some rock sections previously collected from Collieston by Dr. D.J. Fettes. (pers. comm.).

Such rocks have been found at only two localities during the present study:

a) At Collieston on the Aberdeenshire Coast (NK 041284)
   specimen 43962
b) Near Whyntie Head on the Banffshire Coast (NJ 631659)
   specimens 43923; 43924 and 43926.

The Collieston coast section has not been studied in detail though specimens collected near Collieston Harbour (Appendix I) and the work of Fettes (1968) suggest that the assemblages and metamorphic sequence are essentially similar to those described from the Ythan Valley.

Specimen 43962 shows abundant crystals of ortho-amphibole with a well developed preferred orientation over most of the slide. They occur in a fine grained groundmass of granoblastic quartz, plagioclase and opaques. Cordierite rich lenses also occur with their long dimensions parallel to the amphibole orientation. These lenses may be composed of large cordierite crystals or aggregates of small crystals. Where amphibole occurs within them it tends to have random orientation. Small crystals of biotite

At higher grades sillimanite occurs in similar rocks as small clumps of fibrolite sometimes growing on biotite crystals and occasionally appears to replace the edges of andalusite crystals.

As sillimanite becomes more common, andalusite crystals may be seen partially replaced by large plates of muscovite and rarely by aggregates of plagioclase feldspar (specimen 44038).

At higher grades, close to the contact of the Haddo House gabbro east of Methlick (NJ 860373) a boulder field occurs. Some rocks from this locality (specimen 44041, Plate 19b) show large crystals of orthoclase in association with quartz biotite cordierite plagioclase muscovite and sillimanite. The sillimanite in this specimen occurs both as fibrolite and as clumps of stumpy prisms which may possibly represent inverted andalusite crystals.

The sillimanite isograd as shown on Maps 3 and 5 is based on the field recognition of coarse muscovite replacement of andalusite porphyroblasts, a criterion which was used by Ashworth (1972) to place the equivalent isograd in Banffshire. This was chosen as a mapping criterion because coarse muscovite is easily identifiable in hand specimen in the field whilst small clumps of fibrolite can only be observed in thin section. Ashworth (1972) has shown that the appearance of fibrolite is always accompanied by coarse muscovite replacement of andalusite in Banffshire and this is equally true of the present rocks.

Several textures are of interest with respect to the growth of the porphyroblasts, which are best illustrated using two rocks from Braes of Gight (NJ 820387).

In rocks with low modal andalusite, this mineral occurs as irregular masses and stringers growing around and between cordierite porphyroblasts (specimens 44010, 44012 Plate 9).

Where andalusite is modally high it shows well developed crystals which often partially enclose cordierite porphyroblasts (specimen 44013, Plate 10) or their pseudomorphs. The two porphyroblast minerals in this association are separated by an area of granoblastic-polygonal biotite and quartz or less commonly biotite, quartz and plagioclase which appears to have replaced the cordierite mimicking its original shape. Within the recrystallized zone biotite shows no preferred orientation although it does so strongly in the groundmass outside the porphyroblasts. Andalusite adjacent to the recrystallized zone shows an overgrowth which is in optical continuity with the main crystal but less rich in inclusions of opaque material and at its boundary can be seen to finger out to biotite (commonly) and plagioclase (rarely) apparently replacing them whilst quartz takes up the area between advancing fingers.

These textures are clearly related to those previously described with respect to specimen 43943 and their significance is discussed in Chapter 7.

occur scattered through the rock but muscovite does not occur.

This rock type occurs as a thin laterally continuous unit amongst andalusite cordierite schists.

Ortho-amphibole rocks occur in a similar situation at Whyntie Head. Here two beds occur together. The upper bed some two inches in thickness carries crystals of amphibole along with biotite in a groundmass of quartz, plagioclase and opaques (specimen 43926). The lower unit, four to five inches in thickness, contains a more complex assemblage (specimen 43923). In this rock abundant amphibole as associated with cordierite staurolite and rarer granet porphyroblasts which are set in a groundmass of quartz, plagioclase, biotite and ilmenite. The amphibole occurs both as individual crystals and as radiating aggregates of crystals (Plate 19a). It may be seen included in cordierite and in contact with staurolite and garnet. Within this specimen garnet occurs as larger more abundant crystals in a horizon which lacks cordierite though rare small garnets also occur associated with cordierite in layers which are rich in the latter mineral.

The positive optic sign and birefringence (~.02) of the amphibole in these rocks suggest that it is gedrite.

A summary of the occurrence of minerals and important assemblages is given in figure 2.1. for the Banffshire coast section.

CHAPTER 3

MINERALOGY

3.1. Chlorite

Seventeen analyses of chlorites carried out during the present study are given in Appendix III (i) along with three unpublished analyses provided by J. Ashworth, all from rocks of the Banffshire coast.

As previously mentioned in Chapter 2 chlorite occurs both as

a) primary chlorite aligned in the schistosity
b) secondary chlorite with a cross cutting relationship to the schistosity.

All analysed chlorites are Ripidolites on the classification of Foster (1962) with the exception of two primary chlorites from the cordierite zone (specimen 43870) which are Brunsvigites, (see figure 3.1(a)). The analyses as a whole show a restricted range of Fe^{+2}(total) : R^{+2} replacement (0.46 - 0.59) whilst there is a weak tendency for the secondary chlorites to show lower values in association with increased Al substitution for Si in the tetrahedral sites. The water content, as estimated by difference is, in eight of the analyses, slightly in excess of the maximum of 13.5% as suggested by Foster (1962).

Electron microprobe analysis will not distinguish the valency

state of iron so that no direct evidence can be advanced for the role of Fe^{+3} in the structure of these chlorites. It is however possible to make some estimate of the importance of Fe^{+3} in the structure.

Figure 3.1 (b) shows a plot of octahedral versus tetrahedral aluminium. Foster (1962) has pointed out that chlorites in which the charge balance between octahedral and tetrahedral sheets is maintained by the straightforward replacement of $Al^{IV}Al^{VI} \rightleftharpoons R^{++}Si$ will show a ratio of 1 : 1, $Al^{IV} : Al^{VI}$, which is represented by a line in the diagram. For chlorites plotting below the line the charge balance requires to be maintained by the introduction of some other trivalent cation of which Fe^{+3} is the most likely contender. Most of the Buchan chlorites, however, plot above this line (i.e. have excess octahedral aluminium) only one analysis (secondary chlorite specimen 43894) showing a serious deficiency in Al^{VI}. Although this does not discount the possible presence of Fe^{+3} in the structure of these chlorites the amount present is likely to be limited. Foster (1962) has shown that excess trivalent cations in octahedral positions maintain the charge balance by replacement of divalent cations in the ratio 2 : 3 and thus give rise to a deficiency in the number of octahedral positions occupied. A plot of Al^{VI} + Ti in excess of Al^{IV} versus octahedral positions occupied (Figure 3.1 (c)) indicates a close adherance to this 2 : 3 ratio and suggests that Fe^{+3} is not an important constituent of those chlorites which have $Al^{VI} > Al^{IV}$.

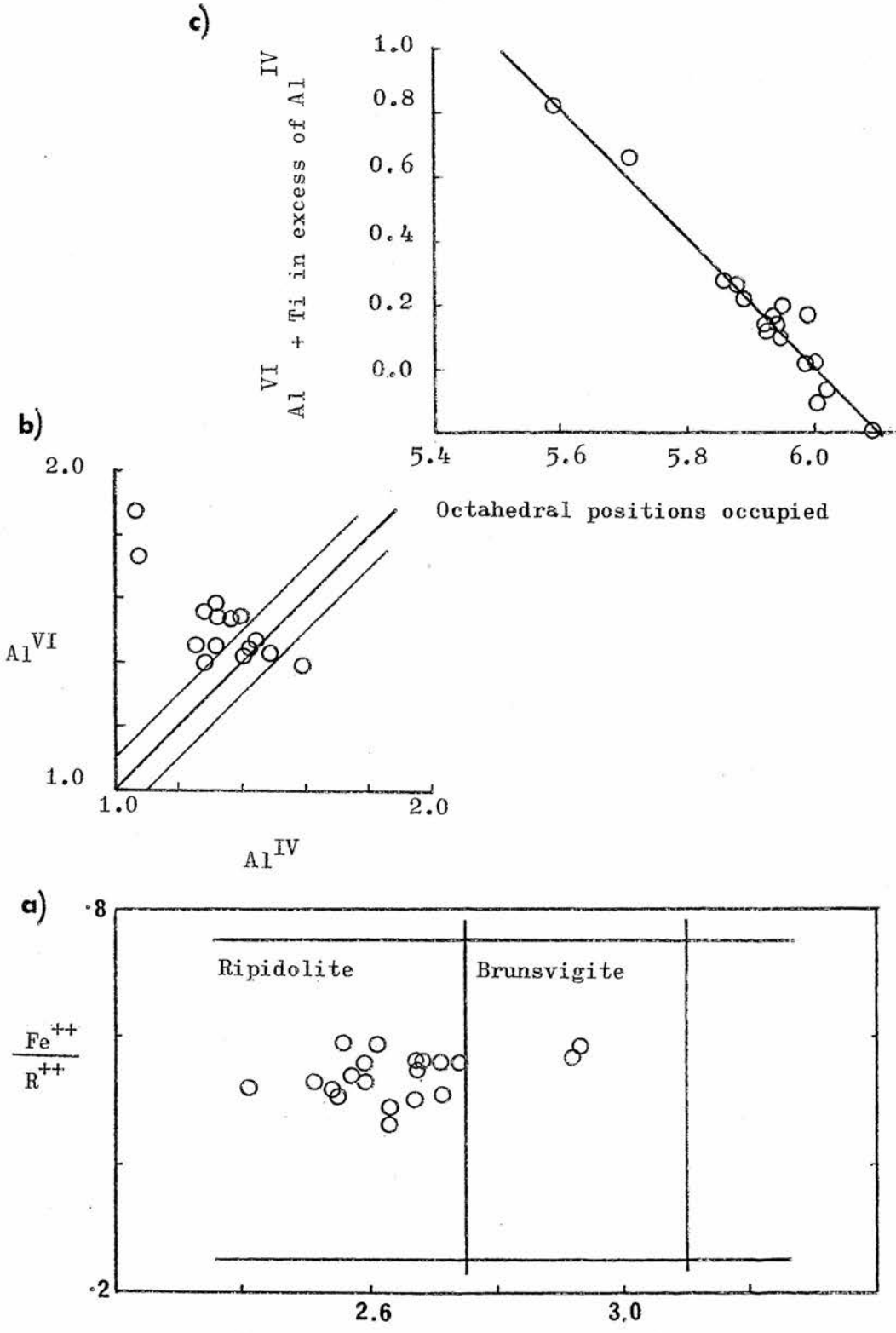

Figure 3.1 : Some features of the mineralogy of chlorite from the Dalradian rocks of Buchan.

3.2. White Mica

White micas from the Buchan rocks range in composition from phengite (Velde 1965) with 18% celadonite solid solution in the biotite zone to near ideal muscovite in the andalusite and staurolite zones. Figure 3.2(a) shows an S A F plot of analysed white micas (see Appendix III (ii)) similar to those used by Butler(1967) etc. Biotite zone white micas are compared with those from similar grades elsewhere in figure 5.1(a). All analyses show a deficiency in the alkali site with respect to ideal muscovite and all are poor in the paragonite molecule with Na/Na+K ranging from .38 to .56 which are low values compared with those reported by Guidotti (1970) but are comparable with some white micas reported by Evans and Guidotti (1966) and Deer, Howie and Zussman (1962).

Comparison of the five analysed white micas with the paragenetic fields as suggested by Cipriani et al (1970) shows that they are not comparable with low grade white micas from kyanite bearing sequences. Figure 3.2(b) shows that the Buchan analyses plot close to the 'orthoclase isograd' paragenetic field (field 7 of Cipriani et al 1971, figure 5). Taking into account the fact that these micas come from a cordierite-andalusite bearing sequence, the above relation is in accord with the experimental results of Velde (1965) which indicate that phengite solid solution in muscovite becomes restricted with both increasing temperature and decreasing pressure.

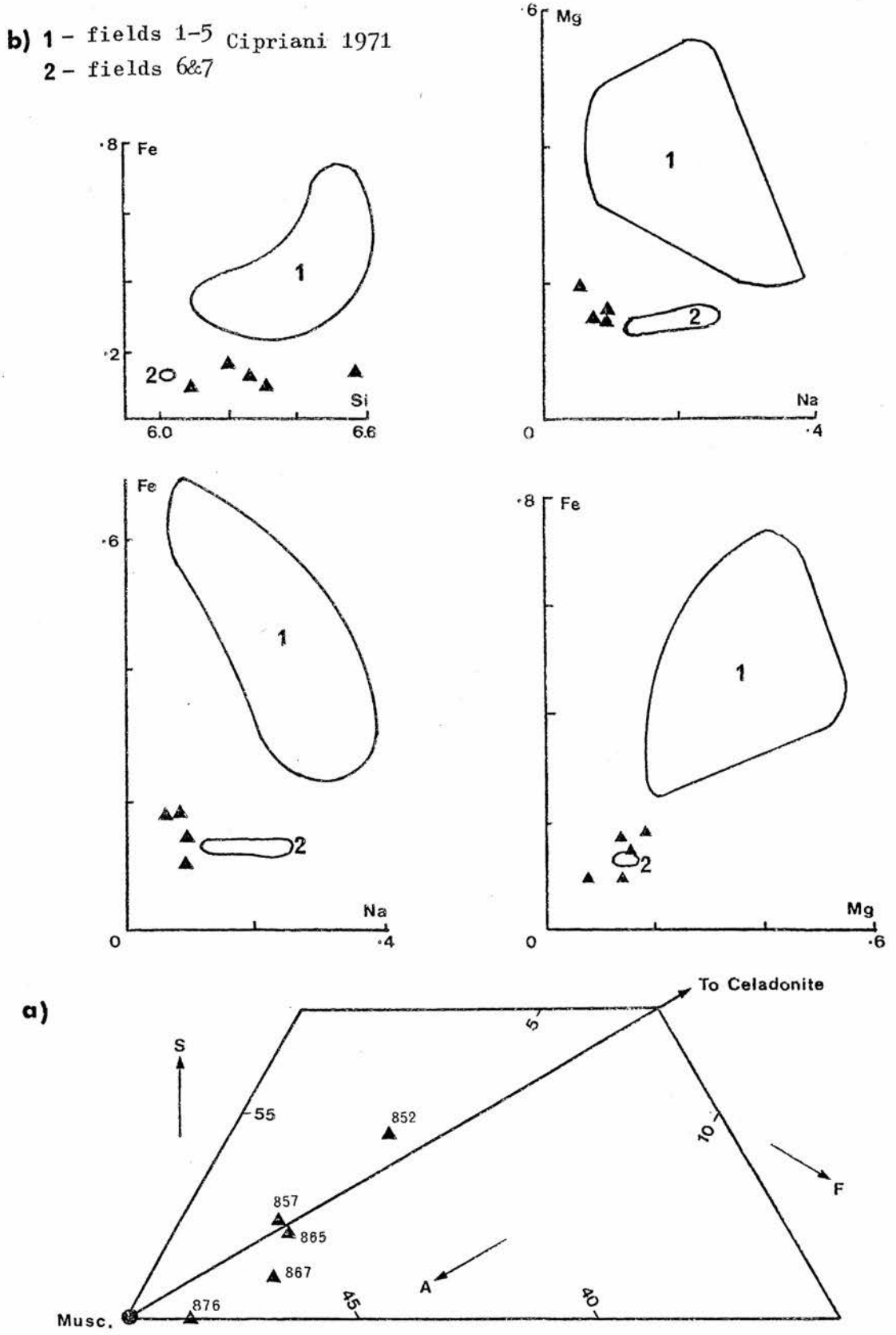

Figure 3.2 : Some features of the mineralogy of white micas from the Dalradian rocks of Buchan.

Extremely fine grained pale green micas occassionally occur in slates from the lower grade parts of the biotite zone (see 43852, last analysis Appendix III (i)). This analysis shows a high iron content and somewhat higher Na content than all the other analyses. It is not clear whether these represent particularly celadonite rich phengites or white mica - chlorite aggregates or laminates, though the large excess octahedral occupancy indicated by the calculated structural formula suggests the latter.

White mica is also a consistent constiuent of 'spots' in the cordierite zone. X-ray diffraction traces of both groundmass and spot material indicated the presence of the 2M polymorph (Yoder and Eugster 1955) in all cases and suggested the presence of the 1M polymorph in some spots.

3.3. Biotite

Analyses of biotites from the rocks of Buchan are listed in Appendix III (iii). All the analyses show a defficiency in total alkalies with respect to ideal biotite compositions, (e.g. Deer Howie and Zussman 1962). Potassium is by far the most important cation in this X site varying from 1.3 to 1.95 atoms per formula unit whilst sodium accounts for a maximum of 0.15 formula positions but is generally less than 0.08.

Tetrahedral aluminium is always in excess of 2.00 atoms per formula unit and may rise to 2.80, so that these biotites contain

considerable amounts of the eastonite molecules. Aluminium in biotites may be interpreted as being involved in three substitutions Deer et al (1962); Foster (1960), $KAl^{IV} = Si$; $Al^{VI}\ Al^{IV} = R^{++}\ Si$ and $Al^{VI} = R^{++}$ the last involving a decrease in octahedral sites occupied in order to maintain the charge balance. The relation between Al^{IV} and Al^{VI} in the Buchan biotites is examined in figure 3.3(a) after correction for Al^{IV} balanced by monovalent cations. Bioties involving no other R^{+++} ions should approximate to a 1 : 1 ratio straight line analogous to that previously discussed with respect to the chlorites. The plot however shows a wide scatter with a slight bias towards biotites with excess octahedral Al. All the biotites contain Titanium in varying amounts up to 0.33 formula positions and virtually all those showing defficiency in Al^{VI} (figure 3.3(a)) plot above the line when Ti is considered (see figure 3.3(b)). A notable exception is the biotite from the ortho-amphibole rock, 43962, which shows an overall negative charge of .08 as follows:

$$(K_{1.66})\ \underbrace{(Mg_{3.09}\ Fe_{2.11}\ Mn_{0.01}\ Ti_{0.18}\ Al_{0.60})}_{5.98}\ (Si_{5.32}\ Al_{2.68})\ O_{20}(OH)_4$$

(+ 0.94 above the octahedral group; − 1.02 above the tetrahedral group)

and it seems likely that this charge is balanced by some Fe^{+++} in the structure. Of those biotites plotting above the line in figure 3.3(a), excess Al^{VI} may in some cases be interpreted as replacing R^{++} in a 2 : 3 ratio (Foster 1962) e.g. biotite 4 specimen 7108:

$$(K_{1.57})\ \underbrace{(Mg_{1.83}\ Fe_{2.78}\ Mn_{0.02}\ Al_{1.20})}_{5.83}\ (Si_{5.58}\ Al_{2.43})\ O_{20}(OH)_4$$

(+ 0.86 above the octahedral group; − 0.86 above the tetrahedral group)

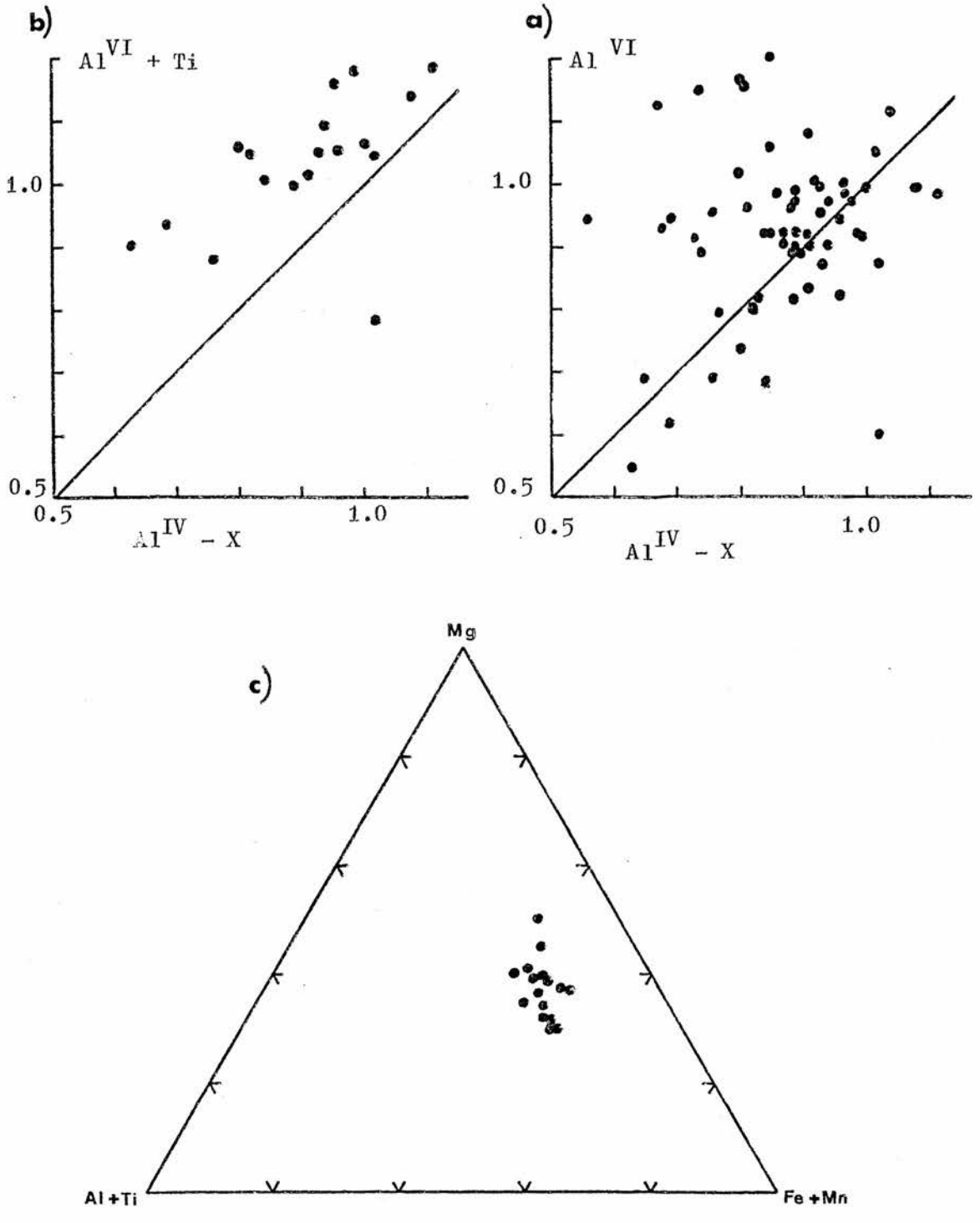

Figure 3.3 : Some features of the mineralogy of biotite from the Dalradian rocks of Buchan.

where 0.34 Al replaces 0.51 R^{++} leaving 0.17 vacant [Y] positions so that transition towards a dioctahedral form is present to a limited extent. The Y - site defficiency, however, never exceeds 0.34 positions. The range of octahedral site occupancy is shown in figure 3.3(c). There is no obvious relationship between number of sites occupied by any ion and metamorphic grade.

3.4. Garnet

Garnet compositions are consistently iron rich, ranging from 65% to 76% of the almandine molecule, (see Appendix III(vi)). With the exception of the garnet from the gedrite bearing rock (specimen 43923) the compositional range is restricted, and occurs largely as a result of variations in the relative proportions of almandine and spessartine molecules.

Almandine	65 - 72%
Pyrope	7 - 9%
Spessartine	15 - 23%
Grossular	4.2- 5%

whilst garnets from 43923 are richer in almandine and pyrope but poorer in spessartine and grossular.

Almandine	74.0 - 76.4
Pyrope	15.6 - 16.1
Spessartine	5.6 - 8.0
Grossular	1.9 - 2.4

All garnets show a close approximation to 6 Si atoms per formula unit, a general relation noted by Deer, Howie and Zussman (1962),

but generally show a slight excess occupancy in the X site and a slight deficiency in the Y site. This is probably due to allocation of Fe^{+++} along with Fe^{++} to the X site instead of to the Y site however since the Y deficiency is small errors introduced by neglecting ferric iron are probably negligible.

No optical zoning is apparent. Probe traverses however, indicate that slight zoning is present in some cases. This is less clearly marked than that reported by other workers (e.g. Atherton and Edmunds 1966, Atherton 1968) but indicates that crystal margins are enriched in iron relative to centres. The situation with regard to MgO and MnO is less clear. Garnet from specimen 7236 shows slight relative marginal enrichment in MgO and depletion in MnO whilst the other garnets show virtually no change.

3.5. Staurolite and Cordierite

Analysis of staurolite and cordierite in the Buchan rocks proved difficult due to the vast numbers of tiny inclusions, generally of quartz in the former, but of virtually any groundmass material in the latter mineral.

Some of the staurolite analyses (Appendix III (v)) have low totals. This is not due to the presence of Zn (e.g. Guidotti 1969) which proved to be just on the limits of detection and though Co and Ni were not analysed it seems unlikely that they would be present in sufficient quantity to explain the difficient totals. The analyses do however recalculate to structural formulae which are comparable with those given in the

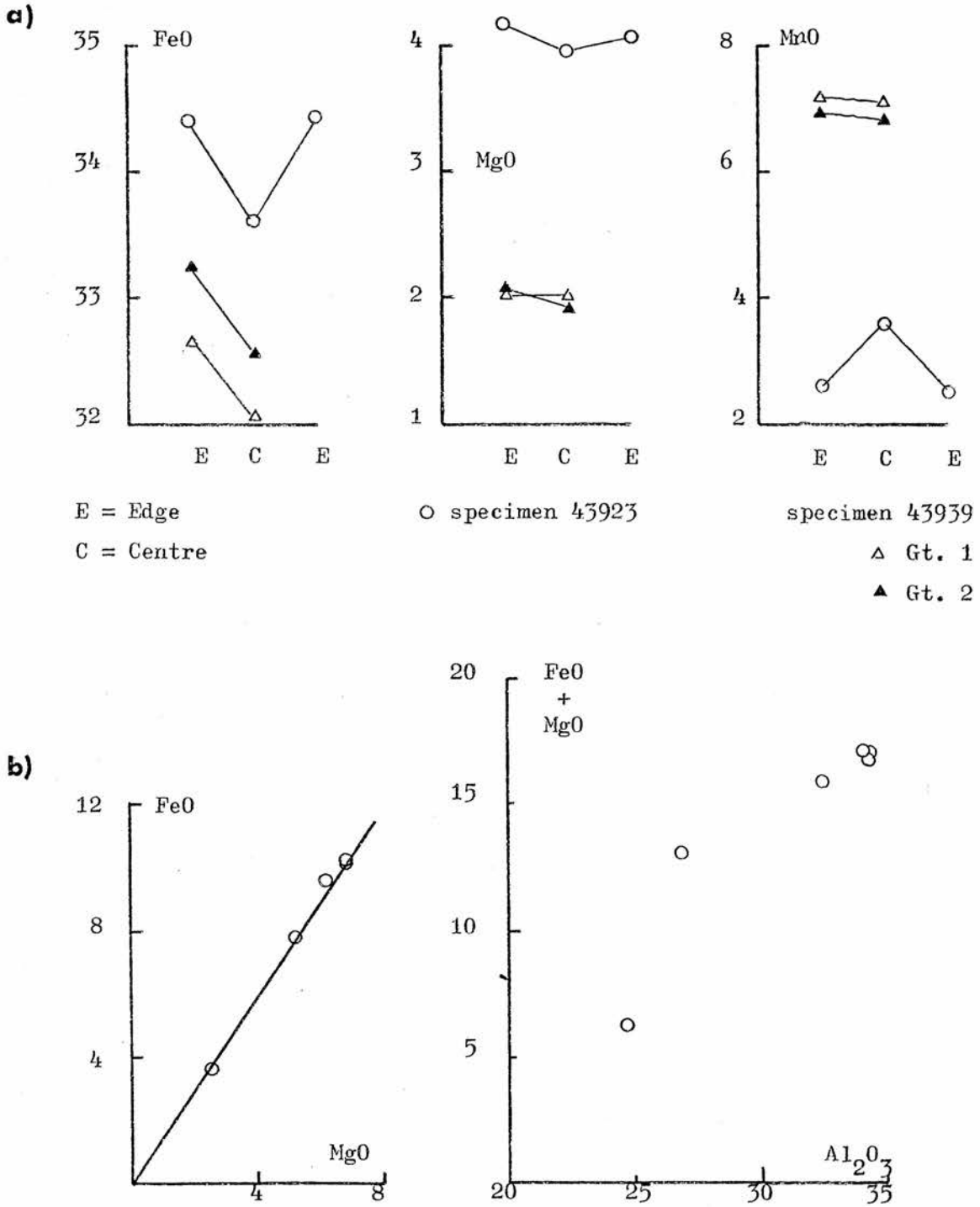

Figure 3.4 : Some features of the mineralogy of a) garnet and b) cordierite from the Dalradian rocks of Buchan.
All plots in wt. %.

literature (e.g. Juurinen 1956; Deer et al 1962; Chinner 1965; Hounslow and Moore 1967). The range of 100 MgO/MgO+FeO+MnO is strictly limited between 14 and 20 whilst 100 MnO/MgO+FeO+MnO may rise to 2.5.

In addition to the inclusion problem, cordierite analysis also proved difficult on account of wide spread partial alteration. Even the freshest porphyroblasts typically show marginal alteration to pinitic material but this may also occur as irregular internal patches. When the pinite is yellow and/or isotropic it may easily be avoided. However analyses indicate that material intermediate between fresh cordierite and pinite also occurs, having all the optical characteristics of normal fresh cordierite. Figure 3.4(b) shows analyses of 'cordierite' and pinite from a single porphyroblast (44029). Pinitisation would appear to proceed with loss of Al and R^{++} but notably does not change the M/FM ratio. This is also true of other specimens and as such the analyses listed in Appendix III (iv) represent those which had the highest measured Al and R^{++} for a rock or porphyroblast. Two analyses of cordierite from specimen 43927 show higher than normal Al content associated with considerable alkali substitution and low R^{++} . These cordierites do not show the excess of X Y ions over the ideal 5 per formula unit which Deer et al (1962) consider typical of alkali rich varieties. The excess of Al outside the six membered rings suggests that some of it may be located in octahedral sites, the charge balance being maintained by introduction of monovalent alkali ions. Cordierite 2

(specimen 43927) gives the following formula:

$$Al_{3.0}\left[(Na,K)_{0.3}\ (Mg,Fe)_{1.4}\ Al_{0.3}\right]\qquad\left[Si_{5.0}\ Al_{1.0}\right]\qquad O_{18}$$

where 0.6 R^{++} ions have been displaced by 0.3 Al and 0.3 R^{+} ions by the replacement of R^{++} = Al R^{+}. However, it seems unlikely that K, Na ions can be accommodated by the octahedral cordierite sites and these are probably located in the large channels parallel to z (Deer et al 1962; Gibbs 1966) presumably leaving some sites unoccupied.

Analysed cordierites show a range of M/FM values between 53 and 72 whilst 100 MnO/MgO+FeO+MnO may rise to 2.0.

CHAPTER 4

Bulk Rock Chemistry

4.1. Introduction

Major element analyses were carried out on thirty three bulk samples; 28 from the Banffshire Coast, 4 from the Ythan Valley and one from Collieston Harbour. The resultant data are tabulated in Appendix II. Mineral assemblages with locality grid references and analytical methods are given in Appendices I and IV respectively.

Two analyses from the Banffshire Coast (Read 1923) and seven from the Ythan Valley (Gribble 1966) are available from the literature.

Several of the analyses listed have poor totals, particularly those from the Macduff slate group. This may be due to components which have not been analysed, for instance carbonaceous material, which is prominent in some rocks, or to low H_2O values associated with poor decomposition of staurolite or reactions producing CO_2 from carbonaceous material.

The accurate determination of FeO proved impossible for many rocks due to considerable amounts of a) staurolite (and garnet) which proved difficult to dissolve b) sulphides and carbonaceous materials which give rise to anomalously high FeO values (Wilson 1955).

Since all rocks contain some sulphide all FeO values determined can be considered at best as only an approximation.

For the sake of comparison in the following text figures the analyses were all recalculated to a standard oxidation ratio where $\frac{100Fe_2O_3}{Fe_2O_3+FeO}$ = 14.78 which was the average of those analyses with the most satisfactory FeO determinations. This is justified on the grounds that very little variation in assemblages of opaque minerals occurs (for more details see Chapter 5 page 119), suggesting that variations in fO_2 were restricted.

4.2. Compositional Range of the Metasediments

A number of lithological types may be recognised on the basis of bulk composition and field relations. Some selected analyses are shown in Table 4.1.

Type I, II, III lithologies

Type I lithologies are typically pelitic having relatively low silica, high alumina and high K_2O/Na_2O ratios, (analyses 1 and 2, Table 4.1). Such lithologies generally occur as distinct beds, seldom greater than two feet thick and presumably represent original clay rich sediments.

Type II lithologies differ in having an excess of soda over potash, reflecting a high plagioclase content, (analyses 4 and 5). They generally occur as the upper portions of graded units. Such rocks must represent immature silty sediments similar to the Moine garnet schists discussed by Butler (1965) though the Buchan

Analysis	1	2	3	4	5	6	7	8	9
Spec. No.	43931	43919	43981	43902	43927	Will. (8)	Snell. (12)	43910	43962
SiO_2	49.67	48.34	69.30	55.45	49.84	49.16	50.39	48.25	50.43
Al_2O_3	27.00	26.77	13.08	23.61	24.67	28.21	26.82	22.00	18.26
FeO	6.94	4.92	6.96	5.53	6.93	10.38	9.13	7.94	11.99
MgO	3.06	2.62	3.03	1.45	4.34	1.84	2.00	2.52	7.46
MnO	0.04	0.04	0.10	0.09	0.06	0.19	0.14	0.10	0.32
CaO	0.50	1.11	0.76	3.20	1.48	1.88	1.80	7.82	1.73
Na_2O	0.96	0.84	0.94	4.58	5.17	3.00	3.22	0.65	5.78
K_2O	6.08	6.87	2.97	1.44	3.23	1.83	2.84	2.49	0.25
TiO_2	1.04	1.12	0.49	1.03	0.84	1.01	0.18	0.84	1.58
P_2O_5	0.06	0.58	nd	0.05	0.04	0.47	na	6.07	0.14
H_2O^+	4.25	4.88	2.49	2.38	2.34	2.76	2.77	1.68	0.96
Total	99.60	98.09	100.12	98.81	98.94	100.73	99.29	100.36	98.91
Lithological Group	I	I	Semi Pelite	II	II	II	II	III	gedrite rock

nd - not detected na - not analysed

analyses 6 and 7 from Williamson (1953) and Snelling (1957)

Table 4.1 : Selected analyses of Dalradian metasediments

Figure 4.1 : Ca-Na-K and AKF diagrams showing the range of bulk rock compositions in Buchan

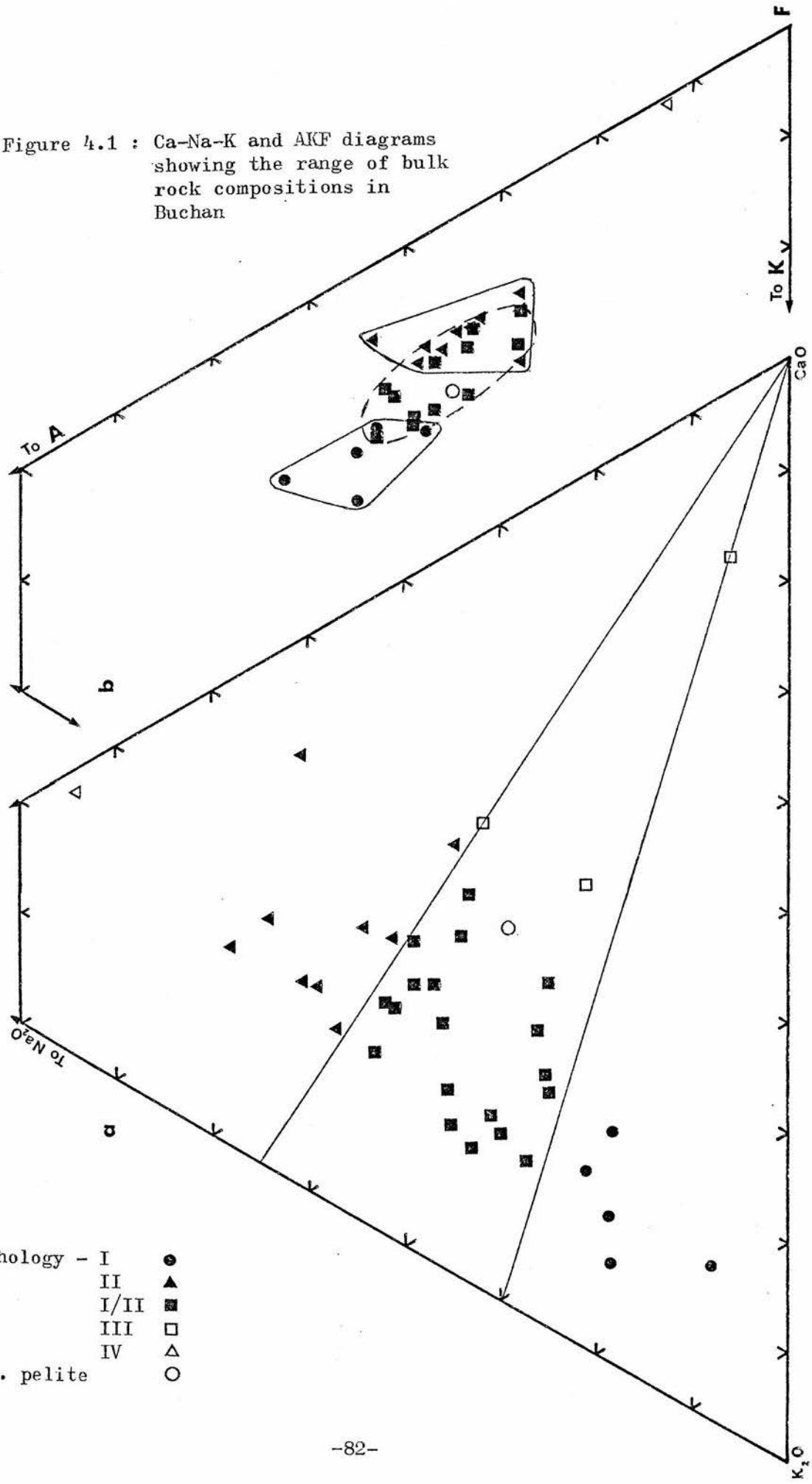

Lithology - I ●
II ▲
I/II ■
III □
IV △
Ave. pelite ○

rocks must have been either originally more argillaceous or better graded, being richer in alumina and poorer in silica. Type II lithologies have been previously reported from the Dalradian of the Southern Highlands (e.g. Williamson 1953, Snelling 1957, Mather 1970) - see analyses 6 and 7 Table 4.1.

The analyses as a whole show a gradation of K_2O/Na_2O ratios and no distinct compositional boundaries have been taken between intermediate types and type I and type II lithologies of $Na_2O/Na_2O + K_2O$ equal to 0.3 and 0.55 respectively, see figure 4.1(a).

In figure 4.1(b) these rocks have been plotted in an AKF diagram. Type II lithologies plot close to the A-F side showing no overlap with type I whilst intermediate lithologies fill up the area between and overlap with each.

There is no obvious correlation between $Na_2O/Na_2O + K_2O$ and $MgO/MgO + FeO$ ratios of the rocks though there is a suggestion that type II lithologies show a wider range of MgO/MgO+FeO than type I lithologies (Figure 4.2(a) and Table 4.3).

Bulk compositions related to the above types, with similar molecular ratios of elements, except for a generally higher silica content, are found (e.g. analysis 3, Table 4.1). These indicate dilution of types I and II lithologies with quartz, and merge with rocks described as semi-pelites in the field. This effect

Specimen	Zone	Assemblage (+ ms + qz)	molecular proportions			
			Al_2O_3- (total alks + CaO)	K_2O	FeO+MgO+MuO	$\frac{100MgO}{FeO+MgO+MuO}$
43860	Biotite	chl.-biot.	41.1	13.2	45.7	41.5
43867	Cordierite	cord.-biot. (1st spots)	40.9	13.6	45.5	42.0
43876	Andalusite	andal.-cord.-biot.	39.1	14.7	46.2	39.1
43904	Staurolite	staur.-andal.-biot.	40.6	13.4	46.0	41.6

Table 4.2 : Comparison of the bulk compositions of selected metasediments from different grades on the Banffshire coast.

	$\frac{100MgO}{MgO+FeO}$ (range)	No. of specimens
(a) Lithology Type		
Type I	43.8 - 52.7	5
Type I/II	37.6 - 50.0	20
Type II	35.1 - 55.0	8
Type III	38.6 - 48.0	6
(b) Stratigraphic Group		
Macduff Slates	38.4 - 42.0	5
Fyvie Schists	38.9 - 49.3	10
Boyndie Bay Group	(35.1) 38.3 - 47.6	17
Whitehills Group	40.6 - 55.0	9
(c) Index Mineral Zone		
Biotite	38.4 - 42.0	5
Cordierite	37.6 - 47.3	3
Andalusite	38.3 - 46.3	6
Staurolite	(35.1) 38.6 - 55.0	22

Table 4.3 : Ranges of iron-magnesium ratios in relation to lithology, stratigraphic level and metamorphic grade.

is illustrated in figure 4.5(a), which shows a well defined trend of decreasing alumina content as silica increases. Figure 4.5(b) shows silica in relation to the ratio $Na_2O/Na_2O + K_2O$.

In distinction to the above, type III lithologies occur as rare dark horizons, 2 to 3 inches thick. They are essentially pelitic, but have high CaO and P_2O_5 values reflecting a high apatite content (analysis 8, Table 4.1). These rocks must represent originally phosphoritic shales. The rocks 43912 and 43913 are typical of varieties which are transitional between type I/II and type III lithologies. During metamorphism these rocks behave as normal pelites except in their unusually high apatite content.

A comparison of the bulk compositions discussed above with the average pelite of Shaw (1956) indicates that the Buchan rocks are less siliceous and more aluminous. The only analysed Buchan rock which is more siliceous than Shaw's average is the semi-pelite specimen 43981 (analysis 3, Table 4.1) so that the former plots near the top of the trend shown in figure 4.5(a). This relation in fact holds true with respect to Scottish Dalradian pelites and meta-greywacke siltstones as a whole (Williamson 1953; Snelling 1957; Atherton 1968; Mather 1970). In other respects the average pelite represents a reasonable mean for the Buchan rocks, generally plotting in or close to the field of intermediate type I/II lithologies.

The composition of the Buchan rocks is compared with a sample of

Highland border rocks (Atherton and Brotherton 1974) in figures 4.2 and 4.3. Their data show a well defined compositional field for 43 out of 44 analyses, the 44th showing high alumina values and plotting apart from the rest. All the Buchan analyses fall within the general compositional field of Atherton and Brotherton (1974) in figures 4.2(b), (c) and 4.3 and show some high alumina types which are transitional towards the high alumina pelite of those workers. Figure 4.2(a) which is an a f m plot, suggests that the Buchan rocks may be biased towards slightly more magnesian compositions than those from the Highland Border, but this could be due to differences in oxidation ratio (see section 4.1).

Also shown in figure 4.2 are the limits of potential chloritoid bearing compositions suggested by Hoschek (1967) and which have been shown to be applicable to the Highland Border rocks by Atherton and Brotherton (1974). None of the Buchan rock compositions falls conclusively in the potential chloritoid region of all three diagrams (figure 4.2(a), (b) and (c)), however those which may be marginally suited to chloritoid production under suitable conditions are identified by the inclusion of specimen numbers. These rocks have also been plotted in the AKF diagram (figure 4.3). In view of the lack of conclusive evidence that potential chloritoid compositions are present, it should be stressed that the absence of chloritoid assemblages in Buchan could be due to a lack of these correct compositions rather than to any controlling influence of intensive variables.

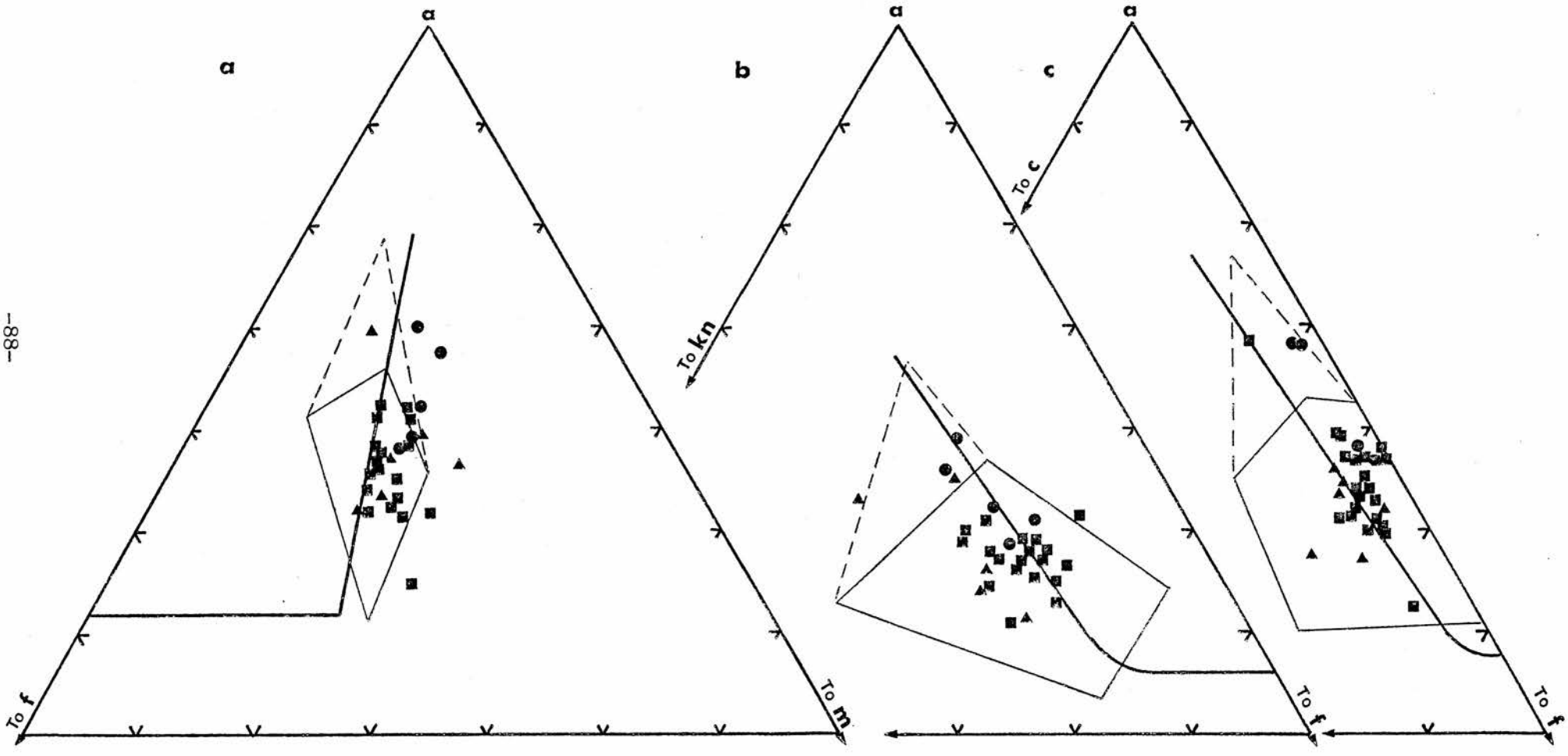

Figure 4.2 : Comparison of bulk compositions present in Buchan with those of Atherton and Brotherton (1974) and the compositional limites of chloritoid (Hoscheck 1967). (heavy lines)

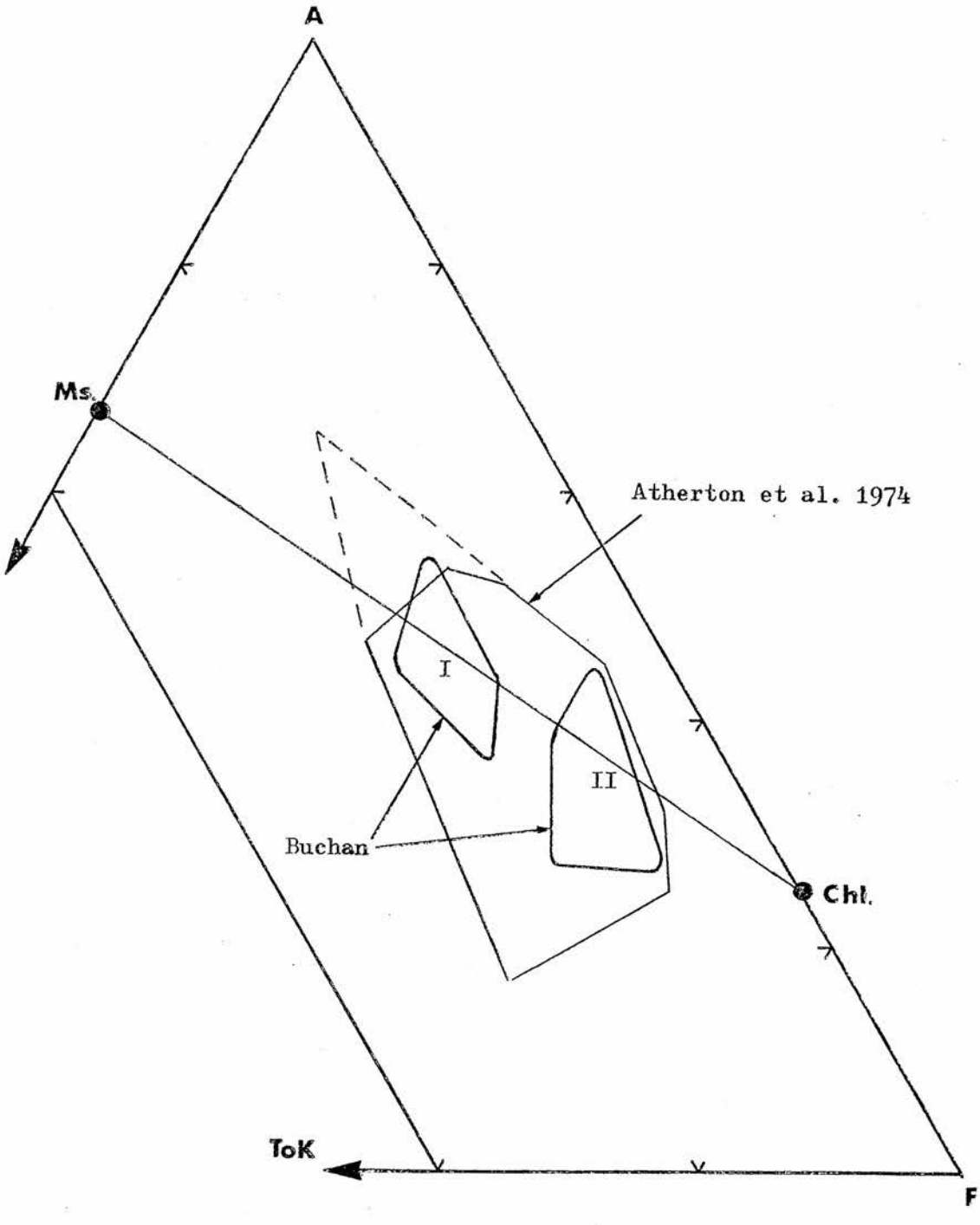

Figure 4.3 : AKF diagram comparing bulk compositions present in Buchan with those of Atherton and Brotherton (1974).

Analysed rocks from the staurolite zone have been plotted in figure 4.4. There is no obvious general compositional relationship between staurolite bearing and staurolite free varieties. Staurolite bearing types straddle the compositional boundary proposed by Hoschek (1967) but appear to be biased towards less aluminous bulk compositions.

The range of 100MgO/MgO+FeO (M/FM) ratios in the Buchan rocks is generally restricted between 37.5 and 50.0 so that higher and lower values are rare (figure 4.5(c)). These more extreme values tend to be restricted to those lithologies which are also more extreme with respect to Na_2O/Na_2O+K_2O ratio. Type II lithologies show the widest range of M/FM values accounting for both the highest and lowest recorded values whilst type I lithologies show a relatively restricted range which is biased towards high values (Table 4.3(a), figure 4.5(c)).

Since the lithological types appear to be unequally distributed between stratigraphic groups there is a resultant variation in compositional range at different stratigraphic levels and concentration of the more extreme types, I and II at lower stratigraphic levels gives rise to a wider range here, particularly with respect to alumina and potash (see figure 4.1(b)). Ranges of M/FM are given in Table 4.3 (b).

It is notable that the two specimens 43902 and 43927 which have

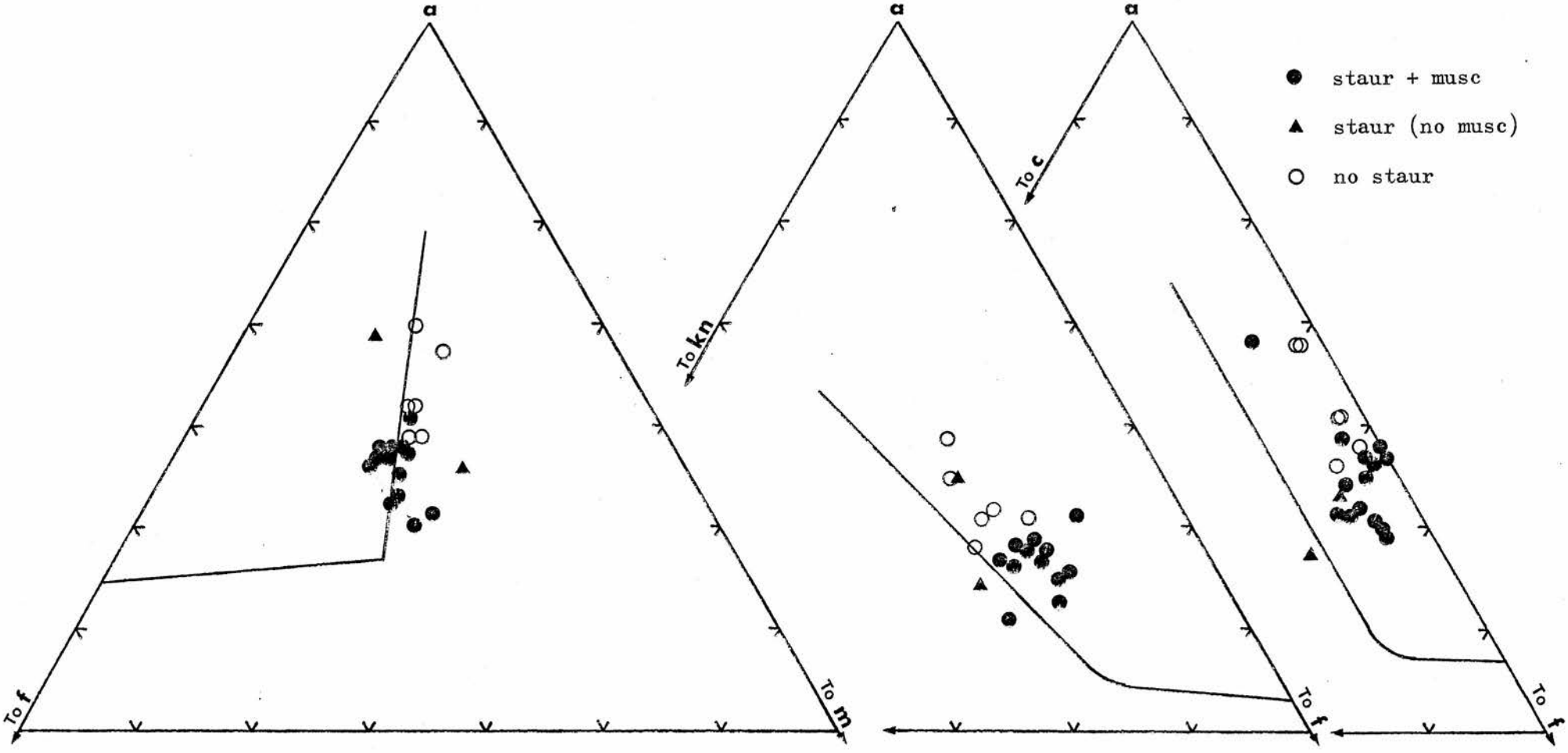

Figure 4.4 : Staurolite zone bulk compositions in relation to the compositional stability limits of staurolite as suggested by Hoscheck (1967).

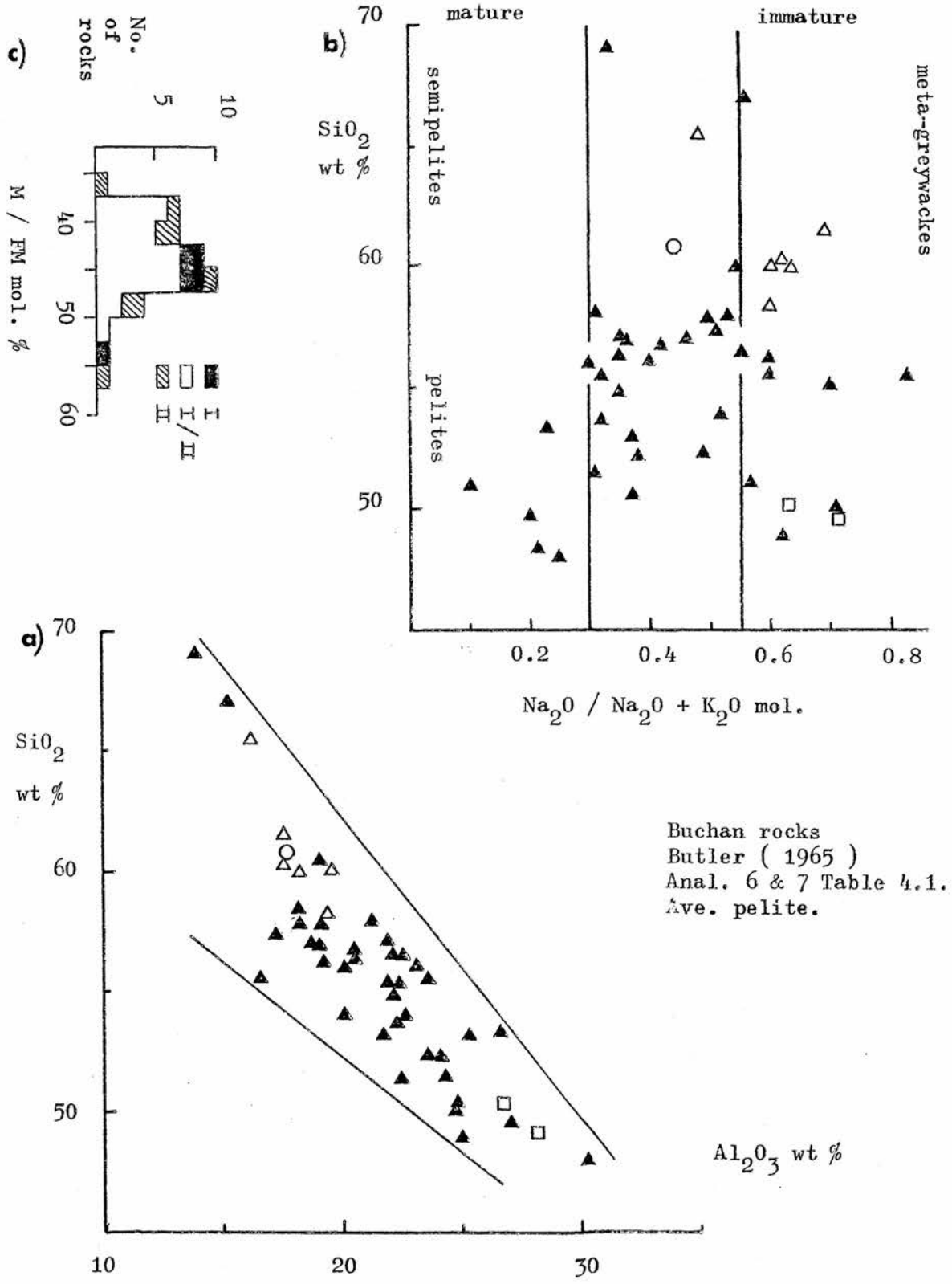

Figure 4.5 : Plots of (a) Al_2O_3 vs SiO_2
(b) Na_2O/Na_2O+K_2O vs SiO_2 and
(c) histogram of M/FM values for bulk rock analyses from Buchan.

the lowest (35.1) and highest (55.0) M/FM values respectively both carry all three of the minerals staurolite, andalusite and cordierite and andalusite commonly occurs in rocks with M/FM < 50.0. As a result the limiting value of 54.0 proposed by Atherton and Brotherton (1972, 1973) for kyanite bearing rocks obviously does not apply equally to andalusite. The basis for this limiting value has been criticised by Harte (1973) however it is in reasonable agreement with estimated mineral compositions for the assemblage Al_2SiO_5- staur-biot-musc-qz. advanced in Chapter 6 page 207 (see figure 6.13).

Despite the lack of any general compositional relationship between staurolite bearing and staurolite free rocks of the staurolite zone, at any one locality cordierite bearing rocks have M/FM greater than staurolite bearing rocks which lack cordierite with the exception of one specimen (43902) as follows:

	Staur Rocks (No Cord.)	Cord bearing Rocks
Boyndie Bay	38.6 - 46.4	46.6 - 47.6
Whitehills	42.9 - 50.0	52.7
Whyntie Head	40.6	55.0

These cordierite bearing rocks appear to show a trend of increasing M/FM upgrade, but they are rare at high grade and the number of analyses are consequently restricted.

4.3 Compositional changes during metamorphism

As mentioned previously there is a tendency for the rocks to show more compositional variation as one moves to lower stratigraphical levels. Since the metamorphic grade also increases stratigraphically downwards, the higher grade rocks will tend to show more

compositional variation than the lower grade rocks. This is more likely to be due to original compositional differences built in during sedimentation than to any large scale metasomatic or differentiation processes. It might still be argued that some of the mineralogical differences seen in an upgrade traverse could be due to changes in bulk composition rather than external P,T, etc. conditions. It can, however, be shown (Table 4.2) that rocks of virtually identical bulk chemistry occur in each zone and there register different mineral assemblages. The range of M/FM ratios in each zone is given in Table 4.3. Although these ranges differ from zone to zone, this is mainly due to the presence or absence of magnesian varieties, the most iron rich varieties remaining fairly constant at around M/FM = 38.0, (again with the exception of the one rock 43902, shown in parenthesis). It will be shown in Chapters 5 and 6 that it is this most iron rich available bulk composition which controls the position of the isograds.

Many workers have recognised progressive changes in both oxidation ratio and water content during metamorphism (e.g. Shaw 1956). Because of the problems of accurate FeO determination, it is impossible to draw any conclusion with respect to oxidation ratio for the Buchan rocks. Average water contents calculated for three grades gave the following:

Biotite Zone	3.44	(3.44)
Cordierite / Andalusite Zones	2.36	(2.74)
Staurolite Zone	3.38	(3.41)

which suggests no systematic decrease with increasing grade. The variation at any one grade is, however, greater than the difference between the averages. This may be due to analytical or statistical unreliability, though duplicate analyses were apparently consistant, or anomalously high water contents at high grade may be due to some development of late chlorite. At the same time, water content seems to be partially related to lithology, type I having consistently higher values (mica rich) than type II (mica poor) the ranges of values showing no overlap as follows:

Type I	3.5 - 5.6
Type II	1.5 - 3.5

Averages calculated on intermediate type I/II lithologies only do however give a similar result (values in parenthesis above).

4.4. Type IV lithologies

Lithological type IV is distinguished on thin section and field criteria as that of the ortho-amphibole bearing rocks, which occur in distinct beds, continuous along the strike despite being only 2 to 3 inches thick, (see Chapter 2, page 62). A bulk analysis of one specimen of this type (Table 4.1, anal. 9), shows the high Fe, Mg and Na associated with low K and Ca which the mode suggests. In the field these rocks show all the characteristics of original sediments. Such rocks have been described from many localities (Eskola 1914, Tilley 1937, Lal 1969, Joplin 1968) and many theories have been advanced for their origin.

a) Metasomatism of aluminous sediments or volcanics generally with introduction of Mg or Mg + Fe^{++}
(e.g. Eskola 1914, Seki and Yamasaki 1957).

b) Metamorphic differentiation in the cores of small folds in argillaceous sediments.
(e.g. Tuominen and Mikkola 1950).

c) Metasomatism of basic igneous rocks.
(e.g. Tilley 1937, Bugge 1943).

d) Regional metamorphism of ultra basic rocks.
(e.g. Anderson 1931, Kulp and Brobst 1954).

e) Regional metamorphism of impure (dolomitic?) argillaceous sediments.
(e.g. Prider 1944, Rao 1974).

f) Metamorphism of altered basic lavas.
(e.g. Vallance 1967).

g) Partial melting of pelitic rocks with subsequent removal of the melt leaving an Fe, Mg rich residue.
(e.g. Grant 1968).

In Buchan many of these theories may be discounted. There is no evidence for partial melting or major metasomatism within the bedded sequences and it would be hard to explain how these processes could be limited to single beds without having any noticeable effect on adjacent beds. Similarly there is no evidence of structurally (or

mechanically) controlled metamorphic differentiation since the ortho-amphibole bearing unit shows no particular relation to the structures. Although the field relations do not support the presence of magma, these units could represent mafic tuffs or altered mafic tuffs. However, in view of the similarity of some aspects of type IV compositions and type II compositions (principally with respect of alkalies), such rocks could possibly represent extremely immature sediments in which some ferromagnesian phase still remained partially unaltered or which were rich in chlorite. This suggestion may be strengthened by figures 4.1 (a) and (b) in which specimen 43962 plots on the extreme end of the trend shown by lithologies I and II.

CHAPTER 5

Mineral Compatibility and Solid Solution Variations in Relation to Grade

The purpose of this chapter is to analyse the relations of mineral assemblages found at each grade and to investigate their dependence on bulk chemical composition and conditions of metamorphism.

5.1. The Biotite Zone

The location and extent of this zone and the petrography of the rocks occurring within it have been described in chapter 2 sections 1 and 2 respectively.

The zone is symmetrical about a low grade axis which will be referred to as the lower biotite zone where slates lacking biotite may occur.

The assemblages occurring in this zone are shown below whilst their distribution may be read from Map 3 (page 99).

B.1 white mica - chlorite

B.2 white mica - chlorite - biotite

B.3 white mica - biotite

MAP 3

The distribution of Biotite zone assemblages in the Banff-Fyvie area N.E. Scotland.

Sillimanite isograds Banff-Huntly area after Ashworth 1972.

Cordierite isograds slightly modified after sheets 86,87, 96,97 (1" series) Geological Survey of Scotland.

▼ assemblage B 1

▲ assemblage B 2

△ assemblage B 3

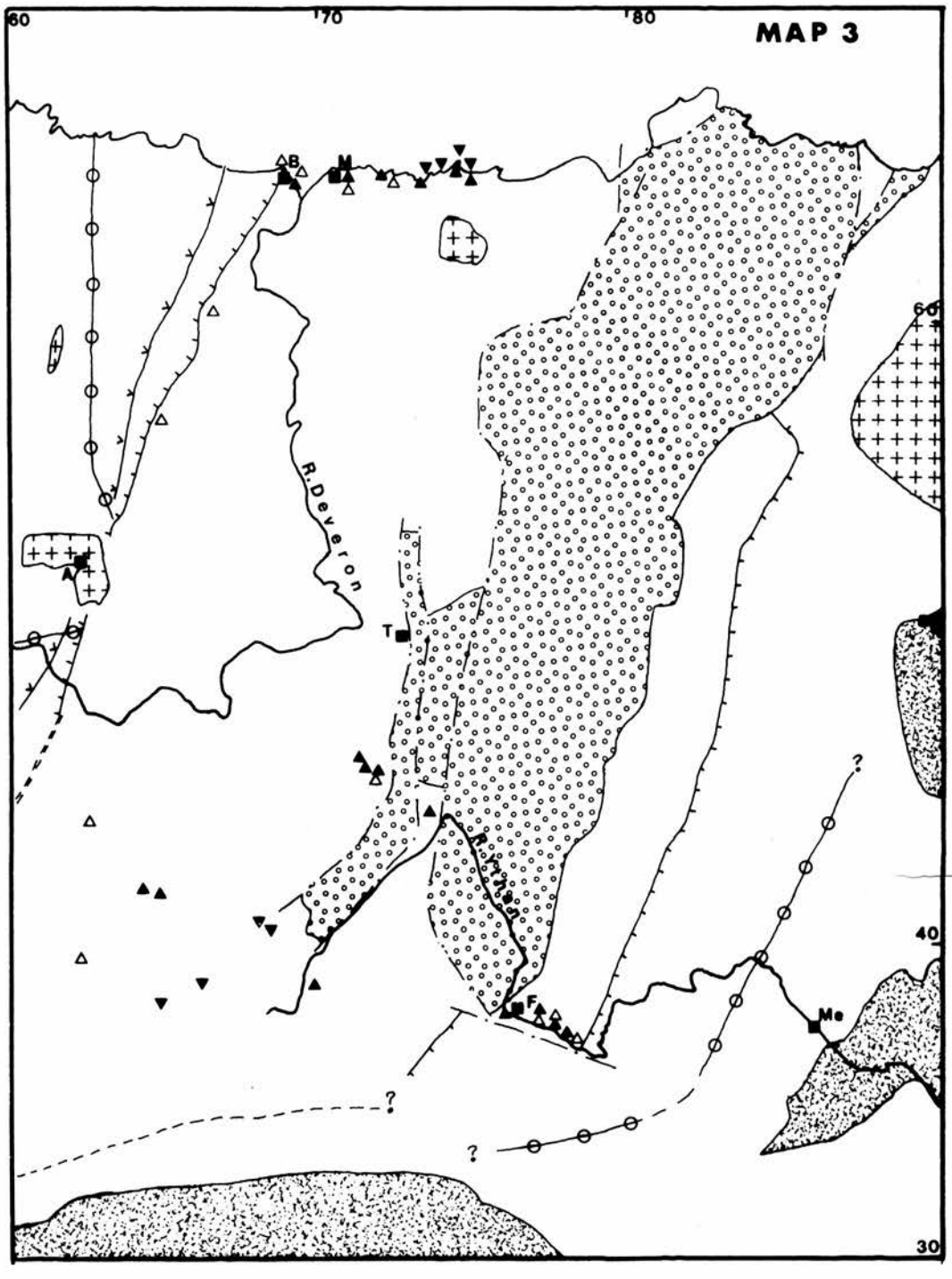

Old Red Sandstone

Dalradian

Gabbro

Granite

Cordierite

Staurolite

Sillimanite

A considerable amount of data and discussion is available in the literature with regard to chlorite and biotite zone minerals (e.g. Lambert 1959; McNamara 1965; Velde 1965,1967; Butler 1967; Brown 1967,1968; Guiddotti 1969; Mather 1970; Cipriani et al 1971; Ramsay 1973; Ono 1969a,b).

Most authors have shown that white micas under such conditions are phengitic in composition and tend to show a decrease in phengite content upgrade (e.g. Lambert 1959, Mather 1970, Ramsay 1973).

The composition of white micas from Banffshire has already been mentioned in chapter 3. Figure 3.2. shows that there is a tendency for phengite content to decrease upgrade reaching essentially muscovite compositions in the andalusite zone. Within the biotite zone the limited data indicates a drop from $Celadonite_{.19}$ at the lower/upper biotite zone boundary, to $Celadonite_{.12}$ in its higher grade parts near the cordierite isograd.

Such a result is in agreement with the experimental work of Velde (1965) which suggests that celadonite solid solution in muscovite is limited by increasing temperatures. Velde also suggests that a similar effect might also be found as a result of decreasing pressure.

Figure 5.1(a) shows fields of biotite zone white mica compositions plotted in part of a S A F diagram. It is notable that the biotite zone white micas from Barrovian sequences (Lambert 1959, Butler 1967,

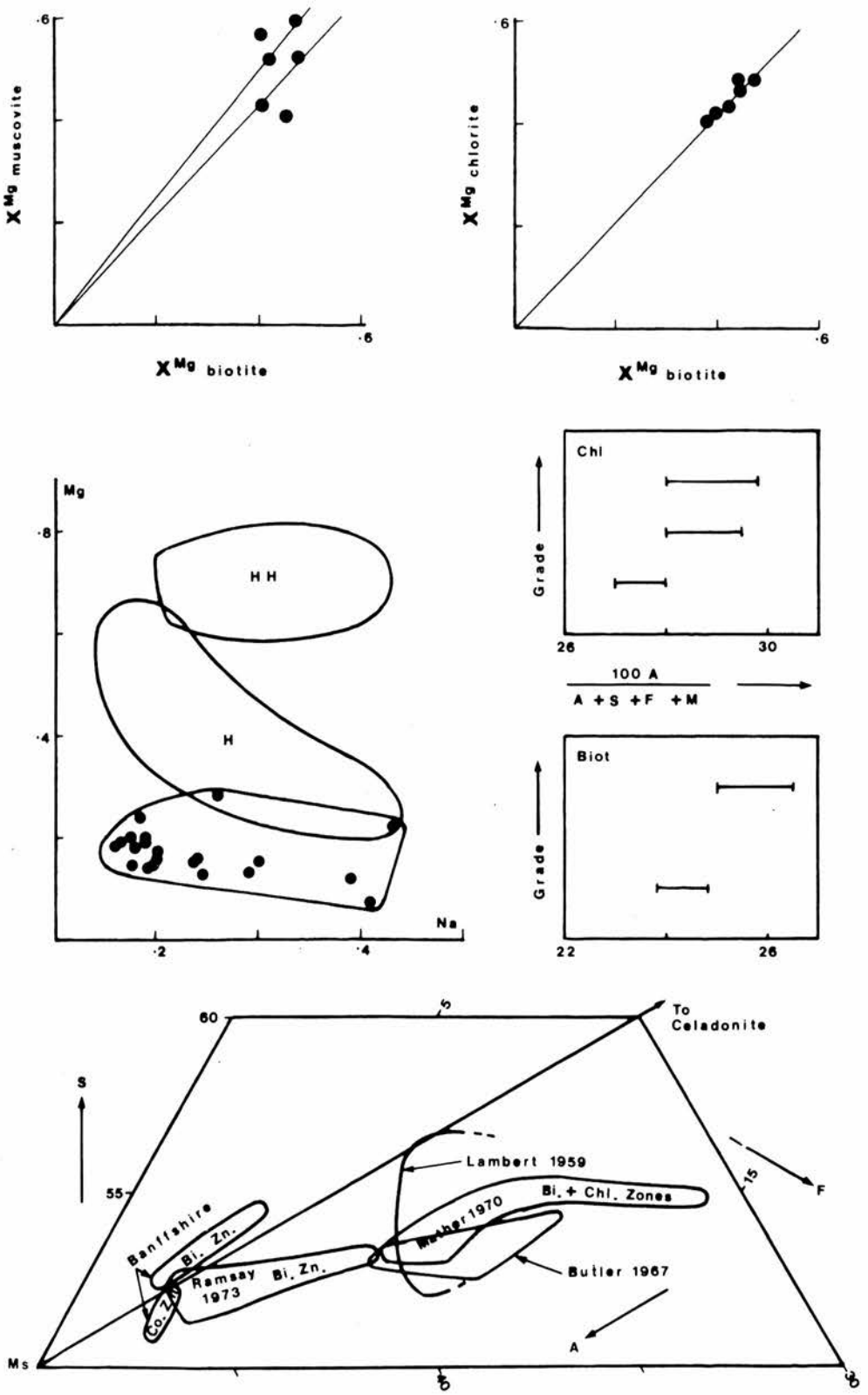

Figure 5.1: (a) Comparison of biotite + chlorite zone phengites from different terrains in part of a SiO_2 - Al_2O_3 - FeO +MgO plot.(b) relationship between number of Mg and Na cations per formula unit in phengites (after Cipriani et.al. 1971);(c)&(d) tentative relationship between Al max. in chlorite and biotite and grade in the biotite zone (Banffshire coast); (e) & (f) graphs of Fe and Mg distribution between muscovite and biotite (e) and chlorite and biotite (f).

Mather 1970) are distinctly more phengite rich than those from similar grade in low pressure (cordierite producing) sequences (Ramsay 1973, this study).

Cipriani et al (1971) suggested that a diagram showing Atom per cent Mg plotted against Na could be used to discriminate between white micas formed at different pressures. Although they were able to give good definition to high and intermediate pressure fields data from low pressure facies series were restricted at that time. In Figure 5.1(b) fields of high and intermediate pressure white micas have been taken from figure 3 of Cipriani et al (1971) whilst the field of low pressure white micas has been constructed using data from Cipriani et al (1971) Ramsay (1973) Ono (1969) and this study. The diagram shows a well defined field for low pressure white micas at low Mg content and only a small overlap with the field for intermediate pressures. The value of this diagram is perhaps reduced if the data of Mather (1970) are considered since four of his five phengite analyses have anomalously low Mg contents (for a Barrovian Sequence)and would suggest a much larger overlap of the two fields.

Compositional trends in biotite and chlorite are not so clearly related to grade. Ramsay (1973) noted a marginal increase in Mg/Fe ratio of chlorite and metagreywacke biotite when approaching the cordierite isograd, whilst Mg/Fe of pelite biotites were independent of grade. The present study shows no relation of Mg/Fe ratio of either mineral to grade. Ramsay (1973) also shows

a tendency towards higher Al content in biotite with increase in grade. Figure 5.1(c) and (d) show Al content of biotite and chlorite from three grades in the biotite zone. Notably there is a considerable range at each grade and within individual specimens. This range is probably due to minor bulk composition variations within the rock. However there does seem to be a general tendency for the maximum Al content at each grade to increase, both in biotite and chlorite.

Distribution of Fe and Mg between phases

Table 5.1 shows $X^{Mg} = \frac{MgO}{MgO+FeO}$ of muscovite, biotite and primary chlorite from rocks of the biotite and cordierite zones. This shows that the relationship

$$X^{Mg}_{Musc} \qquad X^{Mg}_{Chlorite} \qquad X^{Mg}_{biotite}$$

prevails. This upholds the suggestions of Velde (1965) and Butler (1967) that Mg is distributed in favour of muscovite rather than biotite and of Albee (1965b) that Mg is distributed in favour of chlorite rather than biotite.

Distribution graphs are shown in figure 5.1(e) and (f) for muscovite versus biotite and chlorite versus biotite respectively. In figure 5.1 (f) the data points conform closely to a line of constant distribution although they represent a fairly wide range of grade. Thus $K_D^{Fe-Mg}{}_{Chl-Biot}$ shows no obvious relation to grade. Neither does the distribution coefficient show any obvious relation to pressure since data from Barrovian sequences plot close to the same line (Mather 1970, McNamara 1965).

Specimen Numbers	43852	43857	43858	43860	43865	43867	43870
Muscovite	0.52	0.60	n.d.	n.d.	0.52	0.43	n.d.
Chlorite	0.44	0.49	0.49	0.41	n.p.	n.p.	0.42-0.43
Biotite	0.41-0.43	0.47	0.43-0.45	0.37-0.38	0.47-0.48	0.40-0.41	0.39-0.40
Zone	Biotite				Cordierite		

Table 5.1 : Comparison of Mg/Mg+Fe (cations) for muscovite, chlorite and biotite from the biotite and cordierite zones.

In Figure 5.1 (e) the data points show more scatter and there is a slight indication that $K_D^{Fe-Mg}{}_{biot-musc}$ decreases from the biotite zone towards the andalusite zone. Comparison with the data of Lambert (1959) Butler (1967) and Mather (1970) indicates a similar scatter for higher pressure sequences.

Relation of Mineral Composition to Bulk Composition and Grade

Since biotite zone assemblages involve a relatively small number of phases it is not surprising that mineral compositions vary even at a single locality. Reference has already been made to variations in Al_2O_3 content of the minerals but a considerable range of MgO/MgO+FeO ratios is also present. Ramsay (1973) notes a relation between these two compositional features and suggests that more iron rich chlorites and biotites tend also to be more aluminous (c f fig. 4.1 Ramsay 1973).

Alumina variation in chlorite and biotite from the present study shows no definite correlation with MgO/MgO+FeO ratio, although there is a tendency for the minimum Al content of biotites to increase at more iron rich compositions, and for the Al content of chlorite to be at its lowest at $0.45\ Mg/R^{+2}$.

Since MgO/MgO+FeO variation occurs it appears that an AKF diagram is insufficient to represent assemblages fully. The simplest system required to represent quartz bearing rocks in the biotite zone is Al_2O_3-FeO-MgO-K_2O assuming that other variables eg pH_2O are held constant. The assemblage white mica

chlorite - biotite is trivariant in this system and would be represented by a volume filled with subparallel three phase tie planes so that variations in Mg/Fe ratio of the bulk rock would induce similar variations in the mineral phases. At the same time other factors may complicate the issue. For example, biotite porphs and/or chlorite lenses may be sparsely distributed through the rock. In such a case equilibrium may not have been fully achieved or may have been achieved only on a local scale, and some biotite or chlorite grains may be in equilibrium only with white mica. These two phase assemblages would have a variance of 4 and would allow two compositional variables at fixed grade.

Figure 5.2(a) is an AKF diagram showing the most aluminous biotite and chlorite occurring at the boundary between the lower and upper biotite zones (specimen 43852). Also plotted are bulk rock analyses from the following:

43849 -	lower biotite zone	assemblage B1
43852 -	lower/upper biotite zone boundary	assemblage B2
43860 -	upper biotite zone	assemblage B2

The difference in the bulk compositions is small. Specimen 43852 falls within the triangle phengite-chlorite-biotite, formed from analyses of its constituent minerals, as would be expected. The lower grade specimen 43849 also falls within this triangle. This specimen does not carry biotite which suggests that the

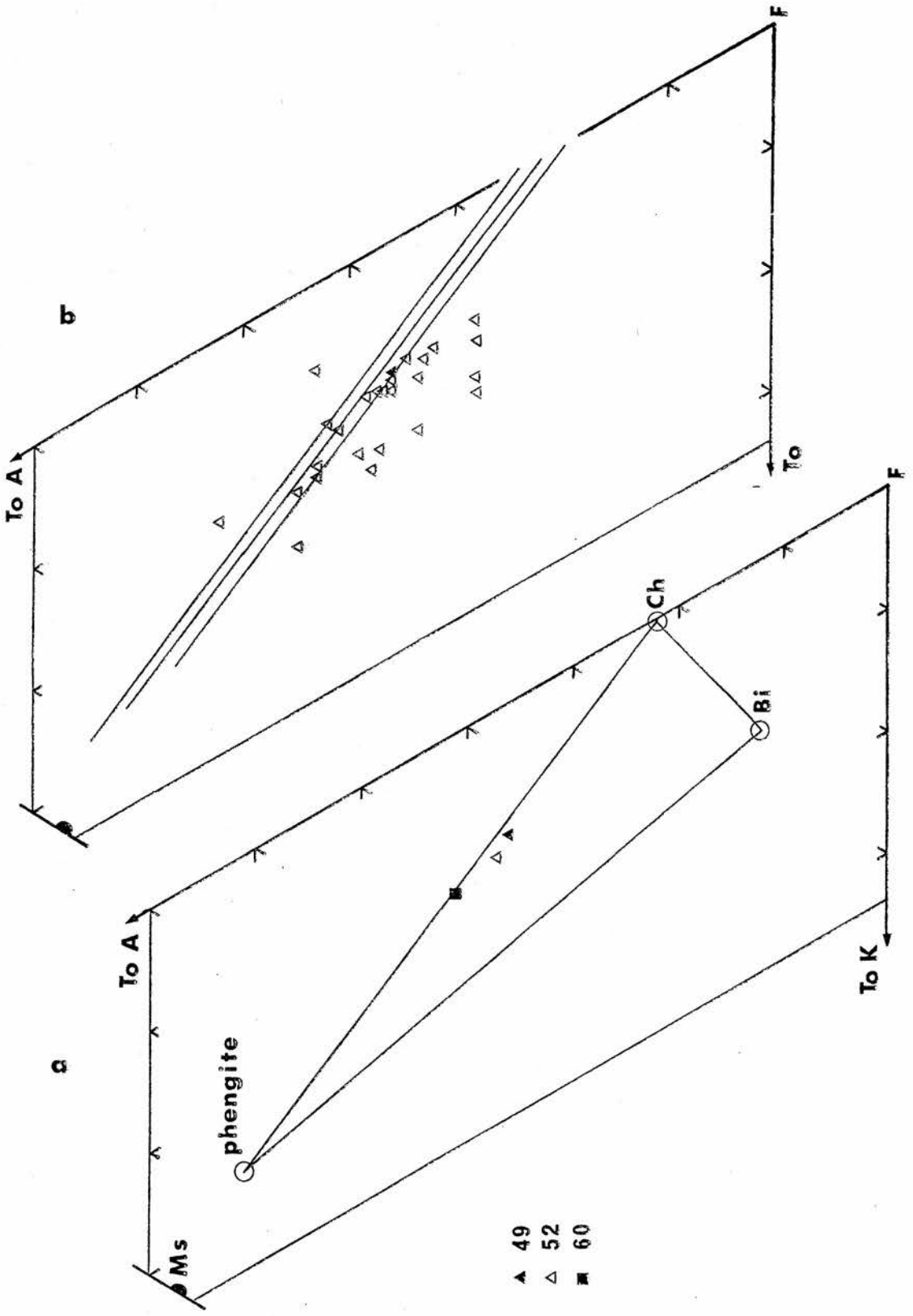

Figure 5.2 : Relationship between bulk composition and potential biotite zone mineral assemblages on the Banffshire Coast.

relevant phengite-chlorite tie line in the three phase assemblage must lie to the alumina poor side of the bulk composition in the lower biotite zone. On the other hand the bulk composition of specimen 43860 from the upper biotite zone plots on the join phengite-chlorite suggesting little or no biotite. This specimen is fairly rich in biotite implying that at this grade the relevant phengite-chlorite tie line in the three phase assemblage must lie to the alumina rich side of the bulk composition.

This information along with data on mineral composition variation with grade (i.e. decrease in phengite content of white mica and increasing maximum Al content of chlorite and biotite) is good evidence to suggest that movement of the white mica-chlorite-biotite stability field controls systematic assemblage changes with grade. (c.f.Mather 1970).

Figure 5.2(b) shows the relationship of the white mica-chlorite-biotite stability field to the range of bulk composition found in the area. The chemical data, though limited, would suggest a slight expansion of the white mica-chlorite-biotite field upgrade since white mica compositions change more rapdily than either biotite or chlorite. However the main control is exercised by the position of the white mica-chlorite edge of this stability field. For grades within the lower biotite zone one third of the bulk composition data points lie above this tie line so that the likelihood of finding the assemblage white mica-chlorite (B1) is high. By the time the lower/upper biotite zone boundary is reached only one eighth of the bulk composition data points lie above the tie line and occurrence of the assemblage B1 is consequently

reduced. By the middle of the upper biotite zone only two points remain above the white mica-chlorite tie line, both of which represent rare bulk compositions.

The occurrence of assemblage B1 will thus become increasingly limited upgrade through the biotite zone although it remains as a potential assemblage throughout.

It is notable from Figure 5.2(b) that the compositional changes referred to above make virtually no change in the position of the white mica-biotite edge of the three phase assemblage. It follows that observed compositional changes should not affect the occurrence of assemblage B3, which is a potential assemblage at all grades in the biotite zone for rocks with higher K/AKF. The widespread occurrence of assemblage B3 immediately below the cordierite isograd is thus more reasonably attributable to the presence of corresponding bulk compositions than to movement of the white mica-chlorite-biotite field. Although no rocks from this locality have been analysed they are obviously more siliceous in the field and it follows from Figure 4.5a that they are correspondingly less aluminous.

Mather (1970) has indicated the presence of the assemblages chlorite-biotite-K-feldspar and chlorite-white mica-K-feldspar in the chlorite zone of Barrows sequence. These assemblages have not been recorded in the Buchan area and the presence of a stable biotite-white mica tie line even in the lowest grade part of the

biotite zone suggests that they are not stable at any stage in the metamorphic sequence.

5.2. The Cordierite Zone

The location and extent of this zone and the petrography of the rocks occurring within it are described in Chapter 2 section 1 and sections 3 and 5 respectively.

Exposure is virtually non existant over most of its outcrop with the exception of the Banffshire Coast (Map 4) and the Valley of the River Ythan (Map 5).

Its lower boundary is the cordierite isograd although it must be emphasised that no fresh cordierite is found here, its original presence being inferred from the presence of 'spots' (Chapter 2 section 5(a)). This boundary as shown on Maps 3 and 4 is that mapped by the Geological survey (Wilson 1882, Read 1923) as the boundary between the Macduff Slates and the Boyndie Bay Group (Map 4) or Fyvie Schists (Map 5). All existing exposures are in agreement with their boundary but many exposures available during their primary mapping have since been destroyed.

On the Banffshire coast the following primary mineral assemblages occur:-

white mica-biotite-'cordierite'-chlorite	C1
white mica-biotite-'cordierite'	C2
white mica-biotite	C3

Assemblage C.2 is the most abundant, whilst assemblage C.3 which is common close to the isograd becomes rare further upgrade. Assemblage C.1. is very rare (2 specimens) and is the only one which does not occur in the Ythan area.

Figure 5.3 shows mineral analyses plotted on a Thompson Projection from the following specimens:

43870 assemblage C.1.

43867 assemblage C.2.

43864
43865 assemblage C.3.

Cordierite 'spots' are only sparsely developed through the rocks close to the isograd and this is reflected in specimen 43867. Biotite compositions vary through the rock in a manner which suggests that equilibrium was only attained on a local scale. $Biotite_1$ is in part of the specimen where no spots occur and is in contact only with white mica and quartz. $Biotite_2$ is at the edge of a spot contacting quartz and white mica and is more iron rich than $biotite_1$. Biotite compositions from specimens 43864 and 43865 which contain no spots also show some variation and are all more magnesian than the biotites of 43867.

The biotite plotted from specimen 43870 is at the edge of a spot and contacting quartz, white mica and chlorite (composition also plotted). This biotite has virtually the same MgO/MgO+FeO ratio as biotite of specimen 43867 however its A^i value (alumina index = $Al_2O_3 - 3K_2O / Al_2O_3 - 3K_2O + FeO+MgO+MnO$) is considerably larger (i.e. less negative).

The compositions of biotites presumably in equilibrium with cordierite (in assemblages C.1 and C.2) coupled with the relatively magnesian and intermediate A' values of biotites co-existing with white mica alone indicate:

a) the biotite-cordierite tie line of 43867 passes on the Fe-rich side of biotite 43870
b) there is a sharp change in biotite A' value as a function of whether or not it coexists with chlorite.

Assuming an A' value of 0.5 the most magnesian cordierite possible would have X cord (100MgO/MgO+FeO) = 36.

It can be seen from figure 5.3 that the mineralogical changes registered at the cordierite isograd could be produced by a bulk chemical composition gradient from magnesian to iron rich across the boundary. This is not upheld by the bulk rock chemistry data, (compare analyses 43860, 43867 Appendix II and table 4.2), the range of Xb in the biotite zone being 38.5 - 4.15 compared with 37.5 - 42.0 in the cordierite zone. Assemblage C.1 however is divariant in the system represented by the Thompson Projection (Chapter 6 section 1) and as a result the compositions of cordierite, chlorite and biotite may vary with grade. If these minerals become more magnesian upgrade causing the stability field of cordierite-biotite-chlorite to migrate to more magnesian compositions, a bulk composition with $A'_{chl} > A'_{b} > A'_{biot}$ (where

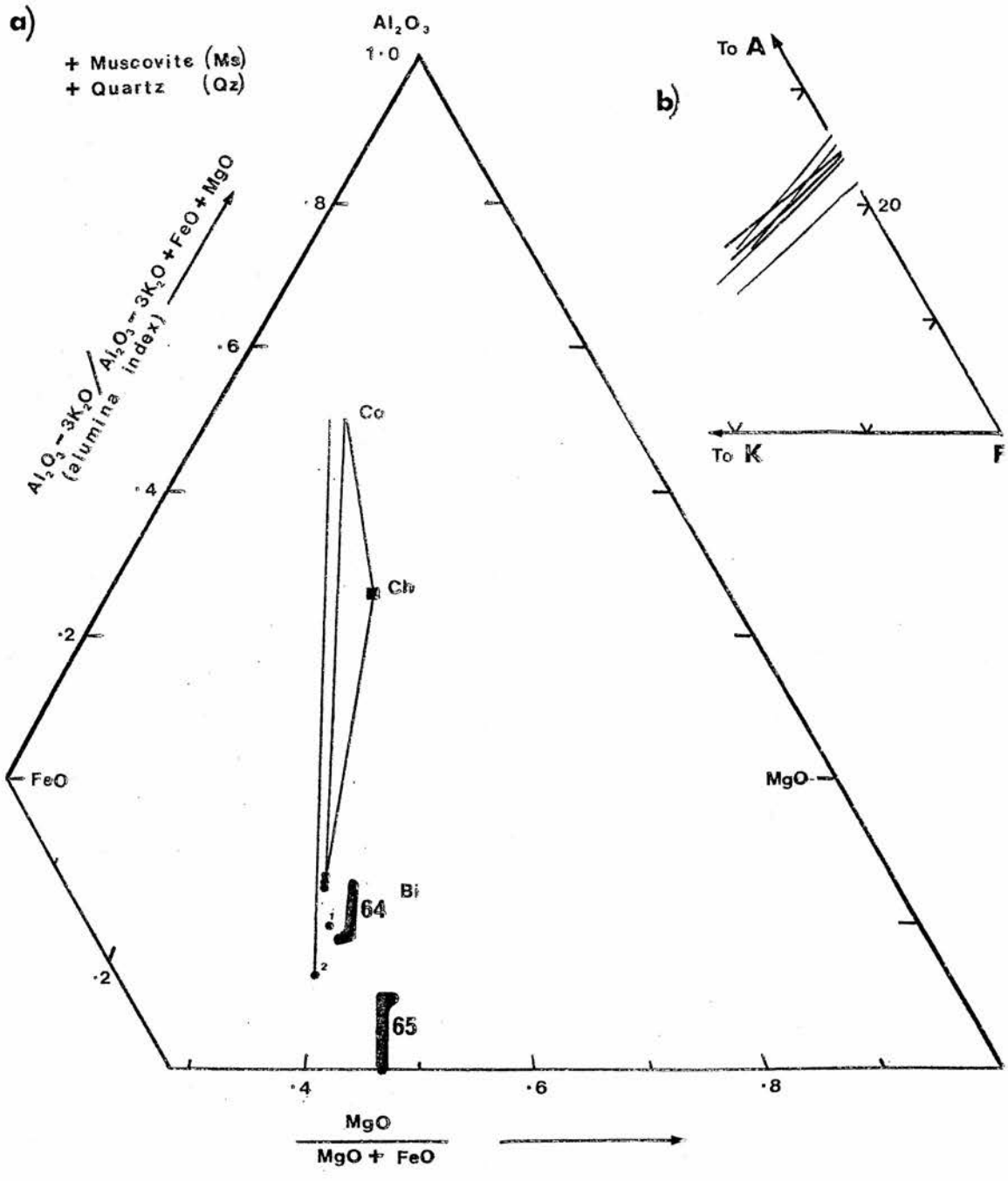

Figure 5.3: (a) Thompson projection showing mineral analyses and assemblages from the cordierite zone (Banffshire coast) (b) AKF diagram of chlorite-biotite pairs.

A'_b = bulk rock alumina index) would register the sequence of assemblages chlorite-biotite → chlorite-biotite-cordierite → cordierite-biotite, which is essentially the change registered in the field. Further more, because of the sharp change in biotite A' between assemblages C.1 and C.2 bulk compositions with $A'_{biot\ (assemblage\ C.1)} > A'_b > A'_{biot\ (assemblage\ C.2)}$ would register the sequence biotite → cordierite-biotite, explaining the decreasing abundance of assemblage C.3 upgrade, which would become restricted to rocks with high potash. Since most of the rocks immediately below the isograd show the assemblage biotite-white mica (B.3 = C.3), this latter assemblage sequence is likely to be the one which occurs most commonly in the field. This, coupled with the very narrow compositional field of assemblage C.1 is adequate to explain the rarity of its occurrence.

Figure 5.3(b) shows coexisting biotite-chlorite pairs from specimen 43870 assemblage C.1 and from the Biotite zone which have been plotted on a standard AKF diagram. From this figure it is evident that the chlorite-biotite tie line of specimen 43870 is more aluminous than any of those from the biotite zone whilst having a compatible slope. White mica at this grade (specimen 43867) contains 0.3 R^{2+} atoms per formula unit compared with 0.55 in the biotite zone suggesting that the concomitant expansion of the volume filled by chlorite biotite white mica tie planes continues from the biotite zone into the cordierite zone.

5.3. The Andalusite Zone

The location and extent of this zone along with the petrography of the rocks occurring within it have been described in chapter 2 sections 1, 3 and 5.

The following primary mineral assemblages occur together with quartz, plagioclase and opaques.

andalusite - cordierite - biotite - muscovite - A.1

cordierite - biotite - muscovite - A.2

Figure 5.4 shows analyses of cordierite and biotite from specimens 43876 and 43873 (assemblage A.1 and A.2 respectively) which occur near the andalusite isograd. The white mica present in specimen 43876 is essentially muscovite with only 0.17 R^{2+} atoms per formula unit, (anal 7 App. III 3). Although cordierite is very common, andalusite is rare in occurrence. This may be partially due to exposure since the upper part of the zone is truncated by the beach at Boyndie Bay. This rarity along with common alteration of cordierite to pinite has precluded any systematic study of mineral compositional variation with grade at this locality. An excellent opportunity is however provided in the Valley of the River Ythan. Read (1952) drew attention to the low dip of the cordierite isograd in this area where it is displaced at least two miles by a normal fault near Fyvie. The andalusite isograd is similarly affected. Andalusite is common above the

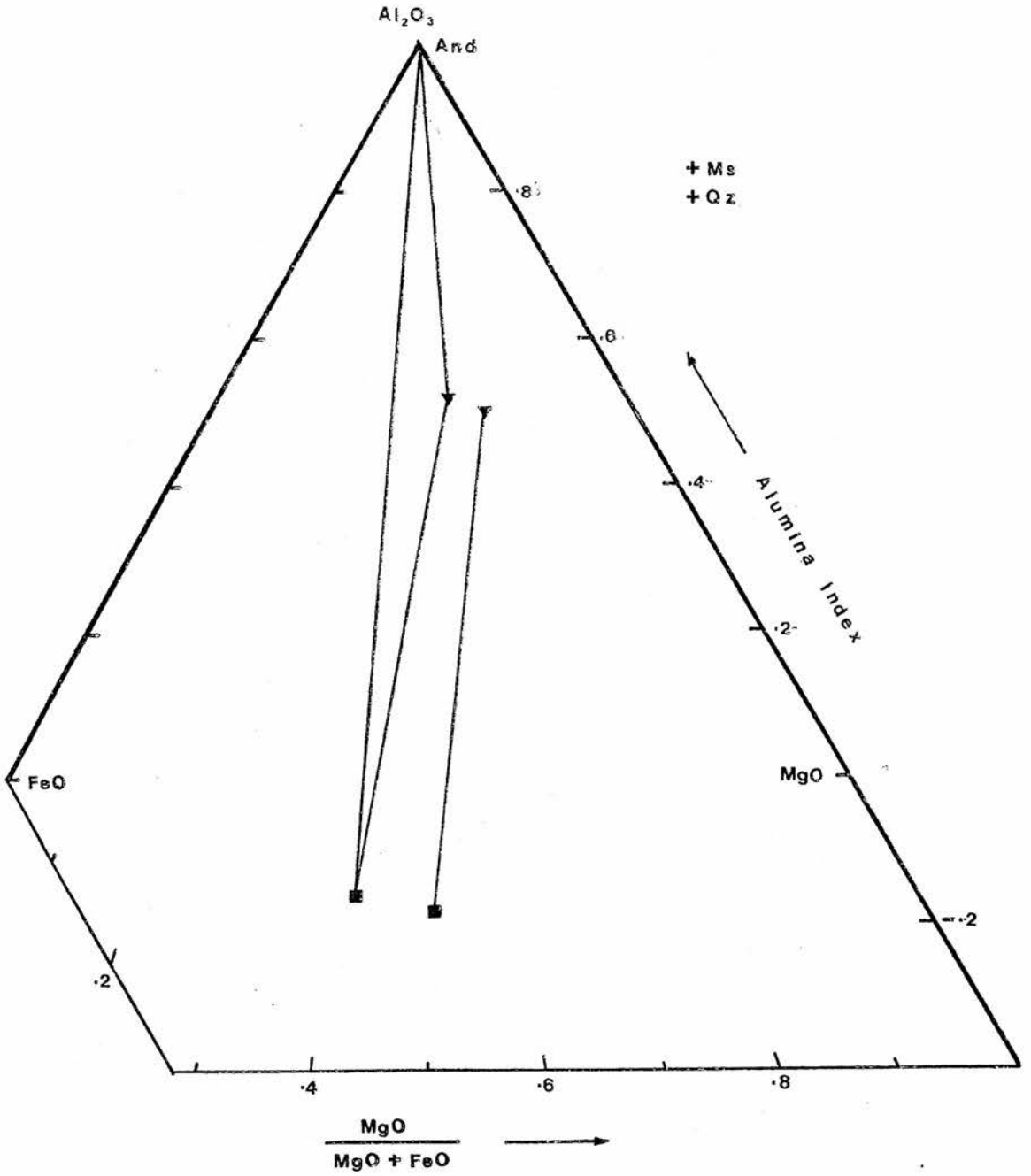

Figure 5.4: Thompson projection showing mineral analyses and assemblages from the Andalusite Zone of the Banffshire Coast.

isograd (NJ 795 380) where the following primary mineral assemblages occur

andalusite - cordierite - biotite - muscovite - A.1

cordierite - biotite - muscovite - A.2

that is essentially similar to the Banff Coast though assemblage A.1 is more common here. Upgrade as far as Braes of Gight (NJ 830 309) the same two assemblages occur in pelitic rocks, assemblage A.2 becoming less common whilst assemblage A.1 becomes more frequent. Close to the Sillimanite isograd near Little Gight (NJ 840 396) a third assemblage

andalusite - biotite - muscovite - A.3

occurs.

Analysis of coexisting cordierite-biotite pairs from assemblage A.2 are presented in figure 5.5. In each case the full assemblage is andalusite-cordierite-biotite-muscovite-quartz-plagioclase-ilmenite-sulphide. The numbered biotites in the diagram refer to the following specimens and grades

1. 43993 lowest grade with andalusite and fresh cordierite
2. 44013 intermediate grade - Braes of Gight
3. 44016 highest grade lacking sillimanite and/or replacement of andalusite by large muscovite plates

Specimen localities are shown on Map 5

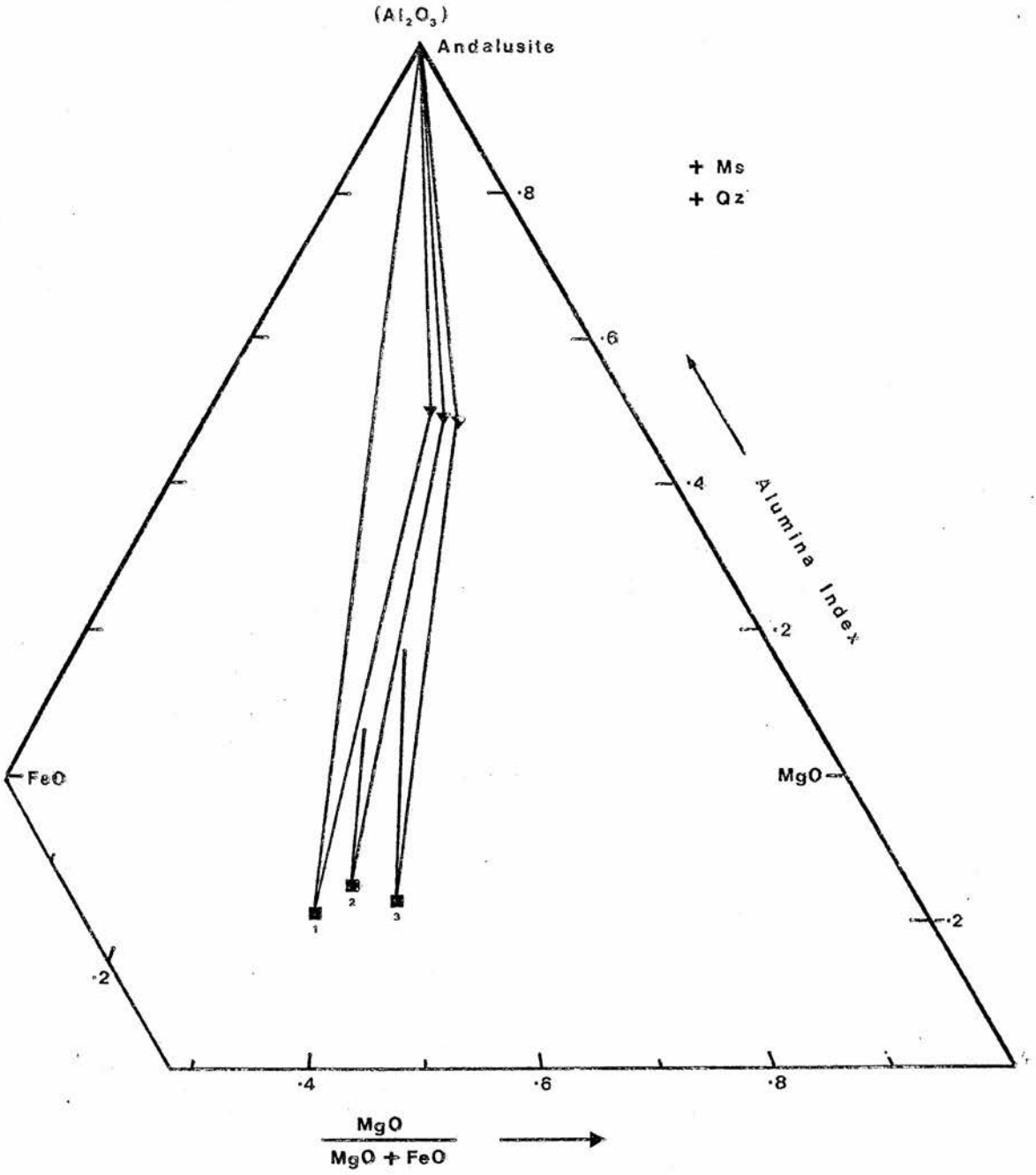

Figure 5.5: Thompson projection representing changes in cordierite and biotite composition across the Andalusite Zone of the Ythan Valley

Figure 5.5 shows that cordierite-biotite pairs coexisting with andalusite have progressively more magnesian compositions apparently simply related to grade. Some workers (e.g. Chinner 1960, Hownslow and Moore 1967) have shown that such variations in mineral composition can be due to variations in fO_2 which can mask the effects of P and/or T. Rocks from this locality, however, register opaque assemblages which indicate only minor variations in fO_2. Neither magnetite nor primary haematite occur in the rocks and the specimens studied contain

43993 ilmenite - rare pyrite

44013 ilmenite - pyrrhotite

44016 ilmenite - rare pyrite

If fO_2 were the controlling factor specimen 44013 associated with the highest fO_2 (Guidotti 1970) (see Figure 5.8(b)) should contain the most magnesian biotite. It does not. Omitting the effect of μH_2O which cannot be monitored it seems most reasonable to attribute the silicate compositional variation to the effect of grade i.e. P and/or T.

The effect of increasing X_{cord} and $X_{biotite}$ upgrade causes the stability field andalusite-cordierite-biotite to sweep across the diagram and encompass more Mg rich bulk compositions as the grade increases. This is in agreement with the observed assemblages in the field, both with respect to the andalusite isograd itself and to assemblages within the andalusite zone.

At the low grades, below the andalusite isograd, the three phase

	Specimen No.	Assemblage	X_{bi}	X_{co}	$K_D^{Fe-Mg}{}_{co-bi}$	Grade within Zone
Ythan Valley	43993	A.1	39.9	52.8	1.68	Low
	44013	A.1	42.9	55.0	1.63	Medium
	44016	A.1	47.4	58.3	1.55	High
Banffshire Coast	43876	A.1	42.5	56.3	1.74	Low
	43873	A.2	51.0	64.0	1.70	Low

Table 5.2 : Chemical data on coexisting cordierite and biotite from the andalusite zone.

$$X = \frac{100\ MgO}{MgO+FeO}$$

assemblage lies at iron rich compositions outside the range of available rock bulk compositions, which show the two phase assemblage cordierite-biotite. As the grade increases the stability field of the three phase assemblage migrates to more magnesian compositions and eventually intersects the most iron rich rock compositions present and generates the andalusite isograd. At higher grades within the andalusite zone the three phase assemblage moves to still more magnesian compositions so that the most iron rich rock compositions register assemblage A.3.

Obviously an isograd of this nature is dependent on the available bulk composition of the rocks, particularly Xb but since $K_{D\ co-bi} = 1$ it is also dependent on alumina index (A_b). The first rocks to register the three phase assemblage will be those with the lowest Xb and highest A'b at any one locality. It is notable that cordierite and biotite in rocks immediately above the isograd on the Banffshire Coast are distinctly more magnesian than those in the Ythan Valley. (compare specimens 43993 and 43876, Table 5.2).

With respect to the Ythan Valley rocks a systematic decrease of $K_{D\ cord-biot}^{Fe-Mg}$ also occurs as the grade increases. Hensen (1971) suggests that such a variation of K_D should be related to temperature assuming ideal mixing within the solid solutions involved.

Evidence from the Banffshire Coast rocks indicates that ideal mixing is not attained and that a slight decrease in $K_{D\ cord-biot}^{FeMg}$

occurs towards more magnesian compositions at a fixed grade. Such a compositionally controlled decrease would only account for about 25% of the variation observed in the Ythan Valley rocks, and if the dependence of K_D on pressure is small (Hensen 1971 page 199) then 75% of the variation may be due to temperature. From Table 5.2 it may be seen that $K_D^{FeMg}{}_{cord-biot}$ in assemblage A.1 at the andalusite isograd on the Banffshire Coast (specimen 43876) is higher than its Ythan Valley counterpart (specimen 43993). Consequently the andalusite isograd on the Banffshire Coast may represent a lower temperature than that of the Ythan Valley.

5.4. The Staurolite Zone

The location, extent and petrography of the rocks occurring in this zone have been described in Chapter 2 sections 1 and 4.

The lower boundary of the zone is the staurolite isograd which is also, on the coast at least, an isograd for garnet. Mineral assemblages within the zone are shown in Table 5.3. Cordierite has been listed in this table for all cases where it is present or pseudomorphs clearly derived from it are present. Recrystallised quartz $\pm$ plagioclase aggregates have not been included (see Chapter 2 section 4 and Chapter 7).

The assemblages fall into four broad groups based on the occurrence of muscovite and garnet.

ASSEMBLAGE	Text Ref. No.
staur - biot - ms	S.1
andal - biot - ms	S.2
cord - biot - ms	S.3
andal - staur - biot - ms	S.4
andal - cord - biot - ms	S.5
staur - cord - biot - ms	S.6
andal - staur - cord - biot - ms	S.7
staur - biot - ms - gt	S.1a
andal - biot - ms - gt	S.2a
andal - staur - biot - ms - gt	S.4a
andal - cord - biot - ms - gt	S.5a
andal - staur - cord - biot - ms - gt	S.7a
andal - staur - biot	S.8
cord - staur - biot	S.9
andal - staur - cord - biot	S.10
andal - staur - biot - gt	S.8a
cord - staur - biot - gt	S.9a
andal - cord - staur - biot - gt	S.10a
gedrite - cord - staur - biot - gt	S.11a
staur - biot - gt	S.12a

Table 5.3 : Mineral Assemblages occurring in the staurolite zone.

i) + muscovite - garnet

ii) + muscovite + garnet

iii) - muscovite - garnet

iv) - muscovite + garnet

All garnet bearing assemblages with the exception of S.11a and S.12a have garnet free equivalents so that in general this mineral appears as an additional phase. Analyses of garnet from the staurolite zone (Appendix III (vi)) show that it contains between 15% and 23% of the spessartite molecule except in the case of specimen 7236 an ortho-amphibole rock in which garnet contains only 6-8% spessartite.

As a first approximation, garnet will be ignored on the grounds that it is an extra phase attributable to the extra component MnO so that the variance of each assemblage is unaffected in terms of the phase rule.

5.4(a). Muscovite bearing assemblages

Assemblage S.4 is the most common assemblage occurring throughout the zone, whilst assemblage S.5 though still common is restricted to the lower grade part and does not occur west of Whitehills. Assemblage S.6 is extremely rare (only one occurrence close to the staurolite isograd). Of the three phase assemblage S.3 is restricted to rocks close to the isograd whilst S.1 is of scattered occurrence through the zone and S.2 is curiously restricted to its higher grade parts, west of Whitehills.

These assemblages always contain quartz and ideally may be projected into the system Al_2O - K_3O - FeO_2 - MgO with the assumption of fixed H_2O (Thompson 1957).

Mineral analyses from specimens 43901 and 15463, assemblage S.5 and S.4 respectively, occurring at Boyndie Bay, are presented in figure 5.6 (For analyses see Appendix III. Analyses from 15463 by John Ashworth). Figure 5.7 shows mineral analyses from assemblage S.4 in which the numbered biotites refer to the following specimens and grades.

1. 15463 Low grade near staurolite isograd. Boyndie Bay
2. 43918 Intermediate grade. Whitehills
3. 43929 Highest grade close to sillimanite isograd. Whyntie Head.

The full assemblage is staurolite-andalusite-biotite-muscovite-quartz-plagioclase-ilmenite-sulphide. (Traces of garnet in 15463 and 43918). The behaviour of this assemblage is similar to that of cordierite-andalusite-biotite in the andalusite zone. Coexisting staurolite-biotite pairs become more Mg rich up grade causing the stability area staurolite-biotite-andalusite to migrate towards more Mg rich bulk compositions. Associated with this compositional change a minor decrease in $K_D^{\text{Fe-Mg}}{}_{\text{Staur-biot}}$ occurs from 0.26 (15463) to 0.24 (43929).

Reliable cordierite analyses have not been obtained from assemblage

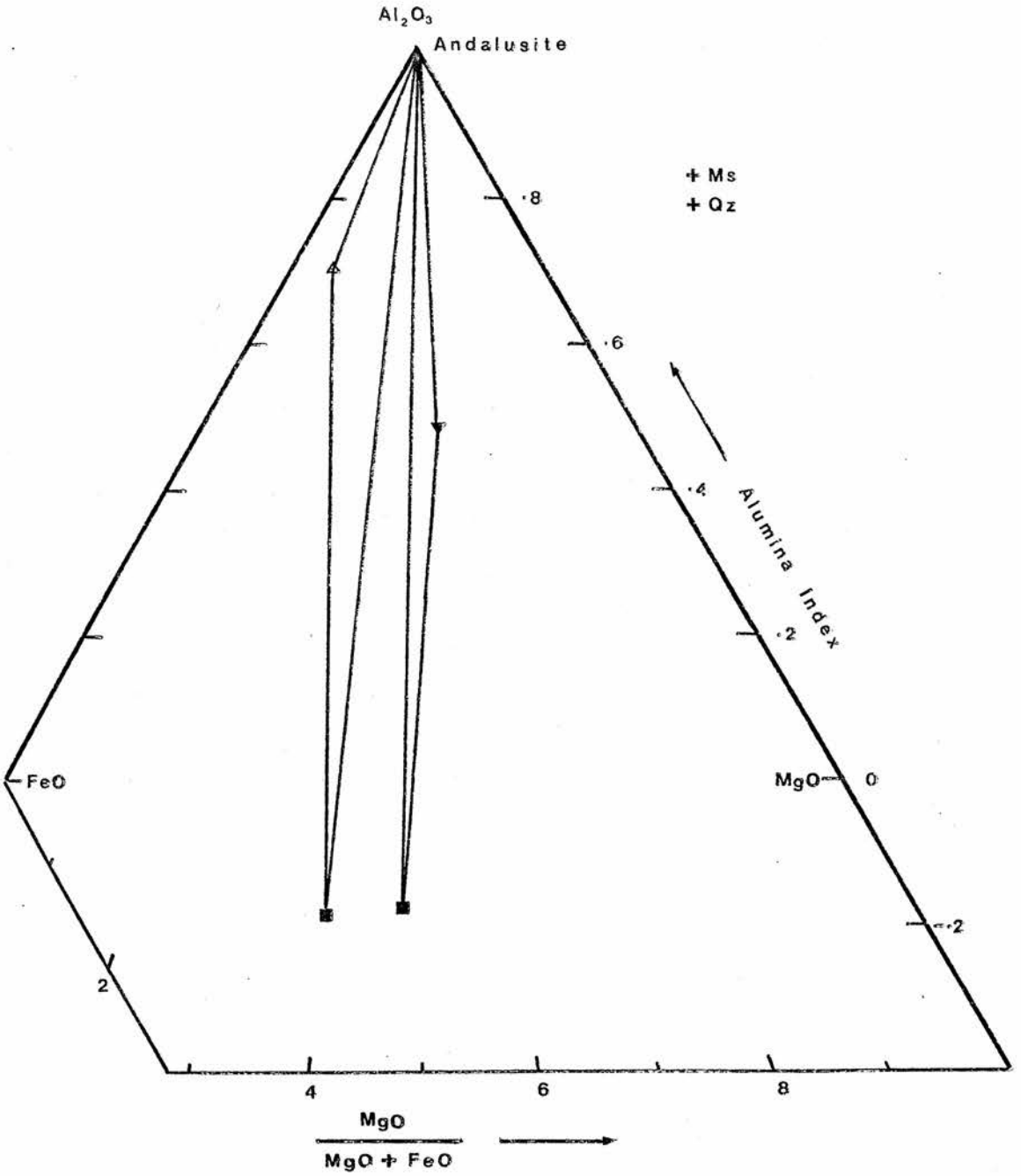

△ staurolite analysis other symbols as in Fig. 5.5.

Figure 5.6: Thompson projection showing assemblages and mineral analyses from the staurolite zone at Boyndie Bay.

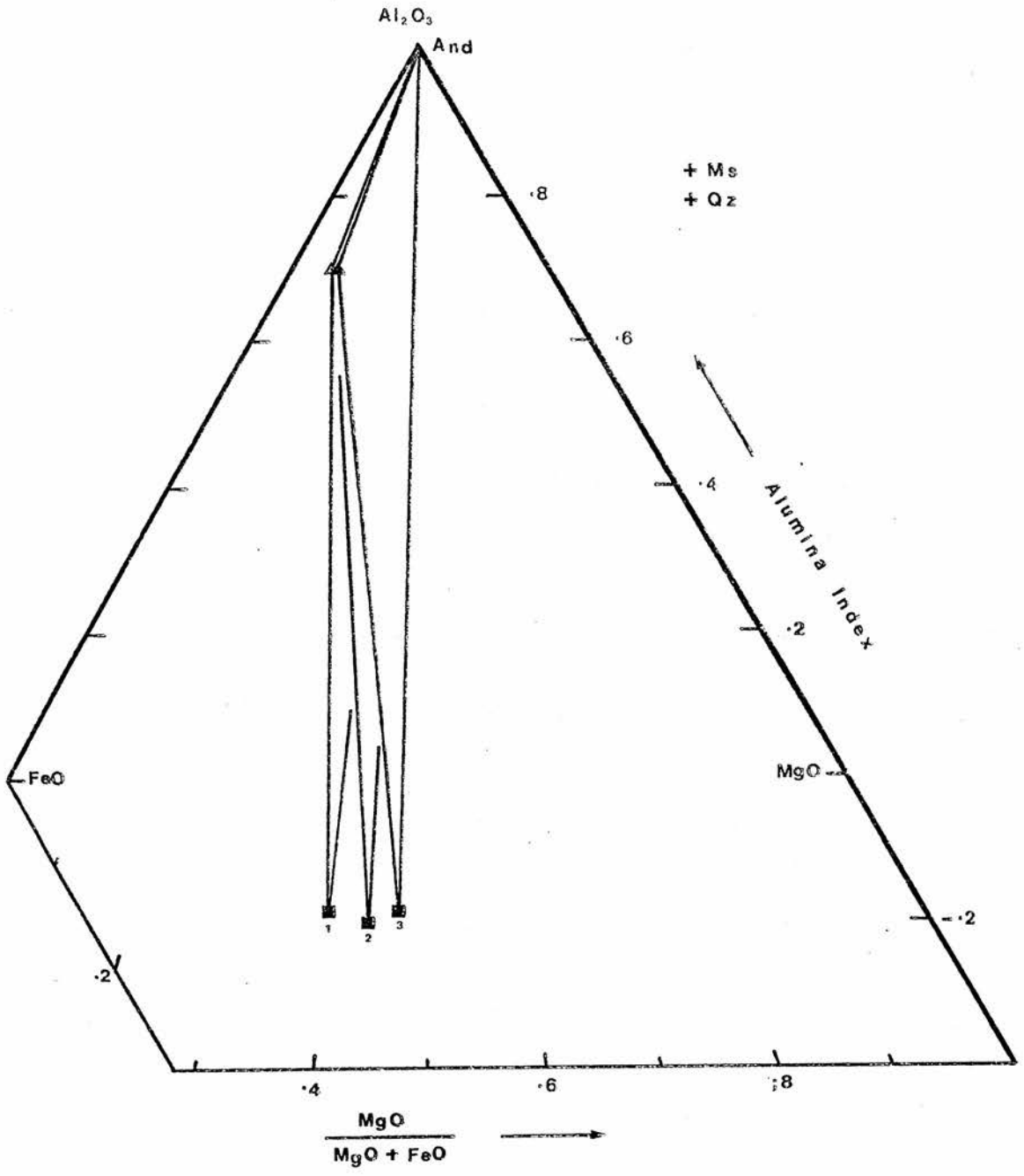

Figure 5.7: Thompson projection showing variation in mineral composition in the assemblage staurolite-andalusite-biotite ($\pm$garnet) across the staurolite zone on the Banffshire Coast.

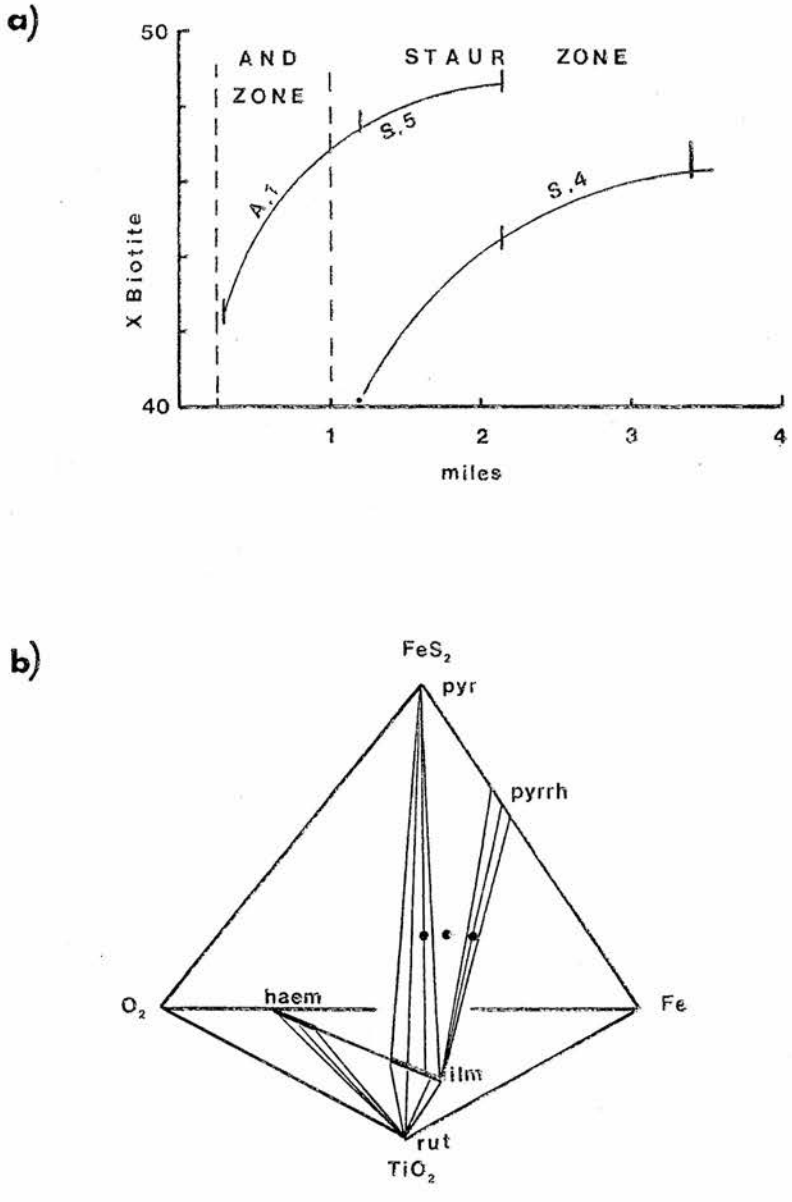

Figure 5.8: (a) Variation in biotite composition in the assemblage cordierite-andalusite-biotite across the andalusite and staurolite zones. (Banffshire Coast)
(b) Opaque mineral assemblages from the rocks of Buchan (after Guidotti 1970).

S.5 within the staurolite zone. Biotite analyses from specimens 43901 (Boyndie Bay) and 43919 (Whitehills) are plotted in figure 5.8(a) which is simply a graph of X biotite against distance above the cordierite isograd as an index of grade. Also plotted on this figure is the biotite composition from specimen 43876 (Andalusite Zone) which has the same assemblage. The figure shows that biotite in assemblage S.5 also becomes more magnesian up grade although it apparently does so much less rapidly in the staurolite zone than in the andalusite zone.

Again it seems unlikely that variations in composition of minerals in either of these assemblages could be attributed to variations in fO_2 though this is undoubtedly the case in other areas (e.g. Hounslow and Moore 1967). Opaque assemblages in the analysed rocks are as follows:

15463	ilmenite - pyrite	Assemblage S.4
43918	ilmenite - pyrite - rare pyrrhotite	
43929	ilmenite - pyrite	
(43876	ilmenite)	Assemblage S.5
43901	pyrite- ilmenite	
43919	ilmenite	

suggesting that although variations in fO probably occurred they are likely to have been small (Figure 5.8(b)). With respect to assemblage S.4., 43918 carries the assemblage associated with the lowest fO_2 and should therefor have the most iron rich silicate compositions were this the controlling factor. It does not.

A grade control on the stability fields of andalusite-staurolite-biotite and andalusite-cordierite-biotite is in good agreement with the distribution of these assemblages in the field. Below the staurolite isograd the stability field of assemblage S.4 lies in very iron rich bulk compositions, outside the range of bulk rock chemical compositions occurring in the field (Xb 35-55). At this grade assemblage S.5 lies in intermediate compositions and appears in the rocks. As the grade increases the two stability fields move to more magnesian compositions and at the staurolite isograd the most iron rich bulk composition available registers assemblage S.4., whilst more magnesian rocks may still show assemblage S.5. Strictly, the first rock to register assemblage S.5 should be the most iron rich irrespective of its A b in contrast to the andalusite isograd, since the controlling tie line is now andalusite - biotite, representing a constant MgO/MgO+FeO ratio. In fact bulk rock analyses are not directly relatable to figures 5.6. and 5.7. due to other constituents (opaques garnet etc) and modes are virtually impossible to establish due to the inhomogeneity of the rocks. See Chapter 2. However, it is notable that at each locality there is no overlap between the compositions of rocks carrying the two assemblages.

Boyndie Bay	Assemblage S.4 Xb	38 - 45.5	Assemblage S.5 Xb	46.7
Whitehills		43 - 50		52.7

At grades higher than that attained at Whitehills, assemblage S.5 must lie at magnesian compositions and is no longer recorded.

Assemblage S.3 is in good accord with this model since it is restricted in occurrence to localities close to the staurolite isograd. On the other hand assemblage S.2 should also be common at this locality but it does not occur at all until grades higher than that attained at Whitehills. Its absence is probably due to the fact that cordierite, having previously grown large porphyroblasts, tends to react only at its margins, the centres of porphyroblasts becoming insulated from the rest of the rock, or less likely to slow reaction rates. At the same time the stability field of this assemblage is narrow (see figure 5.6) and this may further reduce the likelihood of its occurrence.

5.4(b) Muscovite free assemblages

Assemblages lacking muscovite also occur in the staurolite zone with considerable regularity.

Assemblage S.10 (Table 5.2) is the most common of these. It can only be represented fully within the tetrahedron Al_2O_3- K_2O - FeO - MgO (AKFM) in which it forms a narrow volume lying between the planes andalusite - biotite - cordierite of assemblage S.5 and andalusite - biotite - staurolite of assemblage S.4. Its relationships to assemblages S.4 and S.5 may be shown in a projection from andalusite on to the base of the AKFM tetrahedron. This gives a KFM projection valid for rocks containing quartz and andalusite still with the assumption of fixed H_2O. A projection of this type is used for rocks from Boyndie Bay in Figure 5.9(b). It shows assemblage S.10 (specimen 43894) along with the two muscovite bearing assemblages previously discussed.

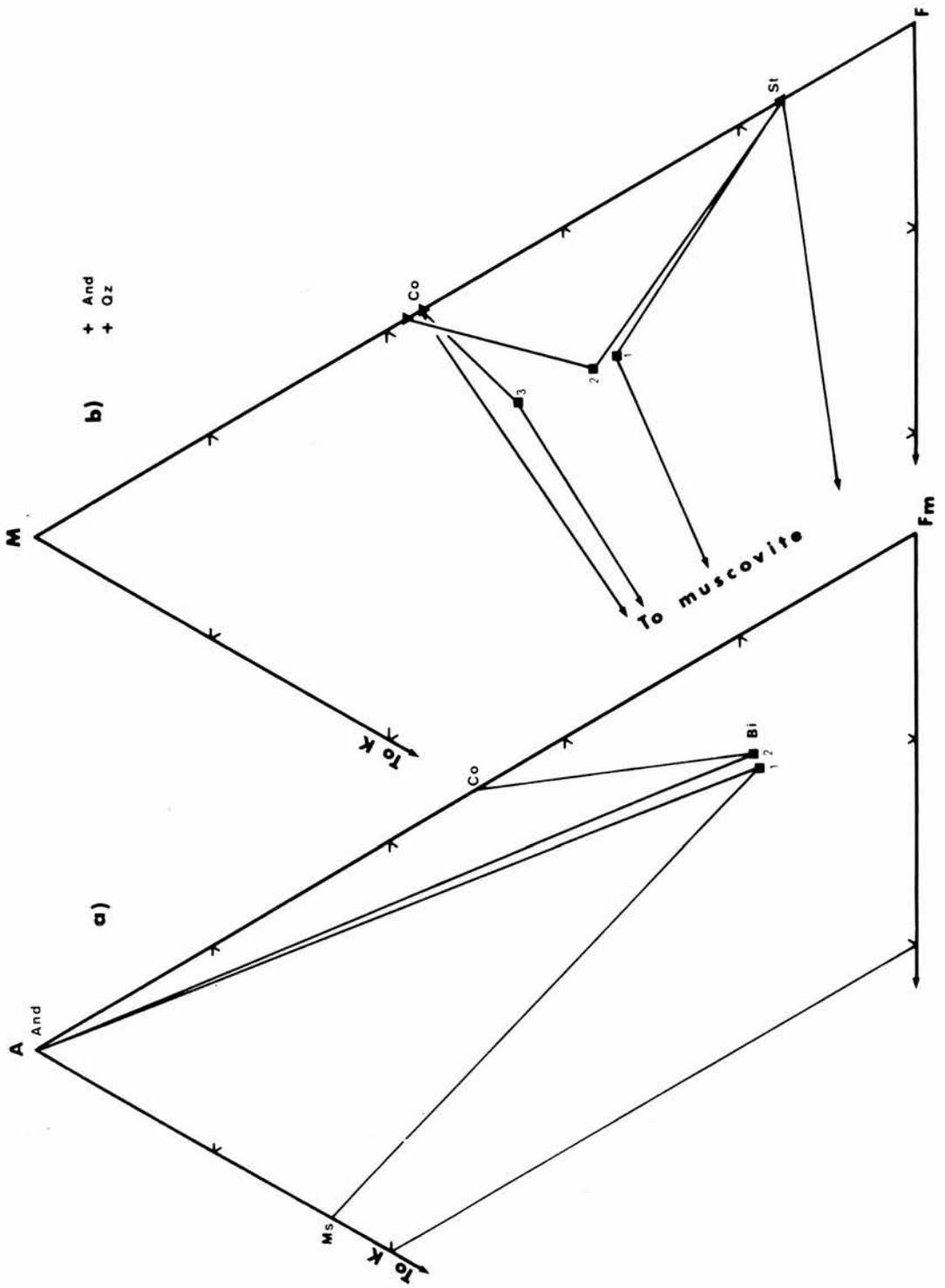

Figure 5.9: AKFm diagram (a) and KFM projection from andalusite (b) representing parageneses and mineral compositions near Boyndie Bay (NJ 670648).

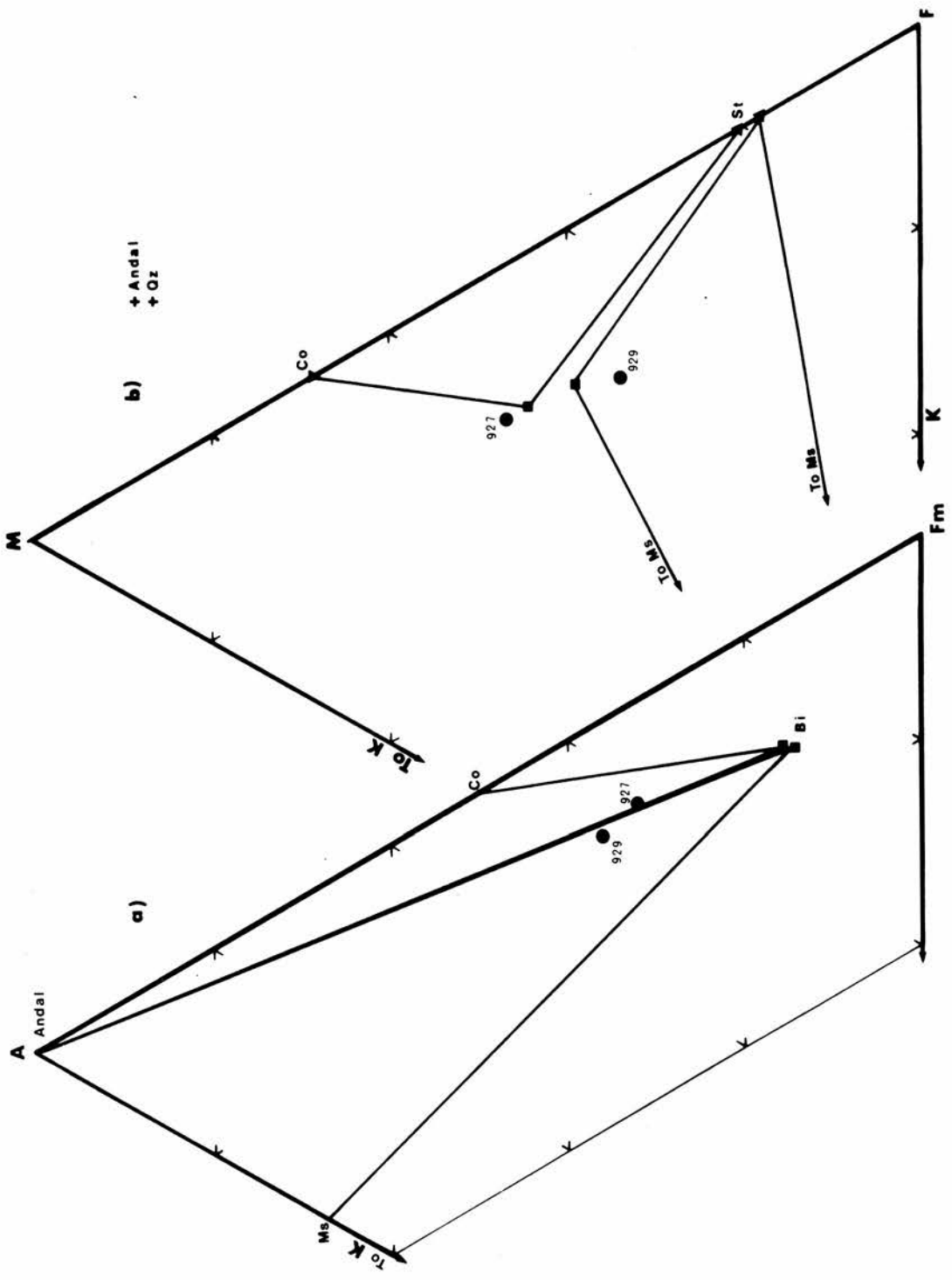

Figure 5.10: AKFm diagram (a) and KFM projection from andalusite (b) for rocks near Whyntie Head (NJ 631659).

The biotite in the muscovite free assemblage (for analyses see Appendix III (ii)) has an 100 MgO/MgO+Feo ratio (X biot) intermediate between those of the two muscovite bearing assemblages though closer to that of assemblage S.4. There is however no detectable difference in X staur between the two assemblages (analyses in Appendix III (v)). Crossing of tie lines near cordierite is not thought to be real but due to a poor analysis (Cordierite 43901) which has a low total and will be neglected hereafter.

Figure 5.10 (b) is similar andalusite projection for rocks just below the sillimanite isograd at Whyntie Head showing analyses from specimens 43929 (assemblage S.4) and 43927 (assemblage S.10). Assemblage S.5 does not occur at this grade. X biotite (assemblage S.10) is again notably larger than X biotite (assemblage S.5) whilst the difference between the two biotite compositions has increased (c.f. figure 5.9). Staurolite (assemblage S.10) is distinctly more magnesian than staurolite (assemblage S.5) at this grade, again suggesting that the difference in composition has increased with grade. Careful comparison between figures 5.9 and 5.10 will also reveal that cordierite biotite and staurolite in specimen 43927 are all more magnesian than the corresponding minerals in specimen 43894 (analyses Appendix III (iv), (ii) and (v) respectively). This suggests that the divariant assemblage S.10 behaves in a manner analogous to assemblages S.4 and S.5, its constituent Fe-Mg silicates becoming more Mg rich upgrade. The available mineral data relevant to these three assemblages has been compiled in the form of graphs in figure 5.12, graphs (a),

(d) and (e) being relevant to the present discussion. X biotite in each assemblage has been chosen as an index of grade and the other mineral compositions related to it. X values for each mineral may be rapidly read from these graphs for comparative purposes. Other data from specimens 43945 (Kinnairdy), 43939, 43942 (Maundenea Quarry) have also been introduced here. These specimens are from inland localities (see Appendix I for locations) and have been used along with specimens from the Banffshire Coast to produce Map 6 which shows the staurolite zone contoured for constant mineral composition in assemblages S.4 and S.10. It is notable that the rate of change of mineral compositions falls off rapidly west of Whitehills. This could be a metamorphic phenomenon but is in fact more likely to be due to post metamorphic folding. Johnson (1962) notes that the third generation folds in the area are later than the metamorphic climax. These folds are related to the Boyndie Syncline "which is an enormous monocline with several subordinate folds occurring as steps on its limbs". These steps produce 'flat belts' in the steep limb of the Boyndie Syncline (i.e. belts of low regional dip) one of which occurs immediately west of Whitehills. It appears that the F_3 folds have folded the metamorphic surfaces not only on a regional scale leaving the lowest grade (Biotite Zone) rocks in the core of the Boyndie Syncline, but also on a fine scale within the staurolite zone near Whitehills.

Also shown in figure 5.12, graphs (c) and (f) are plagioclase compositions coexisting with assemblages S.4 and S.10 respectively.

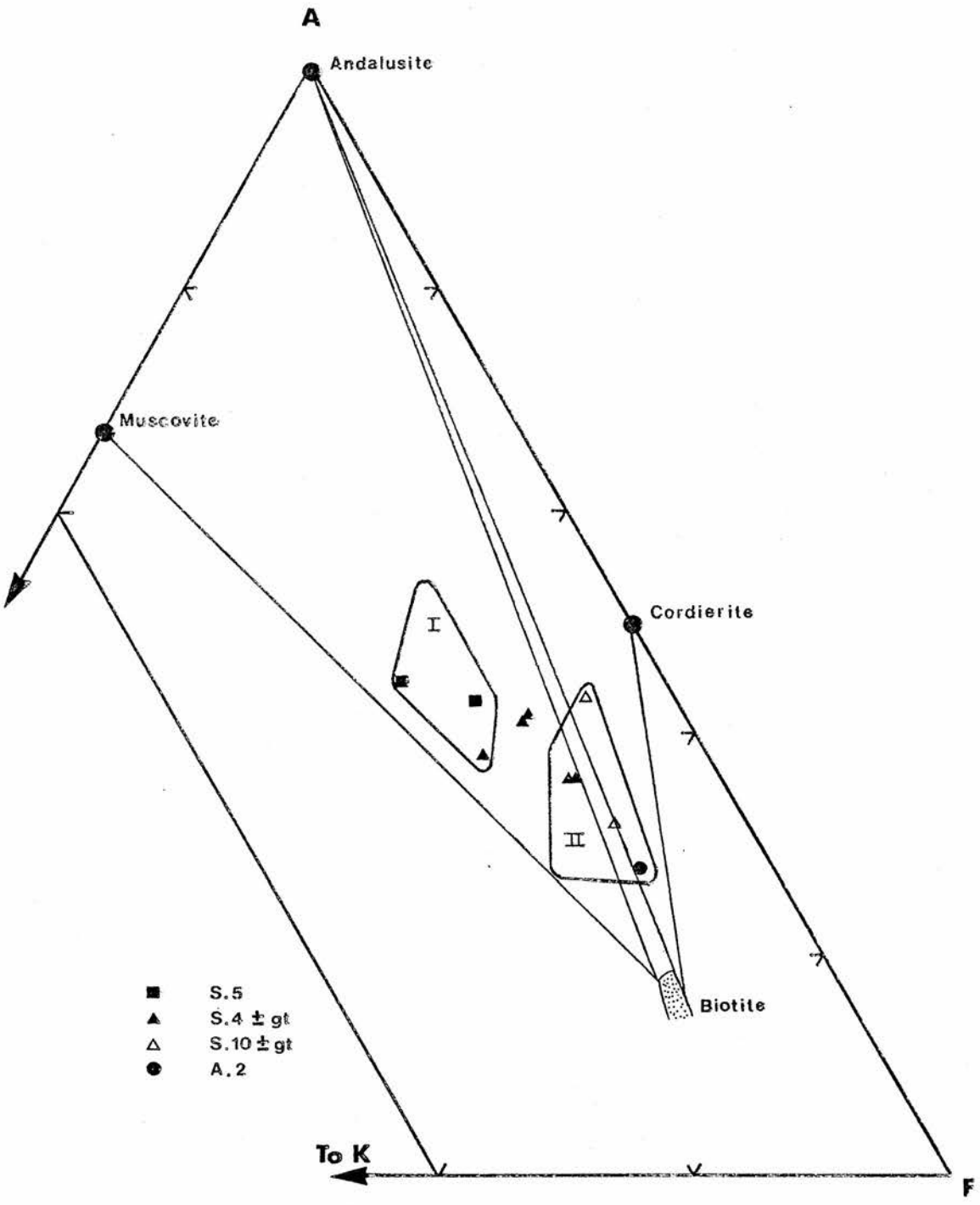

Figure 5.11: AKF diagram to illustrate the relationship between bulk rock composition and potential assemblage sequence with increasing grade.

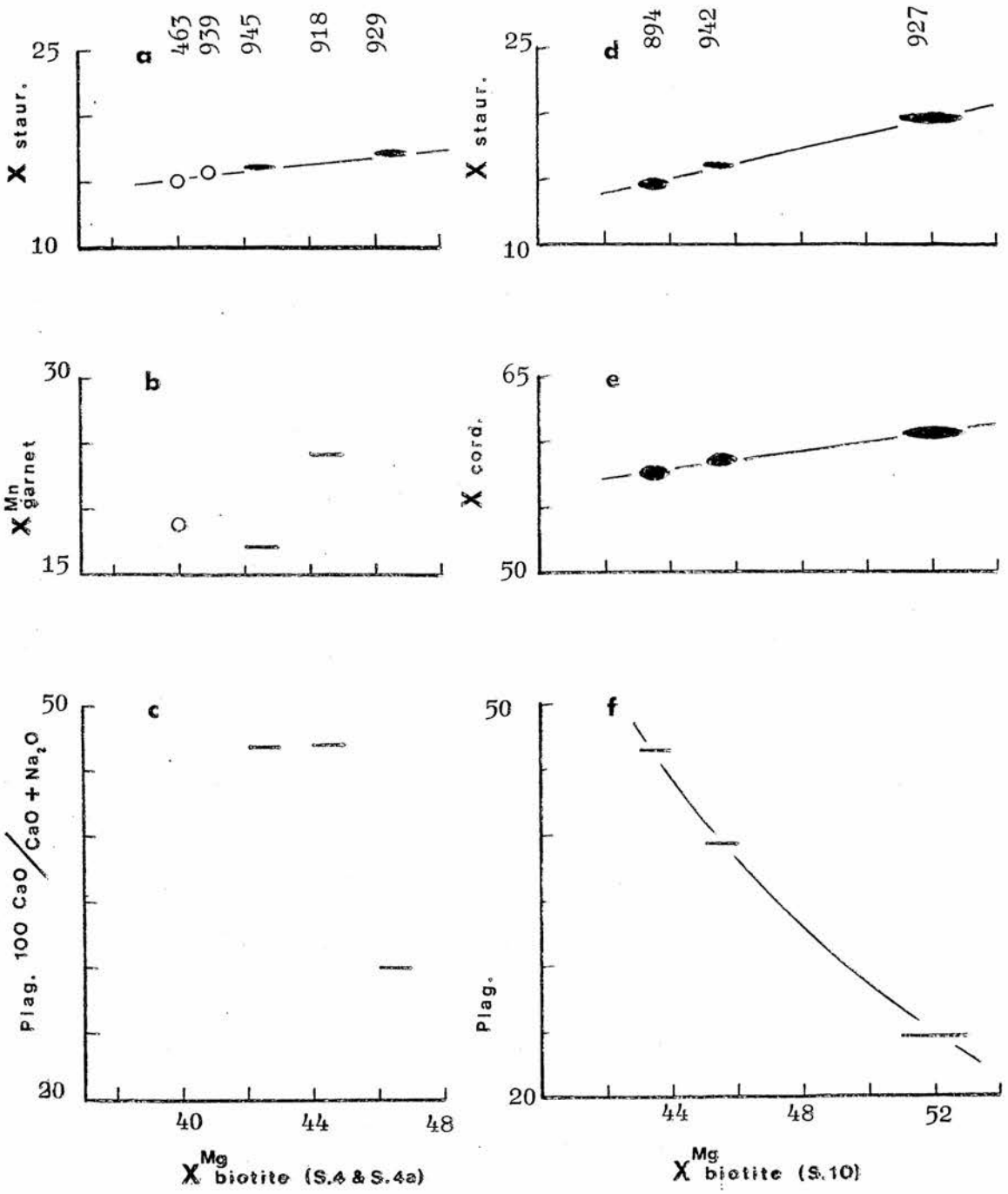

Figure 5.12: Compositional variation in minerals of the staurolite zone. Ellipses indicate internal variation within single specimens. Open circles, no information on internal variation. Lines, information on biotite variation only.
X^{Mg} = 100 MgO/MgO+FeO+MnO; X^{Mn} = 100 MnO/MgO+ FeO+MnO.

Although there is a suggestion of a trend towards more sodic compositions up grade, plagioclase compositions are more clearly related to the $CaO/CaO+Na_2O$ of the bulk rock, figure 5.19(b).

Bulk Compositions giving rise to muscovite free assemblages

Figure 5.11 is a standard AKF plot showing staurolite zone andalusite - biotite tie lines from assemblages S.4 and S.10 at Boyndie Bay and Whyntie Head. Biotite compositions are marked with the specimen number. Also plotted are the fields of Lithology II bulk compositions and Lithology I bulk compositions (see Chapter 4 section 2). A number of actual rock compositions have also been plotted. (See figure caption for assemblages).

As all three assemblages S.4., S.5 and S.10 move to more magnesian compositions together upgrade it can be seen from the figure that a biotite andalusite tie line will exert a control over the upgrade assemblage which is realised in the following manner.

Lithology I (and also Lithology I/II) compositions lie in the triangle andalusite - biotite - muscovite, and on passing from the andalusite to staurolite zones will register the assemblage change S.5 → S.4, previously discussed on page 130of this chapter. The more potassic of Lithology II bulk compositions will also register this change.

Rock compositions falling in the triangle andalusite - biotite - cordierite, ie. less potassic Lithology II compositions, will behave differently. In these compositions the staurolite isograd will represent a change from assemblage S.5 to assemblage S.10 (neglecting intermediate trivariant assemblages). On moving further upgrade, compositions in this triangle could again diverge. The actual rock compositions falling in this triangle are two muscovite free rocks from the staurolite zone (specimens 43902, 43927) and an andalusite zone rock carrying the assemblage cordierite - biotite - muscovite (specimen 43873). This rock may be regarded as a potential muscovite free rock were it to occur in the staurolite zone. These three rocks occur in the triangle andalusite - staurolite - biotite so that on moving to higher grades within the staurolite zone they would eventually register the muscovite bearing assemblage S.4. Any compositions in the triangle staurolite - cordierite - biotite (no analysed representatives) would on the other hand move into other muscovite free assemblages possibly bearing gedrite (see Chapter 5 section 6).

5.5 MnO as a component and the parageneses of garnet

From the common occurrence of manganiferous garnet in these rocks it is apparent that MnO must be an important variable despite the low concentration, generally $\leq$ 0.2%, indicated by the bulk rock analyses of Appendix II.

Figure 5.13 is an FeO-MgO-MnO plot of all analysed staurolite

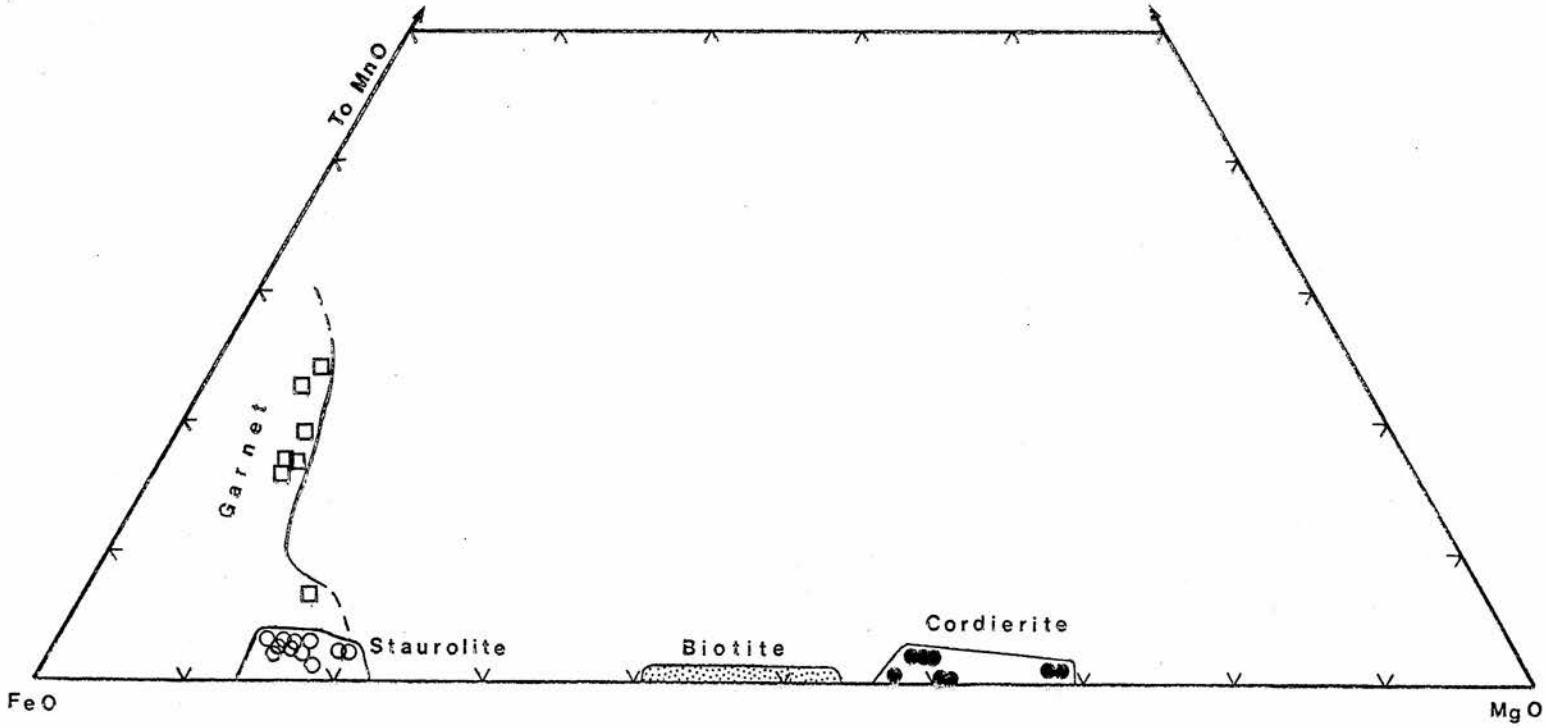

Figure 5.13: FeO - MgO -MnO plot of all analysed staurolite zone minerals.

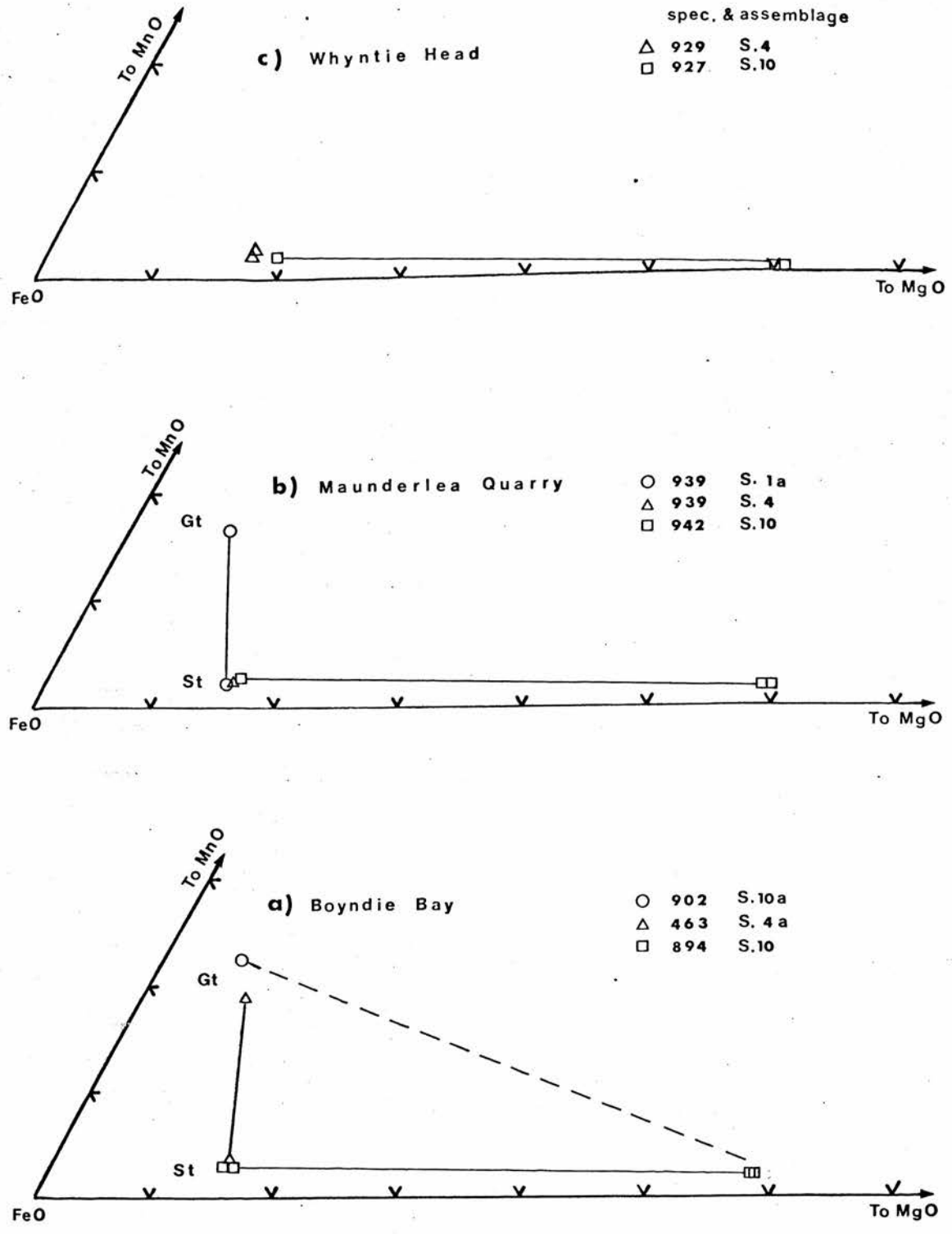

Figure 5.14: FeO - MgO - MnO plots showing relationships between staurolite, cordierite and garnet. Tie lines join co-existing pairs.

zone minerals similar to figure 7 of Albee (1965b), and shows that MnO is distributed in favour of the mineral phases in the order

Garnet > Staurolite ≥ Cordierite > Biotite

Garnet and biotite have a similar range of MnO/FeO+MgO+MnO as those reported by Albee neglecting one very MnO rich garnet reported by him. In order to represent MnO as a component it is necessary to use a three dimensional model. Two such models are available.

a) A tetrahedron using a Thompson Projection as a base with MnO as the top apex. This is similar to the model used by Osberg (1971) for rocks in Maine similar to those under discussion, and is applicable to rocks bearing quartz and muscovite.

b) A tetrahedron using a KFM andalusite projection as a base which is applicable to rocks bearing quartz and andalusite.

Although phase relationships can only be shown qualitatively on these models in perspective view, they can be usefully treated taking a few phases at a time on an FeO-MgO-MnO plot. By its very nature the evidence is tenuous but it does give rise to a consistant model for garnet parageneses which is summarised in two perspective models in figure 5.18.

Figure 5.14 shows analyses of garnet, staurolite and cordierite

from three localities plotted in FeO-MgO-MnO. Figure 5.14(a) (specimens from Boyndie Bay) shows that staurolite and cordierite even in the garnet free assemblage S.10 have X^{Mn} 2.0 whilst garnet (assemblage 4a) has X^{Mn} of almost 20. As previously noted any variation in $X^{Mg}_{staurolite}$ between the two assemblages is not detectable though $X^{Mn}_{staurolite}$ in the latter assemblage is marginally higher. Two garnet analyses from specimen 43902 (assemblage S.10a) are also plotted. Garnet contacting partially altered cordierite is notably more manganese rich than that of assemblage S.4a.

At slightly higher grade (Fig. 5.14(b) - Maunderlea Quarry) staurolite in assemblages S.10, S.4 and S.1a has a decreasing X^{Mg} just within the limits of detection, whilst near the sillimanite isograd (Figure 5.14(c) - Whyntie Head) the difference between $X^{Mg}_{staurolite}$ in assemblages S.10 and S.4 has increased. $X^{Mn}_{staurolite}$ has remained essentially constant between 2.0 and 3.0 per cent at all grades.

Garnet commonly occurs in narrow bands which appear to be related to the original bedding in a manner which implies a compositional control. It may also occur as rare crystals spread sparsely through the rock.

Analyses of contacting mineral pairs and triads were carried out on three garnet rich specimens (43939, 43940, 43945). Within each specimen mineral compositions were found to vary from place to

Specimen No.	43939						43940			
Mosaic	1.st-bi-gt-ms			2.st-bi-and-ms		3.gt-bi-ms			1.st-bi-gt-ms	2.gt-bi
Mineral	st	gt	bi	st	bi	gt	bi		gt	bi	gt - bi
$\frac{100\ MgO}{MgO+FeO+MnO}$	15.1	8.3	42.4	15.7	40.9	8.7	41.9		7.7	42.8	8.9	40.4
$\frac{100\ MnO}{MgO+FeO+MnO}$	2.5	16.7	0.4	2.6	0.5	16.0	0.6		19.1	0.4	16.7	0.4
$\frac{100(Al_2O_3-3K_2O)}{Al_2O_3-3K_2O+FeO+MgO+MnO}$	72.5	25.2	-17.5	70.0	-15.1	25.1	-15.6		25.0	-17.0	26.0	-16.5
K_D^{Fe-Mg} gt-bi		0.123				0.132			0.111			
MnO correction		0.117				0.112			0.134			
Corrected K_D		0.240				0.244			0.245			

Table 5.4 : Chemical data on selected rocks from the staurolite zone.

Specimen No.	43945							
Mosaic	1.st-bi-gt-ms			2.st-bi-and-ms		3.gt-bi-ms		
Mineral	st	gt	bi	st	bi	gt	bi	
$\frac{100MgO}{MgO+FeO+MnO}$	14.5	8.8	42.7	15.8	43.0	9.5	43.2	
$\frac{100MnO}{MgO+FeO+MnO}$	2.3	17.0	0.4	2.6	0.6	17.1	0.4	
$\frac{100(Al_2O_3-3K_2O)}{Al_2O_3-3K_2O+FeO+MgO+MnO}$	70.0	26.0	-16.0	70.0	-16.0	26.0	-19.0	
K_D^{Fe-Mg} gt-bi	0.127					0.138		
MnO Correction	0.119					0.120		
Corrected K_D	0.246					0.258		

Table 5.4 : continued

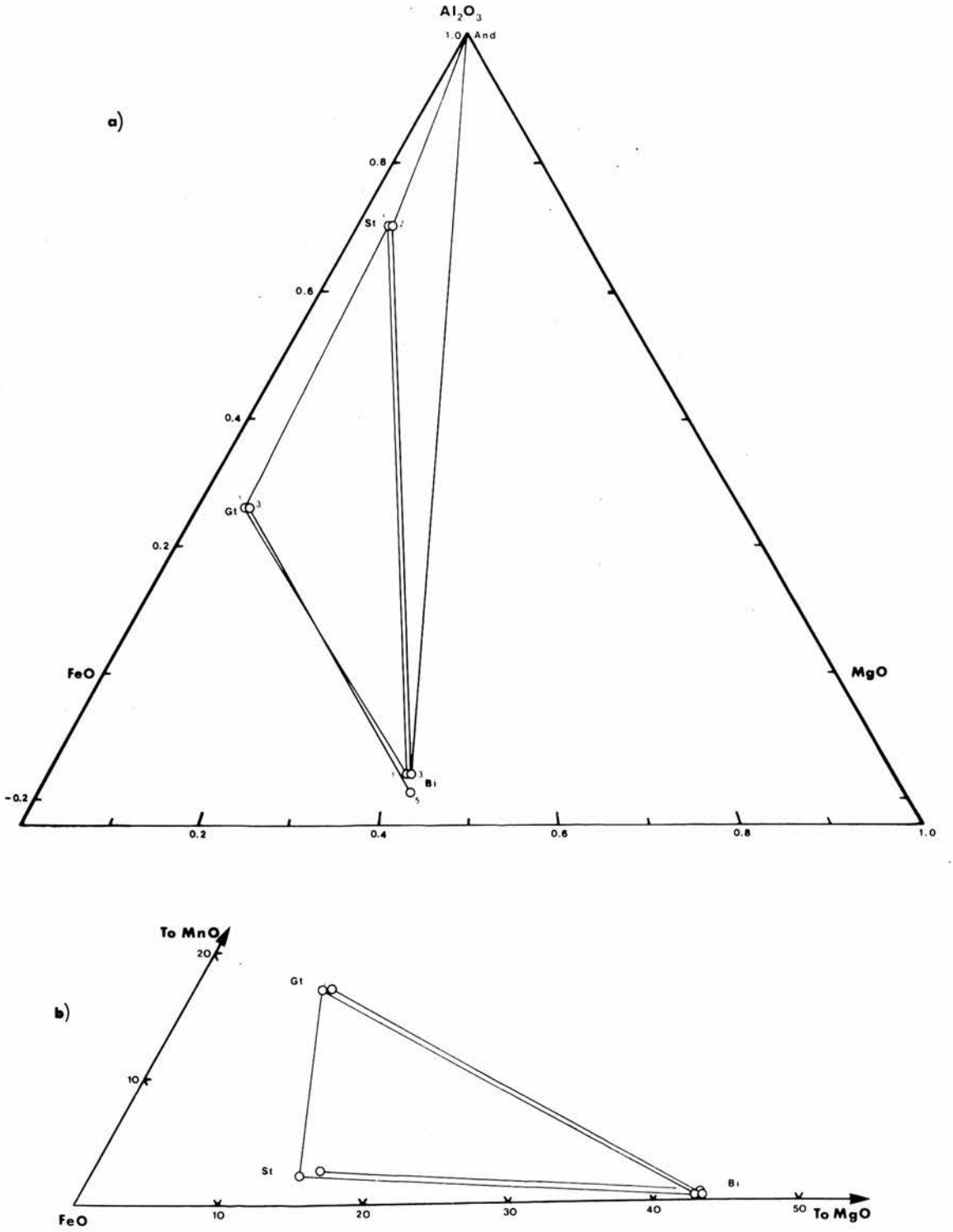

Figure 5.15: Chemical data from co-existing mineral mosaics in specimen 43945 near Kinnairdy (NJ 612501) presented in (a) Thompson projection (b) FeO -MgO -MnO plots.

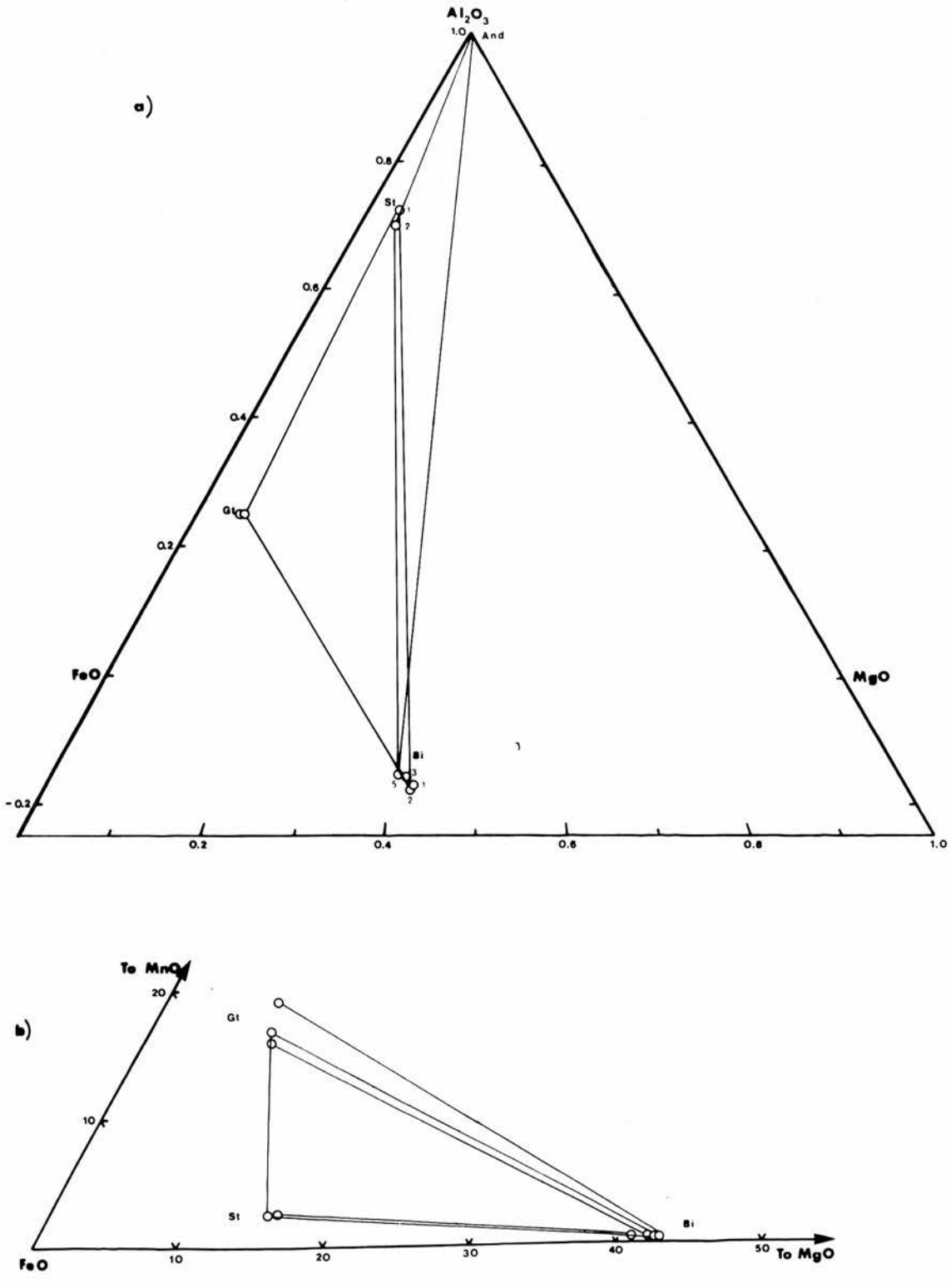

Figure 5.16: Chemical data from co-existing mineral mosaics in specimens 43939 and 43940 from Maunderlea Quarry (NJ 633563).

place in the rock. Mosaic assemblages and relevant chemical data are presented in table 5.4.

The data for specimen 43945 have been plotted to show compositional relationships in figure 5.15. Mineral tie lines on this diagram all show a sensible relationship. Although garnet-biotite tie lines cross on the muscovite projection (figure 5.15(a)) this problem is quickly resolved by the FeO-MgO-MnO plot (figure 5.15(b)) which indicates that the tie line for mosaic 3 lies at higher MnO values than its counterpart for mosaic 1.

The data for specimens 43939 and 43940 representing adjacent beds some one inch apart, are shown in figure 5.16. The range of compositions of garnet and biotite are larger for this specimen. Again garnet - biotite tie lines which cross in figure 5.16 (a) may be resolved by plotting in FeO - MgO - MnO (figure 5.16(b)) although one tie line (not plotted) for a mosaic 5 which is not associated with muscovite has a completely different slope.

Other crossed tie lines are less easy to explain. Biotite and staurolite constitute a mineral pair adjacent to an andalusite porphyroblast. This tie line is notably more Fe rich than the tie line biotite - staurolite which is in contact with garnet (Figure 5.16(a)) and this causes the tie line biotite - stuarolite to cross biotite - andalusite. A consideration of MnO (Figure 5.16 (b)) does not resolve this situation as both tie lines have virtually idential MnO contents.

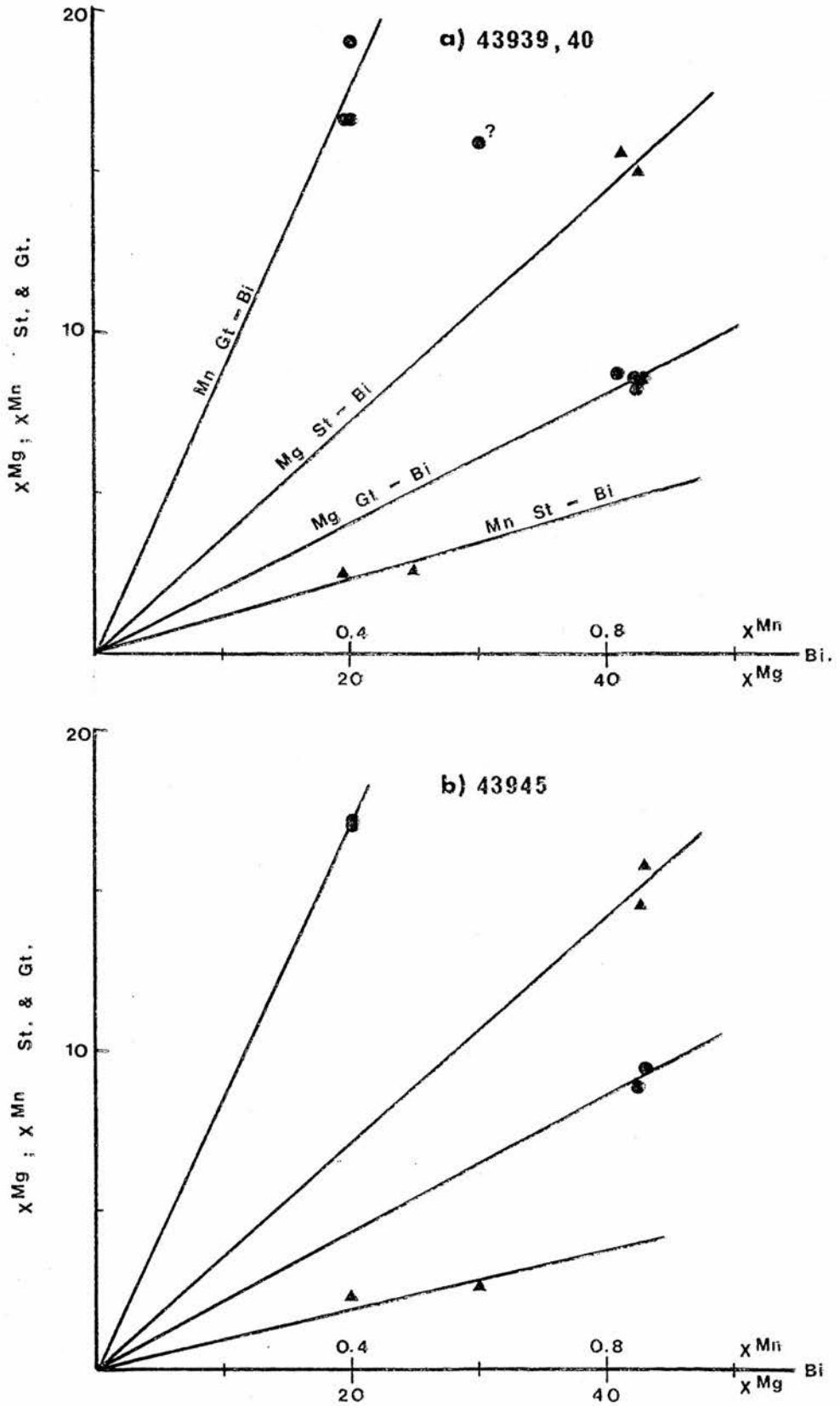

Figure 5.17: Graphs showing the distribution of Fe, Mg and Mn between co-existing phases from specimens (a) 43939 & 43940 (b) 43945.

Osberg (1971) has pointed out that variations in mineral composition through a single specimen are strong evidence that local or mosaic equilibrium has been attained where such variations can be shown to have occurred at a fixed K_D for the minerals and components in question (i.e. fixed T). Assuming that external variables are the same for the whole specimen, deviations from such a fixed K_D may be explained in terms of analytical error, departure from equilibrium or the effects of other components which have not been taken into account.

Distribution diagrams for Fe, Mg and Mn are presented in figure 5.17 for the two specimens under discussion. All the plots are relatively consistant with variations at constant K_D with the exception of X^{Mg}_{staur} vs X^{Mg}_{biot} which with respect to specimens 43939 and 43940 in particular seems to vary at right angles to a line of constant K_D on the plot.

Since the weight of evidence in figures 5.15, 5.16 and 5.17 points towards the achievement of mosaic equilibrium it would seem reasonable to turn to either analytical error or other component effects to explain the behaviour of biotite - staurolite tie lines.

Staurolite is in general difficult to analyse in these rocks due to the large number of inclusions which it invariably contains. This implies that some analyses may contain impurities but at the same time it is not always possible to place the electron probe beam on the grain at a spot immediately adjacent to a contacting grain. This might not be serious if it were possible to prove that

each individual staurolite crystal was internally homogeneous however the numerous inclusions often make this impossible, and in many cases where crystals are small, only two or at a maximum three spots may be found which are large enough to accept the electron probe beam. As a result, staurolite analyses are likely to be the least reliable.

The effect of other components may also be present due to Ca, Zn, Ti etc. in either biotite or staurolite. Zinc has been shown by other workers (e.g. Guidotti 1970) to be important in some staurolites however this is not the case in Banffshire where zinc was found to be barely above the limits of detection. Titanium in biotite is however detectable and shows a tendency to increase with increasing $X^{Mg}_{biotite}$. Taking an empirical relationship from a plot of weight per cent TiO_2 against $X^{Mg}_{biotite}$ suggests an increase of 1.3 per 0.1 weight per cent TiO_2 . However projecting to an equal TiO_2 content does not only fail to resolve the crossed staurolite-biotite tie lines but also causes crossing of garnet biotite tie lines.

Considering the small compositional differences involved it seems most reasonable to attribute the crossed staurolite-biotite tie lines to experimental error.

Recognition of MnO as an additional variable implies that each of the three phase assemblages (+ musc and quartz) staurolite - garnet - biotite; andaulusite - stuarolite - biotite; andalusite - cordierite - biotite is in fact trivariant and will be represented

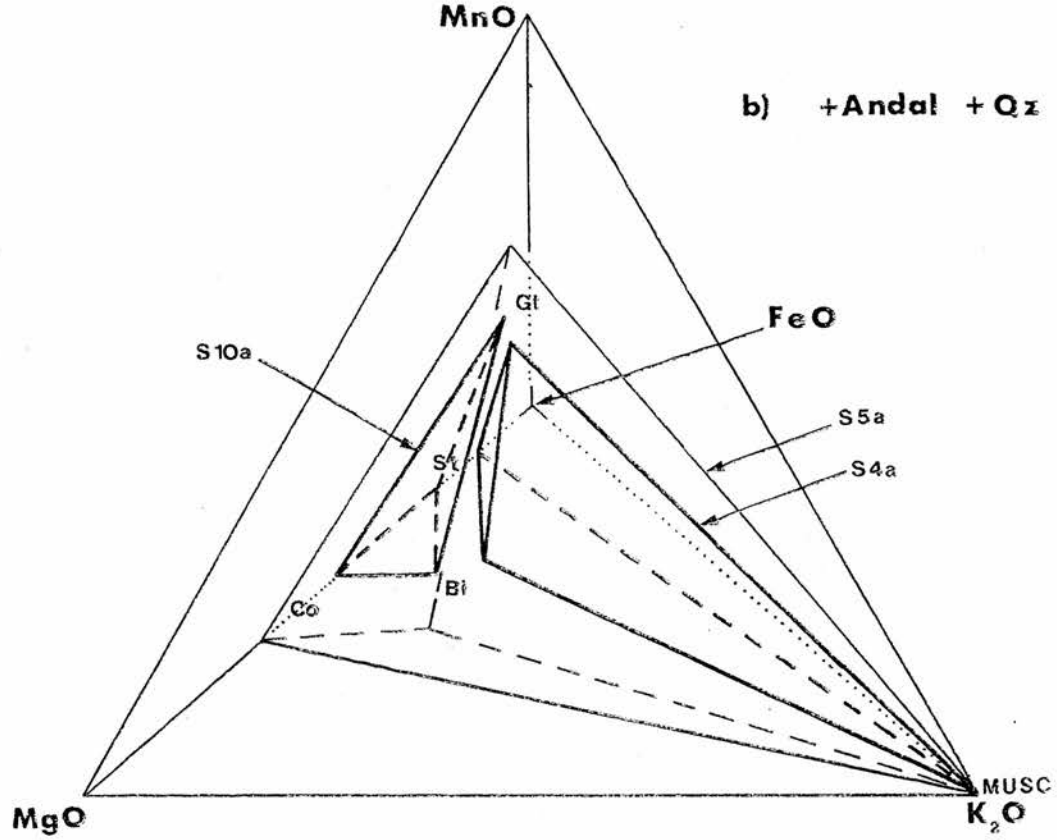

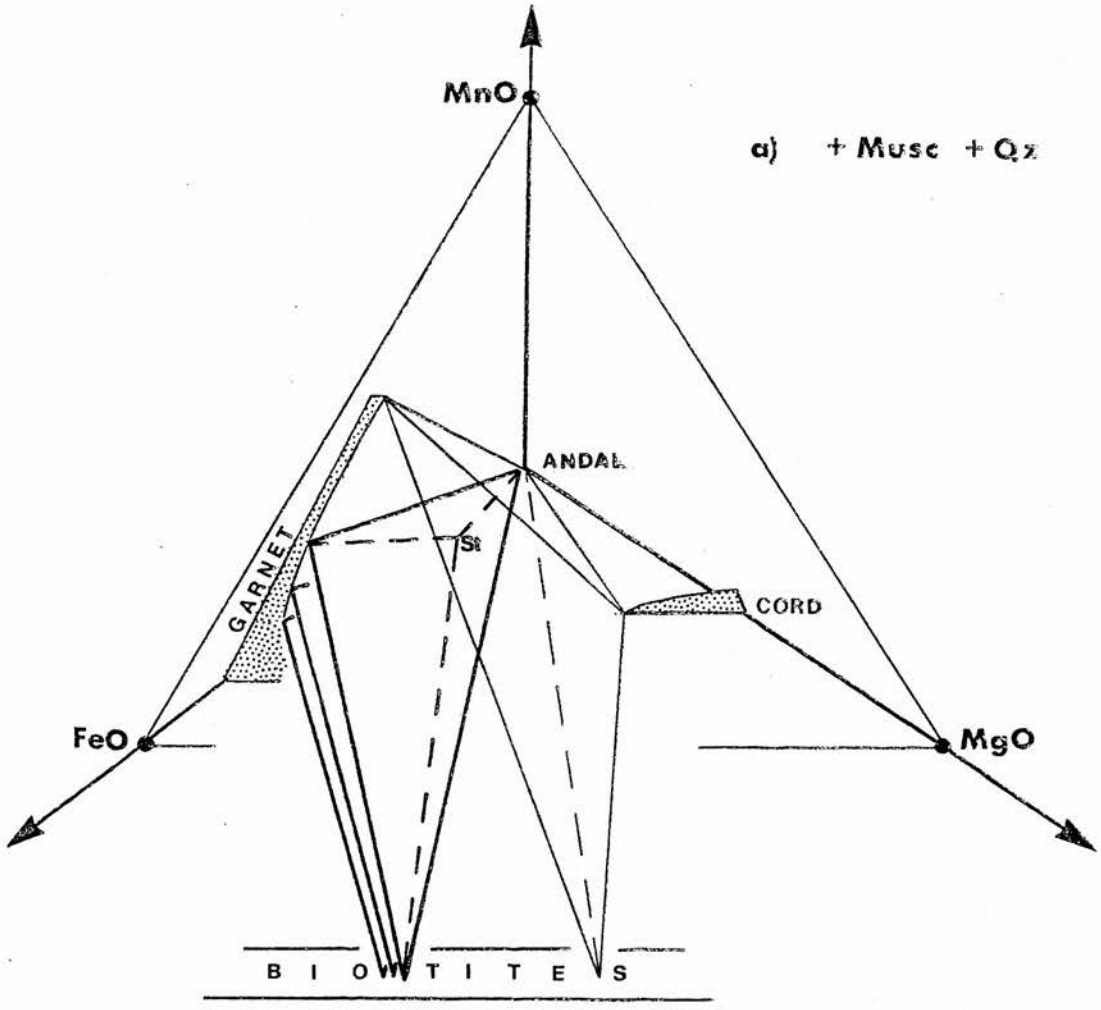

Figure 5.18 : Perspective models representing garnet parageneses in the staurolite zone.

by tie planes in the system shown in figure 5.18(a). Mineral compositions in each of these assemblages can vary at P, T fixed.

It is notable that minor variations in mineral composition are the rule within any particular specimen. This does not negate the evidence previously put forward to show that systematic variations are detectable which are attributable to grade differences. The internal variations within each specimen have been represented in figure 5.12 as the axes of the plotted ellipses. These show that the internal variations are much smaller than the variations due to grade in the two assemblages S.4 and S.10. This is not however true of garnet compositions.

Because of the orientation of garnet - biotite tie lines in FeO-MgO-MnO space small variations in bulk compositions at low MnO values can cause considerable variation in the composition of garnet whilst having only a minor effect on the coexisting biotite.

As a result any grade controlled variation of garnet composition is virtually impossible to pick out, and the present results seem to show random variation. Any systematic study would require data from 6 phase mosaics which remain divariant but are virtually impossible to find or alternatively from enough 5 phase mosaics to define the 6 phase volume.

Distribution of Fe^{++} and Mg between garnet and biotite

Systematic studies of $K_{D_{gt-bi}}^{Fe-Mg}$ (e.g. Albee 1965a, Lyons and Morse 1970) have indicated that the distribution coefficient is related

to grade, its value increasing as grade increases. Albee (1965a) noted that it is also related to the manganese content of the garnet so that projection to an arbituary standard value of X_{gt}^{Mn} (generally 0) is necessary before making comparisons between data from different metamorphic grades. He suggested the following average values of K_D, after projection to $X_{gt}^{Mn} = 0$, for a typical 'Barrovian' sequence:-

garnet	zone	0.2
staurolite	zone	0.215
kyanite	zone	0.23
sillimanite + k'spar	zone	0.3 - 0.37

Provided that the pressure dependence of the distribution coefficient is small values obtained from rocks of the staurolite zone of the present study should be comparable with values for the kyanite zone discussed by Albee (1965a). (i.e. Al_2SiO_5 - staurolite - garnet - biotite - muscovite is stable in each). However $K_D^{FeMg}{}_{gt-bi}$ for seven garnet-biotite pairs from samples 15463, 43939, 43940, 43045, 43918 gave an average value of 0.29 ± 0.02, close to Albee's value for the sillimanite + k'spar zone. The discrepancy is too large to be attributed to the pressure dependence of K_{Dgt-bi}^{Fe-Mg} computed by Albee (1965a) as $2\frac{1}{2}\%$ / Kb which would suggest a pressure differential of 9Kb between the two sequences. There is no systematic variation of K_D across the staurolite zone in Buchan.

Limited data from 'Buchan Type' sequences in other metamorphic terrains are available from the literature (Osberg 1971, Fleming

1972). The data of Osberg (1971) from South Central Maine are from one staurolite zone locality and after correction for X_{gt}^{Mn} gave $K_{D\ gt-bi}^{Fe-Mg} = 0.285 \pm 0.015$, which is in good agreement with that obtained for Buchan.

The data of Fleming (1972) are not so encouraging. These are from andalusite and staurolite rocks from the Mount Lofty Ranges and yield corrected K_D of 0.178 - 0.238. This is a much lower value than that reported by Osberg (1971) and this study, and furthermore covers the range of values given by Albee (1965a) for the garnet to the kyanite zone. The situation with respect to $K_{D\ gt-bi}$ is obviously not clear and the low value for the Australian rocks is further complicated by the fact that they carry fibrolite in addition to andalusite.

Saxena (1973) Sen and Chakraborty (1968) have suggested that $K_{D\ Gt-bi}^{Fe-Mg}$ requires further correction for components other than MnO which may be incorporated in either mineral. Saxena (1973) further suggests that after such modifications a transformed K_D may be used to derive a temperature value. Such a calculation for the Buchan rocks gave an anomalously low value of 350°C.

Distribution of Ca between garnet and plagioclase

Kretz (1964) suggested that the ratio X An/ X_{gt}^{Ca} where:

X An = An/An+Ab in plagioclase

X_{gt}^{Ca} = 100 CaO/CaO + FeO + MgO + Mno in garnet

might be useful as a relative pressure indicator. A great deal of

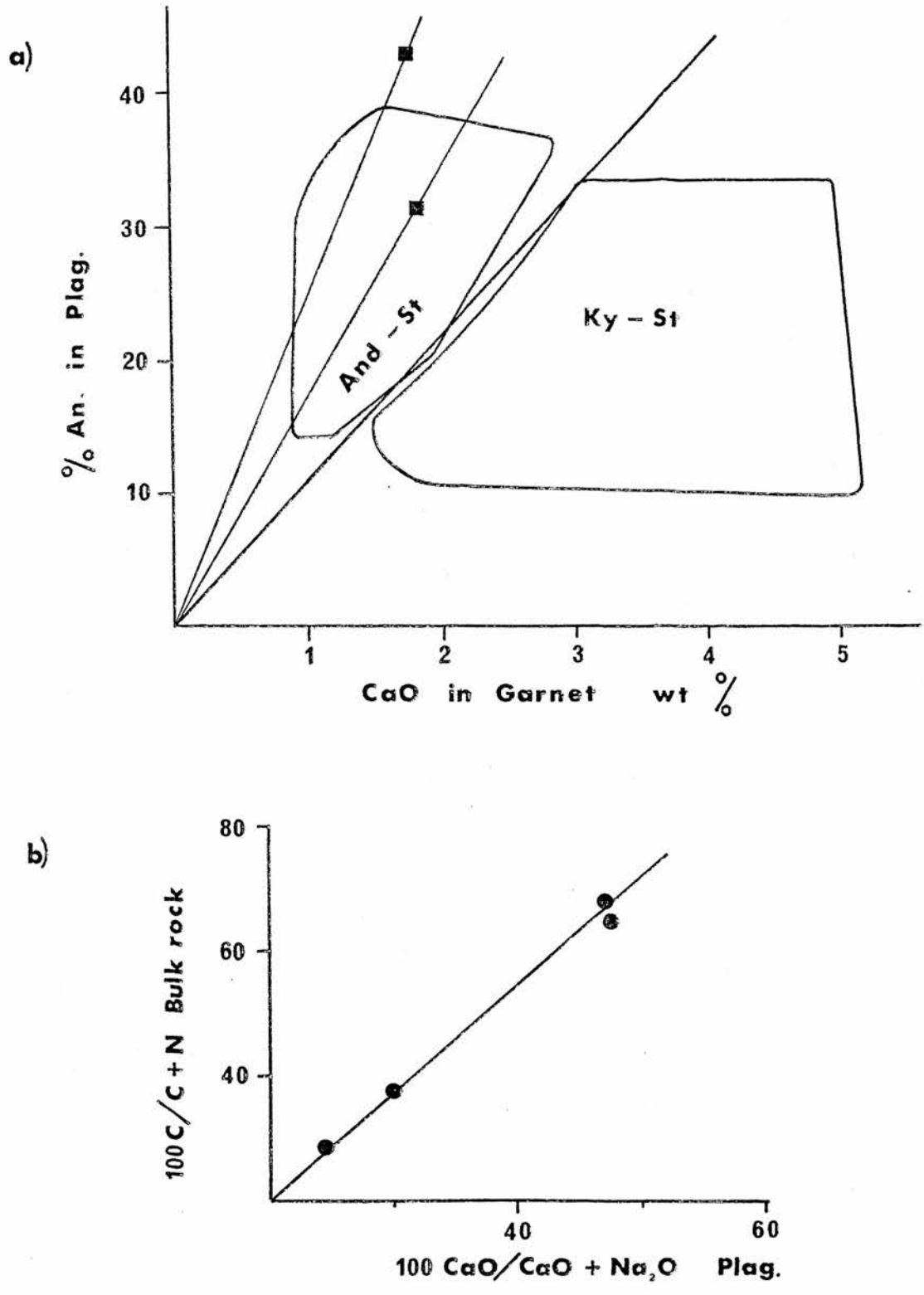

Figure 5.19: The relationship between (a) CaO in garnet and % An in co-existing plagioclase. Ky-Sill and And-Sill fields after Kepezhinskas (1973); (b) the composition of plagioclase and the host rock.

evidence has been amassed by Kepezhinskas (1973) in support of this suggestion, for rocks within the middle grades of metamorphism. Figure 5.19(a) shows the relationship between anorthite molecule content of plagioclase and the CaO content of coexisting garnet. The fields occupied by mineral pairs from the staurolite (kyanite) and staurolite (andalusite) zones are shown after Kepezhinkas (1973 figure 2) along with two specimens 43945 and 43918 from Buchan. These two rocks plot clearly within the low pressure field and also suggest an upgrade pressure increase within the staurolite zone in Buchan.

5.6. Rocks containing the ortho-amphibole Gedrite

Gedrite bearing assemblages are rare and it is notable that the ortho-amphibole never occurs in association with muscovite (see Chapter 2 section 6). As such these rocks could perhaps be treated along with the other muscovite free rocks but their unusual potash deficient bulk compositions (see Chapter 4 section 4) render them a special case.

The rocks may be treated within the chemical system previously discussed. Mineral compositions from specimens 43923 (Banff Coast) and 43962 (Collieston Harbour) have been plotted on an AFM diagram in figure 5.20. All assemblages also contain biotite.

The complete assemblage in specimen 43923 is:- staurolite - gedrite - cordierite - garnet - biotite - plagioclase - quartz - ilmenite. Though cordierite and garnet tend to be concentrated in distinct

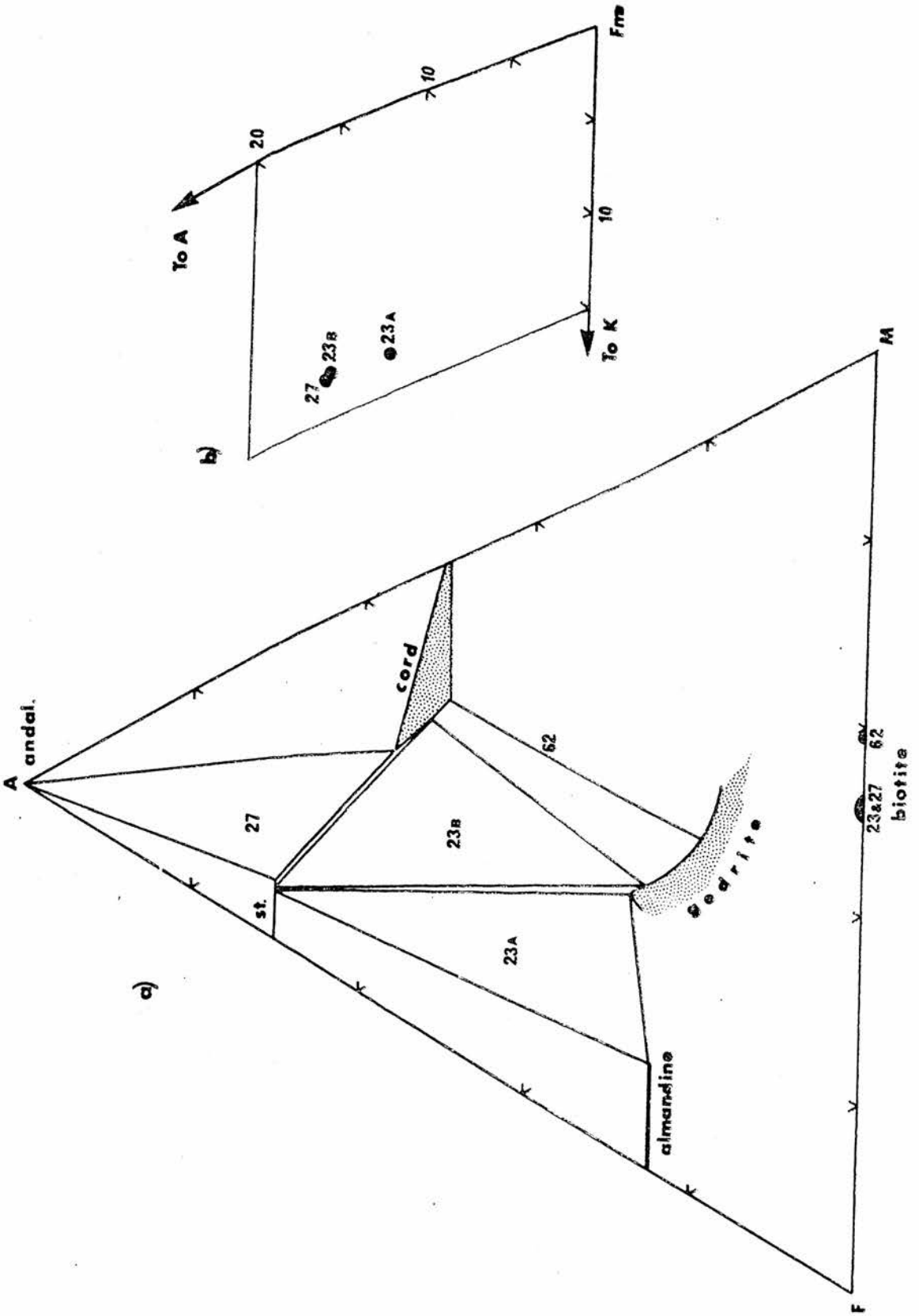

Figure 5.20: Assemblages and mineral compositions in muscovite free rocks near Whyntie Head (NJ 631659).

bands small rare garnets do occur within cordierite rich horizons. Based on this almost complete separation of the two minerals and the Almandine rich nature of the garnet in this rock (Alm 76 Py 16 Spess 6) it may be valid to treat these horizons as distinct assemblages to a first approximation. The sensible relationship of staurolite-gedrite tie lines in figure 5.20 supports this. Staurolite-corderite tie lines also show a sensible relationship when specimen 43923 is considered in relation to specimen 43927 (assemblage S.10.). Even though the relative M/FM of cordierite in these two rocks is apparently inverted the tie lines do not cross because of the high alumina content of cordierite in the latter assemblage (see chapter 3 section 5).

Although specimen 43962 is from a different locality it has also been plotted on this diagram as it gives some indication of the orientation of cordierite-gedrite tie lines in more Mg rich bulk compositions, and indicates that gedrite tends to become more aluminous at more iron rich compositions.

All the assemblages shown in figure 5.20 invariably carry biotite in addition. Although there is a small range of X_{biot} in each rock the biotite associated with assemblages S.10 and S.11a have essentially the same MgO/MgO + FeO ratios. The biotite, however, in the gedrite bearing rocks tends to be less aluminous than that from assemblage S.10. These biotite compositions are represented in an AKF plot, figure 5.20 (b) whilst their MgO/MgO + FeO ratios are represented on a linear scale in figure 5.20 (a).

Maps 4 & 5

Map 4: The distribution of assemblages and isograds in the Banff - Aberchirder area.

Map 5: The distribution of assemblages and isograds in the Fyvie - Methlick area.

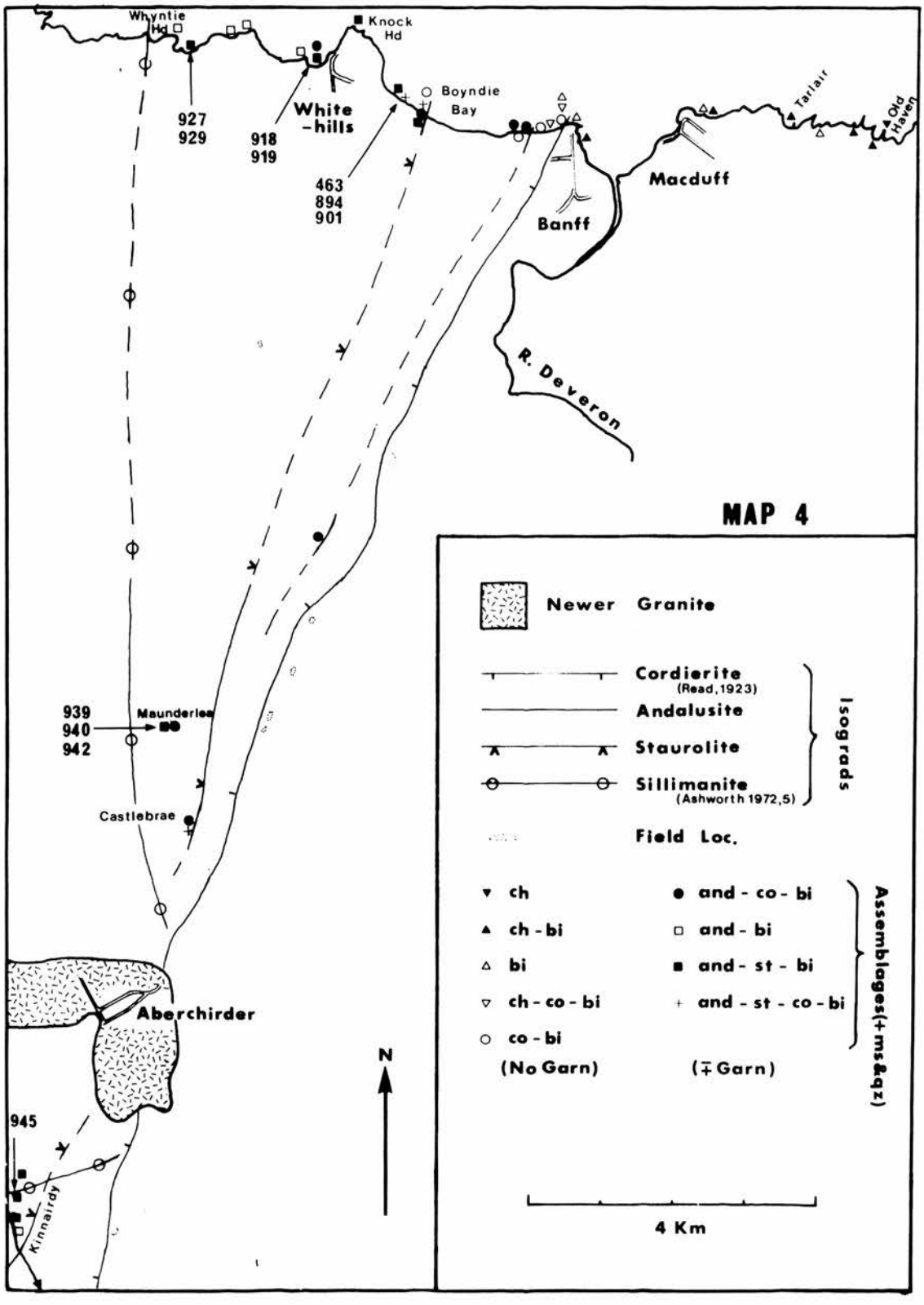
Whyntie Hd
Knock Hd
Boyndie Bay
927
929
White -hills
918
919
463
894
901
Tarlair
Old Haven
Macduff
Banff
R. Deveron
939
940
942
Maunderlee
Castlebrae
Aberchirder
945
Kinnairdy
N
MAP 4
Newer Granite
Cordierite
(Read, 1923)
Andalusite
Staurolite
Sillimanite
(Ashworth 1972,5)
Isograds
Field Loc.
ch
ch - bi
bi
ch - co - bi
co - bi
(No Garn)
and - co - bi
and - bi
and - st - bi
and - st - co - bi
(∓ Garn)
Assemblages(+ms&qz)
4 Km

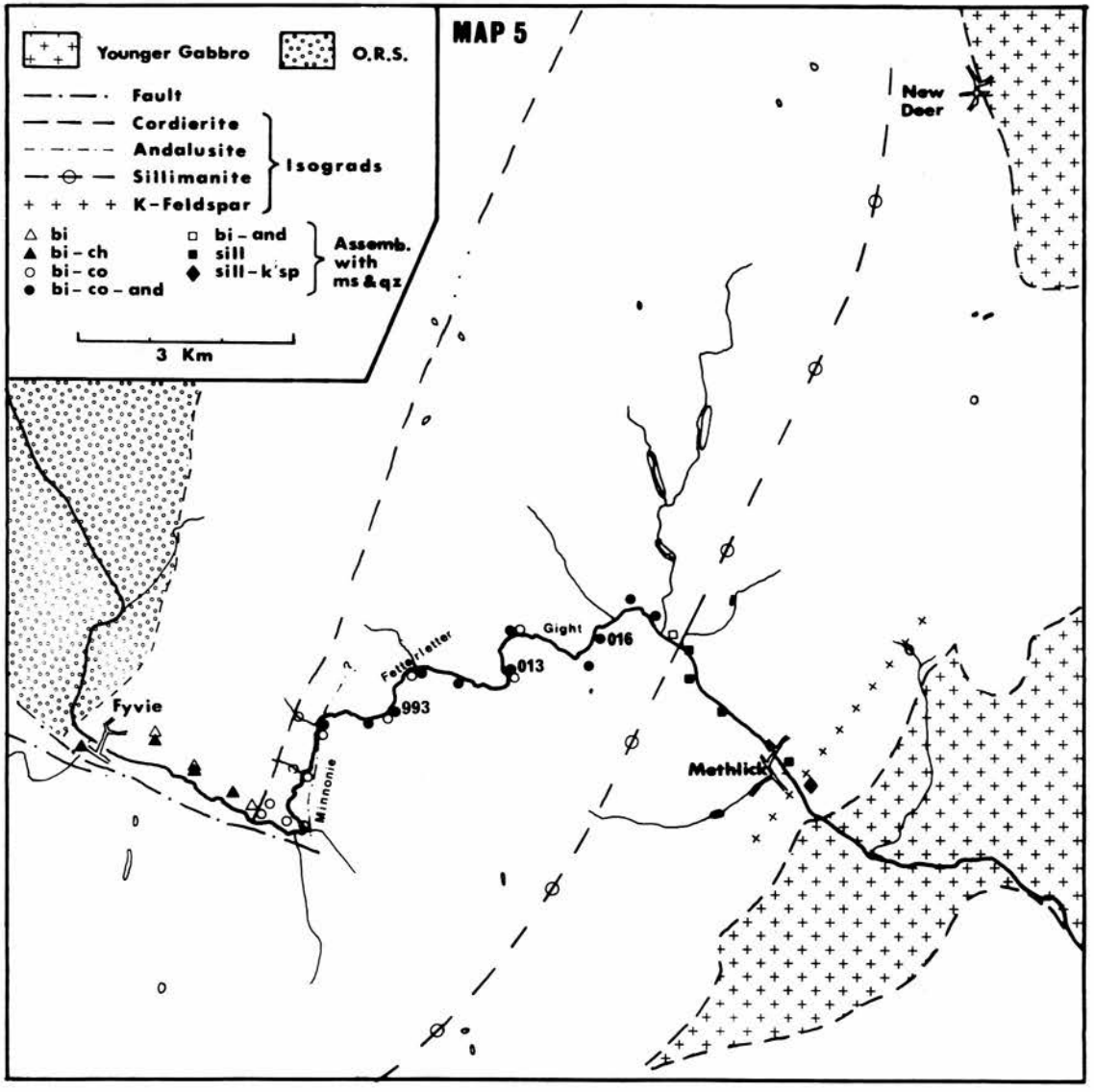
MAP 5
Younger Gabbro
O.R.S.
Fault
Cordierite
Andalusite
Sillimanite
K-Feldspar
Isograds
bi
bi-ch
bi-co
bi-co-and
bi-and
sill
sill-k'sp
Assemb. with ms & qz
3 Km
New Deer
Fyvie
Minmonie
Fetterletter
993
013
Gight
016
Methlick

CHAPTER 6

Inter-relations and Implications for the Intensive Parameters of Metamorphism

6.1. Introduction

The purpose of this chapter is to consider chemical and thermodynamic aspects of the mineral assemblages and reactions which govern the first upgrade appearance of the minerals: cordierite, andalusite, staurolite and garnet; and in conjunction to consider their relations and implications with regard to temperatures and pressures of metamorphism and petrological data from other metamorphic terrains.

In Chapter 5, mineral assemblages were largely considered in terms of the systems Al_2O_3 - K_2O - FeO - MgO - SiO_2 - H_2O (AKFMSH) and Al_2O_3 - K_2O - FeO - MgO - SiO_2 - H_2O - MnO (AKFMSHMn), and these two model or ideal systems will also be used in the present chapter. The adoption of these systems is largely justified on the grounds put forward by Thompson (1957) and allows use to be made of the 'Thompson Projection' from muscovite for muscovite and quartz bearing assemblages. The phases ilmenite, sulphide, apatite and tourmaline are considered to be stabilised by the additional components TiO_2, SO_2, P_2O_5, B_2O_3 and these phases and components are believed to have little significant effect upon equilibria discussed subsequently for the phases: quartz, white mica, chlorite, biotite, cordierite, andalusite, staurolite and garnet. The only major departure from Thompson's (1957) treatment is to

consider garnet to be always stabilised by the additional component MnO. This is because the garnets are characteristically MnO-rich and occur as an additional phase to other mineral assemblages (Chapter 5 section 5), resulting in some assemblages of six solid phases which would have negative variance in AKFMSH at constant T, P_s and u H_2O. Thus where garnet phase equilibria are considered, MnO is treated as an independent chemical component and the system becomes AKFMSHMn.

With regard to the two potentially important variables fO_2 and μH_2O, little precise information is available for the rocks in question. The fO_2 appears to have been probably uniformly low (see Chapter 5 sections 3 and 4) whilst, in the absence of any indication to the contrary, μH_2O is considered, following Thompson (1957) to have been constant.

6.2. Resume of the major mineral assemblages occurring on the Banffshire Coast.

Idealised phase relations for rocks bearing muscovite and quartz in each of the biotite, cordierite, andalusite and staurolite zones, are shown in figure 6.1. Where possible mineral compositions have been plotted for the low grade boundary of each zone.

Within the lowest grade part of the biotite zone the range of available bulk compositions show the two assemblages:-

chlorite - phengite (B1)

chlorite - biotite - phengite (B2)

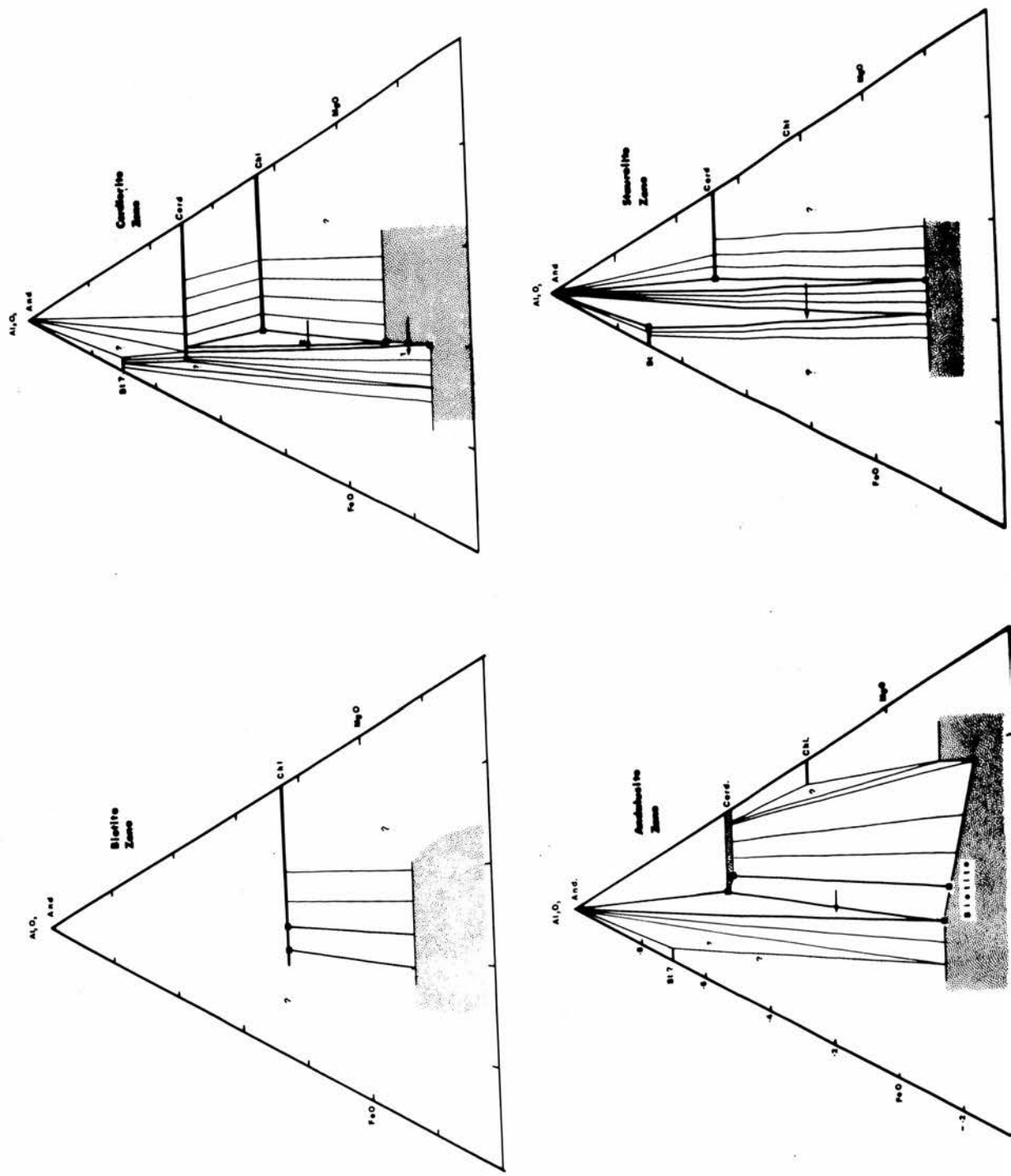

Figure 6.1: Thompson projections representing mineral assemblages in the (a) biotite (b) cordierite (c) andalusite (d) staurolite zones.

With increasing grade, the volume occupied by muscovite - chlorite - biotite tie planes expands, principally in response to the restriction of white mica compositions towards ideal muscovite (Chapter 5 section 1). This has the effect of raising the plane filled by phengite - chlorite tie lines to more aluminous compositions than those normally encountered in the rocks and thus eliminates assemblage (B1).

In the higher grade part of the biotite zone, pelitic rocks show assemblage (B2) whilst more siliceous (and therefore correspondingly less aluminous (figure 4.5(b)) semipelites show the assemblage biotite - phengite (B3).

Near Banff, the cordierite isograd is encountered in rocks which are largely semipelitic, and the assemblage change across it is essentially as follows:-

biotite - phengite	(C3)	) cordierite
cordierite - biotite - phengite	(C2)	) isograd

This assemblage biotite - phengite (C3) persists in some rocks whilst in rare cases primary chlorite is present along with cordierite giving the important assemblage:-

cordierite - biotite - chlorite - phengite (C1)

Figure 6.1(b) shows assemblages just above the cordierite isograd, which is considered to be generated by a grade controlled movement of the three phase triangle cordierite - biotite - chlorite (i.e. assemblage C1), to more Mg-rich compositions,

(See Chapter 5 section 2 for full discussion). The assemblage changes at the isograd, predicted by this model are shown by two short arrows in figure 6.1(b). The arrow labelled 1 corresponds to the assemblage change (B3) - (C2) the more normal case in the field, whilst the arrow labelled 2 indicates how assemblage (C1) may develop from asseblage (B2).

The andalusite isograd is encountered near Scotstown. At this grade the white mica is close to muscovite in composition and the assemblage change is essentially as follows:-

cordierite - biotite - muscovite (C2) below } Andalusite
andalusite - cordierite - biotite - muscovite (A1) above } Isograd

The assemblage cordierite - biotite - muscovite (A2) ≡ (C2) persists above the isograd. This isograd is considered to be generated as a result of upgrade movement of the stability field of (A1) to encompass more Mg-rich bulk compositions, (see Chapter 5 section 3). The assemblage change at the isograd predicted by the model is shown by the short arrow in figure 6.1(c).

Immediately west of Boyndie Bay the staurolite isograd is encountered. Here the range of assemblages is more complex (Table 5.2) but may be summarised as follows; neglecting garnet:

andalusite - staurolite - biotite - muscovite (S.4)
andalusite - cordierite - biotite - muscovite (S.5) ≡ (A.1)
andalusite - staurolite - cordierite - biotite (S.10)

In this zone upgrade Mg-enrichment of biotite may be demonstrated in each of the assemblages (S.4) (S.5) and (S.10). Mg-enrichment of staurolite also occurs in assemblages (S.4.) and (S.10) though much less rapidly, (Chapter 5 section 4). The model for the staurolite isograd is thus similar to those for the two isograds discussed above.

As the stability fields of assemblages (S.4) (S.5) and (S.10) move to encompass more Mg rich bulk compositions upgrade, the assemblages will change, though the actual changes registered will depend on the potash content of the rocks. The assemblage change predicted for rocks with excess muscovite throughout (potash rich) is shown by the short arrow in figure 6.1d i.e. (A1.) = (S.5) → (S.4) whilst potash poor rocks will register the change (A.1) = (S.5) → (S.10) (see figure 5.11).

The evidence for the appearance of garnet in the rocks is less clear. The component MnO is obviously involved (see Chapter 5 section 5) but the appearance of garnet seems intimately linked with the staurolite isograd on the Banffshire coast since the two minerals appear together. The evidence put forward in chapter 5 suggests that the rare assemblage andalusite - cordierite - biotite - garnet (S.5a) is also a potential assemblage below the staurolite isograd and this is supported by its rare occurrence in the andalusite zone near Rosehearty (Johnson 1962). Near Whitehills, the two assemblages andalusite - staurolite - biotite - garnet (S.4a) and andalusite - cordierite - biotite (S.5) occur together, (specimens 43918,43919).

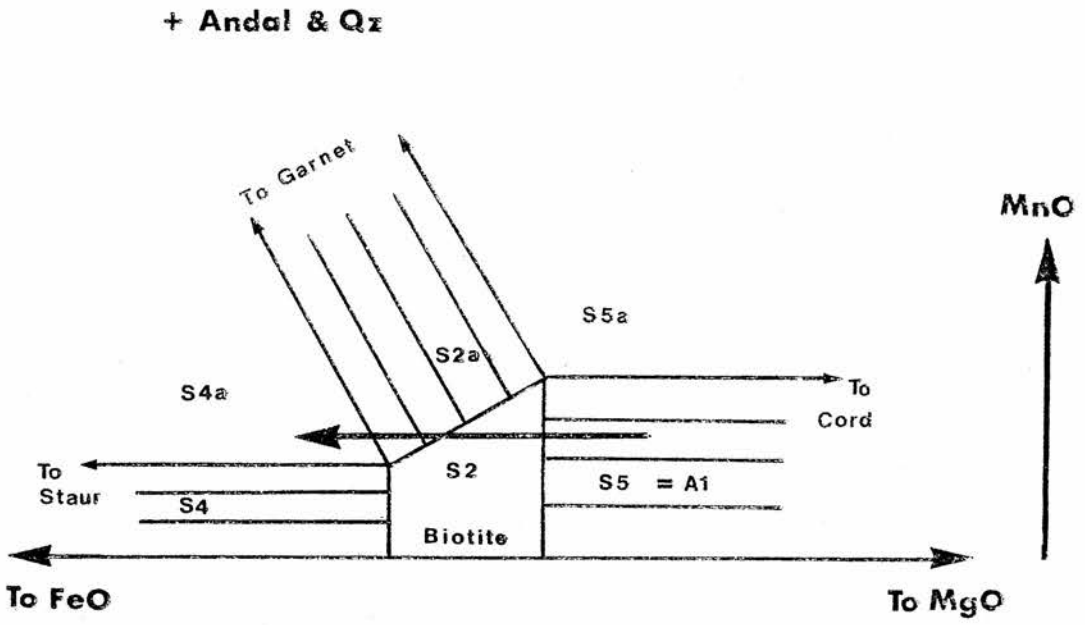

Figure 6.2: A model for the appearance of garnet at the staurolite isograd.

The maximum MnO content in biotite from each of these specimens is essentially the same and this suggests that biotite in equilibrium with the potential assemblage S.5a must be MnO richer, (see figure 6.2). Some support is given to this by the relations in figure 5.14a which shows that garnet in equilibrium with cordierite - biotite - andalusite, though in assemblage S.10a is more MnO rich than garnet in assemblage 4a.

Figure 6.2 shows, schematically, the probable arrangement of tie lines near biotite compositions. If this is correct, bulk compositions registering assemblage S.5a require to have a much higher MnO content than those registering S.4a and this is a likely reason for the rarity of the former assemblage. The predicted assemblage change, as a result of biotite compositions becoming more Mg-rich upgrade, is shown by the arrow in figure 6.2 for bulk compositions with the critical MnO content below that required to realise S.5a but above that required to register S.4a.

6.3. Reactions representing assemblage changes on the Banffshire Coast

Thompson (1957) has pointed out that metamorphic reactions may occur in two ways. Where a phase or phase assemblage becomes unstable with respect to another, for some change in external conditions in a given system, a sharp topological discontinuity will occur. Such "Discontinuous Reactions" are univariant and may be represented as a line on a P,T plot. Alternatively, where

some or all of the phases in an assemblage are solid solutions these will, in general, show continuous compositional variation in response to changing external conditions. This is achieved by "Continuous Reaction" between phases (di-or multi-variant) and will result in a continuous shift of the assemblage's compositional stability field. The isograd reactions occurring in Buchan are clearly of this type (Chapter 6 section 2). For a fixed bulk composition, the stability of a divariant equilibrium may be considered in terms of P, T and X (composition of phases), and may be projected onto the P,T plane where it will usually appear as a parallel sided or wedge shaped region. This will hereafter be referred to as a "divariant transition field" for the sake of brevity but it should be remembered that its width and position in P,T space are functions of the bulk composition chosen and the distribution of critical components between phases (i.e. width of compositional stability field of the assemblage) as well as P and T.

Reactions representing divariant equilibria may be written in two ways:

(a) Equations which represent the movement of assemblage stability fields by changes in the chemical composition of phases. (e.g. Chinner 1965, Evans and Guidotti 1966, Guidotti 1970). Such reactions will hereafter be termed 'Incremental Reactions' in this study.

(b) Equations which represent net assemblage changes from

one side of a divariant transition field to the other. (e.g. Hess 1969, Hensen 1971). Such reactions will hereafter be termed 'Net Reactions' for the purposes of this study.

The two types are of course intimately linked since net reactions are undoubtedly brought about by incremental reactions. The binary system albite - anorthite serves to illustrate the relationship (Figure 6.3a).

In this system there are two trivariant fields separated by a divariant (isobarically univariant) melting loop. Consider the crystallization of a liquid of composition Ab_{30}. The net reaction linking assemblages on either side of the divariant melting loop would be:-

$$L \rightleftharpoons plag_{ss}$$

which refers to the temperature interval T_1 to T_3. Equally, incremental reactions could be written as follows:-

from T_1 to $T_1 - \delta T$:- $L \rightleftharpoons L_{Ab.richer} + plag.ss$

from $T_3 + \delta T$ to T_3 :- $L + plag._{ss} \rightleftharpoons plag.ss_{Ab.richer}$

Incremental reactions are usually written for the edges of divariant transition fields where a phase appears or disappears as above (c.f. Chinner 1965) but can equally be written for increments of T (or P etc) within the field, e.g.:-

from T_2 to $T_2 - \delta T$:- $L + plag._{ss} \rightleftharpoons L_{Ab.richer} + plag.ss_{Ab.richer}$

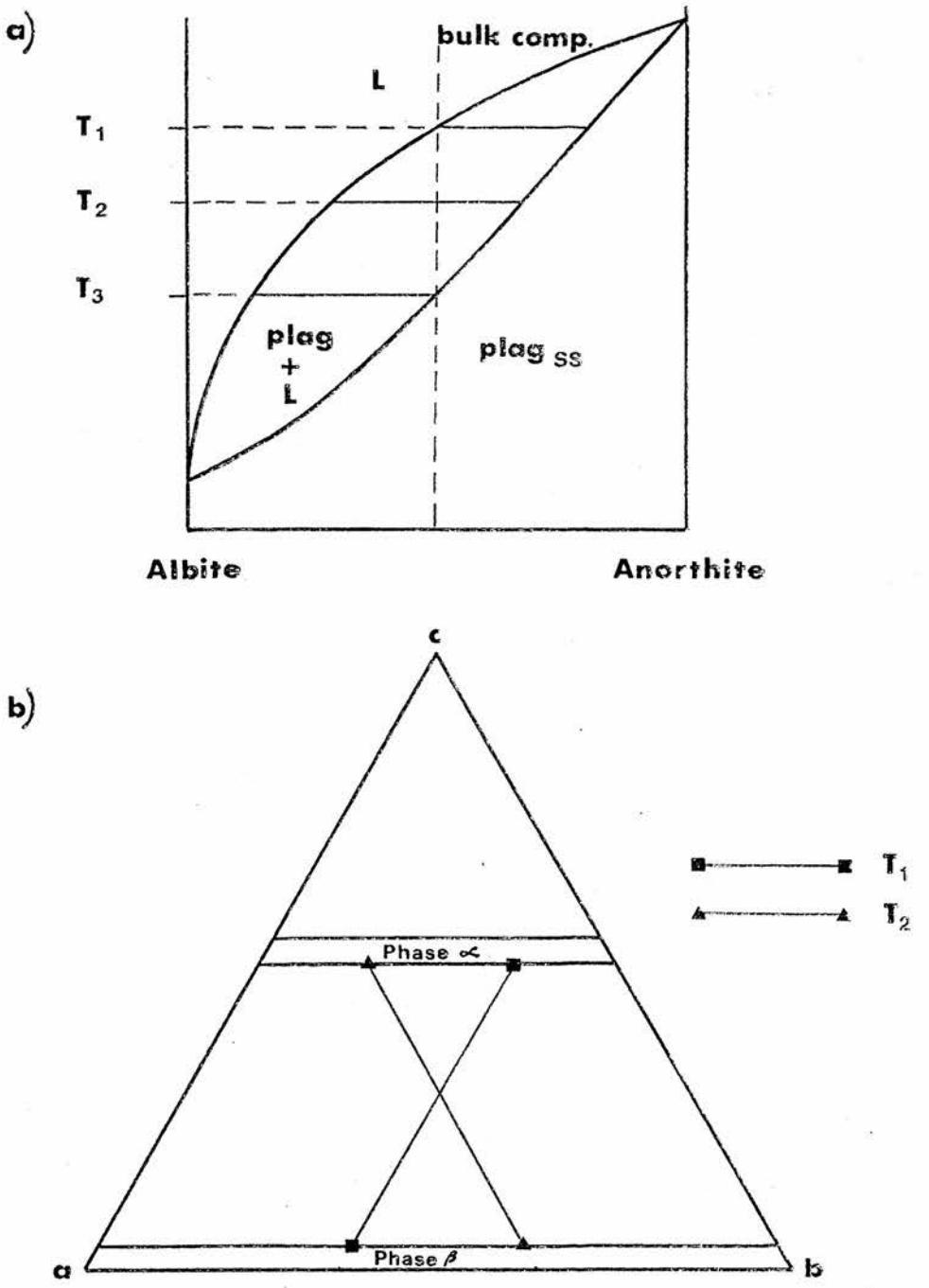

Figure 6.3: T - X sections illustrating di- and tri- variant equilibria in binary and ternary systems. a) The system albite-anorthite (after Bowen, 1928). b) The hypothetical system abc.

All of the above reactions involve two phases and are thus divariant in the binary system. Both types have points of merit. Incremental reactions are often cumbersome but can give information on the actual compositions of phases, whilst net reactions gain in simplicity but may lose the detail. Both types of reaction will be used in the following discussions.

Trivariant continuous reactions may also occur (Figure 6.3b). In a ternary system these will be of the form:

$$\alpha + \beta = \alpha_{\text{a richer}} + \beta_{\text{b richer}}$$

and will produce changes in the distribution of components between phases. In quaternary and multicomponent systems these may also effect the appearance and disappearance of phases.

It is now possible to write equations for isograd reactions based on the assemblage and chemical data presented in Chapter 5 and summarised in Chapter 6 section 2. Reactions are written so that the low grade assemblage appears on the left.

Assemblage changes at the cordierite isograd may be represented by the net reaction (omitting quartz and H_2O):

chlorite + muscovite $\rightleftharpoons$ cordierite + biotite 1

or alternatively by incremental reactions as follows:-

chlorite + biotite + muscovite $\rightleftharpoons$
cordierite + chlorite$^*_{\text{Mg richer}}$ + biotite$^*_{\text{Mg richer}}$ 1a

Where $X_{chlorite}^{*} = 42$, and $X_{biotite}^{*} = 40$

$$\text{cordierite} + \text{chlorite} + \text{biotite} + \text{muscovite} \rightleftharpoons \text{cordierite}_{\text{Mg richer}} + \text{biotite}_{\text{Mg richer}} \qquad 1b$$

Reaction 1a represents the beginning of stability of the divariant four phase assemblage (C.1). However, the compositional stability field of this assemblage appears to be very narrow such that remaining chlorite will be rapidly consumed by further incremental reactions culminating in reaction 1b. The position of the isograd in the field marks the line where reaction 1a occurs for the most Fe-rich bulk compositions present.

Assemblage changes at the andalusite isograd may be represented by the net reaction:-

$$\text{cordierite} + \text{muscovite} \rightleftharpoons \text{andalusite} + \text{biotite} \qquad 2$$

or alternatively by an incremental reaction for the beginning of the divariant transition field of assemblage A.1 :-

$$\text{cordierite} + \text{biotite} + \text{muscovite} \rightleftharpoons \text{cordierite}^{*}_{\text{Mg richer}} + \text{biotite}^{*}_{\text{Mg richer}} + \text{andalusite} \qquad 2a$$

Where $X_{cordierite}^{*} = 56\ (53)$, and $X_{biotite}^{*} = 42.5(40)$

(Values in brackets for Ythan Valley)

Further incremental reactions with increasing grade result in the

conversion of assemblage 1.A into either andal.- biot.- musc. or andal. - biot. - cord., depending on whether cordierite or muscovite is completely consumed first. This is a function of the K_2O content of the bulk rock compositions (see Figure 5.11).

(K rich case) andalusite + biotite (musc.left)
Mg richer

cordierite + biotite + muscovite ⇄ 2b

(K defficient case) andalusite + cordierite + biotite
Mg richer Mg richer
(no musc. left)

The staurolite isograd in the field is generated in muscovite bearing rocks by a net reaction as follows:-

andalusite + biotite ⇄ staurolite + muscovite 3

The beginning of stability of assemblage S.4 may be represented by the incremental reaction:

andalusite + biotite ⇄
staurolite* + biotite* + muscovite 3a
Mg richer

Where $X_{biotite}^{*} = 40$, and $X_{staurolite}^{*} = 15$.

The appearance of assemblage S.10 in these rocks appears to be brought about by a net reaction

cordierite + andalusite ⇄ staurolite 4

from rocks committed to the K defficient group by reaction 2b.

This net reaction takes place within the quaternary system AKFM by the incremental reaction

cordierite + biotite + andalusite ⇌
cordierite (Mg richer) + biotite + staurolite (Mg richer) 4a

which marks the beginning of stability of the divariant assemblage S.10.

The appearance of garnet at the staurolite isograd gives rise to assemblage (S.4a) which is divariant in the system AKFM-Mn. However, a net reaction analogous to reaction 3 shows garnet on the wrong side of the equation:

andalusite + biotite + garnet ⇌ staurolite + muscovite 5

The model proposed in figure 6.2. is actually a two stage process which may be written as two incremental reactions.

andalusite + biotite ⇌ biotite + muscovite + garnet (Mg richer, Mn poorer) 5a

andalusite + biotite + garnet ⇌
biotite + muscovite + $garnet_1$ + staurolite 5b
Mg richer Mn poorer

Although no direct evidence can be put forward for the compositional trend in garnet as this reaction proceeds it is likely that $garnet_1$ is poorer in MnO as some of this component is taken up in staurolite. Note that reaction 5a is in fact trivariant in the above system.

Before discussing these reactions further, it is necessary to consider the topology of the systems in question with respect to possible univariant equilibria occurring in them.

6.4. Phase relations in the system A K F M S H

The relations summarised above indicate the close association of andalusite, staurolite, cordierite, chlorite, biotite, muscovite and quartz. Assuming their stable coexistence together with a fluid phase defines an invariant point in this six component system. Eight curves, representing univariant equilibria, radiate from this invariant point, each of which involves seven phases, (i.e. the invariant assemblage with one phase absent in each case). In accordance with normal usage (e.g. Albee 1965c, Zen 1966) these univariant reactions will be identified by reference to that phase which is absent, the mineral name being placed in parentheses.

The methods used in deriving the stable order of the univariant reactions around an invariant point have been derived by Schreinemakers (1915 - 1925) and summarised by Zen (1966) whilst the types of reactions encountered have been discussed by Hess (1969). Information pertaining to the relative distribution of Fe^{++} and Mg between the ferro-magnesian phases has been discussed by Albee (1965c, 1972), Hess (1969), Ramsay (1974) and Guidotti et al (1975). The MgO/MgO+FeO ratios used in the following analysis have been taken from the chemical data presented in Chapter 5 and summarised in figure 6.1 as staur $<$ biot $<$ cord $<$ chl.

Mineral	MgO	FeO	Al_2O_3	SiO_2	K_2O	H_2O	V(cm^3)
Andal	-	-	1	1	-	-	51.5
Ky	-	-	1	1	-	--	44.2
Staur	0.4	1.6	4.5	4	-	0.5	223
Cord	1	1	2	3	-	0.5	233
Chl	2.8	2.2	1	3	-	4	209
Musc	-	-	1.5	3	0.5	1	141
Biot	1.2	1.8	0.5	3	0.5	1	151
Garn	0.3	2.7	1	3	-	-	115
Ksp	-	-	0.5	3	0.5	-	109
Qz	-	-	-	1	-	-	23

Table 6.1 : Composition of phases and molar volumes used in determining reactions and reaction slopes in the model system AKFMSH.

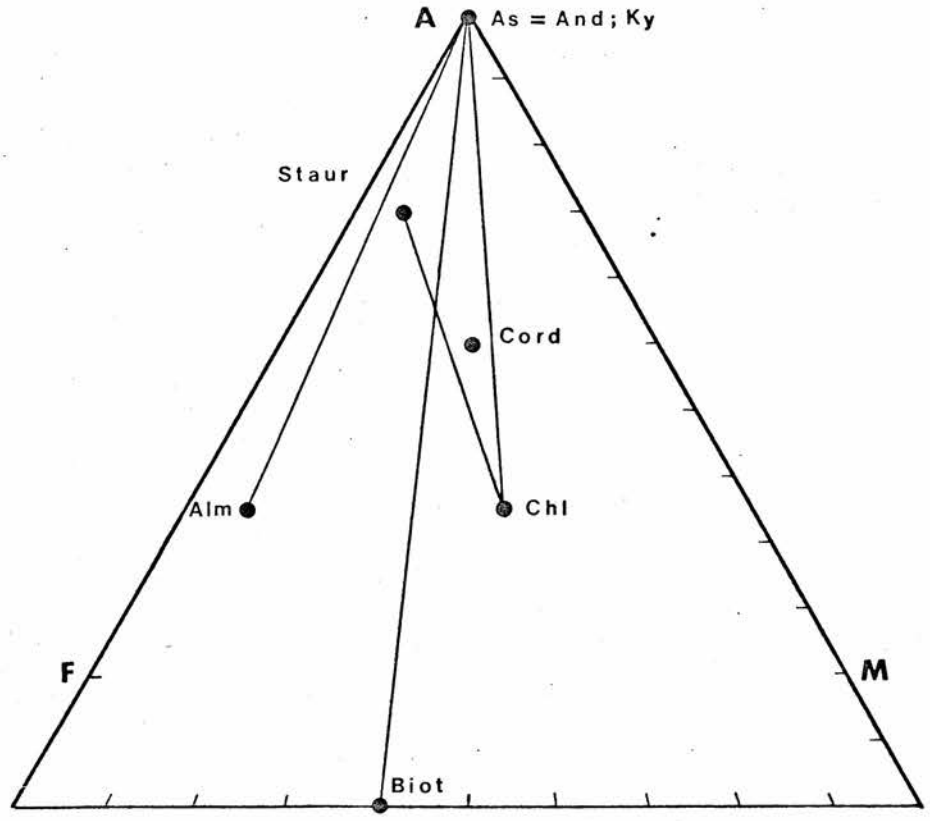

Figure 6.4: Compositional relationships between minerals used in construction of P,T grids, as projected from muscovite.

By initially considering only those rocks which contain excess muscovite, quartz and fluid, three of the eight possible univariant reactions become metastable, (see appendix in Ganguly 1968) i.e. (Ms); (Qz); (fluid). Figure 6.5. shows a P,T projection of the above invariant point together with the five univariant curves generated from it, whilst the compositions of phases used in determining and balancing univariant reactions are shown in Table 6.1 and figure 6.4.

The slopes of the reactions were calculated as follows from the Clapeyron equation (e.g. Klotz 1964)as modified by Albee (1965c).

$$\frac{dP}{dT} = \frac{\Delta S}{\Delta V}$$

For a dehydration reaction

$$[A] \rightleftharpoons [B] + n.\ H_2O$$

$$\Delta S = \left(S_s^{\beta} + n_{H_2O} \cdot \Delta S_{H_2O}\right) - S_s^{A} = \Delta S_{solids} + n_{H_2O} \Delta S_{H_2O}$$

$$\Delta V = \left(V_s^{\beta} + n_{H_2O} \cdot V_{H_2O}\right) - V_s^{A} = \Delta V \text{ solids} + n_{H_2O} V_{H_2O}$$

ΔS_{H_2O} is the entropy change associated with the release of 1 mole of H_2O

ΔS_{solids} is taken to be composed of two parts (Hess 1969).

$$\Delta S_{solids} = \Delta S_c + \Delta S_m$$

Where Δ Sc = entropy change as a result of coordination changes (taken to be largely due to Al).

Δ Sm = entropy change as a result of mixing, which has been neglected (Hess 1969).

Slopes of univariant reactions were thus calculated from the relation:-

$$\frac{dP}{dT} = \frac{\Delta Sc/nH2O + \Delta SH2O}{\Delta Vsolids/n_{H2O} + V_{H2O}}$$

Molar volume data was taken from Robie and Waldbaum (1968) for the solid phases and is shown in Table 6.1, whilst the extrapolations made by Hess (1969) on the data of Holser and Kennedy (1959) were taken for V_{H2O}.

Δ Sc was estimated by reference to entropy data of Fyfe (1967) for the Al_2SiO_5 polymorphs (after Hess 1969)* whilst ΔS_{H2O} was taken from Fyfe, Turner and Verhoogen (1958), after (Albee 1965c).

The balanced reactions with calculated slopes are shown in Table 6.2. Strictly speaking, the reactions should be shown as curves due to variations in volume expansion (α), isothermal compressibility (β) and composition (X) of the phases involved. Such variations are likely to have relatively small effect on dP/dT as far as the solid phases are concerned, (Thompson 1955) however variations (particularly V) for water may have a marked effect. Slopes have therefore been calculated for pressures below and above 4kb using 24 cc/mole and 18 cc/mole respectively for V_{H2O} to show the sense of inflection of the reaction curves with changes in pressure. Slopes were also calculated for those reactions likely to involve kyanite as the stable Al_2SiO_5

* See Hall (1970) for discussion of further refinement of ΔSc.

Phase Absent	Reaction	(>4kb) dP/dT	(<4kb)
(Andal)	st + 1.31 chl + 0.69 ms + 8.32 qz = 3.25 co + 0.69 bi + 4.12 H_2O	+ 24	+ 20.5
(Biot)	st + 2 chl + 5.5 and + 14.5 qz = 6 co + 5.5 H_2O	+ 19.8	+ 17.4
(Chl)	st + 2 co + 2 ms = 10.5 and + 2 bi + 3.5 qz + 1.5 H_2O	- 45	- 73
(Staur)	chl + 8 and + bi + 9 qz = 4 co + ms + 2 H_2O	+ 20	+ 18.2
(Cord)	st + 0.5 chl + 1.4 ms + 0.9 qz = 6.44 and + 1.44 bi + 2.5 H_2O	+ 48.5	+ 35.5

Table 6.2 : Univariant reactions occurring about the invariant point (Alm,Ctd) in the system AKFMSH. Reactions (Staur) and (Cord) have dP/dT of + 14.8 and respectively if kyanite is the stable Al_2SiO_5 polymorph dP/dT in bar/deg.

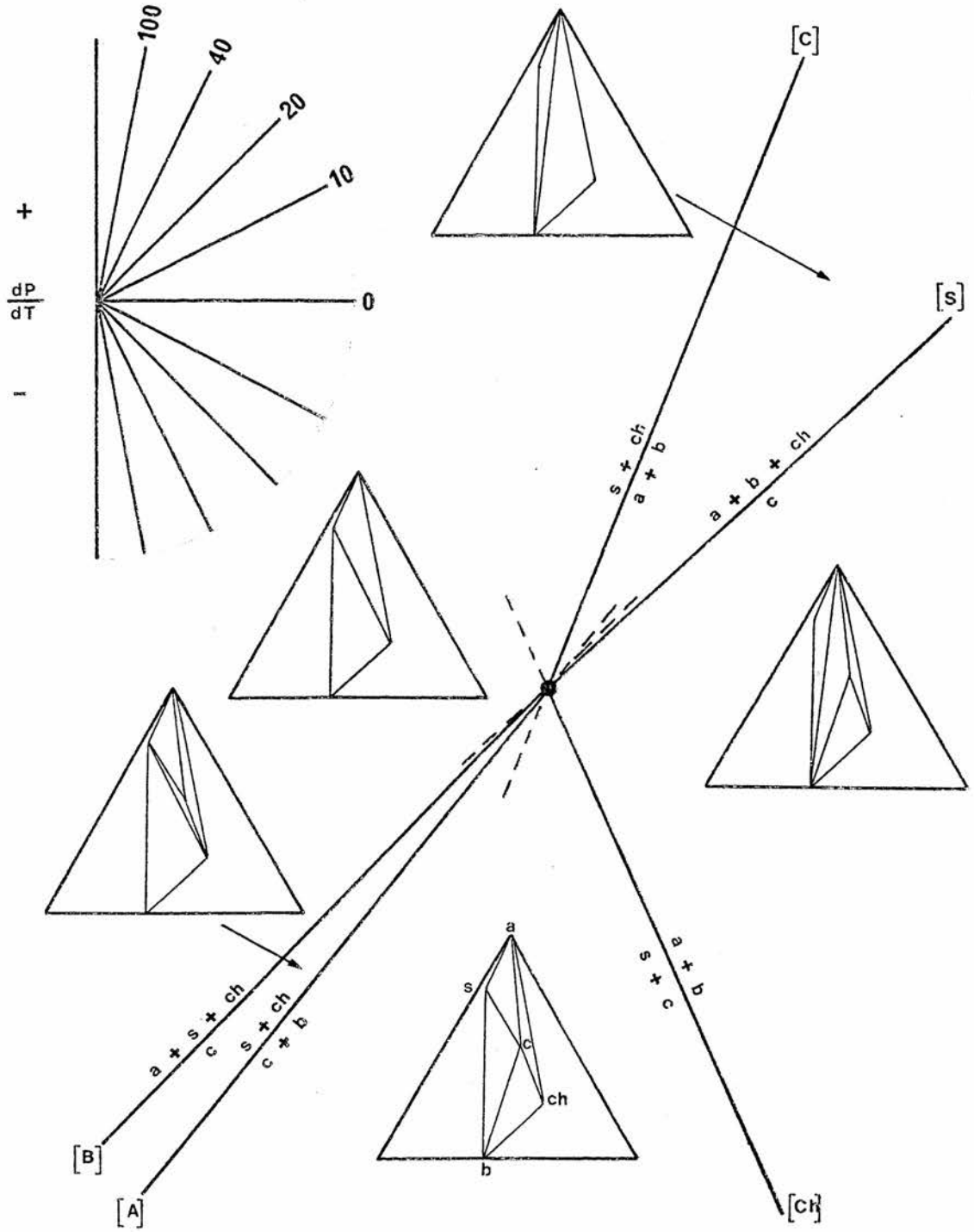

Figure 6.5: Univariant equilibria and mineral fàcies occurring about the invariant point (Gtd,Gt) in the system AKFMSH. (excess musc., quartz and fluid).

polymorph at higher pressures (i.e. (staurolite); (cordierite)).

It should be noted that the value of some slopes is quite uncertain, particularly for reactions involving cordierite where a large proportion of ΔS is a result of Aluminium co-ordination changes. It is therefore better to consider calculated slopes as an indication of dP/dT rather than specific values.

6.4a The Invariant Point

The invariant point shown in figure 6.5 has not been experimentally investigated. It does, however, appear in several published P,T grids for the system A - K - F - M - S - H :-

Invariant point [G,Ct] in figures 4 and 4B of Albee (1965)
[Ct,G] in figure 7 of Hoschek (1969)
[G,H] in figure 3 of Hess (1969)
[Chd,Gr] in figure 1 of Kepezhinskas (1973)

Hess (1969) places the invariant point at 4kb; 575°C, whilst Hess (1970) (in Miyashiro 1973 Fig.3-9) places it at slightly lower pressure and higher temperature. This is in reasonable agreement with experimental work on the stabilities of the individual minerals. The stable coexistence of staurolite, cordierite and chlorite at this point requires that it should lie within the determined stability fields of each mineral. Richardson (1968) Ganguly (1968, 1972) Seifert (1970), Seifert and Schreyer (1970), Bird and Fawcett (1973) etc. This data suggests that the invariant point lies somewhere in an essentially triangular P,T

field (at fO_2 = QFM) between 1.5kb, 500°C; 4.5kb, 575°C and 6.5kb, 635°C, which suggests temperatures a little lower than those shown by Hess (1969, 1970).

6.4b The Univariant Reactions and their relationship to other invariant points

The reactions shown in figure 6.5. vary from those shown in the literature (Albee 1965c, Hess 1969 etc) in slope and in some cases in reaction assemblages. This is a function both of the actual and relative MgO/MgO+FeO ratios chosen for the minerals. The effect of decreasing V_{H2O} with increasing pressure is predictably to increase dP/dT for reactions which have positive slopes and to decrease dP/dT for reactions which have negative slopes. Reactions which cross the Al_2SiO_5 phase boundaries may undergo a marked change in slope as a result of changes in ΔSc.

The terminations of reactions shown in figure 6.5 are of importance in delineating the mineral facies in the system. A general Schreinemakers analysis involving almandine garnet but neglecting chloritoid indicates a topology similar to that of Hess (1969) though the univariant reactions (Gt,Bi); (And,Bi) and (Ch,Bi) all have very similar slopes suggesting that the invariant point (Bi) is metastable as shown in Hess (1970 in Miyashiro 1973). This analysis indicates the stable existence of an invariant point (And) causing termination of the reaction (Gt,And). However, in the light of experimental work on the stabilities of staurolite and chloritoid, the extension

of reactions involving staurolite to very low temperatures seems unlikely. These reactions, e.g. (Gt,Bi)(Gt,And) must interfere with others involving chloritoid. The topology as shown by Albee (1965c fig.4B) and Hoschek (1969 fig.7) is thus preferred to that of Hess (1969, 1970).

Figure 6.6. shows a possible topology for the system in the temperature range 450 - 750°C at pressures up to 8kb. The figure is a synthesis of the work of Albee (1965c) Hess (1969) and Hoschek (1969) taking into account the available experimental data from the end member systems and the relative MgO/MgO+FeO ratios of the minerals as proposed in this study. The terminology of invariant points in this figure is based on Albee (1965c).

In the high temperature part of the grid around the invariant point (Ch,Ctd), garnet has been taken to have MgO/MgO+FeO less than staurolite, but in the lower temperature regions around the invariant points (Bi,Alm); (AS, Alm) and (AS,Ch), andalusite, staurolite, chloritoid and almandine compositions have been taken as colinear to simplify phase relations. This is not a serious simplification for the assemblages under discussion, and only those reactions which are involved in terminating univariant reactions and facies fields shown in figure 6.5. have been plotted for clarity.

The reaction (Alm,Ctd,St) is predicted from calculated slopes to steepen up pressure away from the invariant point (Alm,Ctd)

Figure 6.6 In- and uni- variant equilibria in the model system AKFMSH (modified after Albee (1965c) and Hess (1969)).

Al_2SiO_5 polymorphs - Richardson et al (1969)

musc + qz = Al_2SiO_5 + potash feldspar - Evans (1965)

pyrophyllite = Al_2SiO_5 + qz shown schematically between 400° and 500° (Althaus 1966; Hemley 1967; Kerrick 1968).

● - invariant point in AKFMSH with K-feldspar absent.

■ - invariant point in AKFMSH involving K-feldspar

▼ - invariant point in the end member system AKMSH

——————— - univariant equilibria in AKFMSH

——————— - univariant equilibria in AKMSH

—·——·— - univariant equilibria in AFMSH

Equilibria near the invariant points (As,G); (As,Ch) and not directly related to the discussion, are omitted for clarity.

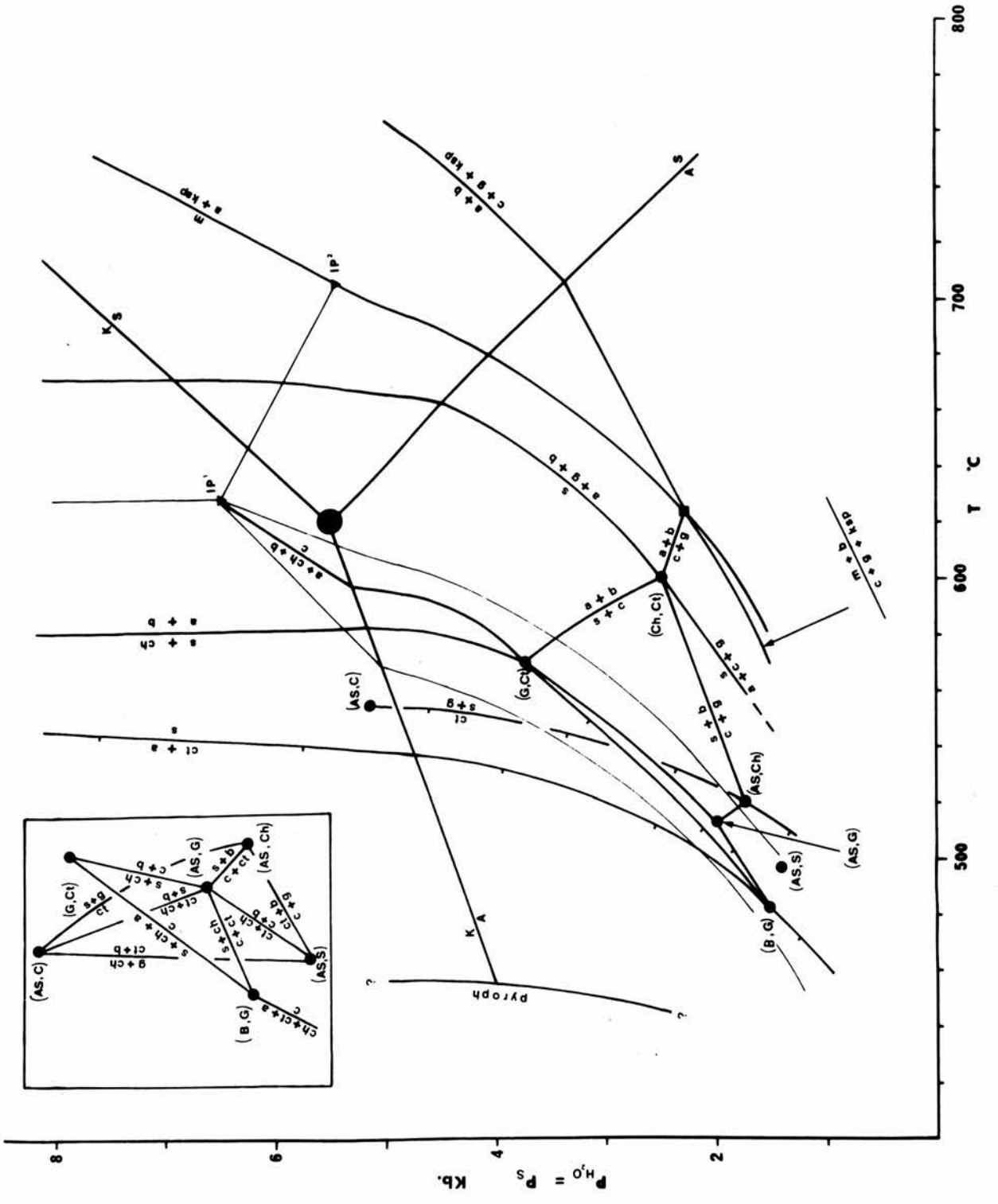

AS; a: Al_2SiO_5 polymorph
B ; b: biotite
C ; c: cordierite
Ch;ch: chlorite
Ct;ct: chloritoid
G ; g: almandine
ksp : potash feldspar
m : muscovite
S ; s: staurolite
AKMSH invariant point terminology after Bird & Fawcett (1973).

eventually interfering with the andalusite, kyanite inversion curve. In the kyanite field its slope is shallower and the reaction must eventually end in the invariant point Ip' (Bird and Fawcett 1973) in the endmember system A-K-M-SiO_2- H_2O. This invariant point gives rise to reactions which are univariant in this endmember system. (thin lines in figure 6.6). The reaction (Alm,Ctd,St) must lie between the two curves bounding the stability field of Mg Cordierite + Mg Chlorite with excess muscovite and quartz (Seifert 1969, Seifert and Schreyer 1970, Bird and Fawcett 1973).

The reaction (Alm,Ctd,Co) steepens up pressure and in the absence of high pressure (Co) invariant points (Richardson 1968) will continue to very high pressure.

The Reaction (Alm,Ctd,Bi) becomes shallower in slope down pressure, eventually terminating in the degenerate invariant point (Alm,Bi), and along its length must lie in the stability field of Mg Cordierite + Mg Chlorite. The invariant point (Alm,Bi) in turn gives rise to the degenerate reaction (Gt,Bi,Chl,Cord) which is the reaction experimentally defined by Richardson (1968)* for the low temperature stability limit of staurolite + quartz.

The grid may then be positioned with respect to the invariant point Ip., the stability field of Mg Cord + Mg Chlorite and the reaction chloritoid + Al_2SiO_5 = Staurolite + quartz.

* The phases in this reaction contain some Mg so that it will occur at slightly higher temperature than Richardson's (1968) reaction for pure Fe phases.

6.4c Divariant reactions in the system A K F M S H

Each stable nondegenerate univariant reaction involving 4 phases (+ musc, qz,vapour) can give rise to 4 divariant equilibria involving 3 phases (+ musc, qz, vapour). For example, the reaction (Ctd,Alm,Chl) gives rise to 4 nondegenerate divariant equilibria which may be specified by the non participation of four phases.

(Ctd,Alm,Chl,Bi)

(Ctd,Alm,Chl,AS)

(Ctd,Alm,Chl,St)

(Ctd,Alm,Chl,Co)

Each of these equilibria can give rise to a reaction where solid solutions are involved.

In a ternary system there are three types of divariant reaction involving three phases. Reactions may proceed as a result of:

a) 1 phase changing composition; 2 remain fixed

b) 2 phases changing composition; 1 remains fixed

c) all 3 phases changing composition

The fourth possibility (all three phases remaining fixed) is trivial since no reaction will take place. This is the general case where no solid solutions are involved. These three types of divariant reaction are special cases on a spectrum of possibilities since the rate of change of the solid solution compositions is also of importance. It is clear that type c) reactions will approach type b) reactions where one phase changes composition very slowly. The situation is entirely analogous to the cotectic

crystallisation of two phases from a liquid and in theory all complications known to occur in that situation may equally occur here.

Although divariant assemblages in the system AKFMSH contain six phases, the above will still hold provided the compositions of muscovite, quartz and vapour remain fixed.

Each nondegenerate divariant reaction will intersect with a number of univariant reactions (involving musc, quartz and vapour) on a P,T diagram. The univariant phase boundaries will wholly or partially limit the stability field of that divariant reaction. (Hensen 1971).

For example the reaction (Ctd,Alm,Chl,AS) will intersect the univariant phase boundaries (Ctd,Alm,Chl); (Ctd,Alm,AS); (Ctd,Chl,AS) and (Alm,Chl,AS) which will wholly define the stability field of that reaction (i.e. the reaction cord+musc $\rightleftharpoons$ staur+biot is stable over the whole mineral facies).

In other cases a divariant reaction may be stable over more than one mineral facies or only part of a mineral facies.

6.4d The stability of isograd forming divariant reactions

The three divariant reaction/assemblages forming isograds in Buchan are:

cordierite - chlorite - biotite - muscovite - quartz (C1) & reaction 1

cordierite - andalusite - biotite - muscovite - quartz(A1) & reaction 2

staurolite - andalusite - biotite - muscovite - quartz(S4) & reaction 3

or (alm,ctd,staur,AS); (alm,ctd,chl,staur) and (alm,ctd,chl,cord) respectively.

The stability field of assemblage (C1) is limited on its low temperature margin from a pressure maximum at the invariant point Ip', (in AKM-SiO_2-H_2O) by the univariant curve (alm,ctd, staur), marking the breakdown of the stable pair cordierite - muscovite, and by (alm,ctd,AS) and (alm,AS,staur) marking the breakdown of cordierite - biotite. At higher temperatures the stability field of (C1) is limited by the univariant reaction for the breakdown of Mg Chlorite plus muscovite in the AKM end member system. This reaction involves the same phases as reaction 1 and represents the high temperature limiting case of the divariant reaction when all the phases become pure Mg endmembers.

The stability field of assemblage (A.1) is limited on its low temperature and pressure margins by the univariant curves (alm, ctd,staur); (alm,ctd,chl) and (ctd,staur,chl) marking the breakdown of the stable pairs cordierite - muscovite and Al_2SiO_5 - biotite, whilst on its high temperature margin it is limited by the degenerate reaction for the breakdown of muscovite + quartz (Evans 1965, Althaus et al 1970). The high pressure limit is again formed by a limiting case of the divariant reaction in the AKM- end member system, on this occasion involving the breakdown of Mg - Cordierite + muscovite.

The stability field of assemblage (S.4) is limited by the reactions (alm,ctd,cord) and (alm,ctd,chl) marking the breakdown of

andalusite - biotite and by the reaction (ctd,chl,cord) marking the breakdown of staurolite - muscovite. This last reaction has a fairly shallow calculated slope and it is not clear whether it extends to high pressure or not. There are two possibilities. The reaction intersects with the Fe- end member reaction (Richardson 1968).

$$\text{Fe-staurolite} + \text{quartz} = \text{Almandine} + Al_2SiO_5$$

at an invariant point in the AKF endmember system involving staurolite biotite almandine AS and muscovite, as figured by Hoschek (1969 fig.5). The stability field of assemblage (S.4) would in this case terminate on the reaction mentioned above. Alternatively the reaction (ctd,chl,cord) may become steeper as the pressure increases approaching the Fe-endmember reaction without ever reaching it. This is the relation shown in figure 6.6. and implies a slight narrowing of possible stability field of assemblage (S.4). Whichever relation is chosen, this assemblage will be stable to pressures in excess of 8kb.

The stability fields of these three assemblages, as inferred from figure 6.6., are shown in figure 6.7. These show the maximum stability field of each assemblage for any bulk composition. Some bulk compositions in the system will never show these assemblages but in general a fixed bulk composition with A^i_b ($100\ Al_2O_3-3K_2O/Al_2O_3-3K_2O+FeO+MgO$) between - 10 and + 50 and intermediate X_b ($100MgO/MgO+FeO$) will register each assemblage over a divariant transition field (Hensen 1971).

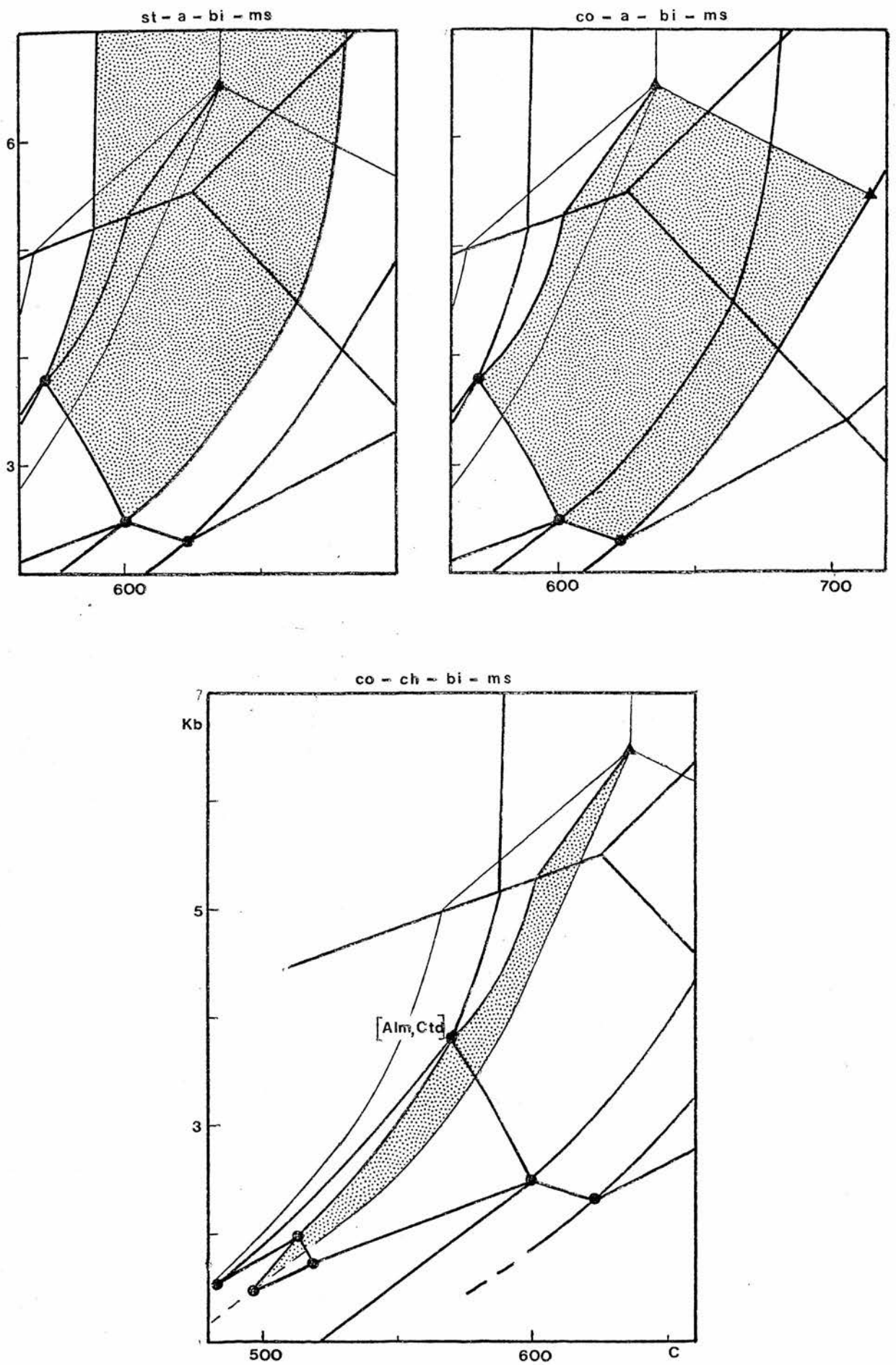

Figure 6.7: Stability fields of isograd forming divariant reaction/assemblages as deduced from figure 6.6.

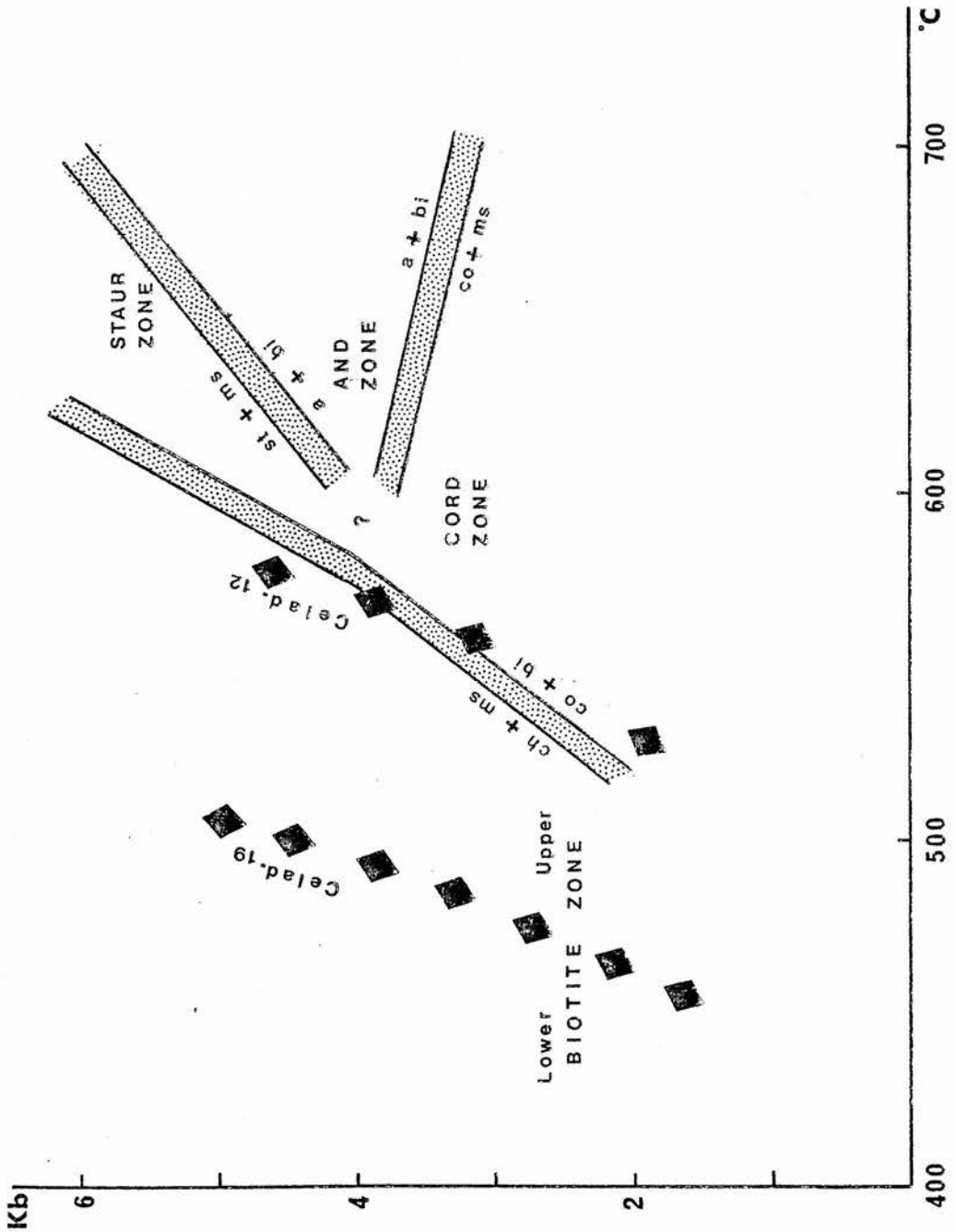

Figure 6.8: Relationships between divariant transition fields (assemblages C.1; A.1; S.4) and phengite stability.

It is of importance to know the general slope of these divariant transition bands. On passing through such a transition band, a rock will undergo two second order transitions (Thompson 1955) but no first order transitions. These second order transitions are represented for the three reactions in question by the incremental reactions 1a, 1b; 2a, 2b; 3a, 3b. The slope of these reactions cannot be obtained by the Clapeyron equation since there is no sudden change in entropy or volume, though these parameters do change rapidly over the range of T and/or P involved in the transition band. Thompson (1955) has suggested that the slope of such a transition band may be approximated by considering the changes in S and V to occur abruptly at a metastable or unstable equilibrium which will occur within the divariant band. This may be achieved for the present reactions, by an approximation which allows the compositions of all phases involved to lie in one plane. The divariant reaction then becomes a degenerate univariant reaction, lying within the divariant transition field, for which a slope may be calculated (i.e. the net reaction in each case). However, in most cases only endmember volume data is available so that the dP/dT obtained must be treated with extreme caution.

Average calculated slopes for reactions 1, 2 and 3 are shown in figure 6.8, in accordance with the stability fields shown in figure 6.7. A steep positive slope for reaction 1 and a shallow negative slope for reaction 2 have previously been experimentally demonstrated for the AKM endmember system (Seifert 1969, Bird and Fawcett 1973) whilst positive slopes with dP/dT of reaction 1

transition field greater than dP/dT of reaction 3 transition field have been demonstrated by Hirchberg (in Winkler 1967 p.180) and Hoscheck (1969). The mineral compositions and reactions used in calculating these slopes are shown in Table 6.3. The reactions have been written so that the high entropy assemblage appears on the right.

It is of great interest to note that, although reactions 1 and 2 are crossed from low to high entropy assemblages in an upgrade direction, reaction 3 is apparently crossed from the high to the low entropy side. This must indicate that the PT path represented by the upgrade sequence on the Banffshire coast becomes strongly pressure controlled on or before the staurolite isograd. This is of course upheld by the occurrence of kyanite bearing assemblages further along the coast at Portsoy (NJ5966) and is also indicated by the distribution of Calcium between garnet and plagioclase as mentioned in Chapter 5 p.155 .

As previously shown the temperature range within which reaction 1′ can occur is closely defined by the experimental data. This temperature is in good agreement with that deduced independently from white mica compositions close to the cordierite isograd. The breakdown temperatures of phengites near the lower/upper biotite zone boundary and the cordierite isograd have been taken from Velde (1965 figure D) and are plotted on figure 6.8.

6.4e Analysis of divariant reactions near the invariant point (Alm,Ctd)

The order of divariant reactions about a univariant reaction may be determined in a manner analogous to the treatment of univariant reactions around an invariant point. This requires that the bulk composition be arbitarily fixed and for the purposes of the present analysis the following are set:

X_b - fixed but unspecified

A'_b - fixed where $A'_{chl} > A'_b > A'_{biot}$

where X = MgO/MgO+FeO subscript b refers to bulk composition

A' = Al_2O_3-$3K_2O$/Al_2O_3-$3K_2O$+FeO+MgO

The choice of A'_b intermediate between chlorite and biotite means that only biotite bearing equilibria will be represented, others with higher A'_b being unstable for the chosen bulk composition. This applies to all equilibria whatever their variance. As such the univariant reaction (Bi)* is unstable leaving only four reactions with F = 1 around the invariant point. Each of these reactions is metastable over most of its range apart from a short section where it affects the chosen X_b. The actual stable section need not be specified unless X_b is specified.

* the additionally absent minerals (Alm,Ctd) are dropped for simplicity in this section since they are absent from all equilibria.

Phases absent in addition to Alm. and Ctd.	Reaction	dP/dT (bar/deg)
(AS,St) Reaction 1	chl + ms + 2 qz = biot + co + 3.5 H_2O	+ 32
(Ch,St) Reaction 2	3 co + 2 ms = 8 and + 2 biot + 7 qz + 1.5 H_2O	- 5
(Ch,Co) Reaction 3	6 st + 4 ms + 6 qz = 31 and + 4 biot + 3 H_2O	+ 20
(St,Co)	3 chl + 5 ms + qz = 8 and + 5 biot + 12 H_2O	+ 104
(AS,Co)	3.1 chl + 4.1 ms = 1.6 st + 4.1 biot + 2.9 qz + 15.6 H_2O	+ 95
(AS,Ch)	2.3 co + ms = 0.8 st + biot + 8.3 qz + 0.75 H_2O	+ 3.3

Table 6.3 : Some biotite bearing divariant reactions near the invariant point (Alm,Ctd) in the system AKFMSH.

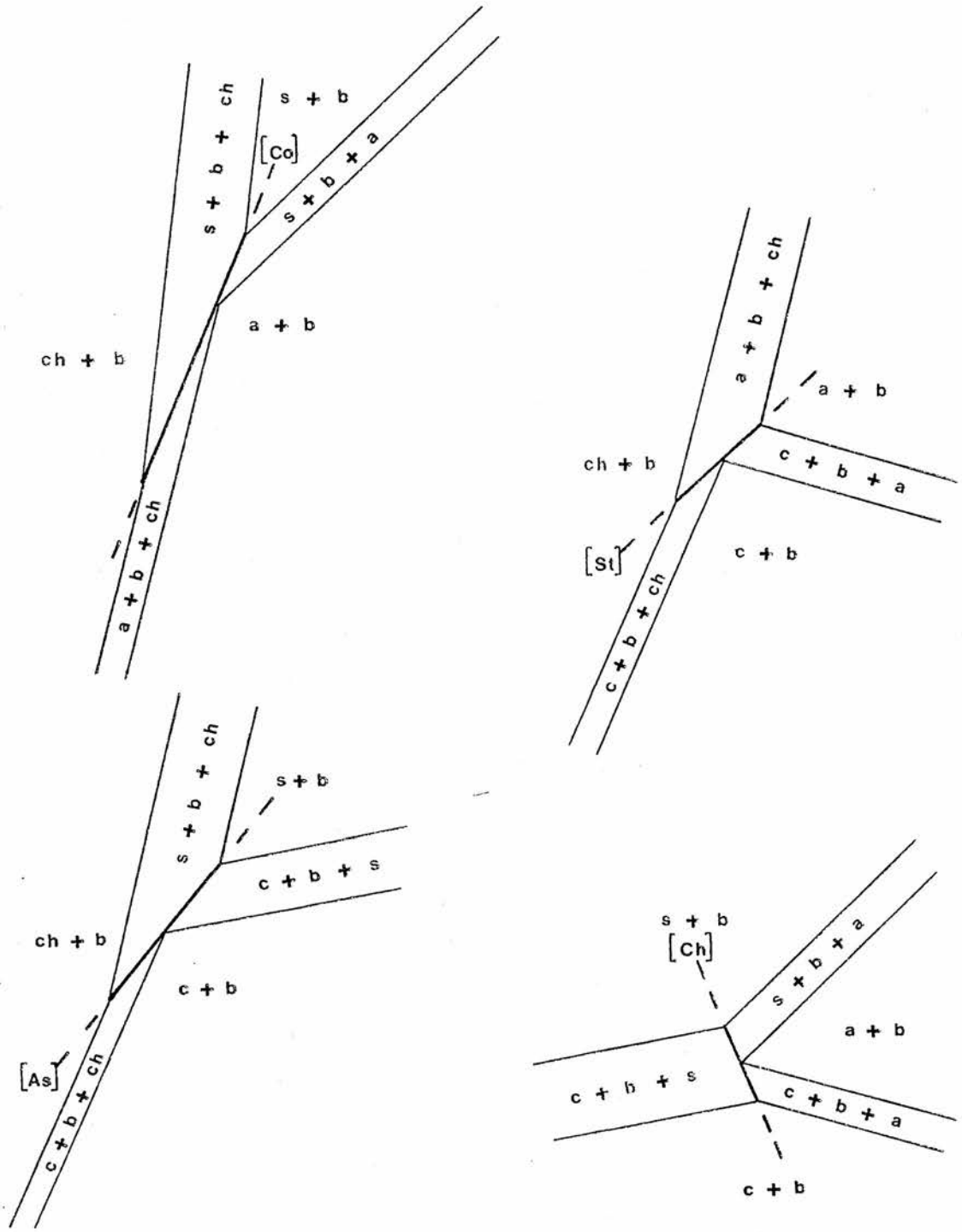

Figure 6.9: Analyses of biotite bearing divariant equilibria in AKFMSH near the invariant point (Alm,Ctd).

Each univariant reaction has three divariant reactions (+Ms+ Bi+Qz) which converge upon it. As the divariant reactions converge the compositions of the phases involved in them converge reaching equality on the univariant reaction.

The arrangement of divariant reactions about a section of univariant reaction for each case is shown in figure 6.9 whilst reactions and slopes are tabulated in Table 6.3. Slopes of univariant reactions are taken from figure 6.5.

Experimental data relevant to reactions (AS,St); (ch,Co); (ch,st) have already been discussed p.194 whilst a positive slope for reaction (AS,Co) has been demonstrated by Hoschek (1969). Reactions (AS,Ch); (Co,St) have received no experimental treatment.

In a manner analogous to fitting invariant and univariant equilibria, these divariant analyses may be fitted together to form a grid. There are two possible stable combinations for assemblages with excess biotite. These are shown in figure 6.10.

For low values of X_b(Fe-rich) the reactions (AS,Co) and (As,St) intersectat low temperatures on the univariant reaction (AS) and the reactions (Co); (St) are entirely metastable (figure 6.10(a)) as is the invariant point. At higher values of X_b (Mg rich) these two divariant reactions intersect at higher temperatures, their intersection moving progressively along the univariant reaction (AS) eventually reaching the invariant point,

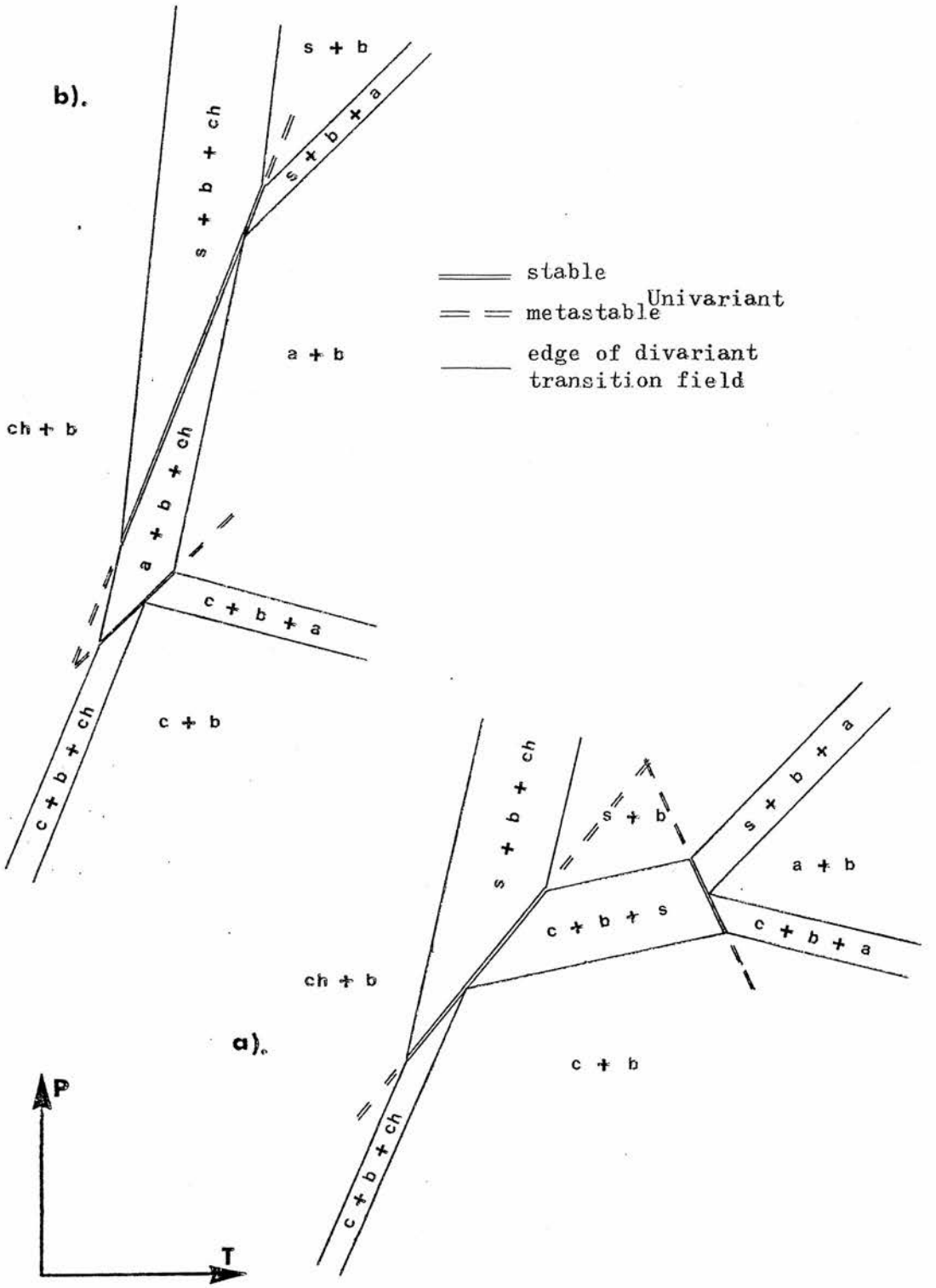

Figure 6.10: P,T grids showing equilibria near the AKFMSH invariant point (Alm,Ctd) for fixed bulk compositions with A b between -20 and + 25. a) Fe-rich b) Mg-rich

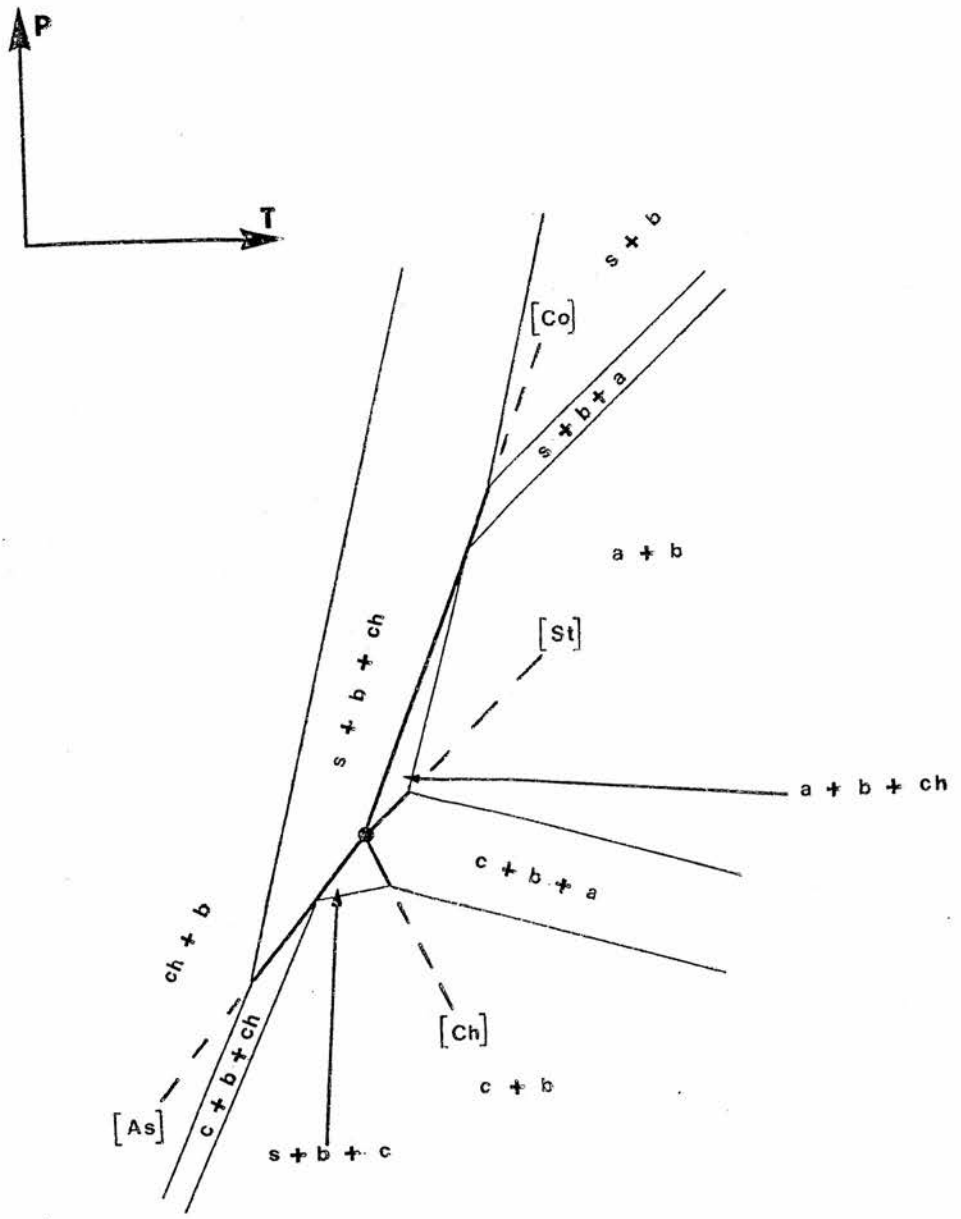

Figure 6.11: Topology of equilibria near the invariant point (Alm,Ctd) for critical bulk compositions with intermediate M/FM.

(figure 6.11). At this point the reaction (Co,St) becomes stable, as do sections of the univariant reactions (Co) and (St). At still higher values of X_b, the reaction (As,Ch) becomes unstable along with the two univariant reactions (As) and (Ch), the topology evolving into that shown in figure 6.10(b).

Before deciding which topology is most applicable to the Banffshire rocks, it is necessary to consider the compositions of minerals both in the reactions and in assemblages in the field, and at what X_b the topology changes from that of figure 6.10(a) to that of figure 6.10(b). The sense of movement with varying P,T may be read from the above figures. This may be checked for consistency by comparison with experimental data on the stabilities of end member minerals which have a bearing on restrictions and expansions of solid solution series.

The work of Turnock (1960) Seifert (1969), Grieve and Fawcett (1974) etc., indicate that Mg chlorite is stable to much higher temperatures than Fe chlorite. Between these two stability limits, intermediate chlorites are likely to be restricted to increasingly more Magnesian compositions as the temperature rises. Because the breakdown curves have positive slopes, there will also be a tendency for chlorite to become Mg richer down pressure though the pressure effect is likely to be less marked.

Conversely, the experimental data of Seifert (1969), Seifert and Schreyer (1970) Schreyer and Yoder (1964) Schreyer (1965)

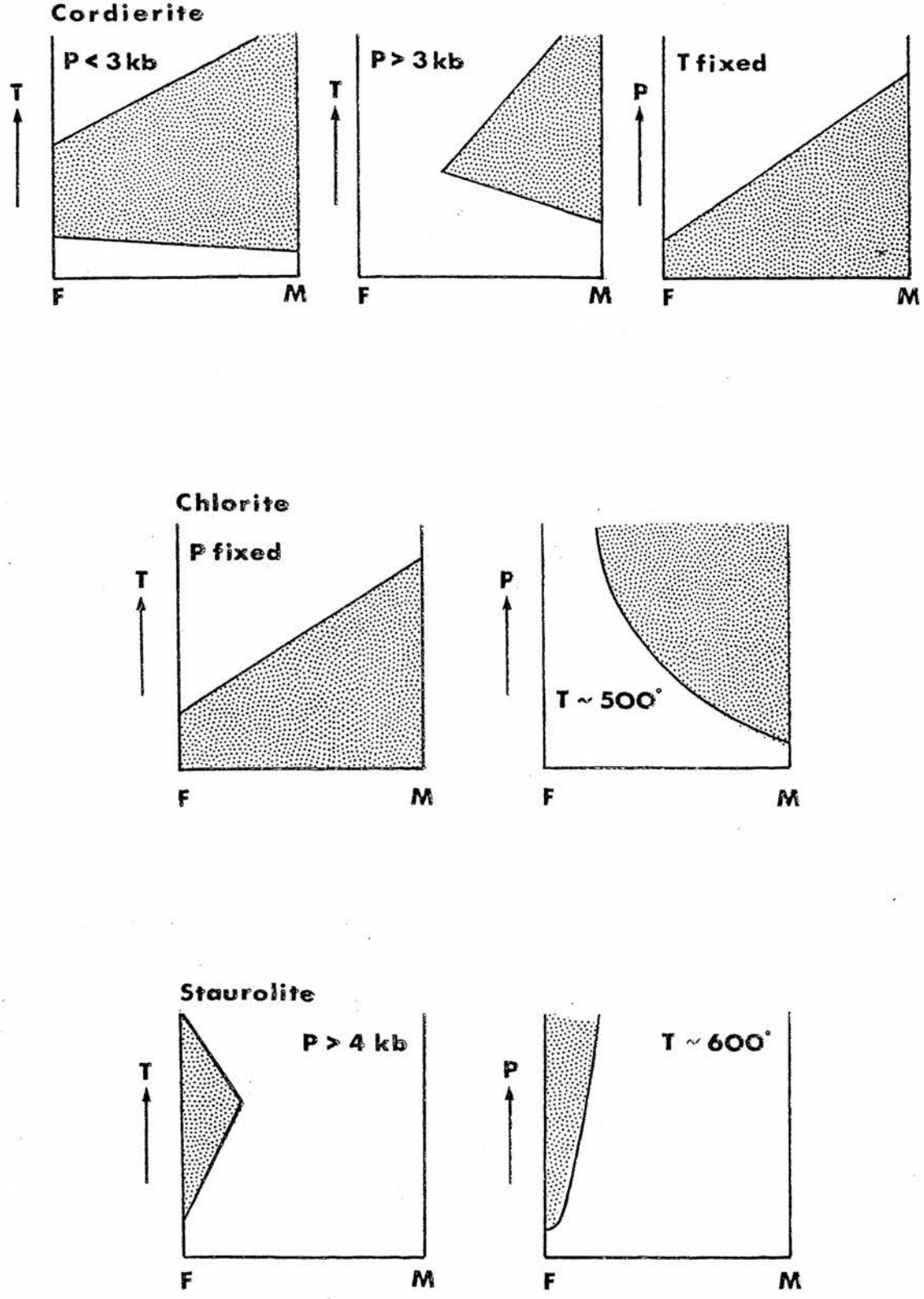

Figure 6.12: The extent of solid solution with varying P,T in chlorite, cordierite and staurolite as suggested by end member stability fields (see text)

Richardson (1968) Grieve and Fawcett (1974) etc., indicate that cordierite compositions are likely to be more dependent on pressure than temperature, becoming more magnesian as pressure increases (c.f. Hensen 1971, Hensen and Green 1971, 1972, 1973). The data of these last workers also shows that cordierite becomes more magnesian up temperature in the higher pressure and temperature ranges. This is in agreement with the negative slope of reaction 2 and probably holds true for intermediate P,T ranges also. At low pressures the situation is not so clear since both Fe and Mg cordierite become stable at virtually identical temperatures (compare Seifert and Schreyer (1970), Mg chl + andal + qz $\rightleftharpoons$ Mg cord and Schreyer (1965) Fe chloritoid + qz $\rightleftharpoons$ Fe cord.), so that a complete solid solution series may exist at very low pressures.

Richardson (1968) has pointed out that the stability field of Fe-staurolite + quartz is a maximum so that Mg bearing varieties will become stable at higher and breakdown at lower temperatures than the pure Fe end member.

Solid solution ranges based on the above data are shown schematically in figure 6.12.

It is to be expected that where these minerals are involved in divariant reaction equilibria, there compositional trends will, in general, reflect the variations in the solid solution range,

either extending or restricting compositional stability fields in response to them. Where more than one of these minerals is involved, complications may arise, for the composition of one mineral may change in response to solid solution restrictions or expansions in the other. This will probably be the general case with respect to the mineral biotite which has a wide solid solution range over all of the P,T region under discussion.

The above data suggests that divariant equilibria involving cordierite are likely to be strongly pressure controlled, moving to encompass more Magnesian (higher X_b) compositions up pressure (c.f. (Ch,St); (Ch,AS)), though in the lower P,T ranges e.g. (AS,St) this need not follow. Reactions involving chlorite are likely to be strongly temperature controlled moving to encompass more magnesian compositions up temperature (c.f. (AS,St); (St,Co); (AS,Co)). Reactions involving staurolite are likely to be temperature controlled but also weakly pressure controlled becoming more Mg rich in the lower temperature stability ranges (c.f. (AS,Co)) and more Fe rich in the higher temperature ranges (c.f. (Ch,Co)) as temperature increases and probably weakly Mg rich as pressure increases.

The sense of movement of the divariant equilibria shown in figures 6.10 and 6.11 is thus wholly in accord with the experimental evidence.

The experimental evidence of Hoscheck (1969) and Hirschberg (in Winkler 1967) show that the divariant transition fields of

reactions (AS,St) and (As,Co) approximate to univariant reactions. These are, however, undoubtedly divariant and the experimental evidence suggests that the transition fields are very narrow and move to Mg rich compositions very quickly. This in turn suggests a very rapid restriction of chlorite compositions near the upper stability temperature of Mg chlorite. This is, of course, upheld by petrological evidence since rocks in the upper part of biotite ($\pm$ garnet) zones normally show extensive chlorite solid solutions (e.g. figure 6.1a this study, Atherton 1968, Albee 1965(b), Green 1963).

The most useful aspect of divariant equilibria is the variable character of the mineral compositions. If enough data is available, it is possible to contour the stability field of the assemblage with respect to composition of the constituent phases (e.g. Hensen 1971, Hensen and Green 1973). The uses of this technique are obvious since the P and T of formation of the assemblage will be uniquely defined by the composition of its constituent minerals. The only way to achieve such a contoured P,T grid properly is by the use of elaborate experiments (e.g. Hensen and Green 1971, 1972) and would represent a major project for the reactions under discussion. However, it is possible to show the general form of the contours for assemblages (A.1) and (S.4) with reference to only very limited experimental data and petrological information from the Dalradian.

Consider assemblage (S.4) i.e. the reaction (Ch,Co). A fixed bulk composition moving up temperature at fixed pressure will enter

the divariant assemblage across a staurolite - biotite tie line and leave it across an andalusite - biotite tie line. Since andalusite - biotite tie lines occur at constant MgO/MgO+FeO, the composition of the biotite on leaving the divariant equilibrium will be the same as Xb. Doing this for a number of fixed pressures indicates that the high temperature boundary of the divariant transition field is an X biotite contour where X biotite is equal to the chosen Xb. For figures illustrating this relation see Hensen (1971).

The slope of the high temperature boundary for this reaction has been experimentally defined by Hoschek (1969 fig.1).

From the present study and that of Chinner (1965) it is clear that biotite with 100MgO/MgO+FeO close to 50 is in equilibrium with assemblage S.4 both in the andalusite and kyanite stability fields. A straight line can now be drawn within the stability field of assemblage S.4 as defined in figure 6.7, using Hoschek's slope so that it crosses the andalusite-kyanite inversion curve. The data of Richardson et al (1969) have been used to locate this boundary. This line represents X biotite = 50. It is not exactly defined but is fairly well located to $\pm$ 10°C within the confines of the grid. The spacing of other X biotite contours is unknown at this point.

The divariant reactions (Ch,Co) (assemblage S.4) and (Ch,St) (assemblage A.1) are known to intersect on the univariant reaction

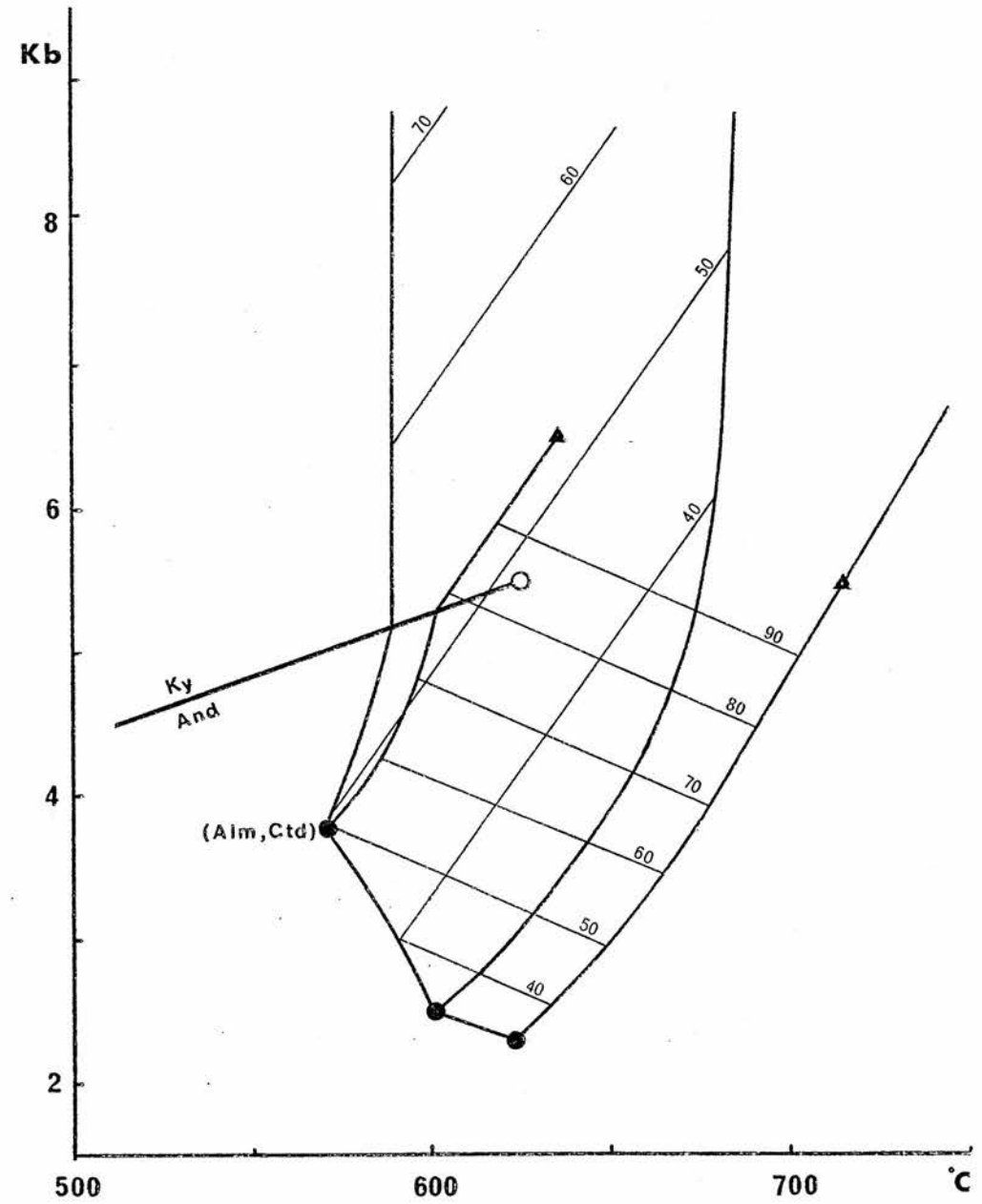

Figure 6.13: Part of figure 6.6. showing the stability fields of the assemblages staur.-andal.-biot.-musc.;cord.-andal.-biot.-musc; contoured for biotite composition in each assemblage. (see text for method of estimating contours).

(Ch). The intersection of the above X biotite = 50 for the former assemblage with the univariant reaction (Ch) or its metastable extension, thus also locates one end of the equivalent X biotite contour for the latter assemblage. The slope of this contour is taken for consistency as the average between that of the calculated net reaction and the Mg end member reaction.

On the assumption that contours are straight and equally spaced, other X biotite contours may be constructed for assemblage (A.1) such that X biotite = 100 lies close to the experimental Mg end member reaction. X biotite contours can now be constructed for assemblage (S.4) parallel to the original one and passing through the intersections of X biotite contours (assemblage A.1) with the univariant reaction (Chl).

Even if left at this stage, the model allows the P,T location of coexisting S.4& A.1 assemblages where the biotite compositions are known. It is not suggested that numerical P,Ts should be interpreted too literally, however the model does allow the relative P,Ts of related specimens to be represented. It should be noted that even after this lengthy construction, the X biotite = 40 contour (Assemblage S.4) lies within the experimental error of Hoschek's experimentally determined upper boundary for Xb = 40. Actual P,Ts may thus be reasonably accurate though this must await proper experimental confirmation. Biotite contours are shown in figure 6.13.

Further refinement of the grid by adding cordierite and

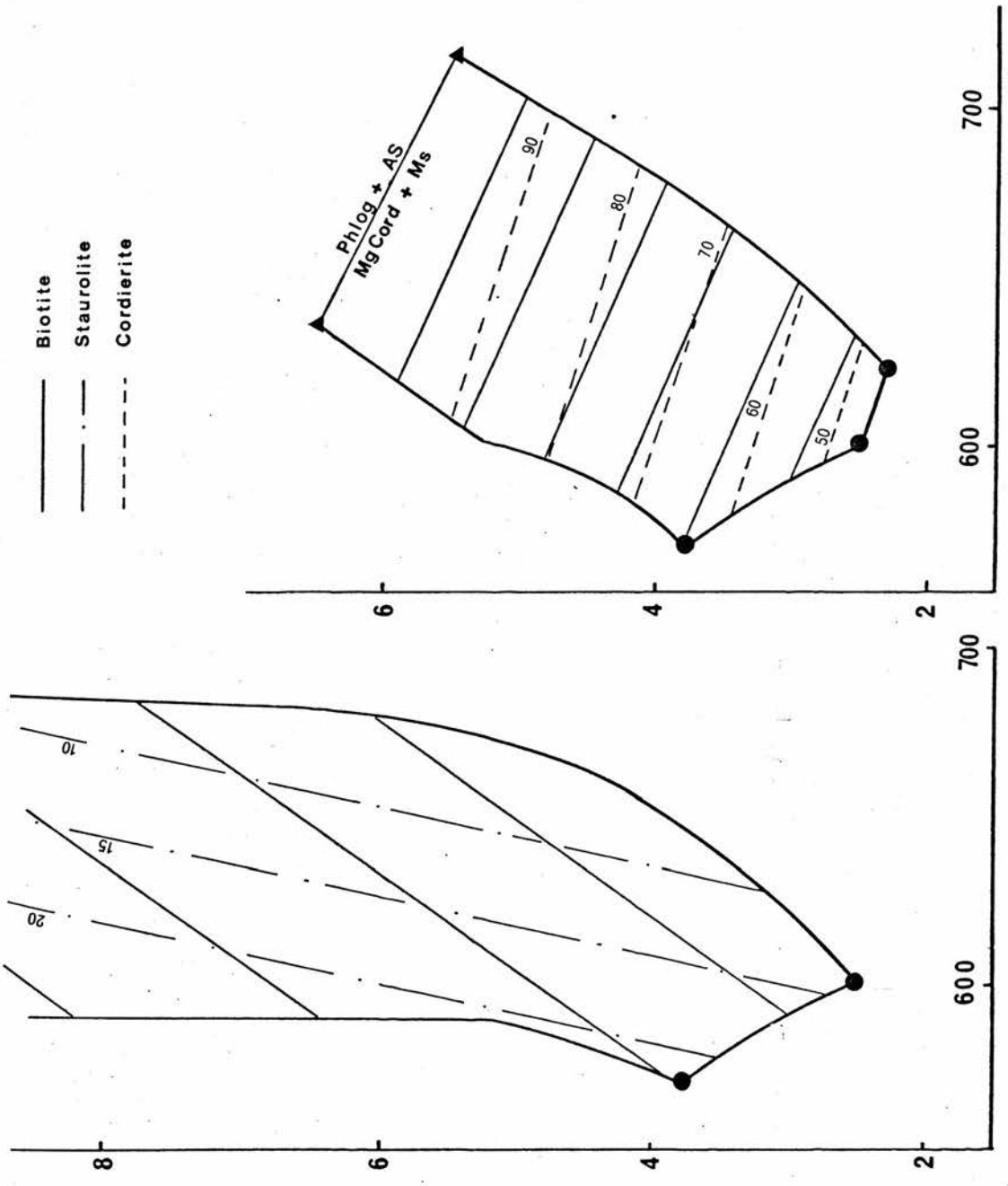

Figure 6.14: Biotite contours of figure 6.13 in relation to staurolite and cordierite contours.

staurolite contours may be attempted using the chemical data from Buchan as presented in Chapter 5. The slopes of these contours (figure 6.14) are highly imprecise. Cordierite contours were estimated using the K_D data from the Ythan Valley which indicates a shallower slope than the biotite contours by specifying a T interval of $20^{o}C$ for a K_D interval of 0.06 and using a figure based on that of Hensen (1971 Appendix 1). Staurolite contours were assumed to have a steep positive slope (based on data of Richardson 1968) allowing a maximum X staur = 25. A reference point was then located at X staur = 15 for specimen 15463 by taking PT where the biotite contours cross for X biot = 40 (15463) (S4) and X biot = 48 (43901) (S5). Staurolite contours were then estimated by eye, taking the data of Chinner (1965) into account.

These figures indicate that the topology change over referred to on page 202 and figures 6.10 and 6.11 occurs in bulk compositions close to Xb = 50. Biotite compositions of isograd assemblages, however, suggest that these take place in compositions with Xb close to 40, as follows:

Specimen 43870	Cordierite Isograd Banff Coast	X biotite = 40
Specimen 43993	Andalusite Isograd Ythan	X biotite = 40
Specimen 43876	Andalusite Isograd Banff Coast	X biotite = 42.5
Specimen 15463	Staurolite Isograd Banff Coast	X biotite = 40

The topology of the divariant grid as shown in figure 6.10(a) is thus more applicable to the Buchan rocks in the P,T location of isograd reactions.

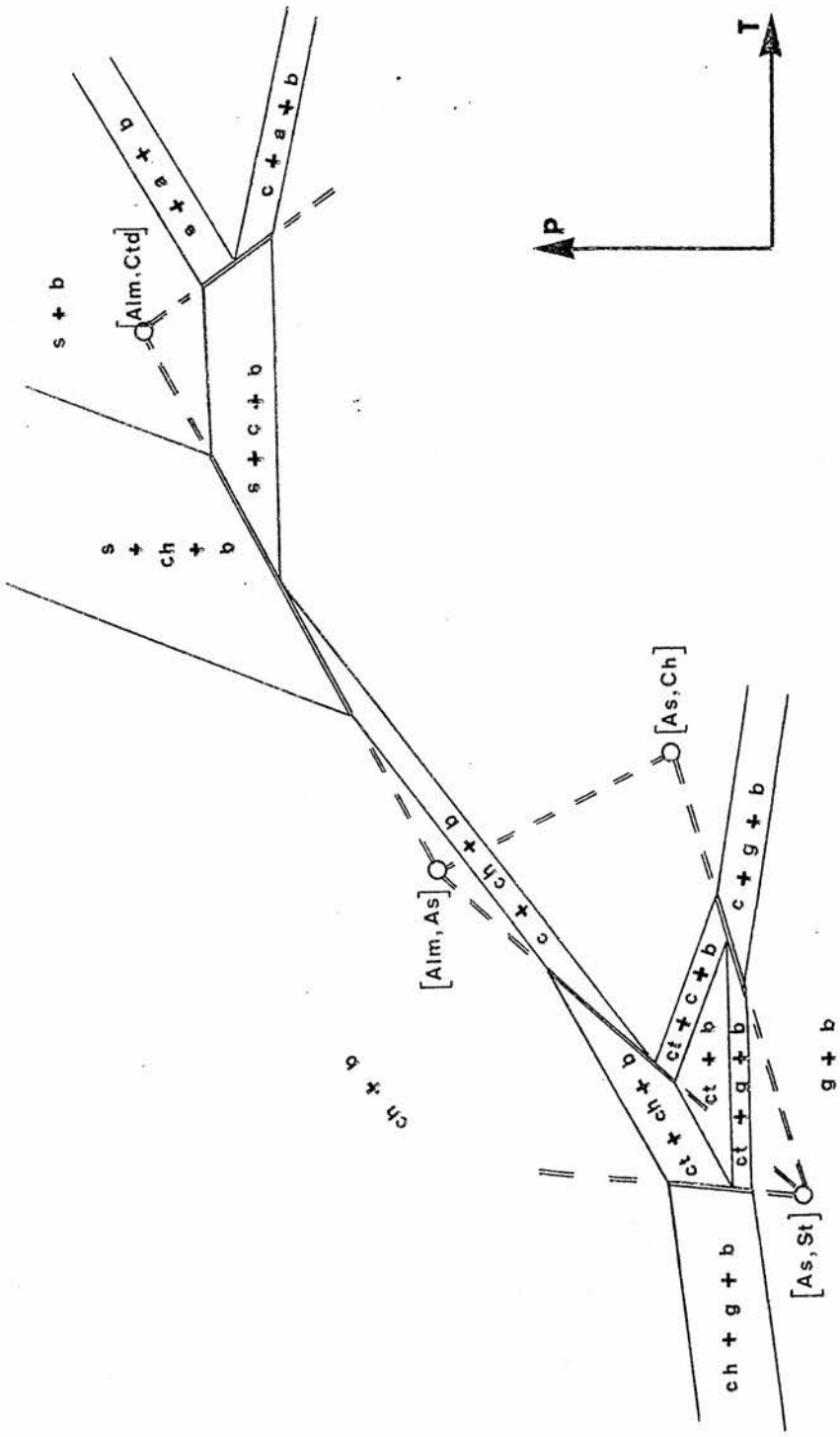

Figure 6.15: Equilibria for biotite bearing rocks (Fe-rich case) near the AKFMSH invariant points (Alm, As); (As,Ch); (As,St) (see figure 6.6.) in relation to those of figure 6.10 (a).

6.4f Extension of the divariant grid to wider ranges of P and T

A similar analysis of divariant equilibria for univariant reactions associated with other invariant points allows the divariant grid to be extended to encompass a wider range of temperature and pressure. Such a grid for reactions on the low pressure and low temperature side of the invariant point (alm,ctd) is shown in figure 6.15. The stability field of chloritoid is notably restricted, even in relatively Fe rich compositions. As Xb becomes more magnesian, divariant reaction (alm,ctd,AS,st) occurs at higher temperatures as previously discussed, the reactions near (Alm,Ctd) evolving as before (figures 6.10, 6.11). Simultaneously the field of chloritoid and biotite becomes progressively smaller and eventually is entirely suppressed as the field of almandine and biotite migrates to very low pressures.

6.5. Phase relations in the end member system A-F-M-S-H

A possible topology for phase relations in this system is shown in figure 6.16. Invariant points in the system A-K-F-M are indicated so that the grid may be directly compared with figure 6.6. Only invariant points above the high temperature breakdown of chloritoid are shown. Gedrite has been included in this analysis since it appears as a rare but regular constituent of muscovite free rocks in many metamorphic terrains. Experimental evidence shows that gedrite (or anthophyllite) can occur as a stable phase in the high temperature part of the grid (Greenwood 1963, Grieve and Fawcett 1974, Green and Vernon 1974).

Mineral Absent	Reaction	dP/dT (bar/deg)
(and)	st + 1.05 chl + 7.27 qz $\rightleftharpoons$ 2.2 co + 0.57 ged + 3.01 H_2O	+ 21
(chl)	st + 2 co $\rightleftharpoons$ 6.1 and + 1.2 ged + 0.7 qz + 0.3 H_2O	- 17
(st)	chl + 0.6 ged + 5.8 and + 7.6 qz $\rightleftharpoons$ 4 co + 2.6 H_2O	+ 15
(co)	st + 0.5 ch + 3.1 qz $\rightleftharpoons$ 0.9 + 3.2 and + 1.6 H_2O	+ 37
(ged)	st + 2 ch + 5.5 and + 14.5 qz $\rightleftharpoons$ 6 co + 5.5 H_2O	+ 17

Table 6.4 : Reactions occurring about the invariant point (Alm,Ctd) in the system AFMSH.

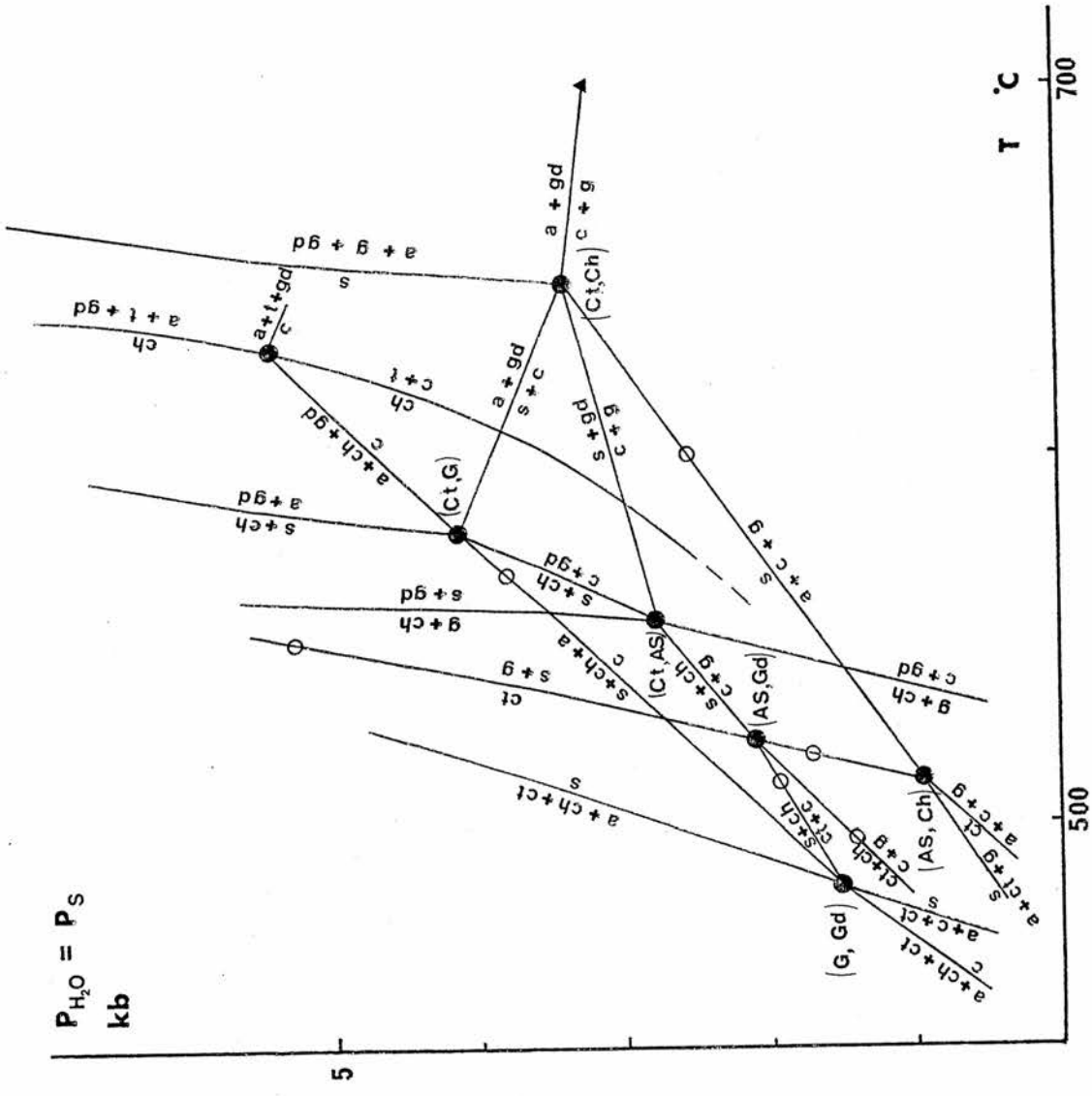

Figure 6.16: In- and Uni- variant equilibria in the system AFMSH. Open circles - invariant points in AKFMSH (see figure 6.6.) Degeneracies between ct;s;g;a, partially removed. See Harte (1975) for relations near (Gd,G) (=(B,G) fig. 6.6.) and (AS,Ch). These relations do not affect the reactions involving gedrite. gd=gedrite; t=talc; other abbreviations as in figure 6.6.

Theoretical grids involving orthoamphibole and other K_2O defficient assemblages have been given by Grant (1968) and Korikovskiy (1969).

Figure 6.16 shows five stable invariant points involving the phases Alm, staur, cord, ctd, chl, Al-silicate and gedrite. The reaction (Ctd,Alm,St) which involves the mineral chlorite cannot extend to very high temperatures and probably terminates where it meets the reaction Mg -chlorite + Qz = cordierite + talc (Fawcett and Yoder 1966) at an invariant point involving talc. The reaction (chl,ctd,st) terminates at $700^{o}C$ 3kb in an invariant point in the Fe end member system involving Al_2SiO_5, gedrite, almandine and cordierite as shown by Greive and Fawcett (1974).

The most important invariant point in this system with respect to the Buchan rocks is (Ctd,Alm). Table 6.4 shows the univariant reactions occurring about this point along with their calculated slopes.

It has previously been shown (Chapter 5 section 4b, Chapter 6 section 2) that the muscovite free assemblage

andalusite - staurolite - cordierite - biotite (S.10)

mimicks the behaviour of assemblage (S4) as its constituent minerals become more magnesian upgrade. This must be achieved by means of the net divariant reaction

cordierite ⇌ andalusite + staurolite reaction 4

(though see page with respect to biotite).

Although there is no direct evidence of grade controlled compositional change in the assemblage

staurolite - cordierite - gedrite - biotite

it seems likely this divariant assemblage will behave in a similar manner.

Neglecting biotite for the moment, these two divariant assemblages may be usefully treated in the system A F M - SiO_2 - H_2O.

Figure 6.16 indicates that assemblages S.10 and S.11 are stable in K_2O defficient rocks at temperatures above the AKFMSH reaction

musc+staurolite+cordierite ⇌ andalusite+ biotite (Alm,Ctd,Chl)

and thus the existence of the stable pair staurolite-cordierite in rocks lacking muscovite is entirely compatible with assemblages (S.4) and (S.5).

6.5a Divariant reactions in the system A F-M-S-H

Analyses of divariant reactions occurring near the invariant point (Alm,Ctd) are shown schematically in figures 6.17a and 6.17b for the conditions Xb fixed with $A'_{staur} > A'_b > A'_{cord.}$ and $A'_b = 25$ respectively.

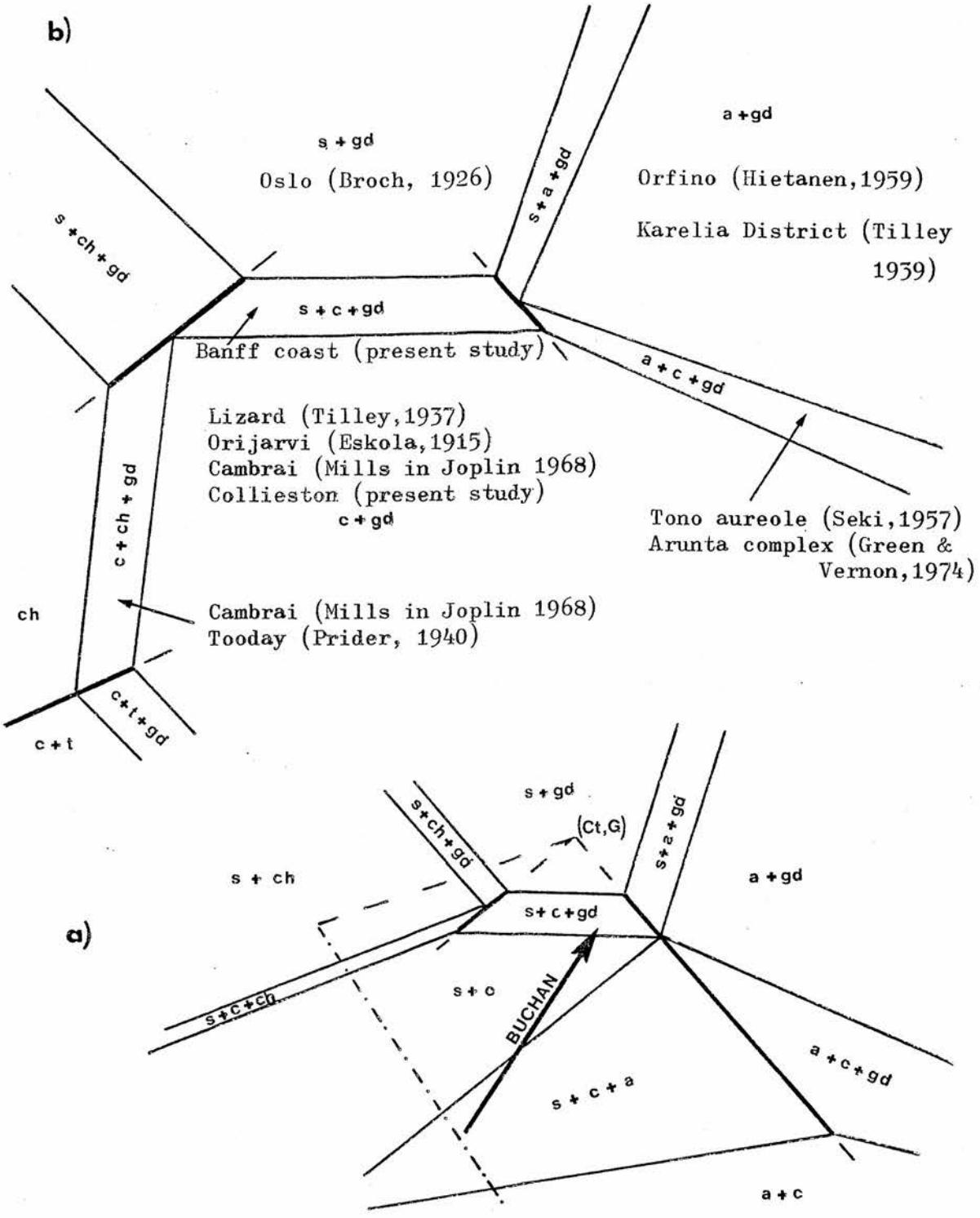

Figure 6.17: Divariant equilibria in AFMSH (a) A'_{co} A'_{b} A'_{st}
(b) $A'_{b} = 25$

The divariant reaction (4) cord + andal $\rightleftharpoons$ staur is of course related to reactions (2) and (3) since the phase relations (figure 5.10) define X staur assemblage (S.10) $>$ X staur assemblage (S.4) and X cord assemblage (S.10) $<$ X cord assemblage (S.5) at the same external conditions. Staurolite and cordierite contours on the stability field of assemblage (S.10) must therefore be closely related to the contours for assemblages (S.4) and (A.1 = S.5). For compositions truely in the AFM ternary system the divariant transition field for Xb fixed must therefore be very wide at high temperature, narrowing rapidly down temperature. This is shown schematically in figure 6.17a. At higher pressures a fixed Xb may pass from assemblage (S.10) into gedrite bearing assemblages via the divariant reaction

$$\text{cord} \rightleftharpoons \text{staur} + \text{gedrite}$$

which would appear to be responsible for the introduction of ortho amphibole assemblages on the Banffshire coast.

It should be noted that the introduction of small amounts of K_2O into the system will stabilise biotite as an extra phase without disturbing the topology of phase relations outlined above. The addition of biotite will however stabilise the assemblages at much lower values of $A'b$. It will also cause a narrowing of the divariant transition fields as bulk compositions become more K rich or less A' rich.

A similar analysis of divariant reactions occurring at lower $A'b$ values is instructive. Figure 6.17b shows the general P,T

relationships of most ortho-amphibole assemblages (ignoring garnet & assemblages with other amphiboles) which have been reported in the literature. The P,T distribution of cordierite-orthoamphibole and Al_2SiO_5-orthoamphibole assemblages is essentially in agreement with that broadly proposed by Hietanen (1959), whilst Green and Vernon (1974) have presented petrographic and experimental evidence for the occurrence of reaction

$$\text{cordierite} = \text{orthoamphibole} + Al_2SiO_5$$

The most interesting feature of figure 6.17b is that virtually all ortho-amphibole assemblages, despite a very varied origin of the original bulk composition, may be produced by straight forward metamorphism.

Although it was previously noted that small amounts of K_2O added to the system would merely produce a little biotite as an additional phase, this is only true for reaction (4) so long as the rock is on the high temperature side of the AKFM-SiO_2-H_2O reaction (Alm,Ctd,Chl)

$$\text{staurolite} + \text{cordierite} + \text{muscovite} = \text{andalusite} + \text{biotite}$$

On the low temperature side of this reaction addition of K_2O to the assemblage andal - staur - cord will give rise to muscovite as an extra phase, since andalusite - biotite no longer constitutes a stable join.

6.6. Phase relations in the system A-K-F-M-S-H-Mn Uni- and Divariant Reactions

Although garnet is a potentially useful index mineral, its readiness to accept manganese in solid solution and the marked affect which this has on its stability field (Hsu 1968) has rendered isograds mapped on its appearance virtually useless as indicators of grade. Garnet bearing assemblages are, however, frequently treated in the system A-K-F-M-SiO_2 - H_2O (e.g. Hess 1969). Almandine is of course stable in this system and must be considered when constructing P,T grids, but it is probably only safe to use these for interpretation of garnet bearing assemblages when these are not accompanied by other assemblages in which garnet appears as an extra phase.

Before a more rigorous treatment of garnet bearing assemblages can be attempted the affect of manganese on the phase relations must be taken into account.

Figure 6.18 shows, schematically, a possible topology for the complex system A-K-F-M-S-H-Mn which is consistent with phase relations in the manganese free system. The number of phases involved in these two systems is the same, chlorite, Al_2SiO_5, staurolite, chloritoid, cordierite, biotite and garnet (muscovite, quartz and fluid present in excess). As a result this system has only seven possible invariant points, fewer than the Mn-free system.

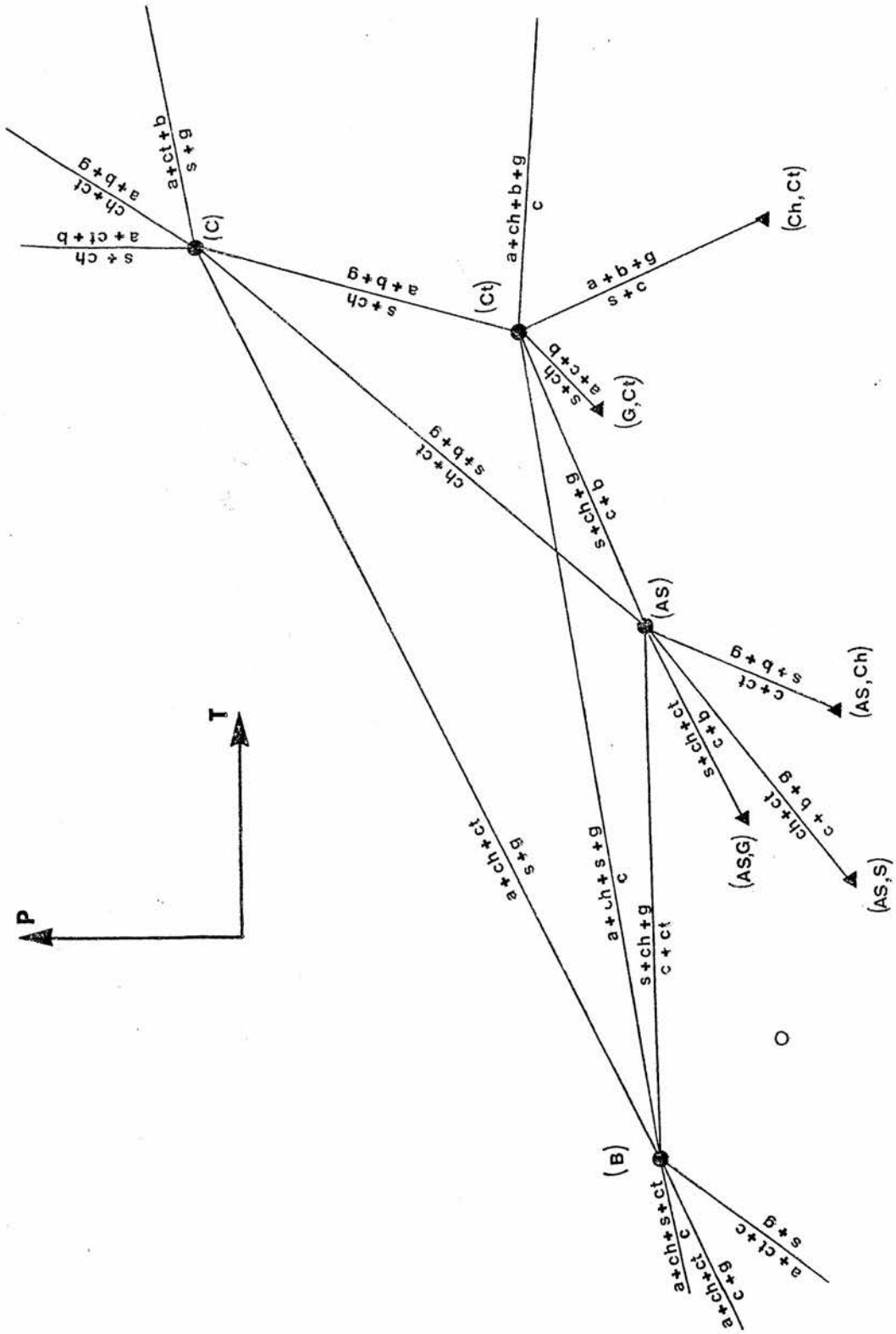

Figure 6.18: In- and uni- variant equilibria in the system AKFMSHMn. Triangles - invariant points in the system AKFMSH.

Only scanty evidence is available with regard to Mn distribution between these phases. For the purposes of constructing the grid Mn has been considered to be distributed in the following manner:

Garnet (Spess) $\gg$ Chloritoid $>$ Staurolite, Cordierite $>$ Chlorite, biotite, Al_2SiO_5

based on the evidence advanced in Chapter 5 along with the data of Albee (1965(b)) and Kramm (1973). Because five of these phases lie in or very close to the plane AFM, actual values are critical.

The most important invariant point with respect to the Buchan assemblages is (Ctd) which is shown in figure 6.18.

The reaction (Ctd,Ch) marks the breakdown of the stable join staurolite - cordierite in Mn bearing rocks. This must occur at higher pressures and temperatures than in Mn free rocks since the reaction (Ctd,Spess) is generated from the invariant point (Ctd,Alm) in the Mn free system. Divariant reactions occurring about the reaction (Ctd,Ch) for the condition Xb fixed $A'chl > A'b > A'biot$ and at Mn values greater than staurolite are shown in figure 6.19(a). The distribution of assemblages is identical to that of figure 6.10a except that spessartine is present as an additional phase in each case. This situation represents much higher MnO contents than are normally found in the Buchan rocks. If the distribution of Mn between phases has been correctly defined, there is a critical region between the above case and the

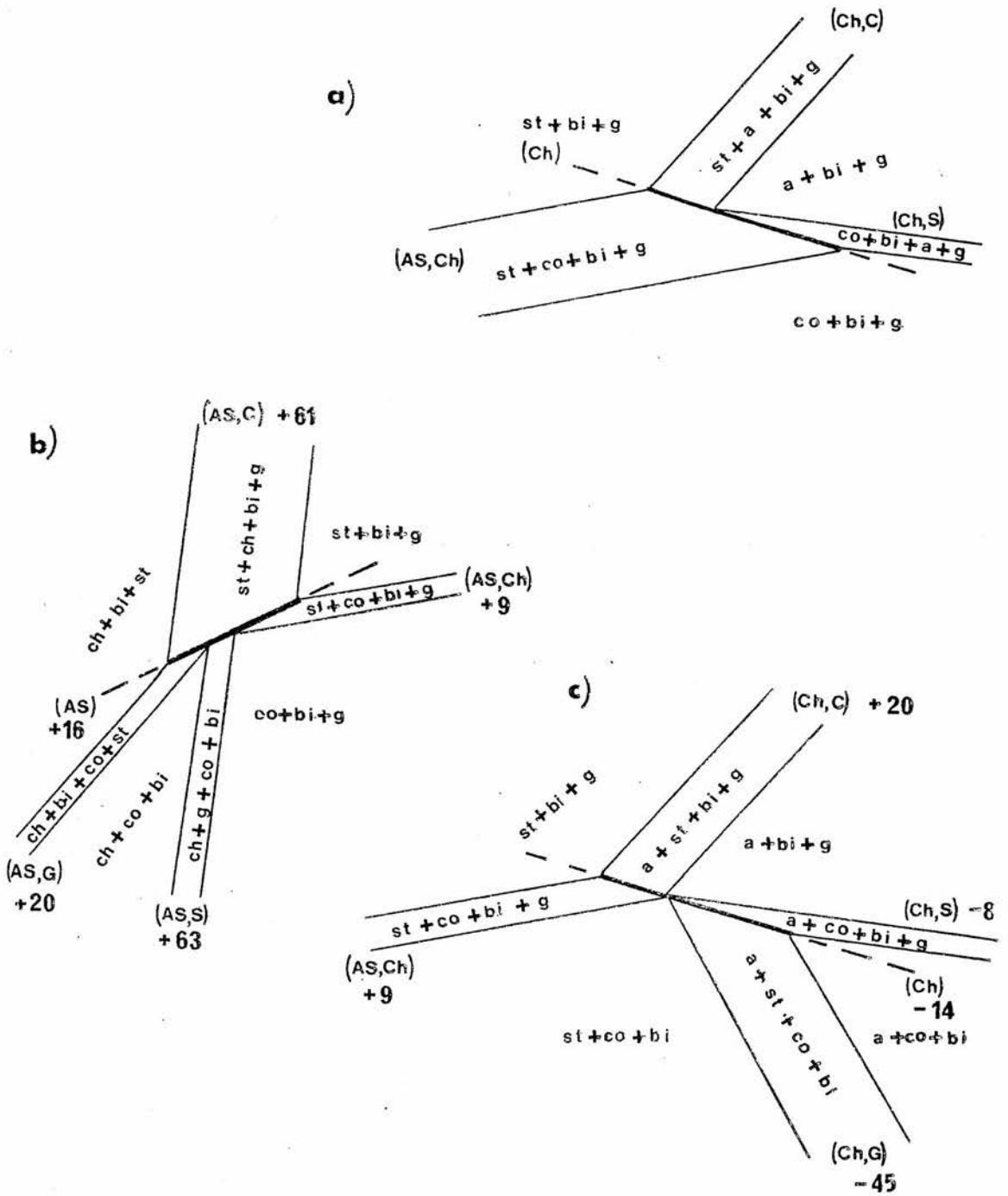

Figure 6.19: Divariant equilibria occurring about the univariant equilibria (Ctd,As); (Ctd,Ch) in AKFMSHMn.

Mn free system, i.e. where bulk compositions lie just above the AFM plane.

General analyses for divariant reactions occurring about the two univariant reactions [AS] and [Chl] are shown in figure 6.19(b) and (c). These show two divariant equilibria, [AS,G] and [Ch,G] respectively, which are stabilised by small amounts of manganese but show no garnet development. These are typical of the four phase assemblages often encountered in the field and so commonly dismissed as disequilibrium.

The reaction [Ch,G] is univariant in the Mn free system (see figure 6.6.). From the topology outlined in figure 6.18 its divariant equivalent occurs at higher temperatures and thus its constituent minerals (chiefly cordierite and staurolite) must become Mn richer up temperature. At the same time its constituent minerals must become more Mg rich progressively up pressure along its length. This is clear from figure 6.10 and 6. 11. As a result, for a fixed bulk composition, a large part of this assemblage's divariant transition field must become metastable in a manner analogous to that of the univariant reactions previously discussed.

6.6a Analysis of multivariant equilibria in the system A-K-F-M -MnO - SiO_2 - H_2O

Each divariant equilibrium involving four phases (+ musc, quartz, fluid) may give rise to four trivariant equilibria. Considering only equilibria involving biotite reduces this to three in each case.

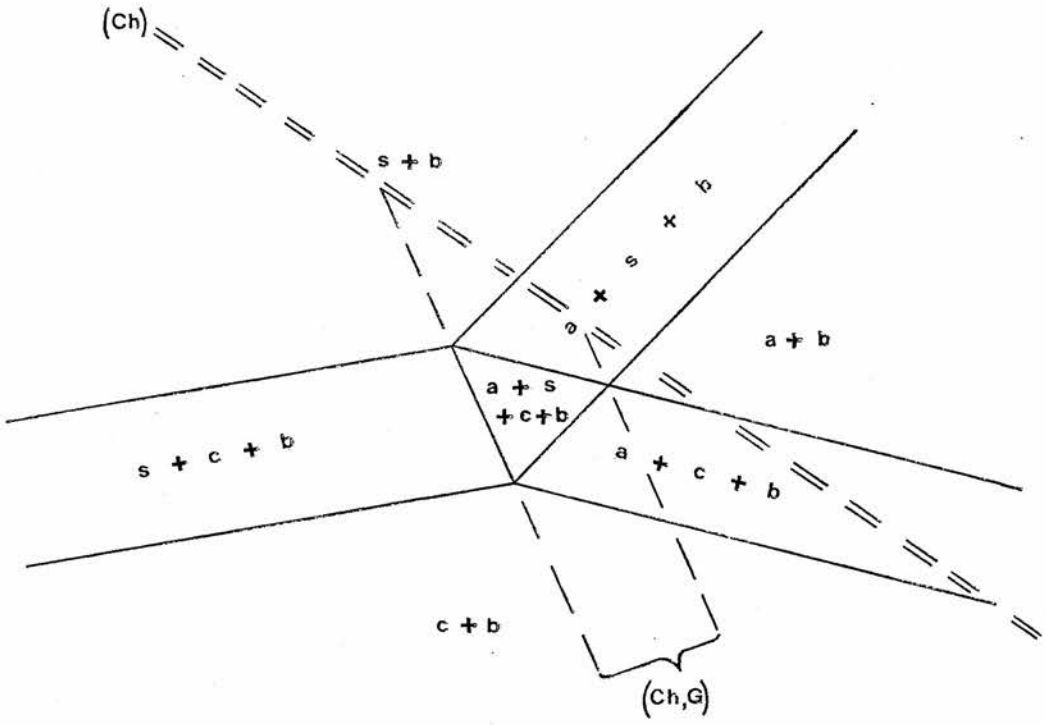

Figure 6.20: Multi variant equilibria occurring near the divariant equilibrium (Ctd,Ch,G) in AKFMSHMn.

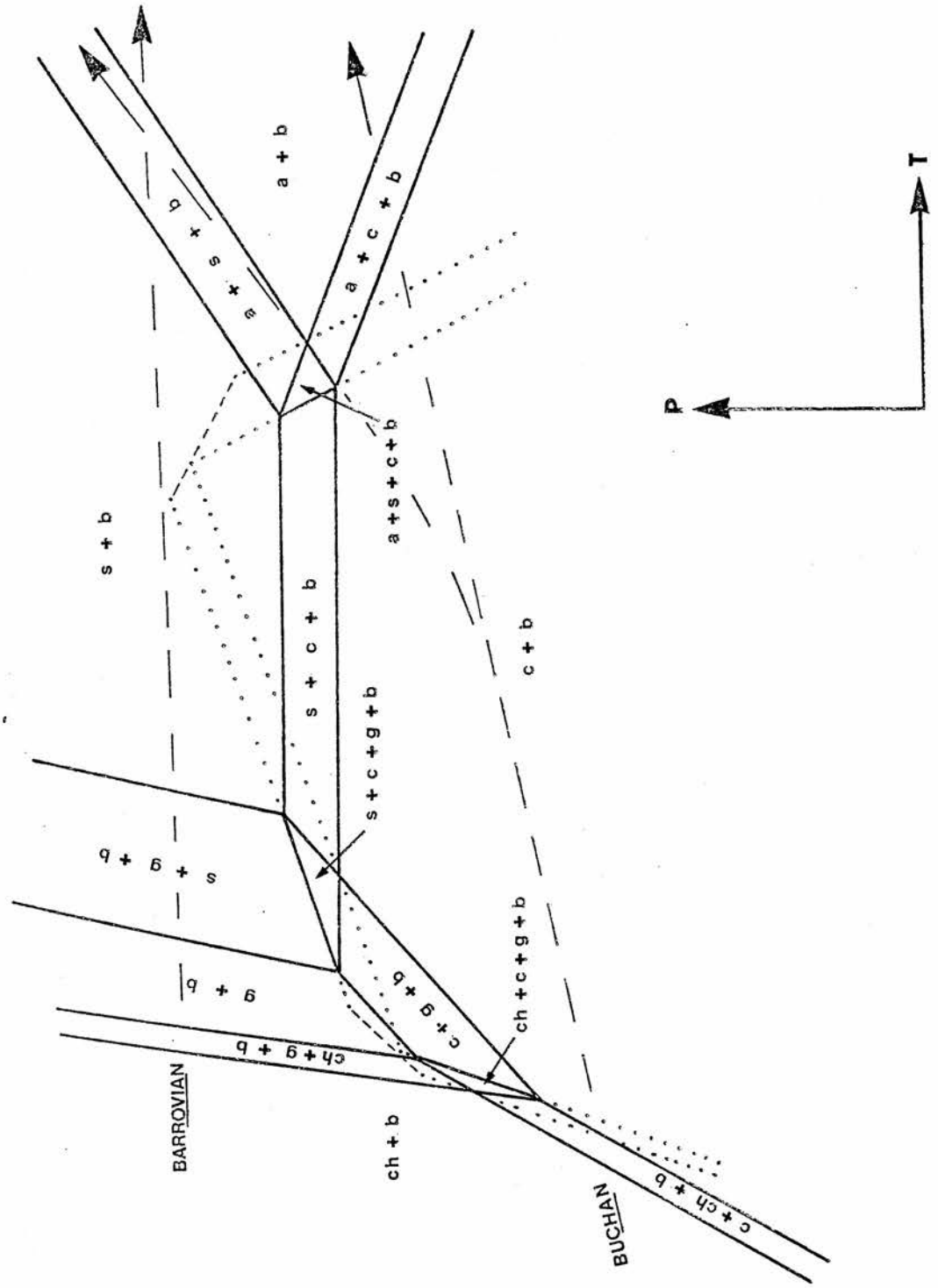

Figure 6.21: Schematic P,T grid showing a possible relationship between equilibria in AKFMSHMn.

Consider the reaction (Ch,G). It may give rise to the three trivariant equilibria (Ch,G,St); (Ch,G,AS) and (Ch,G,Co). The order of these around the divariant equilibrium may be deduced in exactly the same manner as before and are shown in figure 6.20.

The two divariant analyses of figure 6.19(b) and (c) may be joined together by means of the reaction (As,Ch). Although this is not the only way of joining divariant analyses in this system, it is the most relevant for present purposes. An analysis of trivariant equilibria leads to the topology shown in figure 6.21.

This model is in excellent agreement with assemblages in muscovite bearing rocks on the Banffshire coast and even accounts for the presence of staurolite and cordierite assemblages close to the staurolite isograd. The P,T path shown in figure 6.21 predicts the following assemblages upgrade:

1. chl - biot	F = 4
2. chl - biot - cord	F = 3
3. cord - biot	F = 4
4. andal - cord - biot	F = 3
5. staur-cord-andal-biot	F = 2
6. staur - andal - biot	F = 3

The occurrence of the assemblage garnet - andalusite - staurolite - biotite immediately above the staurolite isograd requires that these rocks should be on the high temperature side of the

reaction (Ch). This is not necessarily a drawback providing that the stability area of the divariant assemblage (Ch,G) is close to the univariant reaction (Ch) as shown in figure 6.21. Under these circumstances it is possible to explain all assemblages near the staurolite isograd, given a sufficient range of bulk compositions, in equilibrium terms including the rare maximum phase assemblage (S6a) which could theoretically be univariant.

It is notable that assemblages (S4) and (A.1=S.5) are trivariant in the system A-K-F-M-MnO-SiO_2-H_2O. In this case their constituent minerals should not show any systematic compositional changes with grade variations. The data advanced in Chapter 5, however, indicates that such systematic variations do occur. These two assemblages probably approximate to divariant equilibria because they lie very close to the AFM face (within MnO/MnO+Feo+MgO = 0.02) see figures 5.16 and 5.18 . This would, in fact, explain the minor variations found at any particular grade.

By varying the bulk composition chosen, the topology of figure 6.21 will evolve in a similar manner to that shown in figures 6.10 and 6.11 for the Mn free system. For more Mg rich bulk compositions, the di- and tri- variant fields will migrate to higher temperatures, some of the divariant reactions becoming unstable (e.g. Ch,G) and others becoming stable (e.g.St,Co). For more Fe-rich bulk compositions, the equilibria will migrate down temperature along the univariant equilibrium (AS), eventually

becoming involved with reactions involving chloritoid. For more Mn rich bulk compositions, the equilibria which do not involve garnet will disappear.

6.7. Relationships between the metamorphism in Buchan and other metamorphic terrains

Metamorphic terrains showing the close association of two or all three of the minerals; staurolite, andalusite and cordierite have been widely reported in the literature from many parts of the world. General relationships between these (Buchan and Abukuma Type, lower pressure) sequences and these involving kyanite $\pm$ staurolite (Barrovian Type higher P) have been recognised for some years (Miyashiro 1961). However the low pressure varieties themselves show considerable variation which is less well understood.

Europe:

Apart from the occurrences in the Dalradian, lower pressure assemblages have been described from many parts of Europe, principally the Hercynian terrain (Zwart 1967, den Tex 1965) but also from parts of the Precambrian Fenno-Scandian shield (Simonen 1960, Magnusson et al 1960) Simonen (1960) has described Pre-Karelian mica schists and gneisses containing garnet, staurolite, kyanite and cordierite whilst the rocks of the Svecofennides show a progressive transition from virtually unaltered greywackes and slates into andalusite - cordierite schists and thence into gneisses containing cordierite and garnet.

Rocks of the Karelide belt show a similar transition in this case into schists bearing staurolite in addition to andalusite and cordierite.

The literature associated with metamorphism of the Hercynian terrain is vast, such that a completely exhaustive discussion of it is beyond the scope of the present work. Many of the areas are, in addition, complicated by polymetamorphic effects both older and younger than the Hercynian (Zwart 1967) however in some areas the effects of Hercynian metamorphism are clearly seen and have been described as follows:

a) Pyrenees	e.g. Guitard and Raguin (1958); Zwart (1962, 1963); Guitard (1965); Autran et al (1966).
b) Spain and Portugal	e.g. Capdevila (1968); Bard (1969 summary in Miyashiro 1973).
c) Massif Central and Montague Noire	e.g. Chevenoy (1958); Schuiling (1960); Forestier (1963); Tobschall (1969).
d) Bohemian Massif	e.g. Bederke (1935); Schreyer (1966); Suk (1964); Schreyer and Blumel (1974).
e) Black Forest - Odenwald	e.g. Wimmenauer (1950); Bossdorf (1961); von Raumer (1973).
f) Other Areas	e.g. Suzuki (1930).

Asia:

It is clear from the syntheses of Dobretsov et al (1965) and Sobolev et al (1967) that these sequences are common in the U.S.S.R. though no detailed assemblage data is given for individual areas. However, Kepezhinskas (1973) indicates that a sequence bearing cordierite, andalusite and staurolite occurs in the South Chuisky Range and another bearing andalusite and cordierite in the Khan-Khukhei Range of the Mongolian Peoples Republic. Both of these belts show a transition into kyanite bearing sequences.

North America:

Lower pressure sequences have been described from several parts of North America, all of which carry andalusite and staurolite ($\pm$ cordierite).

a) Michigan	James (1955)
b) Appalachians	Green (1963); Osberg (1968,1971) Kyanite bearing sequences are also common here (e.g. Albee 1968; Thompson and Norton 1968.).
c) Areas near the Idaho batholith	Hietanen, 1956, 1961, 1962, 1967.

Japan:

Similar sequences are well known from both the Ryoke and Hida metamorphic belts of Japan (Miyashiro 1961). Detailed descriptions are available as follows:

a) Ryoke belt (Shiojiri-Takato Area)	e.g. Oki (1961 (a) and (b)); Katada (1965); Ono (1969 (a) and (b)). The work of Ono is published in Japanese (English abstracts) but a summary is given by Miyashiro (1973 pp 169-172).
b) Ryoke belt (Abukuma Plateau)	e.g. Miyashiro (1958); Shido (1958); Hara et al (1969); Tagiri (1971).
c) Hida belt	e.g. Sato (1968).

Australia:

The metamorphism of Australian belts has been summarised by Joplin (1968). More detailed descriptions are as follows:

a) Cooma-Wantabagery area	e.g. Joplin (1942, 1943).
b) Mount Lofty Range (S.Australia)	e.g. White (1966); Offler and Fleming (1968).

The documented occurrences of these terrains fall into three broad groups:

a) Those showing the occurrence of all three of the minerals andalusite, staurolite and cordierite. e.g. Zwart (1962,1963); Forestier (1963); Guitard (1965); Osberg (1968); Kepezhinskas (1973); Present study. Mount Lofty Ranges (White 1966); Joplin (1968 p. 121).

b) Those lacking cordierite. e.g. Green (1963); Schuiling (1960); Capdevila (1968); James (1955); Bederke (1935).

c) Those lacking staurolite. e.g. Autran (1966); Joplin (1942/43); Katada (1965); Ono (1969 (a) and (b)); Bard (1969); Oki (1961(a)).

Isolated occurrences of kyanite are reported, generally in association with staurolite bearing sequences suggesting that these may be, as suggested by Miyashiro (1961) indicative of slightly higher pressures. Occurrences of kyanite and staurolite in the Central Abukuna Plateau, Japan (e.g. Hara et al 1969) are of uncertain origin. In addition the mineral chloritoid may occur in the lower grade parts of any terrains e.g. Capdevila (1968); Bard (1969) and garnet may be associated with any of the above minerals. Rare occurrences of pyrophyllite have been reported (Tobschall 1969).

In the relatively rare cases where zonal sequences and assemblages have been outlined there is little consistancy in the order of occurrence of isograds even considering only the three main minerals. In most cases isograds are established on the first appearance of index minerals and as such, may not be directly comparable between areas, (e.g. Compare the andalusite isograds of Capdevila (1968) assemblage andalusite - chloritoid - chlorite, and the present study). However, a comparison may be attempted using the first stability with biotite - ms - qz of each of the index minerals staurolite, cordierite and andalusite.

Sequences lacking cordierite are in general consistant with the zonal scheme established for the classical Barrovian area (i.e. staurolite + biotite appears at lower grade than Al_2SiO_5+ biotite) with the exception of the Montagne Noire (Schuiling 1960)

	Grade		
Buchan	cord.	and.	staur.
Maine	staur.	and.	cord.
Mongolia	cord.	staur./and	
E. Pyrenees	cord.	staur.	and.
Mt. Lofty Ranges	and./staur.	cord.	

Table 6.5: Order of occurrence of isograds in sequences producing all three of the index minerals staurolite, cordierite and andalusite. Data of Guitard (1965), Osberg (1968,1971), Joplin (1968), Kepezinskas (1973).

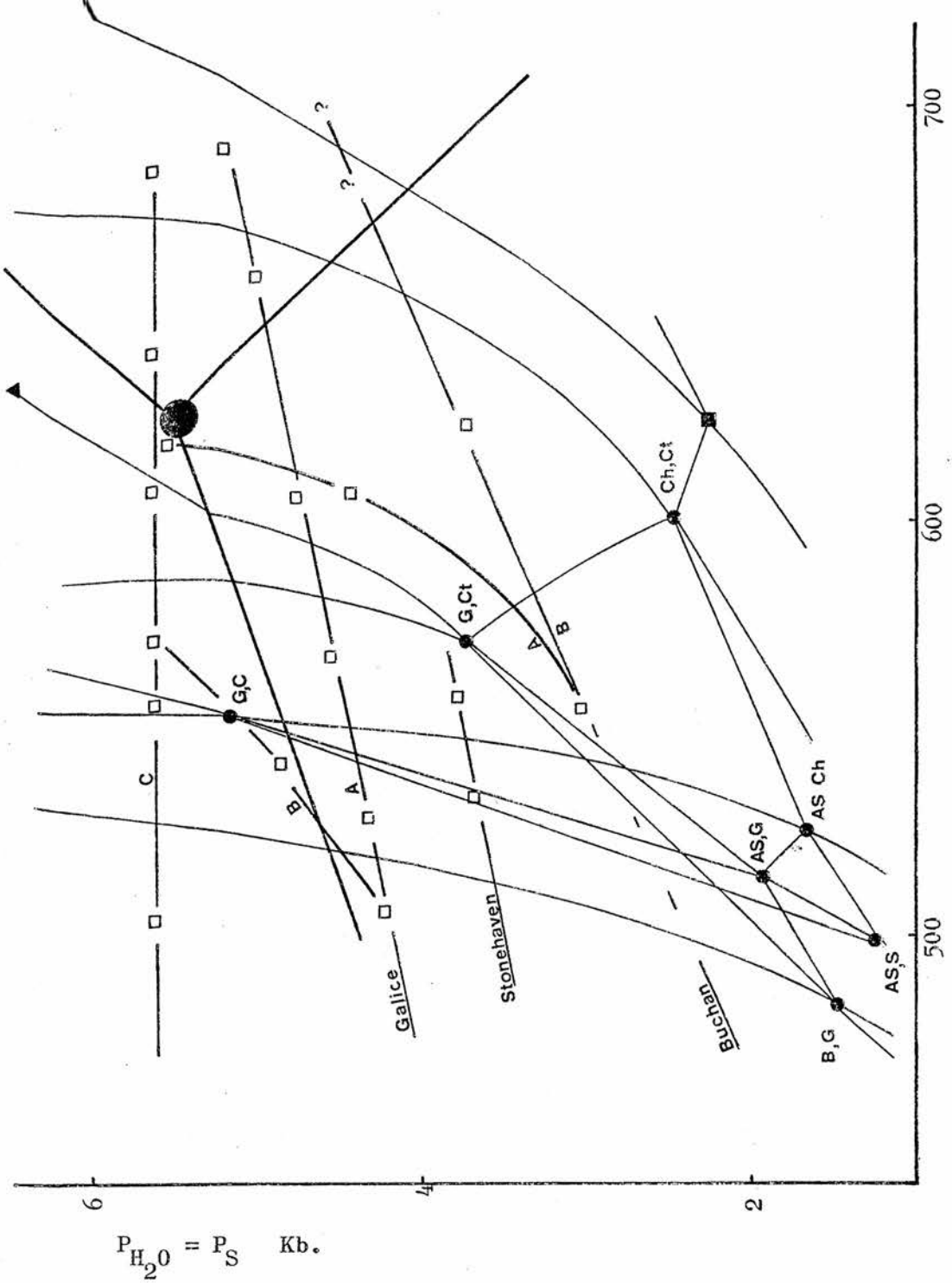

Figure 6.22: Some observed facies series represented in the system AKFMSH. Galice (suites A,B,C) after Capdevila (1968). Stonehaven after Chinner (1967). Buchan A-Banff coast B-Ythan Valley. - observed facies.
see figure 6.6. for reactions.

where these are inverted. Sequences lacking staurolite may show cordierite + biotite stable at lower grades than andalusite + biotite (e.g. Katada 1965; Autran et al 1966), or vice versa (e.g. Ono 1969 (a) and (b)) or at virtually the same time, (Joplin 1968 p. 107). The order of isograds in sequences where all three minerals are present is tabulated in Table 6.5 where data permits.

The most striking feature of the cordierite bearing rocks is their diversity, which is in sharp contrast to the relative consistancy of sequences lacking cordierite. This may reflect the relative complexity of the P,T grids in the low pressure regions.

Adequate data allowing application of P,T grids to these sequences are present in only a few instances. However, where data does permit, there is fairly good agreement between the model systems and observed assemblages. Typically, metamorphic terrains do not show a complete series of potential mineral facies, but those observed generally appear in a logical sequence. Where garnet does not consistantly appear as an extra phase assemblages may be represented in the system A-K-F-M-S-H and the sequences recorded by Capdevila (1968) and Chinner (1967) (Figure 6.22) are shown in relation to those of Buchan (ignoring garnet). The incidence of assemblages with excess phases for the above system appears to be higher in cordierite bearing sequences but is not restricted to them. The following areas may

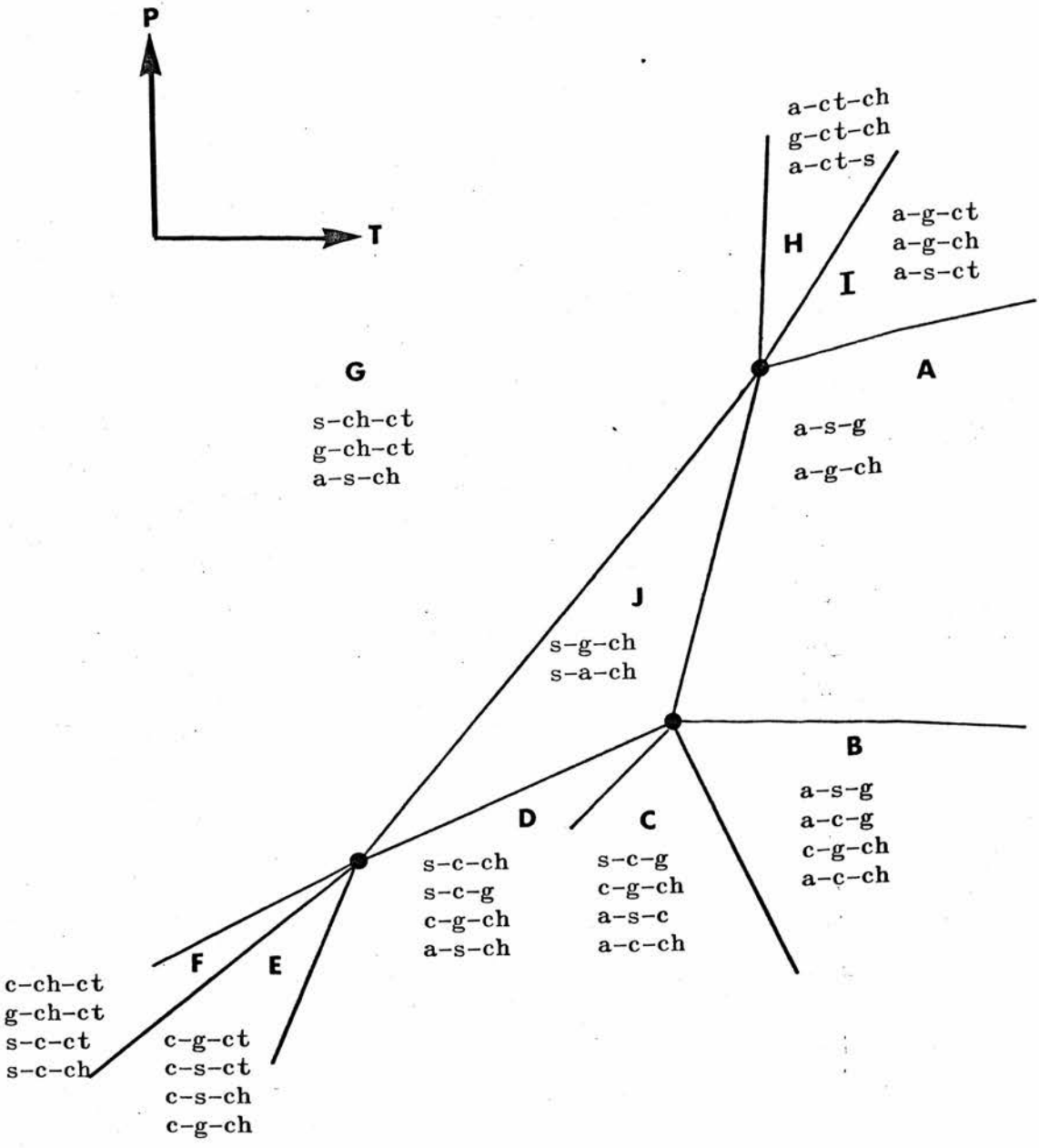

Figure 6.23: Biotite bearing assemblages and mineral facies in the system AKFMSHMn.

be usefully treated in the system A-K-F-M-S-H-Mn., (See Figure 6.23) assuming that chlorite is primary where listed in assemblages.

The Eastern Pyrenees:

Guitard (1965) has recorded a complex sequence of assemblages from the Massif du Canigou as follows:*

Cordierite Zone	co - bi - st - ch - g	J/D
	co - bi - st - g	Facies D
	co - bi - st - ch	
	co - bi - ch - g	
Andalusite Zone	co - bi - st - ch - a	D/C
	co - bi - st - g - a	C/B
	a - co - bi - ch	Facies C
	a - co - st - bi	
	a - st - bi - g	Facies B
	a - co - bi - g	
Sillimanite Zone	a - st - bi - g	Facies B

This series of assemblages may be interpreted as a virtually complete facies series J to B. The five phase assemblage representing the C/B transition occurs at higher grade than that representing D/C in the field. Microcline occurs in the highest grade regions.

* Three phase assemblages are omitted throughout this section.

The South Chuisky Range (USSR):

Kepezhinskas (1973) records the following assemblages in the eastern part of the South Chuisky Range where andalusite is the sole Al_2SiO_5 polymorph.

Cordierite Zone	bi - ch - co	Facies D (or E)
	bi - ch - g	
(no ms)	bi - ch - co - g	
Staurolite Zone	bi - co - st - a	Facies C
	bi - co - ch - a	

In the west where kyanite is the stable Al_2SiO_5 polymorph the following assemblages suggest a higher pressure transition from facies J to A above the K-A inversion

bi - ch - st - a	Facies J
bi - ch - st - g	
bi - ch - st - a - g	J/A
bi - g - st - a	Facies A

Northern New Hampshire:

Green (1963) has described a sequence of metamorphic zones from the Appalachians (Errol Quadrangle) which show the sequence of zones biotite; garnet; staurolite; sillimanite. Andalusite is common in the staurolite zone, appearing slightly later than staurolite. The transition from facies J to A appears to occur within the staurolite zone as follows:

Staurolite Zone	bi - ch - st - g bi - ch - st - a	Facies J
	bi - ch - st - a - g	J/A
	bi - ch - a - g	Facies A (or I)
Sillimanite Zone	bi - a - st - g bi - a - ch - g	Facies A

The assemblage bi - a - st - ch is also reported as common in this zone and as such must remain an anomaly since it is typical of the lower temperature facies J.

Waterville-Vassalboro Area, Maine:

Osberg (1968, 1971) has recorded a sequence of zones chlorite/biotite zone - garnet - staurolite/andalusite - sillimanite. Within the lower grade part of the staurolite zone (Osberg 1968 p. 56) andalusite does not occur with biotite. Assemblages are as follows:

Staur/And Zone		
(lower grade)	bi - ch - st - g	Facies J
(higher grade)	bi - st - a - g	Facies A or B
Cordierite Zone		
(lower)	bi - st - co - g	Facies C or D
(intermediate)	bi - st - co - g - a	C/B
(higher)	bi - a - co - g bi - a - st - g	B

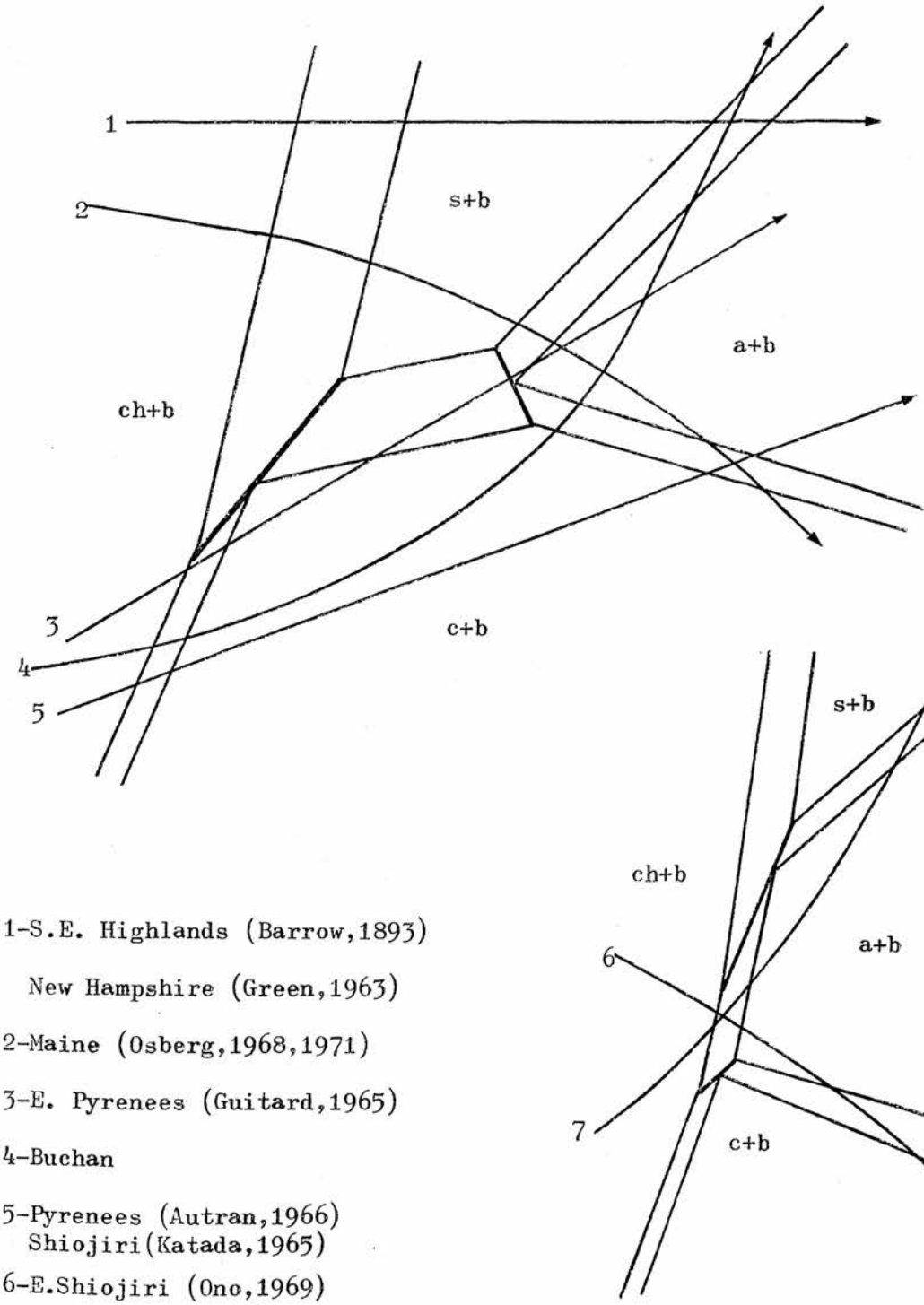

1-S.E. Highlands (Barrow,1893)

New Hampshire (Green,1963)

2-Maine (Osberg,1968,1971)

3-E. Pyrenees (Guitard,1965)

4-Buchan

5-Pyrenees (Autran,1966)
Shiojiri(Katada,1965)

6-E.Shiojiri (Ono,1969)

7-Massif Central (Schuiling,1960)

Figure 6.24: Predicted P,T paths based on order of occurrence of isograds. a) Fe-rich bulk compositions (or lower fO_2) b) Mg-rich bulk compositions (or higher fO_2)

Despite the occurrence of the anomalous assemblage bi - st - a - g in the staurolite/andalusite zone, this suggests a facies series passing below the invariant point (Ctd) from J to B and is thus similar to that of Guitard (1965).

It would appear from figures 6.22 and 6.23 that most facies series are compatible with a largely temperature controlled gradient. The rocks of the Banffshire Coast would appear to be atypical in this respect.

Where adequate data does not allow rocks to be allocated to specific mineral facies it is still possible to gain some information simply from the order of first appearance of the pairs: cordierite - biotite; staurolite - biotite; Al_2SiO_5 - biotite; by applying the divariant grids shown in figure 6.10. Some examples of predicted isograd sequences are shown in figure 6.24.

A possible mechanism for the reaction; cordierite + muscovite = biotite + andalusite.

The following textural relationships were described in Chapter 2.

a) Andalusite commonly occurs in close association with cordierite porphyroblasts, particularly in rocks from the andalusite zone of the Ythan Valley. In rocks with low model amounts of andalusite, this mineral occurs as thing stringers, predominantly between and around cordierite porphyroblasts. (Plate 9). In rocks which are richer in andalusite this mineral commonly shows enclaves which partially surround cordierite porphyroblasts (Plate 10). Within these enclaves the two porphyroblasts are always separated by a mosaic of granoblastic polygonal material composed of predominant quartz with biotite and in some cases plagioclase. The porphyroblasts are related to the granoblastic mosaic in two ways:

i) 'Fingers' of andalusite reach out from the main porphyroblast and appear to replace biotite (commonly) and plagioclase (less commonly). The regions between andalusite 'fingers' are filled by quartz. (Plate 10b).

ii) Pinitization of cordierite margins makes it impossible to recognise any direct replacement relations, however cordierite porphyroblasts appear to be truncated by the granoblastic mosaic which mimicks their original oval shape.

b) In higher grade rocks within the Staurolite zone of the Banffshire coast similar textures occur in rocks which contain no cordierite. Andalusite porphyroblasts commonly show oval enclaves composed entirely of polygonal granoblastic material. (Plate 15). Such enclaves may be almost entirely enclosed in andalusite and are generally composed of:

i) an outer zone close to the andalusite porphyroblast composed of biotite and quartz showing replacement of biotite by the porphyroblast

ii) a central region, composed of biotite, plagioclase and minor quartz, occasionally accompanied by rare stringers of unidentifiable material which may be pinite.

In all cases inclusions within andalusite are restricted to quartz, biotite and ilmenite (occasionally with apatite and carbonaceous material) whilst cordierite where present may include all ground mass phases.

These textures are interpreted as follows. Oval enclaves in staurolite bearing rocks represent prograde pseudomorphs after cordierite. The pseudomorphing is achieved by i) replacement of cordierite by a biotite-plagioclase mosaic, ii) replacement of the biotite-plagioclase mosaic by andalusite.

Following Helgeson (1967), Carmichael (1969) and Eugster (1970) these replacement relations may be represented by ionic equilibria which may usefully be balanced conserving Aluminium as follows:

for replacement i)

$$\text{cordierite} + 7\ \text{quartz} + 7.5\ H_2O + 4(Fe,Mg)^{++} + 2K^+ + 2Na^+ = 2\ \text{albite} + 2\ \text{biotite} + 12H^+ \quad - 6$$

for replacement ii)

$$\text{albite} + \text{biotite} + 8H^+ = \text{andalusite} + 5\ \text{quartz} + 5H_2O + 3(Fe,Mg)^{++} + Na^+ + K^+ \quad - 7$$

Simplified mineral compositions used in these reactions are shown in Table 7.1. Although albite has been used to simplify the calculations the reactions could equally be balanced using a real plagioclase composition.

Reaction 6 consumes quartz. This is not a problem since cordierite contains numerous quartz inclusions. In fact the presence of some quartz in the central portions of completely recrystallised pesudomorphs may suggest that excess quartz is present as inclusions.

Reaction 7 will tend to occur at the interface between plagioclase and biotite so that these two minerals will become separated by intervening areas of andalusite + quartz. It is also notable that this reaction produces much more quartz than andalusite (in approximate ration 7 : 3 by volume). As a result, the reaction may easily become 'choked' by production of excess quartz, and this may explain why so many of these textures are preserved in the rocks.

Andalusite may also occur in complete isolation from cordierite porphyroblasts within specimens showing the above textures. These andalusites tend to be smaller and to occur in muscovite rich parts of the rock. From the net reaction (reaction 2) it is clear that muscovite is likely to be consumed. Although no direct replacement can be observed it is also possible to write a reaction producing andalusite from groundmass muscovite as follows:

muscovite + quartz + $3H_2O$ + $3(Fe,Mg)^{++}$ = andalusite + biotite + $6H^+$ - 8

Following Carmichael (1969) these three reactions, occurring in local adjacent subsystems, may be linked by interchaning cations to form a cycle (Figure 7.1). Taking 3 x reaction 6; 6 x reaction 7 and 2 x reaction 8, exactly balances all free ionic species and gives rise to a net reaction which is exactly equivalent to reaction 2 (see table 6.3).

The reaction path suggested in figure 7.1 is however likely to be an over simplification. For example, the chemical data presented in chapter 5 suggests that the net reaction is brought about by an incremental reaction (2a) effecting a change in X biotite and X cordierite, whereas figure 7.1 treats only total Fe + Mg. The distribution of ilmenite inclusions within andalusite porphyroblasts may have some bearing on this problem. These are generally concentrated near the centres of porphyroblasts and are generally scarcer near the edges particularly around the margins of enclaves. This situation occurs even where ilmenite is virtually lacking in the ground mass, and suggests that the oxide phase is a reaction product. Incorporation of some Fe^{++} in ilmenite would then allow

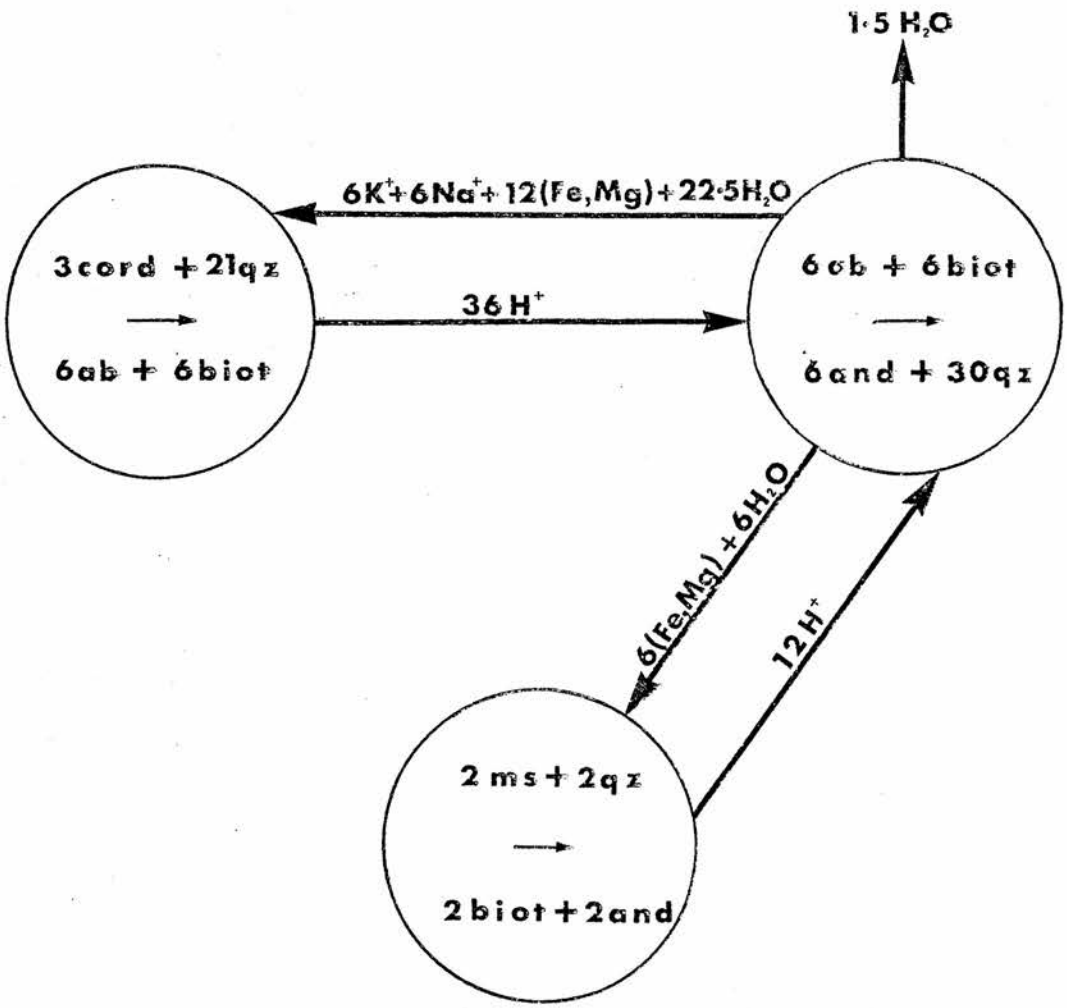

Figure 7.1 : Model of a possible path for the reaction cordierite + muscovite = andalusite + biotite. Each circle represents one microscopic domain.

Mineral	Formula
Andalusite	Al_2SiO_5
Cordierite	$(Fe,Mg)_2\ Al_4\ Si_5\ O_{18} \cdot\ 0.5\ H_2O$
Muscovite	$K\ Al_2\ AlSi_3\ O_{10}\ (OH)_2$
Biotite	$K\ (Fe,Mg)_3\ AlSi_3\ O_{10}\ (OH)_2$
Albite	$Na\ Al\ Si_3\ O_8$
Quartz	SiO_2

Table 7.1 : Simplified mineral compositions used in balancing reactions 6, 7 and 8.

the compositions of cordierite and biotite to become more Mg rich. If this were the case, it might be expected to operate more in the initial stages of reaction whilst the silicate compositions are still relatively iron rich. As the reaction proceeds, less Fe would be released relative to Mg, and consequently less of the oxide phase would be formed. This might explain the decrease in ilmenite inclusions close to enclaves, the andalusite on the edge of which was presumably the last to form.

APPENDIX I

MINERAL ASSEMBLAGES AND LOCALITIES

Appendix I (i) — Silicate assemblages. Quartz and plagioclase (or albite) are ubiquitous and are not listed. Grid references are preceded by the letter NJ except where otherwise stated. Eight figure references are given for important specimens (e.g. near isograds; analysed samples).

Appendix I (ii) — Opaque assemblages in polished sections.

A = andalusite; S = staurolite; C = cordierite;
G = garnet; Ch = chlorite (primary only);
Ms = muscovite; Bi = biotite; Ilm = ilmenite;
Pyr = pyrite; Pyrrh = pyrrhotite

* Specimen of J R Ashworth.

Specimen	A	S	C	G	Ch	Ms	Bi	Others	Locality	Grid Ref.
43842	-	-	-	-	x	x	x		¼ mile East of Garness Head	748647
43843	-	-	-	-	x	x	-			
43844	-	-	-	-	x	x	x		Garness Head	746648
43845	-	-	-	-	x	x	-			
43846	-	-	-	-	x	x	-		⅛ ml. W. Gar. Hd.	743648
43847	-	-	-	-	x	x	-	Carb. material	½ mile East of Old Haven	739647
43848	-	-	-	-	x	x	-	Brown material		
43849	-	-	-	-	x	x	-	Carb. material		
43850	-	-	-	-	x	x	x			
43851	-	-	-	-	x	x	-	Carb. material	Old Haven	734645
43852	-	-	-	-	x	x	x			
43853	-	-	-	-	-	x	x			
43854	-	-	-	-	x	x	x		W. Bay of Gullen	728647
43855	-	-	-	-	-	x	x		E. Bay of Gullen	723647
43856	-	-	-	-	x	x	x		Howe of Tarlair	719647
43857	-	-	-	-	x	x	x			
43858	-	-	-	-	x	x	x			

Specimen	A	S	C	G	Ch	Ms	Bi	Others	Locality	Grid Ref.
43859	-	-	-	-	x	x	x		Macduff	709649
43860	-	-	-	-	x	x	x			
43861	-	-	-	-	-	x	x			707649
43862	-	-	-	-	x	x	x		Banff Harbour S	68976438
43863	-	-	s	-	x	x	x		Banff Harbour N	68906473
43864	-	-	-	-	-	x	x			
43865	-	-	-	-	-	x	x		Boat Hythe	68786473
43866	-	-	-	-	-	x	x			68756470
43867(A)	-	-	s	-	-	x	x			68726470
43867(B)	-	-	-	-	-	x	x			
43868	-	-	s	-	-	x	x			68656470
43869	-	-	s	-	-	x	x			
43870	-	-	s	-	x	x	x	Tourmaline	Seatown	68506460
43871	-	-	s	-	-	x	x	Tourmaline		68406459
43872	-	-	s	-	-	x	x	Tourmaline		
43873	-	-	x	-	-	x	x		Scotstown	68286460
43874	-	-	x	-	-	x	x			
43875	-	-	s	-	-	x	x			68266460
43876	x	-	x	-	-	x	x			68236460
43877	x	-	x	-	-	x	x			
43878	-	-	s	-	-	x	x			68186460

Specimen	A	S	C	G	Ch	Ms	Bi	Others	Locality	Grid Ref.
43879	-	-	x	-	-	x	x		Elf Kirk	67956460
43880	-	-	x	-	-	x	x		Little Tumblers	67806458
43881	-	-	s	-	-	x	x			
43882	-	-	x	-	-	x	x		Tumblers	67606470
43883	-	-	x	-	-	x	x			
43884	-	-	x	-	-	x	x			
43885	x	-	x	-	-	x	x		Firfolds	65335895
43886(A)	x	x	s	x	-	x	x		West side of Boyndie Bay	66656495
43886(B)	x	x	-	x	-	x	x			
43887	x	x	x	-	-	x	x			66606498
43888	x	x	s	-	-	x	x			66556499
43889	x	x	-	-	-	x	x	Apatite		Between 66506500 and 66426511
43890	-	x	-	-	-	x	x			
43891	-	-	x	-	-	x	x			
43892	-	-	x	-	-	x	x			
43893	-	x	?	-	-	x	x			
43894	x	x	x	-	-	-	x			
43895	x	-	?	x	-	x	x			
43896	-	-	x	-	-	x	x			
43897	-	-	?	-	-	x	x			
43898	?	x	?	-	-	x	x			
43899	x	x	x	-	-	x	x			

Specimen	A	S	C	G	Ch	Ms	Bi	Others	Locality	Grid Ref.
43900	-	x	-	-	-	x	x			
43901	x	-	x	-	-	x	x			
43902	x	x	x	x	-	-	x			
43903	-	x	x	-	-	-	x			
43904	x	x	x	-	-	x	x			
43905	x	x	-	-	-	x	x			
43906	x	x	-	x	-	-	x	Apatite	West side	Between
43907	x	x	-	-	-	x	x			
43908	x	x	x	x	-	x	x		of	66356510
43909	x	x	-	-	-	x	x			
43910	x	x	-	-	-	-	x	Apatite	Boyndie Bay	and
43911	x	x	-	-	-	x	x			
43912	x	x	-	-	-	x	x	Apatite		66306520
43913	-	x	-	-	-	x	x	Apatite		
43914	x	x	-	-	-	x	x			
43915	-	x	-	-	-	x	x		Knock Head	65856598
43916	x	x	-	-	-	x	x			65426553
43917	x	x	-	-	-	x	x			
43918	x	x	-	x	-	x	x		Whitehills	65306557
43919	x	-	x	-	-	x	x			
43920	x	-	-	x	-	x	x		Craig Noon	65106562
43921	x	-	-	-	-	x	x		Stake Ness	644660
43922	x	-	-	-	-	x	x			642659

Specimen	A	S	C	G	Ch	Ms	Bi	Others	Locality	Grid Ref.
43923	-	x	x	x	-	-	x	Gedrite	East side of Bay East of Whyntie Head	637658
43924	-	x	x	x	-	-	x			
43925	-	x	x	-	-	-	x			
43926	-	-	-	-	-	-	x	Gedrite		
43927	x	x	x	-	-	-	x			
43928	x	x	x	-	-	-	x			
43929	x	x	-	-	-	x	x			
43930	x	-	-	-	-	x	x		Bay E. of Whyntie Hd.	635657
43931	x	-	-	-	-	x	x		Whyntie Head	634659
43932	x	-	-	-	-	x	x			
43933	x	-	x	-	-	x	x		Castlebrae Quarry	637546
43934	x	x	x	-	-	x	x			
43935	x	x	x	-	-	x	x			
43936	x	-	x	-	-	x	x			
43937	x	x	?	x	-	x	x		Maunderlea Quarry	633564
43938	x	-	x	-	-	x	x			
43939	x	x	-	x	-	x	x			
43940	-	x	-	x	-	x	x	in bands		
	-	x	-	x	-	-	x			
43941	x	-	x	-	-	x	x			
43942	x	x	x	-	-	-	x			

Specimen	A	S	C	G	Ch	Ms	Bi	Others	Locality	Grid Ref.
43943	x	x	-	-	-	x	x	Trace of Sill.	Kinnairdy Bridge	611501
43944	x	x	-	x	-	x	x			
43945	x	x	-	x	-	x	x	Trace of Sill.	Small Quarry by Kinnairdy Castle	611498
43946	x	x	-	-	-	x	x			
43947	x	x	-	x	-	x	x			
43948	x	x	-	-	-	x	x			
43949	x	x	-	-	-	x	x		Banks of Deveron near Kinnairdy	611495
43950	x	x	-	-	-	x	x			
43951	x	-	?	-	-	x	x			
43952	x	-	x	-	-	x	x			
43953	x	-	x	-	-	x	x			
43954	-	-	x	-	-	x	x			
43955	-	-	x	-	-	x	x			
43956	-	-	x	-	-	x	x	Tourm. Sill.	S. of	Between
43957	-	-	x	-	-	x	x			
43958	-	-	x	-	-	x	x	Trace of Sill.	Collieston	NK 041286
43959	-	-	x	-	-	x	x			and
43960	x	-	x	-	-	x	x		Harbour	NK 037281
43961	x	-	x	-	-	x	x			
43962	-	-	x	-	-	-	x	Gedrite		
43963	x	-	-	-	-	x	x			

Specimen	A	S	C	G	Ch	Ms	Bi	Others	Locality	Grid Ref.
43964	x	-	x	-	-	x	x			
43965	-	-	x	-	-	x	x	Sill.	S. of Collieston Harbour	
43966	-	-	x	-	-	x	x			
43967	-	-	-	-	x	x	x			761376
43968	-	-	-	-	-	x	x		Fyrie to	771378
43969	-	-	-	-	-	x	x			774375
43970	-	-	-	-	x	x	x		Ardlogie Mill	
43971	-	-	-	-	x	x	x	Tourm.		775373
43972	-	-	-	-	x	x	x			782370
43973	-	-	-	-	-	x	x			783369
43974	-	-	-	-	-	x	x	Tourm.		78503685
43975	-	-	-	-	-	x	x			78523672
43976	-	-	s	-	-	x	x		Ardlogie Mill	78553671
43977	-	-	s	-	-	x	x			78603668
43978	-	-	s	-	-	x	x		to the	78653663
43979	-	-	s	-	-	x	x			78673685
43980	-	-	s	-	-	x	x		Ords	78603682
43981	-	-	s	-	-	x	x			78903660
43982	-	-	s	-	-	x	x			79233655

Specimen	A	S	C	G	Ch	Ms	Bi	Others	Locality	Grid Ref.
43983	-	-	s	-	-	x	x		Braes of Minnonie	79183668
43984	-	-	s	-	-	x	x			79363765
43985	x	-	s	-	-	x	x			79343780
43986	x	-	s	-	-	x	x			79433774
43987	-	-	s	-	-	x	x			79353777
43988	-	-	s	-	-	x	x		Doolie Bridge to Blaikie Burn	79853805
43989	x	-	s	-	-	x	x			80103795
43990	x	-	s	-	-	x	x			80203805
43991	-	-	x	-	-	x	x			80303808
43992	-	-	x	-	-	x	x			80353812
43993	x	-	x	-	-	x	x			
43994	x	-	x	-	-	x	x		Braes of Blairfowl	80483844
43995	x	-	x	-	-	x	x			807387
43996	-	-	x	-	-	x	x		Featherletter Burn to Round Pot	808388
43997	x	-	x	-	-	x	x			
43998	x	-	x	-	-	x	x			

Specimen	A	S	C	G	Ch	Ms	Bi	Others	Locality	Grid Ref.
43999	-	-	x	-	-	x	x		Fetterletter Burn to Round Pot	810386
44000	x	-	x	-	-	x	x			812386
44001	x	-	x	-	-	x	x			813386
44002	-	-	-	-	-	x	x			818383
44003	-	-	-	-	-	x	x			821384
44004	x	-	x	-	-	x	x		Braes of Gight	821385
44005	x	-	x	-	-	x	x			
44006	x	-	x	-	-	x	x			821386
44007	x	-	x	-	-	x	x			
44008	-	-	x	-	-	x	x			
44009	x	-	x	-	-	x	x			821387
44010	x	-	x	-	-	x	x			
44011	-	-	x	-	-	x	x			
44012	x	-	x	-	-	x	x			
44013	x	-	x	-	-	x	x			82053875
44014	x	-	x	-	-	x	x			831388
44015	-	-	-	x	-	-	-	hble; ep; carb.		

Specimen	A	S	C	G	Ch	Ms	Bi	Others	Locality	Grid Ref.
44016	-	-	-	-	-	x	x	ksp.	Braes of	83223915
44017	x	-	x	-	-	x	x	Tourm.	Gight	
44018	x	-	x	-	-	x	x			819312
44019	x	-	x	-	-	x	x		Bar Strike	822393
44020	-	-	x	-	-	x	x		to Gight Castle	
44021	-	-	x	-	-	x	x			838397
44022	x	-	x	-	-	x	x		Little	839397
44023	-	-	-	x	-	-	-		Gight	
44024	x	-	x	-	-	x	x			840395
44025	-	-	-	x	-	?	x		to	841395
44026	x	-	x	-	-	x	x			839396
44027	x	-	x	-	-	x	x		Waterloo	
44028	?	-	?	-	-	x	x		Bridge	839397
44029	x	-	x	-	-	x	x			841392
44030	x	-	x	-	-	x	x		Chapelhaugh	843392
44031	-	-	-	-	-	x	x			845392
44032	x	-	-	-	-	x	x			845390

Specimen	A	S	C	G	Ch	Ms	Bi	Others	Locality	Grid Ref.
44033	x	-	-	-	-	x	x		Chapelhough	845390
44034	?	-	x	-	-	x	x			843389
44035	x	-	x	-	-	x	x	Sill.	Wood of	845386
44036	x	-	x	-	-	x	x		Wardford	846384
44037	x	-	x	-	-	x	x	Sill.		848383
44038	x	-	-	-	-	x	x	Sill.	to	849382
44039	x	-	x	-	-	x	x	Sill.		852399
44040	-	-	x	-	-	x	x	Sill.	Methlick	858375
44041	x	-	-	-	-	x	x	Sill.		862372
44042	-	-	-	-	x	x	x		Largue	643418
44043	-	-	-	-	x	x	-	Carbn.material	Lenshie	680408
44044	-	-	-	-	x	x	-	Carbn.material		683404
44045	-	-	-	-	x	x	x		Badenscoth Br.	698388
44046	-	-	s	-	-	x	x			733369
44047	-	-	s	-	-	x	x		Waulkmill Wood	736368
44048	x	-	s	-	-	x	x			
44049	-	-	-	-	x	x	x		Largue	648417

Specimen	A	S	C	G	Ch	Ms	Bi	Others	Locality	Grid Ref.
44050	-	-	-	-	x	x	x	Tourm.	Kings Chair	771376
44051	-	-	s	-	-	x	x			79023650
44052	-	-	s	-	-	x	x			78853654
44053	-	-	s	-	-	x	x		The Ords	79083700
44054	-	-	s	-	-	x	x			79103705
44055	-	-	-	-	x	x	x	Carbn.material		
44056	-	-	-	-	x	x	x	Carbn.material		Between
44057	-	-	-	-	x	x	x	Carbn.material		
44058	-	-	-	-	x	x	x			
44059	-	-	-	-	x	x	x		Balquholly	714459
44060	-	-	-	-	x	x	x			
44061	-	-	-	-	-	x	x			and
44062	-	-	-	-	-	x	x			
44063	-	-	-	-	x	x	x			718451
44064	-	-	-	-	-	x	x		Towie	
44065	-	-	x	-	-	x	x			
44066	x	-	x	-	-	x	x			
44067	x	-	x	-	-	x	x		Rosehearty	927677
44068	x	-	x	-	-	x	x	Apatite		
44069	-	-	x	-	-	-	x	Apatite		
44070	-	-	x	-	-	x	x			923673
15463*	x	x	-	x	-	x	x		Boyndie Bay	

APPENDIX I (ii)

Specimen	Ilm.	Pyr.	Pyrrh.	Others
43852	x	-	x	ccp.
43857	x	x	-	
43858	x	x	-	
43859	x	x	-	
43860	x	x	x	
43864	x	-	x	ccp.
43865	x	-	-	rut?
43867	x	-	x	rut?
43870	x	-	x	rut?
43873	x	-	x	ccp.
43876	x	-	-	
43894	x	x	-	ccp.
43901	x	x	-	
43902	x	x	-	rut?
43918	x	x	x	ccp.; rut?
49219	x	-	-	
43922	x	-	x	ccp.
43923	x	-	-	
43927	x	-	-	rut?
43929	x	x	-	
43931	x	-	-	rut?
43939	x	-	-	
43940	x	-	-	
43942	x	-	x	
43945	x	-	x	ccp.
43962	x	-	-	
43993	x	x	-	
44013	x	-	x	ccp.
44016	x	-	-	
15463*	x	x	-	ccp.

rut? = primary? rutile; ccp. = chalcopyrite

APPENDIX II

BULK ROCK ANALYSES

Specimen No.	43973	43978	43981	43998
SiO_2	56.86	56.21	69.30	56.94
TiO_2	1.56	1.23	0.49	1.18
Al_2O_3	18.74	20.56	13.08	19.03
Fe_2O_3*	7.70	7.44	7.74	9.68
MgO	2.31	1.95	3.03	2.69
MnO	0.11	0.07	0.10	0.10
CaO	0.87	0.70	0.76	1.51
Na_2O	2.11	2.05	0.94	1.36
K_2O	4.39	4.62	2.97	3.66
P_2O_5	0.08	0.11	n.d.	0.32
H_2O	2.46	2.88	2.49	2.39
Total	97.19	97.82	100.90	98.86
FeO**	5.13	5.70	5.61	7.22
A	34	39	28	34
K	16	17	12	12
F	50	44	60	54
$\frac{100MgO}{MgO+FeO}$	40.8	37.6	47.3	38.9

BULK ROCK ANALYSES

Specimen No.	43849	43852	43860	43867
SiO_2	53.90	57.80	57.79	54.50
TiO_2	1.07	1.06	0.82	1.08
Al_2O_3	20.10	18.36	19.27	20.00
Fe_2O_3*	9.57	7.79	7.50	8.38
MgO	2.60	2.40	2.32	2.65
MnO	0.11	0.11	0.13	0.08
CaO	1.03	1.02	0.55	0.82
Na_2O	2.27	2.30	1.16	n.a.
K_2O	3.20	3.07	3.81	4.45
P_2O_5	0.27	0.12	0.07	0.14
H_2O	4.07	3.27	3.95	n.a.
Total	98.19	97.30	97.37	(92.10)
FeO**	-	6.24	6.21	6.48
A	36	37	41	41
K	11	12	13	14
F	53	51	46	45
$\frac{100MgO}{MgO+FeO}$	38.4	41.4	41.5	42.0

BULK ROCK ANALYSES

Specimen No.	43873	43874	43876	43888
SiO_2	55.64	56.43	51.46	54.68
TiO_2	0.95	1.14	1.44	0.83
Al_2O_3	16.51	20.48	24.36	22.24
Fe_2O_3*	9.25	7.11	8.11	8.05
MgO	2.43	2.63	2.27	3.05
MnO	0.08	0.09	0.06	0.06
CaO	1.54	0.77	1.66	0.87
Na_2O	2.78	1.68	2.95	n.a.
K_2O	2.75	4.66	4.34	4.49
P_2O_5	0.09	0.10	0.37	0.43
H_2O	1.73	3.08	2.89	4.42
Total	93.75	98.17	99.91	99.12
FeO**	-	4.96	7.18	6.01
A	28	37	39	43
K	10	16	15	13
F	62	47	46	44
$\frac{100MgO}{MgO+FeO}$	38.3	46.0	39.1	46.5

BULK ROCK ANALYSES

Specimen No.	43895	43899	43901	43902
SiO_2	56.30	52.25	55.51	55.45
TiO_2	0.81	1.06	0.88	1.03
Al_2O_3	19.30	24.18	22.57	23.61
Fe_2O_3*	6.30	9.53	6.70	6.15
MgO	2.49	3.16	2.59	1.45
MnO	0.05	0.05	0.03	0.09
CaO	0.99	0.56	0.42	3.20
Na_2O	2.86	1.71	1.52	4.58
K_2O	2.88	4.29	4.86	1.44
P_2O_5	0.05	0.06	0.02	0.05
H_2O	3.39	4.02	3.87	2.38
Total	95.42	100.87	98.97	99.43
FeO**	-	6.01	-	4.67
A	38	42	43	44
K	12	12	16	7
F	50	46	41	49
$\frac{100MgO}{MgO+FeO}$	47.6	43.2	46.6	35.1

BULK ROCK ANALYSES

Specimen No.	43904	43907	43910	43911
SiO_2	53.75	52.33	48.25	53.34
TiO_2	0.98	1.34	0.84	1.03
Al_2O_3	22.36	23.66	22.00	25.39
Fe_2O_3*	8.90	11.01	8.82	9.50
MgO	2.76	4.07	2.52	3.25
MnO	0.07	0.11	0.10	0.10
CaO	0.64	1.56	7.82	0.90
Na_2O	1.33	2.55	0.65	0.84
K_2O	4.49	3.93	2.49	4.28
P_2O_5	0.03	0.12	6.07	0.29
H_2O	3.57	2.45	1.68	3.76
Total	98.88	103.13	101.24	102.68
FeO**	6.23	4.07	7.74	8.59
A	41	33	20	38
K	13	11	11	18
F	46	56	68	44
$\frac{100MgO}{MgO+FeO}$	41.6	45.9	39.6	44.6

BULK ROCK ANALYSES

Specimen No.	43912	43913	43916	43918
SiO_2	5048	54.24	57.36	56.03
TiO_2	1.08	0.77	0.75	1.09
Al_2O_3	24.82	22.32	17.30	20.15
Fe_2O_3*	10.81	6.99	7.37	9.48
MgO	2.96	2.55	3.21	3.10
MnO	0.11	0.07	0.06	0.12
CaO	2.15	3.29	0.86	0.96
Na_2O	1.19	2.83	2.66	1.21
K_2O	3.24	3.52	3.87	3.96
P_2O_5	0.76	0.48	0.04	0.10
H_2O	2.90	2.40	2.75	3.84
Total	100.50	99.46	96.23	100.04
FeO**	7.45	5.92	-	7.79
A	42	32	28	36
K	9	14	15	12
F	49	54	57	52
$\frac{100MgO}{MgO+FeO}$	38.6	45.5	50.0	42.9

BULK ROCK ANALYSES

Specimen No.	43919	43921	43922	43927
SiO_2	48.34	51.07	47.95	49.87
TiO_2	1.12	0.80	1.13	0.84
Al_2O_3	26.77	23.24	30.29	24.67
Fe_2O_3*	5.47	7.81	6.18	7.71
MgO	2.64	2.98	2.41	4.34
MnO	0.04	0.04	0.06	0.06
CaO	1.11	0.52	0.85	1.48
Na_2O	0.84	0.33	1.24	5.17
K_2O	6.87	5.25	5.58	3.23
P_2O_5	0.58	0.11	0.18	0.04
H_2O	4.88	5.51	3.82	2.34
Total	98.66	97.66	99.69	99.75
FeO**	3.97	-	4.80	6.28
A	45	43	53	32
K	20	15	15	11
F	35	42	32	57
$\frac{100MgO}{MgO+FeO}$	52.7	46.7	47.2	55.0

BULK ROCK ANALYSES

Specimen No.	43929	43931	43943	43945	43962
SiO_2	48.81	49.67	57.93	57.15	50.43
TiO_2	0.98	1.04	1.00	1.09	1.58
Al_2O_3	24.96	27.00	21.25	21.90	18.26
Fe_2O_3*	10.46	7.72	8.79	9.66	13.33
MgO	3.55	3.06	3.05	3.39	7.46
MnO	0.07	0.04	0.13	0.21	0.32
CaO	1.32	0.50	1.59	1.16	1.73
Na_2O	4.16	0.96	1.98	1.29	5.78
K_2O	3.91	6.08	3.12	3.54	0.25
P_2O_5	0.07	0.06	0.17	0.14	0.14
H_2O	3.47	4.25	1.63	1.76	0.96
Total	101.76	99.93	100.64	101.29	100.24
FeO**	8.41	6.26	7.28	6.72	11.89
A	36	45	37	38	15
K	11	16	10	10	6
F	53	39	53	52	79
$\frac{100MgO}{MgO+FeO}$	40.6	43.8	44.5	44.6	58.9

APPENDIX III

ELECTRON MICROPROBE MINERAL ANALYSES

na	=	not analysed
nd	=	not detected

*	Partial analysis
**	Analysis performed & kindly donated by Dr J Ashworth.

APPENDIX III (i)

CHLORITE ANALYSES

Specimen No.	43852				43857
	1	2	3	4	
SiO_2	24.50	24.30	24.53	24.17	25.01
TiO_2	0.08	0.13	0.09	0.71	0.08
Al_2O_3	20.67	20.40	21.58	21.31	23.24
FeO	26.72	27.36	27.49	27.26	24.39
MgO	11.45	11.73	11.80	11.56	13.11
MnO	0.33	0.36	0.33	0.38	0.36
≠ Total	83.88	85.43	85.92	85.43	86.45
		No. of ions			
Si	2.74	2.71	2.68	2.67	2.67
Al	1.26	1.29	1.32	1.33	1.33
Al	1.46	1.40	1.46	1.45	1.59
Fe	2.50	2.55	2.51	2.52	2.17
Mg	1.91	1.95	1.92	1.90	2.08
Mn	0.03	0.03	0.03	0.04	0.03
Ti	0.01	0.01	0.01	0.01	0.01
	5.91	5.94	5.93	5.92	5.88
$Fe^{+2} : R^{+2}$	.56	.56	.56	.56	.51
Zone	Biot	Biot	Biot	Biot	Biot

≠ Includes minor alkalies.

CHLORITE ANALYSES

	Specimen No.	43858	43860		43859	
			1	2	1	2
	SiO_2	24.90	24.02	23.22	24.42	24.47
	TiO_2	0.06	0.09	0.09	0.06	0.07
	Al_2O_3	22.14	22.84	22.28	23.68	22.99
	FeO	24.14	28.33	28.72	27.74	28.36
	MgO	12.69	10.83	11.19	11.87	14.22
	MnO	0.36	0.49	0.49	0.48	0.50
≠	Total	84.79	86.60	85.99	88.37	90.67
			No. of ions			
	Si	2.72	2.61	2.56	2.59	2.54
	Al	1.28	1.39	1.44	1.41	1.46
	Al	1.56	1.54	1.45	1.55	1.35
	Fe	2.20	2.58	2.64	2.46	2.46
	Mg	2.06	1.75	1.84	1.88	2.20
	Mn	0.03	0.05	0.05	0.05	0.04
	Ti	0.01	0.01	0.01	0.01	0.01
		5.86	5.93	5.99	5.95	6.06
	$Fe^{+2} : R^{+2}$	.51	.59	.59	..56	.52
	Zone					

≠ Includes minor alkalies.

CHLORITE ANALYSES

Specimen No.	43859	43870		43873	43876
	3	1	2		
SiO_2	25.26	28.17	28.12	25.50	25.36
TiO_2	0.07	na	na	0.09	0.08
Al_2O_3	23.49	23.07	24.12	23.88	23.11
FeO	28.32	26.22	24.89	23.42	27.33
MgO	13.75	10.90	9.75	15.26	12.17
MnO	0.50	0.27	0.28	0.31	0.17
≠ Total	91.46	88.63	87.15	88.52	88.30
		No. of ions			
Si	2.59	2.92	2.93	2.63	2.67
Al	1.41	1.08	1.07	1.37	1.33
Al	1.42	1.73	1.89	1.53	1.54
Fe	2.42	2.27	2.17	2.02	2.41
Mg	2.10	1.68	1.51	2.34	1.91
Mn	0.04	0.03	0.03	0.03	0.02
Ti	0.01	-	-	0.01	0.01
	5.99	5.71	5.59	5.93	5.89
$Fe^{+2} : R^{+2}$	.53	.57	.58	.46	.55
Zone	Biot	Cord	Cord	Andal	Andal

≠ Includes minor alkalies.

CHLORITE ANALYSES

	Specimen No.	43901	43894	15462**	15463**	15464**
	SiO_2	25.49	21.16	23.30	24.31	23.56
	TiO_2	0.09	0.09	na	0.08	na
	Al_2O_3	24.04	22.31	22.68	23.18	23.29
	FeO	24.62	25.78	25.08	27.56	27.56
	MgO	14.39	13.51	13.62	13.18	13.50
	MnO	0.24	0.31	na	0.44	na
≠	Total	88.93	83.20	84.68	88.75	87.91
			No. of ions			
	Si	2.63	2.41	2.55	2.57	2.57
	Al	1.37	1.59	1.45	1.43	1.49
	Al	1.55	1.39	1.47	1.45	1.43
	Fe	2.12	2.45	2.29	2.43	2.45
	Mg	2.21	2.22	2.22	2.07	2.14
	Mn	0.02	0.03	-	0.04	-
	Ti	0.09	0.01	-	-	-
		5.99	6.10	5.98	5.99	6.02
	$Fe^{+2} : R^{+2}$	.49	.52	.51	.54	.53
	Zone	Staur	Staur	Staur	Staur	Staur

≠ Includes minor alkalies.

APPENDIX III (ii)

WHITE MICA ANALYSES

Specimen No.	43852	43857	43865	43867	43876
SiO_2	48.67	46.98	44.13	45.94	44.97
TiO_2	0.30	0.18	0.56	0.40	na
Al_2O_3	32.03	34.66	32.63	35.36	37.12
FeO	1.58	0.87	1.19	1.64	0.86
MgO	0.95	0.72	0.73	0.69	0.35
MnO	0.02	nd	nd	nd	nd
K_2O	8.76	9.56	9.44	9.20	8.52
Na_2O	0.24	0.37	0.37	0.34	na
Total	92.55	93.34	89.05	93.57	91.82
	No. of ions on the basis of 22 oxygen				
Si	6.57	6.31	6.25	6.18	6.10
Al	1.43	1.69	1.75	1.82	1.90
Al	3.67	3.80	3.70	3.78	4.03
Ti	0.03	0.02	0.06	0.04	-
Fe	0.18	0.10	0.14	0.18	0.10
Mg	0.19	0.14	0.15	0.14	0.07
Mn	< 0.01	-	-	-	-
	4.07	4.06	4.07	4.14	4.20
K	1.51	1.64	1.71	1.58	1.47
Na	0.06	0.10	0.10	0.09	-
	1.57	1.74	1.81	1.67	1.47
Zone	Biot	Biot	Cord	Cord	Andal

WHITE MICA ANALYSES

Specimen No.	15463**	43852 green mica
SiO_2	50.21	48.74
TiO_2	na	0.16
Al_2O_3	36.31	26.46
FeO	0.32	8.76
MgO	0.24	3.22
MnO	na	0.11
K_2O	9.05	9.47
Na_2O	0.99	0.94
Total	97.12	97.86
	No. of ions	
Si	6.42	6.55
Al	1.58	1.45
Al	3.90	2.74
Ti	-	0.02
Fe	0.03	0.99
Mg	0.05	0.65
Mn	-	0.01
	3.98	4.41
K	1.48	1.62
Na	0.25	0.25
	1.73	1.87
Zone	Staur	Biot

APPENDIX III (iii)

BIOTITE ANALYSES

Specimen No.	43852				43857
	1	2	3	4	
SiO_2	35.93	37.05	36.12	35.57	35.89
TiO_2	1.67	1.55	1.71	1.61	1.31
Al_2O_3	18.01	17.82	18.41	17.54	19.51
FeO	20.16	20.65	20.32	22.13	19.64
MgO	8.17	8.26	8.58	8.13	9.94
MnO	0.17	0.17	0.14	0.11	0.18
K_2O	8.50	7.03	8.72	7.98	7.37
Na_2O	na	na	na	na	na
CaO	na	na	na	na	na
Total	92.61	92.53	94.00	93.07	93.84
		No. of ions on the basis of 22 oxygen			
Si	5.61	5.73	5.56	5.58	5.48
Al	2.39	2.27	2.44	2.42	2.52
Al	0.94	0.98	0.91	0.82	0.99
Ti	0.20	0.18	0.20	0.19	0.15
Fe	2.63	2.67	2.62	2.90	2.51
Mg	1.90	1.91	1.97	1.90	2.26
Mn	0.02	0.02	0.02	0.02	0.02
	5.69	5.77	5.71	5.82	5.93
Ca	-	-	-	-	-
Na	-	-	-	-	-
K	1.70	1.38	1.71	1.59	1.44
Zone	Biot	Biot	Biot	Biot	Biot

BIOTITE ANALYSES

Specimen No.	43860			43864	
	2	3	4	1	3
SiO_2	34.26	36.42	35.48	35.13	35.59
TiO_2	1.55	1.44	1.51	1.46	1.44
Al_2O_3	19.58	18.99	19.03	19.28	18.90
FeO	22.15	22.36	22.06	21.17	20.69
MgO	7.57	7.60	7.46	8.89	8.73
MnO	0.21	0.25	0.25	0.23	0.23
K_2O	7.60	7.73	7.85	8.78	8.44
Na_2O	0.09	0.09	0.11	na	na
CaO	na	na	na	na	na
Total	93.01	94.88	93.75	94.94	94.02
		No. of ions			
Si	5.37	5.58	5.51	5.40	5.49
Al	2.63	2.42	2.49	2.60	2.51
Al	0.98	1.01	0.99	0.89	0.92
Ti	0.18	0.17	0.18	0.17	0.17
Fe	2.90	2.86	2.86	2.72	2.67
Mg	1.77	1.73	1.72	2.03	2.01
Mn	0.03	0.03	0.03	0.03	0.03
	5.86	5.80	5.78	5.84	5.79
Ca	-	-	-	-	-
Na	0.03	0.03	0.04	-	-
K	1.52	1.51	1.56	1.72	1.66
Zone	Biot	Biot	Biot	Cord	Cord

BIOTITE ANALYSES

Specimen No.	43864	43865			
	4	1	2	3	4
SiO_2	34.91	34.07	34.12	34.53	34.48
TiO_2	1.29	2.95	2.76	2.64	2.64
Al_2O_3	19.15	16.71	17.27	16.32	16.09
FeO	21.20	19.01	18.83	18.06	18.31
MgO	8.58	9.48	9.31	9.09	9.50
MnO	0.23	0.12	0.17	0.18	0.17
K_2O	8.74	9.62	9.35	8.54	8.54
Na_2O	na	na	na	na	na
CaO	na	na	na	na	na
Total	94.10	91.96	91.81	89.36	89.73
		No. of ions			
Si	5.41	5.42	5.42	5.59	5.56
Al	2.59	2.58	2.58	2.41	2.44
Al	0.91	0.55	0.94	0.70	0.62
Ti	0.15	0.35	0.33	0.32	0.32
Fe	2.75	2.53	2.50	2.44	2.47
Mg	1.98	2.25	2.20	2.19	2.28
Mn	0.03	0.01	0.02	0.02	0.02
	5.83	5.69	5.99	5.67	5.71
Zone	Cord		Cord	Cord	Cord

BIOTITE ANALYSES

Specimen No.	43867		43870		
	1	2	1	3	4
SiO_2	35.88	36.69	36.12	35.97	36.00
TiO_2	1.46	1.35	na	na	na
Al_2O_3	18.32	17.60	19.43	19.35	19.86
FeO	20.84	20.67	21.29	21.25	21.45
MgO	8.11	7.90	8.04	8.17	7.93
MnO	0.15	0.20	0.12	0.17	0.18
K_2O	8.28	8.65	7.94	8.01	7.94
Na_2O	na	na	na	na	na
CaO	na	na	na	na	na
Total	93.04	93.06	92.94	92.92	93.36
		No. of ions			
Si	5.59	5.72	5.62	5.60	5.58
Al	2.41	2.28	2.38	2.40	2.42
Al	0.95	0.95	1.18	1.15	1.20
Ti	0.17	0.16	-	-	-
Fe	2.71	2.69	2.77	2.76	2.78
Mg	1.88	1.83	1.86	1.89	1.83
Mn	0.02	0.03	0.01	0.02	0.02
	5.73	5.66	5.82	5.82	5.83
Ca	-	-			
Na	-	-			
K	1.65	1.72	1.58	1.59	1.57
Zone	Cord	Cord	Cord	Cord	Cord

BIOTITE ANALYSES

Specimen No.	43873	43876	43993	44013	44016
SiO_2	35.13	35.20	34.76	35.04	35.19
TiO_2	1.35	1.27	1.44	1.86	1.69
Al_2O_3	20.47	21.12	20.78	19.57	19.99
FeO	18.21	21.17	21.55	20.92	20.43
MgO	10.48	8.82	8.08	8.88	10.42
MnO	0.19	0.11	0.11	0.15	0.15
K_2O	8.79	8.78	8.99	8.13	8.67
Na_2O	na	na	na	na	na
CaO	na	na	na	na	na
Total	94.62	96.47	95.71	94.55	96.54
		No. of ions			
Si	5.33	5.30	5.30	5.37	5.28
Al	2.67	2.70	2.70	2.63	2.72
Al	0.99	1.05	0.99	0.88	0.79
Ti	0.15	0.15	0.17	0.21	0.19
Fe	2.31	2.66	2.75	2.68	2.57
Mg	2.37	2.18	1.84	2.03	2.33
Mn	0.02	0.01	0.01	0.02	0.02
	5.84	6.06	5.76	5.82	5.90
Ca	-	-	-	-	-
Na	-	-	-	-	-
K	1.70	1.68	1.75	1.59	1.66
Zone	Andal	Andal	Andal	Andal	Andal

BIOTITE ANALYSES

Specimen No.	43901			15463**	43919
	1	2	3		1
SiO_2	35.16	35.92	35.49	35.66	35.66
TiO_2	1.33	1.51	1.47	1.60	2.05
Al_2O_3	20.06	20.01	20.00	20.77	19.24
FeO	19.65	19.11	18.55	21.52	18.45
MgO	10.19	9.66	10.26	8.10	9.85
MnO	0.14	0.14	0.15	na	0.17
K_2O	8.64	8.46	8.42	8.88	8.10
Na_2O	na	na	na	0.48	0.25
CaO	na	na	na	na	na
Total	95.17	94.81	94.34	97.01	93.77
		No. of ions			
Si	5.33	5.44	5.39	5.35	5.45
Al	2.67	2.56	2.61	2.65	2.55
Al	0.92	1.01	0.97	1.02	0.88
Ti	0.15	0.17	0.17	0.18	0.24
Fe	2.49	2.42	2.35	2.70	2.36
Mg	2.30	2.18	2.32	1.81	2.24
Mn	0.02	0.02	0.02	-	0.02
	5.88	5.80	5.94	5.71	5.74
Ca	-				
Na	-			0.14	0.07
K	1.67	1.64	1.63	1.70	1.58
Zone	← Staur. →				

BIOTITE ANALYSES

Specimen No.	43919		43918		
	2	3	1	2	3
SiO_2	35.53	35.77	35.28	35.38	35.53
TiO_2	1.78	1.87	1.62	1.77	1.89
Al_2O_3	19.41	19.45	19.67	19.73	19.93
FeO	18.37	18.71	20.23	20.01	19.84
MgO	9.96	9.88	9.23	8.93	8.96
MnO	0.15	0.15	0.25	0.26	0.23
K_2O	8.91	9.07	8.61	8.37	8.77
Na_2O	0.32	0.28	0.28	0.25	0.34
CaO	na	na	na	na	na
Total	94.43	95.18	95.17	94.70	95.49
		No. of ions			
Si	5.43	5.42	5.37	5.41	5.40
Al	2.57	2.58	2.63	2.59	2.60
Al	0.92	0.89	0.91	0.96	0.96
Ti	0.20	0.21	0.19	0.20	0.22
Fe	2.34	2.37	2.59	2.56	2.51
Mg	2.27	2.23	2.09	2.03	2.02
Mn	0.02	0.02	0.03	0.03	0.03
	5.75	5.71	5.81	5.78	5.74
Ca	-	-	-	-	-
Na	-	0.08	0.08	0.07	0.10
K	1.73	1.76	1.67	1.63	1.70
Zone	←		Staur		→

BIOTITE ANALYSES

Specimen No.	43922	43929			43931
		2	3	4	
SiO_2	34.69	34.37	36.97	36.59	34.84
TiO_2	2.19	2.26	2.26	2.15	2.85
Al_2O_3	19.01	20.38	19.57	19.73	18.61
FeO	20.44	19.09	19.41	18.22	19.66
MgO	9.37	9.41	9.46	9.64	9.67
MnO	0.12	0.12	0.12	0.11	0.17
K_2O	8.36	8.63	8.63	8.61	9.24
Na_2O	0.01	0.25	0.28	0.30	0.09
CaO	0.01	0.01	< 0.01	< 0.01	< 0.01
Total	94.20	94.52	96.70	95.35	95.13
		No. of ions			
Si	5.40	5.25	5.49	5.48	5.33
Al	2.60	2.75	2.51	2.52	2.67
Al	0.89	0.92	0.91	0.97	0.68
Ti	0.27	0.26	0.25	0.24	0.33
Fe	2.66	2.44	2.41	2.28	2.51
Mg	2.18	2.14	2.09	2.15	2.20
Mn	0.02	0.02	0.02	0.01	0.02
	6.02	5.77	5.68	5.66	5.75
Ca	-	-	-	-	-
Na	-	0.07	0.08	0.09	0.03
K	1.64	1.68	1.64	1.65	1.80
Zone	Staur	Staur	Staur	Staur	Sill

BIOTITE ANALYSES

Specimen No.	43942			43894	
	1	3	4	1	2
SiO_2	32.82	33.09	33.49	32.78	32.28
TiO_2	1.66	1.56	1.64	1.58	1.54
Al_2O_3	19.68	19.34	19.03	19.19	19.12
FeO	19.28	19.21	18.93	20.35	20.20
MgO	9.04	8.90	9.27	8.91	8.72
MnO	0.15	0.18	0.14	0.14	0.15
K_2O	8.88	8.56	8.31	8.98	8.87
Na_2O	0.18	0.21	0.25	0.18	0.20
CaO	na	0.01	0.01	0.03	na
Total	91.69	91.06	91.07	92.14	91.08
			No. of ions		
Si	5.21	5.28	5.32	5.22	5.20
Al	2.79	2.72	2.68	2.78	2.80
Al	0.90	0.92	0.89	0.82	0.83
Ti	0.20	0.19	0.20	0.19	0.19
Fe	2.56	2.56	2.52	2.71	2.72
Mg	2.14	2.12	2.20	2.11	2.09
Mn	0.02	0.02	0.02	0.02	0.02
	5.82	5.81	5.82	5.85	5.85
Ca	-	-	-	0.01	-
Na	0.06	0.07	0.08	0.06	0.06
K	1.79	1.74	1.69	1.82	1.82
Zone	← Staur →				

BIOTITE ANALYSES

Specimen No.	43927			43940	43939
	1	2	3	1	2
SiO_2	35.42	35.72	35.76	35.62	34.32
TiO_2	1.97	1.74	1.53	1.57	1.47
Al_2O_3	20.33	20.56	21.10	19.36	19.23
FeO	17.74	17.40	16.87	21.50	20.60
MgO	10.57	10.65	10.65	9.07	8.26
MnO	0.11	0.09	0.11	0.15	0.14
K_2O	8.39	8.64	8.65	8.38	8.22
Na_2O	0.61	0.48	0.53	0.13	na
CaO	na	na	0.01	na	nd
Total	95.14	95.28	95.21	95.78	92.24
			No. of ions		
Si	5.32	5.35	5.34	5.41	5.40
Al	2.68	2.65	2.66	2.59	2.60
Al	0.92	0.98	1.06	0.87	0.97
Ti	0.22	0.20	0.17	0.18	0.17
Fe	2.23	2.18	2.11	2.73	2.71
Mg	2.37	2.37	2.37	2.05	1.94
Mn	0.01	0.01	0.01	0.02	0.02
	5.76	5.74	5.72	5.85	5.81
Ca	-	-	-	-	-
Na	0.18	0.14	0.15	0.04	-
K	1.61	1.65	1.65	1.62	1.65
Zone	←		Staur		→

BIOTITE ANALYSES

Specimen No.	43939		43945		
	3	5	1	3	5
SiO_2	34.40	37.97	35.13	33.69	34.49
TiO_2	1.47	1.42	1.56	1.52	1.72
Al_2O_3	19.76	19.39	19.92	19.74	19.61
FeO	20.6	20.40	20.34	20.98	20.47
MgO	8.42	7.98	8.60	9.00	8.78
MnO	0.22	0.18	0.14	0.18	0.15
K_2O	8.22	7.97	8.34	8.37	8.53
Na_2O	na	na	0.18	0.20	0.32
CaO	na	na	na	na	na
Total	93.09	95.31	94.21	93.68	94.07
		No. of ions			
Si	5.36	5.70	5.39	5.25	5.33
Al	2.64	2.30	2.61	2.75	2.67
Al	0.99	1.13	1.00	0.87	0.90
Ti	0.17	0.16	0.18	0.18	0.12
Fe	2.69	2.56	2.61	2.73	2.65
Mg	1.96	1.79	1.97	2.09	2.02
Mn	0.03	0.03	0.02	0.02	0.02
	5.84	5.67	5.78	5.89	5.71
Ca	-	-	-	-	-
Na	-	-	0.05	0.06	0.10
K	1.64	1.53	1.63	1.67	1.68
Zone	← Staur →				

BIOTITE ANALYSES

Specimen No.	43924		43923	43962
	1	2	2	
SiO_2	34.69	34.54	34.32	35.15
TiO_2	1.51	1.37	1.57	1.55
Al_2O_3	21.29	19.99	17.69	18.57
FeO	17.14	18.24	17.69	16.64
MgO	10.22	10.26	11.26	13.70
MnO	0.06	0.05	0.03	0.08
K_2O	8.20	8.25	8.54	8.58
Na_2O	0.29	0.42	0.35	na
CaO	0.01	0.01	na	nd
Total	93.41	93.13	91.45	94.27
		No. of ions		
Si	5.28	5.32	5.41	5.32
Al	2.72	2.68	2.59	2.68
Al	1.11	0.95	0.69	0.60
Ti	0.17	0.16	0.19	0.18
Fe	2.18	2.35	2.33	2.11
Mg	2.32	2.36	2.64	3.09
Mn	0.01	0.01	-	0.01
	5.79	5.83	5.85	5.99
Ca	-	-	-	-
Na	0.09	0.13	0.11	-
K	1.59	1.62	1.72	1.66

Gedrite bearing rocks

APPENDIX III (iv)

CORDIERITE ANALYSES

Specimen No.	43993	44013	44016	43873	43876
SiO_2	47.32	47.30	47.11	47.36	47.39
TiO_2	0.04	0.02	0.02	0.02	0.02
Al_2O_3	32.99	32.91	32.71	33.49	34.18
FeO	10.01	9.80	8.50	7.78	9.23
MgO	6.61	7.24	7.17	8.29	6.93
MnO	0.50	0.73	0.62	0.53	0.34
CaO	0.04	0.01	0.01	0.01	0.01
Na_2O	na	na	na	na	na
K_2O	0.04	0.06	0.88	0.02	0.05
Total	97.55	98.07	97.00	97.50	98.15
	No. of ions on the basis of 18 oxygen				
Si	4.96	4.94	4.96	4.92	4.91
Al	1.04	1.06	1.04	1.08	1.09
Al (+Ti)	3.04	2.99	3.02	2.98	3.05
Fe	0.88	0.86	0.75	0.68	0.80
Mg	1.03	1.13	1.13	1.28	1.07
Mn	0.04	0.07	0.06	0.04	0.02
Ca	-	-	-	-	-
Na	-	-	-	-	-
K	0.01	0.01	0.11	-	0.01
	1.96	2.07	2.05	2.00	1.90

CORDIERITE ANALYSES

Specimen No.	43901	43894		43942	
		1	2	1	2
SiO_2	46.72	45.84	45.43	45.72	45.12
TiO_2	0.02	na	na	na	0.02
Al_2O_3	30.07	31.96	32.41	32.04	31.68
FeO	9.25	8.79	8.96	8.75	8.41
MgO	6.60	7.21	7.07	7.29	7.33
MnO	0.14	0.57	0.48	0.48	0.48
CaO	0.01	na	0.01	0.01	0.03
Na_2O	na	0.31	0.39	0.40	0.45
K_2O	0.04	0.06	0.06	0.06	0.06
Total	92.85	94.68	94.81	94.75	93.58
		No. of ions			
Si		4.94	4.90	4.92	4.92
Al		1.06	1.10	1.08	1.08
Al (+Ti)		3.00	3.01	2.99	2.99
Fe		0.79	0.81	0.79	0.77
Mg		1.16	1.14	1.17	1.15
Mn		0.05	0.04	0.04	0.04
Ca		-	-	-	-
Na		0.07	0.08	0.08	0.09
K		0.01	0.01	0.01	0.01
		2.08	2.08	1.09	2.06

CORDIERITE ANALYSES

Specimen No.	43927		43924		43962
	1	2	1	2	
SiO_2	48.36	45.23	48.20	48.22	48.60
TiO_2	na	na	na	0.02	na
Al_2O_3	33.92	33.02	32.61	32.95	33.53
FeO	5.72	6.12	6.47	6.71	6.22
MgO	5.01	5.26	8.07	7.94	9.52
MnO	nd	0.02	0.22	0.22	0.16
CaO	0.38	0.19	0.04	0.01	na
Na_2O	1.02	0.41	1.14	1.07	na
K_2O	1.74	1.58	0.01	0.01	0.02
Total	96.15	91.83	96.76	97.15	98.05
		No. of ions			
Si	5.08	4.98	5.02	5.01	4.97
Al	0.92	1.02	0.98	0.99	1.03
Al (+Ti)	3.27	3.27	3.02	3.04	3.01
Fe	0.50	0.56	0.56	0.58	0.53
Mg	0.78	0.86	1.25	1.23	1.45
Mn	-	-	0.02	0.02	0.01
Ca	0.04	0.02	-	-	-
Na	0.21	0.08	0.23	0.22	-
K	0.23	0.22	-	-	0.01
	1.76	1.74	2.06	2.05	2.00

CORDIERITE ANALYSES

Specimen No.	44029	(Partial analysis)				
	1	2	3	4	5	Pinite
SiO_2	47.45					
TiO_2	0.02					
Al_2O_3	34.28	34.31	32.36	26.89	34.05	24.70
FeO	9.99	9.93	9.56	7.83	10.22	3.54
MgO	6.80	6.77	6.31	5.14	6.83	2.58
MnO	0.53					
CaO	na					
Na_2O	na					
K_2O	na					
Total	99.04					
		No. of ions				
Si	4.89					
Al	1.11					
Al (+Ti)	2.96					
Fe	0.86					
Mg	1.05					
Mn	0.05					
Ca	-					
Na	-					
K	-					
	1.96					

APPENDIX III (v)

STAUROLITE ANALYSES

Specimen No.	15463**	43894		43927	
		1*	2*	1	2
SiO_2	28.64	na	na	26.94	27.00
TiO_2	0.55	0.50	0.62	0.54	0.58
Al_2O_3	53.50	52.38	52.49	54.44	56.21
FeO	13.46	12.70	13.05	13.32	13.57
MgO	1.38	1.19	1.33	1.89	1.80
MnO	0.56	0.45	0.42	0.32	0.34
Total	98.09			97.45	99.50
		No. of ions on the basis of 48 oxygen			
Si	7.94			7.54	7.47
Al	0.06			0.46	0.53
Al	17.42			17.27	17.55
Ti	0.12			0.12	0.12
	17.54			17.39	17.67
Fe	3.13			3.12	3.14
Mg	0.57			0.79	0.75
Mn	0.13			0.09	0.08
	3.83			4.00	3.97

STAUROLITE ANALYSES

Specimen No.	43929		43939		43942
	1	2	1*	2	1
SiO_2	27.87	28.39	na	25.73	25.19
TiO_2	0.70	0.66	na	na	0.54
Al_2O_3	53.27	52.65	52.03	51.95	52.20
FeO	12.94	13.17	12.09	13.38	13.83
MgO	1.49	1.57	1.24	1.45	1.53
MnO	0.40	0.40	0.36	0.43	0.45
Total	96.67	96.84		92.94	93.74
		No. of ions			
Si	7.80	7.96		7.53	7.34
Al	0.20	0.04		0.47	0.66
Al	17.36	17.31		17.45	17.27
Ti	0.15	0.14		-	0.12
	17.51	17.45		17.45	17.39
Fe	3.03	3.09		3.27	3.38
Mg	0.62	0.65		0.63	0.67
Mn	0.10	0.10		0.11	0.11
	3.75	3.84		4.01	4.16

STAUROLITE ANALYSES

Specimen No.	43942	43945		43923(B)	43923(A)
	2	1*	2		1
SiO_2	24.62	na	27.14	27.20	26.09
TiO_2	0.58	na	0.45	0.41	0.54
Al_2O_3	53.32	52.41	53.99	53.19	52.59
FeO	13.54	13.15	13.37	13.61	11.94
MgO	1.53	1.29	1.46	1.72	1.43
MnO	0.46	0.37	0.40	0.19	0.15
Total	94.05		96.81	96.32	92.74
		No. of ions			
Si	7.15		7.60	7.66	7.58
Al	0.85		0.40	0.34	0.42
Al	17.38		17.42	17.31	17.59
Ti	0.13		0.09	0.08	0.12
Fe	3.28		3.13	3.20	2.90
Mg	0.66		0.61	0.73	0.63
Mn	0.12		0.10	0.05	0.03
	4.06		3.84	3.98	3.56

STAUROLITE ANALYSES

Specimen No.	43923(A)	
	2	3
SiO_2	26.38	26.54
TiO_2	.52	0.56
Al_2O_3	52.18	52.33
FeO	12.54	12.55
MgO	1.34	1.40
MnO	0.12	0.15
Total	93.08	93.43
	No. of ions	
Si	7.66	7.67
Al	0.34	0.33
Al	17.51	17.48
Ti	0.11	0.12
	17.62	17.60
Fe	3.05	3.02
Mg	0.58	0.61
Mn	0.03	0.03
	3.66	3.66

APPENDIX III (vi)

GARNET ANALYSES

Specimen No.	43939				43940
	1 Edge	1 Centre	2 Edge	2 Centre	1
SiO_2	36.12	36.10	36.14	36.06	37.82
TiO_2	0.05	0.05	nd	nd	0.03
Al_2O_3	20.79	20.85	21.01	20.94	20.94
FeO	32.66	32.08	33.26	32.44	31.66
MgO	2.03	2.02	2.15	1.86	1.85
MnO	7.17	7.08	6.96	6.76	8.18
CaO	1.70	1.70	1.54	1.55	1.48
Total	100.52	99.88	101.06	99.61	101.96
	No. of ions on the basis of 24 oxygen				
Si	5.885	5.90	5.86	5.91	6.03
Al	0.115	0.10	0.14	0.09	-
	6.00	6.00	6.00	6.00	6.03
Al	3.88	3.92	3.88	3.96	3.94
Ti	0.01	0.01	-	-	-
	3.89	3.93	3.88	3.96	3.94
Fe	4.45	4.39	4.51	4.45	4.22
Mg	0.49	0.49	0.52	0.45	0.44
Mn	0.99	0.98	0.96	0.94	1.11
Ca	0.30	0.30	0.27	0.27	0.25
	6.23	6.16	6.26	6.11	6.02
		Mol % End Members			
Alm	71.4	71.2	72.2	72.8	70.1
Pyr	7.9	8.0	8.3	7.4	7.3
Spess	15.9	15.9	15.3	15.4	18.4
Gross	4.8	4.8	4.3	4.4	4.2

APPENDIX III (vi) continued

GARNET ANALYSES

Specimen No.	43940	43945		15463**	43918
	2	1	3		
SiO_2	37.40	36.57	35.83	36.96	37.12
TiO_2	0.03	0.03	nd	na	0.02
Al_2O_3	21.39	21.13	21.37	21.26	20.45
FeO	32.31	31.70	31.78	32.32	28.40
MgO	2.18	2.11	2.28	2.19	1.75
MnO	7.21	7.20	7.34	8.36	9.99
CaO	1.56	1.53	1.63	1.33	1.68
Total	102.08	100.27	100.23	102.42	99.41
		No. of ions			
Si	5.96	5.93	5.84	5.40	6.06
Al	0.04	0.07	0.16	0.10	-
Al	3.97	3.97	3.94	3.90	3.93
Ti	-	-	-	-	-
	3.97	3.97	3.94	3.90	3.93
Fe	4.30	4.30	4.33	4.32	3.88
Mg	0.52	0.51	0.55	0.52	0.43
Mn	0.97	0.99	1.01	1.13	1.38
Ca	0.27	0.27	0.28	0.23	0.29
	6.06	6.07	6.17	6.20	5.98
		Mol % End Members			
Alm	71.0	70.9	70.0	69.7	64.8
Pyr	8.5	8.4	8.9	8.4	7.1
Spess	16.1	16.3	16.4	18.2	23.1
Gross	4.4	4.4	4.6	3.7	5.0

GARNET ANALYSES

Specimen No.	43923			43902	
	1 Edge	1 Centre	1 Edge	1*	2*
SiO_2	36.88	37.10	37.16	na	na
TiO_2	0.04	0.04	0.04	na	na
Al_2O_3	21.46	21.20	21.33	21.58	21.66
FeO	34.40	33.60	34.44	31.01	33.12
MgO	4.09	3.98	4.02	1.84	2.17
MnO	2.68	3.61	2.51	9.76	7.35
CaO	0.67	0.83	0.70	na	na
Total	100.22	100.36	100.20		
		No. of ions			
Si	5.92	5.95	5.96		
Al	0.08	0.05	0.04		
Al	3.97	3.96	3.97		
Ti	0.01	0.01	0.01		
	3.98	3.97	3.98		
Fe	4.62	4.50	4.62		
Mg	0.98	0.95	0.96		
Mn	0.36	0.49	0.34		
Ca	0.12	0.14	0.12		
	6.08	6.08	6.04		
		Mol % End Members			
Alm	76.0	74.0	76.4		
Pyr	16.1	15.6	15.9		
Spess	6.0	8.0	5.6		
Gross	1.9	2.4	2.0		

APPENDIX III (vii)

GEDRITE ANALYSES

Specimen No.	43923		43962	
	1	2	1	2
SiO_2	37.76	36.88	41.20	41.23
TiO_2	0.15	0.19	0.23	0.22
Al_2O_3	20.55	19.33	15.82	18.08
FeO	22.92	22.47	23.75	24.09
MgO	8.12	8.64	12.26	9.73
MnO	0.55	0.55	0.60	0.60
CaO	0.15	0.11	0.18	0.18
Na_2O	2.46	2.38	na	na
K_2O	0.07	0.06	0.04	0.35
Total	92.73	90.61	94.08	94.48
	No. of ions on the basis of 22 oxygen			
Si	5.67	5.68	6.06	6.03
Al	2.33	2.32	1.94	1.97
Al	1.31	1.19	0.80	1.15
Ti	0.02	0.02	0.03	0.02
Fe	2.88	2.90	2.92	2.95
Mg	1.82	1.98	2.69	2.12
Mn	0.07	0.07	0.08	0.07
Ca	0.02	0.02	0.03	0.03
Na	0.72	0.71	-	-
K	0.01	0.01	0.01	0.07
	6.85	6.90	6.56	6.41

APPENDIX III (viii)

PLAGIOCLASE ANALYSES

Specimen No.	43945	43918*	43929	43894*
SiO_2	61.79	na	66.78	na
Al_2O_3	23.57	20.84	22.39	na
CaO	6.67	6.42	3.42	6.14
Na_2O	8.13	8.14	8.86	7.80
K_2O	0.21	0.08	0.05	na
Total	100.37		101.50	

Specimen No.	43942*	43927	43923
SiO_2	na	65.92	64.65
Al_2O_3	na	22.78	22.13
CaO	5.00	2.96	3.05
Na_2O	8.50	10.08	10.11
K_2O	na	0.04	0.05
		101.78	99.99

APPENDIX IV

Bulk rock analysis

Major elements excepting FeO and H_2O were determined by X-ray fluorescence spectrometry using a Phillips PW 1212 automatic spectrometer. Rocks were prepared by fusion of 1 part rock powder 1 part La_2O_3 and 6 parts $Li_2B_4O_7$. FeO was determined by the method of Wilson (1955), Na_2O by flame photometry and H_2O by fusion.

Mineral analysis

All mineral analyses were carried out by electron microprobe using a Cambridge Instruments Geoscan (in the department of Mineralogy and Petrology, Cambridge) or Microscan (in the Grant Institute of Geology, Edinburgh), using the methods of Sweatman & Long (1969). Standards were: K-orthoclase; Na-jadeite and pure elements or stoichiometric oxides in all other cases.

REFERENCES

ALBEE, A.L., 1965(a). Distribution of Fe, Mg and Mn between garnet and biotite in natural mineral assemblages. J. Geol. 73, 155-164.

ALBEE, A.L., 1965(b). Phase equilibria in three assemblages of kyanite - zone pelitic schists, Lincoln Mountain Quadrangle, central Vermont. J. Petrology, 6, 246-301.

ALBEE, A.L., 1965(c). A petrogenetic grid for the Fe-Mg silicates of pelitic schists. Am. J. Sci. 263, 512-36.

ALBEE, A.L., 1968. Metamorphic zones in northern Vermont. In Studies in Appalachian Geology, Northern and Maritime, Zen, White, Hadley and Thompson Eds. John Wiley, New York.

ALBEE, A.L., 1972. Metamorphism of pelitic schists: reaction relations of chloritoid and staurolite. Bull. geol. Soc. Am. 83, 3249-68.

ALTHAUS, E., 1966. Die Bildung von Pyrophyllit und Andalusit zwischen 2000 und 7000 bar H_2O - Druck. Naturwissenschaften 53, 105-106.

ALTHAUS, E., 1967. The triple point andalusite-sillimanite-kyanite. An experimental and petrologic study. Contr. Mineral. Petrol. 16, 29-44.

ALTHAUS, E., NITSCH, K.H., & WINKLER, H.G.F., 1970. An experimental re-examination of the stability limits of muscovite plus quartz. Neues. Jb. Miner. 7, 325-36.

ANDERSON, A.L., 1931. Genesis of the anthophyllite deposits near Kamiah, Idaho. J. Geol. 39, 68.

ANDERSON, J.G.C., 1947. The geology of the Highland Border: Stonehaven to Arran. Trans. R. Soc. Edinb. 61, 497-515.

ANDERSON, J.G.C., 1948. Stratigraphic nomenclature of Scottish metamorphic rocks. Geol. Mag. 85, 89-96.

ASHWORTH, J.R., 1972. Migmatites of the Huntly-Portsoy area, North-East Scotland. Unpublished PhD Thesis University of Cambridge.

ASHWORTH, J.R., 1975. The sillimanite zones of the Huntly-Portsoy area in the north-east Dalradian, Scotland. Geol. Mag. 112, 113-136.

ATHERTON, M.P., 1964. The garnet isograd in pelitic rocks and its relation to metamorphic facies. Am. Miner. 49, 1331-49.

ATHERTON, M.P., 1965. The chemical significance of isograds. In Pitcher and Flinn (Eds), Controls of Metamorphism. Oliver and Boyd, Edinburgh 169-202.

ATHERTON, M.P., 1968. The variation in garnet, biotite and chlorite composition in medium grade pelitic rocks from the Dalradian, Scotland, with particular reference to the zonation in garnet. Contr. Mineral. Petrol. 18, 347-71.

ATHERTON, M.P., & BROTHERTON, M.S., 1972. The composition of some kyanite-bearing regionally metamorphosed rocks from the Dalradian. Scott. J. Geol. 8, 203-213.

ATHERTON, M.P., & BROTHERTON, M.S., 1973. Metamorphic index minerals in the eastern Dalradian. Scott. J. Geol. 9, 244-248.

ATHERTON, M.P., & BROTHERTON, M.S., 1974. Metamorphic index minerals in the eastern Dalradian. Scott. J. Geol. 10, 321-324.

ATHERTON, M.P., & EDMUNDS, W.M., 1966. An electron microprobe study of some zoned garnets from metamorphic rocks. Earth Planet. Sci. Lett. 1, 185-193.

AUTRAN, A., FONTEILLES, M., & GUITARD, G., 1966. Discordance du paleozoque inférior métamorphique sur socle gneissique anté hercynian dans le massif Albeires. C. R. Acad. Sci. Paris. Ser. D 263, 317-320.

BAILEY, E.B., 1923. The metamorphism of the south-west Highlands. Geol. Mag. 60, 317-31.

BAILEY, E.B., 1925. Perthshire tectonics: Loch Tummel, Blair Atholl and Glen Shee. Trans. R. Soc. Edinb. 53, 671-698.

BARD, J.P., 1969. Le Metamorphisme regional progressif des Sierras d'Aracena en Andalusie Occidentale (Espagne). Unpublished PhD Thesis - Montpellier.

BARROW, G., 1893. On an intrusion of muscovite-biotite gneiss in the south-eastern highlands of Scotland and its accompanying metamorphism. Q. Jl. Geol. Soc. Lond. 49, 330-54.

BARROW, G., 1912. On the geology of lower Deeside and the southern Highland Border. Proc. Geol. Assoc. 23, 268-273.

BEDERKE, E., 1935. Die regional metamorphose in Altvatergebirge. Geol. Rundschau, 26, 108-124.

BIRD, G.W., & ANDERSON, G.M., 1972. The free energy of formation of magnesian cordierite and phlogopite. Am. J. Sci. 273, 84-91.

BIRD, G.W., & FAWCETT, J.J., 1971. Some metamorphic reactions in the system K_2O-MgO-Al_2O_3-SiO_2-H_2O. Trans. Am. geophys. Un. 52, 377.

BIRD, G.W., & FAWCETT, J.J., 1973. Stability relations of Mg-chlorite-muscovite and quartz between 5 and 10 kb water pressure. J. Petrology, 14, 415-28.

BOSMA, W., 1967. The alteration of cordierite in spotted schists from the central Pyrenees. Geol. Mijnbouw. 46, 96-104.

BOSSDORF, R.H.H., 1961. Das Kristallin von Gadernheim und Landenau im Odenwald. Neues Jb Miner Abh 95, 370-419.

BOWEN, N.L., 1928. The evolution of the igneous rocks. Princeton University Press.

BOWEN, N.L., 1940. Progressive metamorphism of siliceous limestone and dolomite. J. Geol. 48, 225-274.

BOWES, D.R., & CONVERTY, H.J.E., 1966. The composition of some Ben Ledi grits and its bearing on the composition of albite schists in the south-west Highlands. Scott. J. Geol. 2, 67-75.

BROWN, E.H., 1967. The green schist facies in part of eastern Otago, New Zealand. Contr. Mineral. Petrol. 14, 259-92.

BROWN, E.H., 1968. The Si^{+4} content of natural phengites. A discussion. Ibid., 17, 78-81.

BUGGE, J.A.W., 1943. Geological and petrographical investigations in Kongsberg-Bamble formation. Nor. Geol. Unders. 160.

BURNHAM, C.W., HOLLOWAY, J.R., & DAVIS, N.F., 1969. The specific volume of water in the range 1000-8900 bars, 20^{o}-900^{o}C. Am. J. Sci. 267A, 70-95.

BUTLER, B.C.M., 1965. A chemical study of some rocks of the Moine series of Scotland. Q. Jl. geol. Soc. Lond. 121, 163-208.

BUTLER, B.C.M., 1967. Chemical study of minerals from the Moine schists of the Ardnamurchan area, Argyllshire, Scotland. J. Petrology, 8, 233-67.

CAPDEVILA, M.R., 1968. Les types de metamorphisme "intermediares de basse pression" dans le segment hercynien de Galice nord orientale (Espagne). C.R. Acad. Sc. Paris, Ser. D 266, 1924-1927.

CARMICHAEL, D.M., 1969. On the mechanism of prograde metamorphic reactions in the quartz bearing pelitic rocks. Contr. Mineral. Petrol. 20, 244-267.

CARMICHAEL, D.M., 1970. Intersecting isograds in the Whetstone Lake area, Ontario. J. Petrology, 11, 147-81.

CHAKRABORTY, K., & SEN, S., 1967. Regional metamorphism of pelitic rocks around Kandra, Singhbhum, Bihar. Contr. Mineral. Petrol. 16, 210-32.

CHATTERJEE, N.D., 1966. On the widespread occurrence of oxidised chlorites in the Pennine Zone of the western Italian Alps. Contr. Mineral. Petrol. 12, 325-39.

CHEVENOY, M., 1958. Contribution à l'étude des schistes cristallins de la partie N.W. due Massif Central Francais. Mém. Serv. Géol. France, 428.

CHINNER, G.A., 1960. Pelitic gneisses with varying ferrous/ferric ratios from Glen Clova, Angus, Scotland. J. Petrology, 1, 178-217.

CHINNER, G.A., 1961. The origin of sillimanite in Glen Clova, Angus. J. Petrology, 2, 312-23.

CHINNER, G.A., 1965. The kyanite isograd in Glen Clova, Angus. Mineralog. Mag. 34, 132-43.

CHINNER, G.A., 1966. The distribution of pressure and temperature during Dalradian metamorphism. Q. Jl. geol. Soc. Lond. 122, 158-86.

CHINNER, G.A., 1967. Chloritoid, and the isochemical character of Barrow's zones. J. Petrology, 8, 268-82.

CIPRIANI, C., SASSI, F.P., & SCOLARI, A., 1971. Metamorphic white micas; definition of paragenetic fields. Schweiz. miner. petrogr. Mitt. 51, 259-302.

DASGUPTA, H.C., SEIFERT, F., & SCHREYER, W., 1974. Stability of Manganocordierite and related phase equilibria in part of the system $MnO-Al_2O_3-SiO_2-H_2O$. Contr. Mineral. Petrol. 43, 275-294.

DEER, W.A., HOWIE, R.A., & ZUSSMAN, J., 1962. Rock Forming Minerals. vols. 1 to 5. Longman, London.

DEWEY, J.F., & PANKHURST, R.J., 1970. The evolution of the Scottish Caledonides in relation to their radiometric age pattern. Trans. R. Soc. Edinb. 68, 361-89.

DOBRETSOV, N.L., REVERDATTO, V.V., SOBOLEV, V.S., SOBOLEV, N.V., USTAKOVA, Ye.N., & KHLESTOV, V.V., 1965. Distribution of regional metamorphic facies in U.S.S.R. International Geology Review, 8, 1335-1346.

DOWNIE, C., LISTER, T.R., HARRIS, A.L., & FETTES, D.J., 1971. A palynological investigation of the Dalradian rocks of Scotland. N.E.R.C. I.G.S. Report No. 71/9. H.M.S.O.

DUNNING, F.W., 1972. Dating events in the Metamorphic Caledonides: impressions of the symposium held at Edinburgh, September 1971. Scott. J. Geol. 8, 179-192.

ELLES, G.L., 1931. Notes on the Portsoy coastal district. Geol. Mag. 68, 24-34.

ELLES, G.L., & TILLEY, C.E., 1930. Metamorphism in relation to structure in the Scottish Highlands. Trans. R. Soc. Edinb. 56, 621-46.

ERNST, W.G., 1964. Significance of phengitic micas from low grade schists. Am. Miner. 48, 1357-73.

ESKOLA, P., 1914. On the petrology of the Orijarvi region in south western Finland. Bull. comm. geol. Finlande, 40, 1-277.

ESKOLA, P., 1915. On the relations between the chemical and mineralogical composition in the metamorphic rocks of the Orijarvi region. Ibid., 44.

ESKOLA, P., 1920. The mineral facies of rocks. Norsk. Geol. Tidsskr, 6, 143-94.

ESKOLA, P., 1939. Die metamorphen Gesteine. In Die Entstehung der Gesteine by T.F.W. Barth, C.W. Correns and P. Eskola. 263-407. Berlin Julius Springer. Reprinted 1960, 1970.

EUGSTER, H.P., 1959. Reduction and oxidation in metamorphism. In 'Researches in Geochemistry' vol. 1 397-426. New York: John Wiley & Sons.

EUGSTER, H.P., 1970. Thermal and ionic equilibria among muscovite, K-feldspar and aluminosilicate assemblages. Fortschr. Miner. 47, 106-123.

EUGSTER, H.P., & WONES, D.R., 1962. Stability relations of the ferruginous biotite, annite. J. Petrology, 3, 82-125.

EVANS, B.W., 1965. Application of the reaction rate method to the breakdown equilibria of muscovite + quarts. Am. J. Sci. 263, 647-67.

EVANS, B.W., & GUIDOTTI, C.V., 1966. The sillimanite-potash feldspar isograd in western Maine, U.S.A. Contr. Mineral. Petrol. 12, 25-62.

FAWCETT, J.J., 1964. The muscovite-chlorite-quartz assemblage. Yb. Carnegie Instn. Wash. 63, 137-41.

FAWCETT, J.J., & YODER, H.S., 1966. Phase relations of chlorite in the system $MgO-Al_2O_3-SiO_2-H_2O$. Am. Miner. 51, 353-80.

FETTES, D.J., 1968. Metamorphic structures of Dalradian rocks in north-east Scotland. Unpublished PhD Thesis Univ. of Edinb.

FETTES, D.J., 1970. The structural and metamorphic state of the Dalradian rocks and their bearing on the age of emplacement of the basic sheet. In Rolfe, W.D.I., et. al.(eds.) The 'Younger' basic igneous complexes of north east Scotland and their metamorphic envelope. Scott. J. Geol. 6, 108-118.

FETTES, D.J., 1971. Relation of cleavage and metamorphism in the Macduff Slates. Scott. J. Geol. 7, 248-53.

FLEMING, P.D., 1972. Mg-Fe distribution between coexisting garnet and biotite, and the status of fibrolite in the andalusite-staurolite zone of the Mt. Lofty Ranges, South Australia. Geol. Mag. 6, 477-482.

FORESTIER, F.M., 1963. Métamorphism hercynien et anté hercynien das le bassin du Haut-Allien (Massif Central Francais). Bull. Serv. Carte Géol. France, 271, 59, 521-813.

FOSTER, M.D., 1960. Interpretation of the composition of trioctahedral micas. U.S. geol. Surv. prof. Paper, 354-B.

FOSTER, M.D., 1962. Interpretation of the composition and a classification of the chlorites. U.S. geol. Surv. prof. Paper, 414-A.

FRANCIS, G.H., 1956. Facies boundaries in pelites at the middle grades of regional metamorphism. Geol. Mag. 93, 353-68.

FRANCIS, G.H., & HEY, M.H., 1956. The unit cell constants of anthophyllite. Mineralog. Mag. 31, 173-186.

FROST, M.J., 1962. Metamorphic grade and iron-magnesium distribution between co-existing garnet-biotite and garnet-hornblende. Geol. Mag. 99, 427-438.

FYFE, W.S., 1967. Stability of Al_2SiO_5 polymorphs. Chem. Geol. 2, 67-76.

FYFE, W.S., TURNER, F.J., & VERHOOGEN, J., 1958. Metamorphic reactions and metamorphic facies. Mem. geol. Soc. Am. 73, 259.

GANGULY, J., 1968. Analysis of the stability of chloritoid and staurolite and some equilibria in the system $FeO-Al_2O_3-SiO_2-H_2O-O_2$. Am. J. Sci. 266, 277-98.

GANGULY, J., 1969. Chloritoid stability and related parageneses: theory, experiments and applications. Am. J. Sci. 267, 910-44.

GANGULY, J., 1972. Staurolite stability and related parageneses: theory, experiments and applications. J. Petrology,13, 335-65.

GANGULY, J., & NEWTON, R.C., 1968. Thermal stability of chloritoid at high pressure. J. Petrology, 9, 444-66.

GIBBS, G.V., 1966. The polymorphism of cordierite I. Am. Mineral. 51, 1068-87.

GOLDSCHMIDT, V.M., 1915. Geologisch-petrographische studien im Hochgeburge des südlichen Norwegens. III. Die Kalksilikatgneise und Kalksilikatglimmerschiefer im Trondhjem-Gebiete. Vidensk. Skrifter I. Mat-Naturv. Kl (1915) 10.

GOLDSCHMIDT, V.M., 1921. Geologisch-petrographische studien im Hochgeburge des südlichen Norwegens. V. Die Injektionsmetamorphose im Stavanger-Gebiete. Vidensk. Skrifter, 1. Mat-Naturv. Kl. (1926) 10.

GRANT, J.A., 1968. Partial melting of common rocks as a possible source of cordierite-anthophyllite bearing assemblages. Am. J. Sci. 266, 908-31.

GREEN, J., 1963. High level metamorphism of pelitic rocks in northern New Hampshire. Am. Miner. 48, 991-1023.

GREEN, T.H., & VERNON, R.H., 1974. Cordierite breakdown under high pressure hydrous conditions. Contr. Mineral. Petrol. 46, 215-226.

GREENWOOD, H., 1963. The synthesis and stability of anthophyllite. J. Petrology, 4, 317-51.

GRIBBLE, C.D., 1965. Petrological studies of the rocks of the Haddo House and Arnage districts Aberdeenshire. Unpublished PhD Thesis Univ. of Edinb.

GRIBBLE, C.D., 1966. The Thermal Aureole of the Haddo House norite in Aberdeenshire. Scott. J. Geol. 2, 306-313.

GRIEVE, R.A.F., & FAWCETT, J.J., 1970. The synthesis of chloritoid at low pressures. Am. Miner. 55, 517-21.

GRIEVE, R.A.F., & FAWCETT, J.J., 1974. The stability of chloritoid below 10 kb P_{H_2O}. J. Petrology, 15, 113-39.

GUIDOTTI, C.V., 1969. A comment on 'chemical study of minerals from the Moine schists of the Ardnamurchan Area, Argyllshire, Scotland', by B.C.M. Butler, and its implications for the phengite problem. J. Petrology, 10, 164-70.

GUIDOTTI, C.V., 1970. The mineralogy and petrology of the transition from the lower to upper sillimanite zone in the Oquossoc area, Maine. J. Petrology, 11, 277-336.

GUIDOTTI, C.V., CHENEY, J.T., & CONATORE, P.D., 1975. Coexisting cordierite + biotite + chlorite from the Rumford Quadrangle, Maine. Geology, 3, 147-148.

GUITARD, G., 1965. Associations minérales subfacies et type de metamorphisms dans les micaschistes et les gneiss pélitique du Massif du Canigou. Bull. Geol. France, 7, 356-82.

GUITARD, G., & RAGUIN, E., 1958. Sur la présence de gneiss à grenat et hypersthène dans le massif de l'Agly (Pyrénées Orientales). C.R.Acad. Sci. Paris, 247, 2385-8.

HALL, D.J., 1970. Compositional variations in biotites and garnets from kyanite and sillimanite zone mica schists, Orange area, Massachusetts and New Hampshire. Unpublished M.Sc. Thesis, University of Massachusetts.

HARA, I., KANISAWA, S., KANO, H., KURODA, Y., MARUYAMA, T., MITSUKAWA, H., NUREKI, T., UMEMURA, H., & URONO, K., 1969. Poly-metamorphism in the Abukuma Plateau with special regards to the discovery of staurolite and kyanite. (Japanese-Eng. abstract).

HARKER, A., 1928. Normal regional metamorphism. Fennia, 50, No. 36.

HARKER, A., 1932. Metamorphism. A study of the transformation of rock-masses (1st Ed). Methuen, London.

HARKER, A., 1939. Metamorphism. A study of the transformation of rock-masses (2nd Ed). Methuen, London.

HARRIS, A.L., 1962. Structural investigations in the Dalradian rocks between Pitlochry and Blair Atholl. Trans. Edinb. geol. Soc. 19, 256-278.

HARRIS, A.L., & PITCHER, W.S., 1975. The Dalradian Supergroup. In a Correlation of Precambrian rocks in the British Isles. Sp. Rept. geol. Soc. Lond. 6, 52-75.

HARTE, B., 1974. The composition of some kyanite-bearing regionally metamorphosed rocks from the Dalradian. Scott. J. Geol. 9, 239-244.

HARTE, B., (in press). Determination of a pelite petrogenetic grid for the eastern Scottish Dalradian. Yb. Carnegie Instn. Wash. (in press).

HARTE, B., & JOHNSON, M.R.W., 1969. Metamorphic History of Dalradian rocks in Glens Clova, Esk and Lethnot, Angus, Scotland. Scott. J. Geol. 5, 54-80.

HELGESON, H.C., 1967. Solution chemistry and metamorphism. In: Researches in Geochemistry, Vol. 2 P.H. Abelson, Ed. Wiley and Sons New York 362-404.

HEMLEY, J.J., 1967. Stability relations of pyrophyllite, andalusite and quartz at elevated pressures and temperatures. Trans. Am. geophys. Un. 48, 224.

HENSEN, B.J., 1971. Theoretical phase relations involving cordierite and garnet in the system MgO-FeO-Al_2O_3-SiO_2. Contr. Mineral. Petrol. 33, 191-214.

HENSEN, B.J., & GREEN, D.H., 1971. Experimental study of cordierite and garnet in pelitic compositions at high pressures and temperatures. I Compositions with excess alumino-silicate. Contr. Mineral. Petrol. 33, 309-330.

HENSEN, B.J., & GREEN, D.H., 1972. Experimental study of cordierite and garnet in pelitic compositions at high pressures and temperatures. II Compositions without excess alumino-silicate. Contr. Mineral. Petrol. 35, 331-354.

HENSEN, B.J., & GREEN, D.H., 1973. Experimental study of the stability of cordierite and garnet in pelitic compositions at high pressures and temperatures. III Synthesis of experimental data and geological applications. Contr. Mineral. Petrol. 38, 151-166.

HESS, P.C., 1969. The metamorphic paragenesis of cordierite in pelitic rocks. Contr. Mineral. Petrol. 24, 191-207.

HIETANEN, A., 1956. Kyanite, andalusite and sillimanite in the schist in Boehls Butte quadrangle, Idaho. Am. Miner. 41, 1-27.

HIETANEN, A., 1959. Kyanite-garnet gedritite near Orofino, Idaho. Am. Miner. 44, 539.

HIETANEN, A., 1961. Metamorphic facies and style of folding in the Belt series North west of the Idaho Batholith. Bull. Comm. geol. Finlande, 196, 73-103.

HIETANEN, A., 1962. Staurolite zone near the St Joe River, Idaho. U.S. geol. Surv. Prof. Paper, 450-C 69-72.

HIETANEN, A., 1967. On the facies series in various types of metamorphism. J. Geol. 75, 187-214.

HIETANEN, A., 1969. Distribution of Fe and Mg between garnet, staurolite and biotite in aluminium rich schist in various metamorphic zones north of the Idaho Batholith. Am. J. Sci. 267, 422-456.

HINRICHSEN, TH.J., 1968. Hydrothermal investigations and stability relations of synthetic gedrites. Proc. Int. Min. Ass. 243-8.

HIRSCHBERG, A., & WINKLER, H.G.F., 1968. Stabilitäts beziehungen zwischen chlorit, cordierit und almandin bei der metamorphose. Contr. Mineral. Petrol. 18, 17-42.

HOLDAWAY, M.J., 1971. Stability of andalusite and the aluminium silicate phase diagram. Am. J. Sci. 271, 97-131.

HOLSER, W.T., & KENNEDY, G.C., 1959. Properties of water part V. P-V-T relations of water in the range 400-1000°C and 100-1400 bars. Am. J. Sci. 257, 71-77.

HORNE, J.,1886. The origin of the andalusite schists of Aberdeenshire. Min. Mag. 6, 98-100

HOSCHEK, G., 1967. Untersuchungen zum Stabilitätsbereich von Chloritoid und Staurolith. Contr. Mineral. Petrol. 14, 123-62.

HOSCHEK, G., 1969. The stability of staurolite and chloritoid and their significance in metamorphism of pelitic rocks. Contr. Mineral. Petrol. 22, 208-32.

HOUNSLOW, A.M., & MOORE, J.M.Jnr., 1967. Chemical petrology of Grenville schists near Frenleigh, Ontario. J. Petrology 8, 1-28.

HSU, L.C., 1968. Selected phase relationships in the system Al-Mn-Fe-Si-O-H: a model for garnet equilibria. J. Petrology, 9, 40-83.

JAMES, H.L., 1955. Zones of regional metamorphism in the Precambrian of northern Michigan. Bull. geol. Soc. Am. 66, 1455-88.

JOHNSON, M.R.W., 1962. Relations of movement and metamorphism in the Dalradians of Banffshire. Trans. Edinb. geol. Soc. 19, 29-64.

JOHNSON, M.R.W., 1963. Some time relations of movement and metamorphism in the Scottish Highlands. Geol. Mijnbouw, 5, 121-142.

JOHNSON, M.R.W., 1965. Dalradian: in Geology of Scotland G.Y. Craig (Ed). Oliver and Boyd, Edinburgh and London.

JOHNSON, M.R.W., & STEWART, F.H., 1960. On Dalradian structures in north-east Scotland. Trans. Edinb. geol. Soc. 18, 94-103.

JOHNSON, M.R.W., & STEWART, F.H., (Eds), 1963. The British Caledonides. Oliver and Boyd, Edinburgh.

JOHNSTONE, G.S., 1966. British Regional Geology: the Grampian Highlands (3rd Ed), H.M.S.O., Edinburgh.

JOPLIN, G.A., 1942. Petrological studies in the Ordovician of New South Wales. I. Proc. Linn. Soc. N.S.W. 67, 156-196.

JOPLIN, G.A., 1943. Petrological studies in the Ordovician of New South Wales. II. Proc. Linn. Soc. N.S.W. 68, 159-182.

JOPLIN, G.A., 1968. A petrography of Australian metamorphic rocks. Angus and Robertson: Sydney.

JUURINEN, A., 1956. Composition and properties of staurolite. Ann. Acad. Sci. Fennicae, ser A, III (Geol. Geogr.), No.47.

KATADA, M., 1965. Petrography of Ryoke rocks in northern Kiso District, central Japan. J. Japan. Ass. Min. Petrog. econ. Geol. 53, 77-90 (in English).

KENNEDY, W.Q., 1948. On the significance of thermal structure in the Scottish Highlands. Geol. Mag. 85, 229-34.

KEPEZHINSKAS, K.B., 1973. Pressure variability during medium - temperature metamorphism of meta-pelites. Lithos, 6, 145-158.

KERRICK, D.M., 1968. Experiments on the upper stability of pyrophyllite at 1.8 kb and 3.9 kb H_2O pressure. Am. J. Sci. 266, 204-14.

KING, B.C., & RAST, N., 1956. The small scale structures of south-eastern Cowal, Argyllshire. Geol. Mag. 93, 185-95.

KLOTZ, I.M., 1964. Introduction to chemical thermodynamics. W.A. Benjamin Inc., New York.

KORIKOVSKIY, S.P., 1969. Boundaries of the staurolite metamorphic sub facies in the low pressure region. Dok. Acad. Sci. USSR. Earth Science Section, 184, 107-9.

KORZHINSKII, D.S., 1959. Phsicochemical basis of the analysis of the paragenesis of minerals. New York Consult. Bur. Inc.

KRAMM, U., 1973. Chloritoid stability in manganese rich low-grade metamorphic rocks, Venn-Stavelot Massif, Ardennes. Contr. Mineral. Petrol. 41, 179-96.

KRETZ, R., 1959. Chemical study of garnet, biotite and hornblende from gneisses of south western Quebec, with emphasis on distribution of elements in coexisting minerals. J. Geol. 67, 371-402.

KRETZ, R., 1964. Analysis of equilibrium in garnet-biotite-sillimanite gneisses from Quebec. J. Petrology, 5, 1-20.

KULP, J.L., & BROBST, D.A., 1954. Notes on the dunite and the geochemistry of vermiculite at the Day Book dunite deposit, Yancey County, North Carolina. Econ. Geol. 49, 211.

LAL, R.K., 1969. Paragentic relations of alumino-silicates and gedrite from Fishtail Lake, Ontario, Canada. Lithos, 2, 187-196.

LAL, R.K., & SHUKLA, R.S., 1970. Parageneses of staurolite in pelitic schists of Kishangarh, District Ajmer, India. Mineralog. Mag. 37, 561-7.

LAMBERT, R.St.J., 1959. The mineralogy and metamorphism of the Moine schists of the Morar and Knoydart districts of Inverness-shire. Trans.R. Soc. Edinb. 63, 553-88.

LAMBERT, R.St.J., 1965. The metamorphic facies concept. Mineralog. Mag. 34, 283-291.

LYONS, J.B., & MORSE, S.A., 1970. Mg/Fe partitioning in garnet and biotite from some granitic, pelitic and calcic rocks. Am. Miner. 55, 231-245.

McNAMARA, M.J., 1965. The lower greenschist facies in the Scottish Highlands. Geol. FÖr. Stockh. Förh. 87, 347-389.

MAGNUSSON, N.H., THORSLUND, P., BROTZEN, F., ASKLUND, B., & KULLING, O., 1960. Description to accompany the map of pre-quaternary rocks of Sweden. (Sveriges Geologiska Undersökning), Afh. Ser. Ba, 177. Sver. Geol. Unders.

MATHER, J.D., 1970. The biotite isograd and the lower greenschist facies in the Dalradian rocks of Scotland. J. Petrology, 11, 253-75.

MERCY, E.L.P., 1965. Caledonian igneous activity in Geology of Scotland. G.Y. Craig (Ed). Oliver and Boyd, Edinburgh.

MIYASHIRO, A., 1953. Calcium poor garnet in relation to metamorphism. Geochim. cosmochim. Acta, 4, 179-208.

MIYASHIRO, A., 1956. Data on garnet-biotite equilibria in some metamorphic rocks of the Ryoke zone. J. geol. Soc. Japan, 62, 700-702.

MIYASHIRO, A., 1958. Regional metamorphism of the Gosaisyo-Takonuki district in the central Abukuma Plateau. J. Fac. Sci. Univ. Tokyo, Section II, 11, 219-272.

MIYASHIRO, A., 1961. Evolution of metamorphic belts. J. Petrology, 2, 277-311.

MIYASHIRO, A., 1973. Metamorphism and metamorphic belts. George Allen & Unwin.

MUNRO, M., 1970. A re-assessment of the 'younger' basic igneous rocks between Huntly and Portsoy based on new borehole evidence. Scott. J. Geol. 6, 41-52.

NELSON, B.W., & ROY, R., 1958. Synthesis of the chlorites and their structural and chemical constitution. Am. Miner. 43, 707-25.

NEWTON, R.C., 1972. An experimental determination of the high pressure stability limits of magnesian cordierite under wet and dry conditions. J. Geol. 80, 398-420.

OFFLER, R., & FLEMING, P.D., 1968. A synthesis of folding and metamorphism in the Mt. Lofty Ranges, South Australia. J. geol. Soc. Aust. 15, 245-266.

OKI, Y., 1961(a). Metamorphism in the northern Kiso range, Nagamo Prefecture, Japan. (in English). Jap. J. Geol. Geogr. 32, 479-496.

OKI, Y., 1961(b). Biotite in metamorphic rocks. (in English). Jap. J. Geol. Geogr. 32, 497-506.

ONO, A., 1969(a). Geology of the Ryoke metamorphic belt in the Takato-Sioziri area, Nagano Prefecture. J. geol. Soc. Japan, 75, 491-498. (Japanese-English abstract) Summary in Miyashiro 1973, 169.

ONO, A., 1969(b). Zoning of the metamorphic rocks in the Takato-Sioziri area, Nagano Prefecture. J. geol. Soc. Japan, 75, 521-536. Japanese-English abstract. Summary in Miyashiro 1973, 169.

OSBERG, P.H., 1968. Stratigraphy, structural geology and metamorphism of the Waterville-Vassalboro area, Maine. Maine geol. Surv. Bull. 20, 64.

OSBERG, P.H., 1971. An equilibrium model for Buchan-type metamorphic rocks, south-central Maine. Am. Miner. 56, 570-86.

PANKHURST, R.J., 1970. The geochronology of the basic complexes, in Rolfe, W.D.I. et. al. (eds). 'The 'Younger' basic igneous complexes of north-east Scotland and their metamorphic envelope'. Scott. J. Geol. 6, 83-107.

PANKHURST, R.J., 1974. Rb-Sr Whole rock chronology of Caledonian events in north east Scotland. Bull. geol. Soc. Am. 85, 345-50.

PITCHER, W.S. & FLINN, G.W., (Eds), 1965. Controls of Metamorphism. Oliver and Boyd, Edinburgh.

PORTEOUS, W.G., 1973. Metamorphic index minerals in the eastern Dalradian. Scott. J. Geol. 9, 24-43.

PRIDER, R.T., 1944. The geology and petrology of part of the Toodyay district, Western Australia. J.R. Soc. West Aust. 28, 83.

RAMSAY, C.R., 1973. Controls of biotite zone mineral chemistry in Archean meta-sediments near Yellowknife, North west Territories, Canada. J. Petrology, 14, 467-88.

RAMSAY, C.R., 1974. The cordierite isograd in Archaean meta-sediments near Yellowknife, N.W.T., Canada - variations on an experimentally established reaction. Contr. Mineral. Petrol. 47, 27-40.

RAO, T.R., 1974. A bedded deposit of anthophyllite schist in the Precambrian belt of Nellore, South India. Geol. Mag. 111, 221-228.

RAST, N., 1958. Metamorphic history of the Schichallion complex (Perthshire). Trans. roy. Soc. Edinb. 63, 413-31.

von RAUMER, J.F., 1973. Die mineral fazielle Stellung der Metapelite und Metagrauwacken zwischen Heppenheim und Reichelsheim. (Odenwald). Neues. Jb. Miner. Abh. 118, 313-336.

READ, H.H., 1923. The geology of the country around Banff, Huntly and Turriff. Mem. geol. Surv. Scotld. for sheets 86 and 96.

READ, H.H., 1927. The igneous and metamorphic history of Cromar, Deeside, Aberdeenshire. Trans. R. Soc. Edinb. 55, 317-353.

READ, H.H., 1936. The stratigraphical order of the Dalradian rocks of the Banffshire coast. Geol. Mag. 73, 468-73.

READ, H.H., 1950. The dislocated south western margin of the Insch igneous mass, Aberdeenshire. Proc. geol. Ass. Lond. 67, 73-86.

READ, H.H., 1952. Metamorphism and migmatisation in the Ythan Valley, Aberdeenshire. Trans. Edinb. geol. Soc. 15, 265-79.

READ, H.H., 1955. The Banff Nappe. Proc. Geol. Assoc. 66, 1-29.

READ, H.H., & FARQUHAR, O.C., 1956. The Buchan Anticline of the Banff Nappe of Dalradian rocks in N.E. Scotland. Q. Jl. geol. Soc. Lond. 92, 131-56.

RICHARDSON, S.W., 1968. Staurolite stability in part of the system Fe-Al-Si-O-H. J. Petrology, 9. 467-88.

RICHARDSON, S.W., 1970. The relation between a petrogenetic grid, facies series and the geothermal gradient in metamorphism. Fortschr. Miner. 47, 65-76.

RICHARDSON, S.W., GILBERT, M.C., & BELL, P.M., 1969. Experimental determination of kyanite-andalusite and andalusite-sillimanite equilibrium; the alumino-silicate triple point. Am. J. Sci. 267, 259-72.

ROBIE, R.A., & WALDBAUM, D.R., 1968. Thermodynamic properties of minerals and related substances at 298.15 K (250^{o}C) and one atmosphere (1.013 bars) pressure and at higher temperature. U.S. geol. Surv. Bull. 1259.

ROLFE, W.D.I., LAWSON, J.D., DAWSON, J.B., HARRIS, A.L., UPTON, B.G.J., GRANT, D., & GRIBBLE, C.D., 1970. The 'Younger' basic igneous complexes of north-east Scotland and their metamorphic envelope. Scott. J. Geol. 6.

SATO, S., 1968. Precambrian-Variscan polymetamorphism in the Hida massif basement of the Japanese Islands. Tokyo Univ. Educ. Sci. Rep. Sec. C, 10, 15-130.

SAXENA, S.K., 1968. Distribution of elements between coexisting minerals and the nature of solid solution in garnet. Am. Miner. 53, 994-1014.

SAXENA, S.K., 1973. Thermodynamics of rock-forming crystalline solutions. Minerals Rocks and Inorganic Materials Vol. 8 Springer-Verlag. Berlin-New York.

SAXENA, S.K., & HOLLANDER, N.B., 1969. Distribution of iron and magnesium in coexisting biotite, garnet and cordierite. Am. J. Sci. 267, 210-16.

SCHREINEMAKERS, F.A.H., 1965. In- mono- and divariant equilibria. Vol. 2 of collected papers. Penn. State Univ. 322.

SCHREYER, W., 1965. Zur Stabilität des Ferrocordierits. Contr. Mineral. Petrol. 11, 297-322.

SCHREYER, W., 1966. Metamorpher Ubergang Saxothuringikum-Moldanubikum östlich Tirschenreuth/Opf., nachgewiesen durch Phasenpetrologische Analyse. Geol. Rundschau, 55, 491-508.

SCHREYER, W., & BLUMEL, P., 1974. Progressive metamorphism in the Moldanubicum of the Northern Bavarian Forest. Fortschr. Miner. 52, 151-165.

SCHREYER, W., & SCHAIRER, J.F., 1961. Composition and structural states of anhydrous Mg- cordierites. A reinvestigation of the central part of the system $MgO-Al_2O_3-SiO_2$. J. Petrology, 2, 324-406.

SCHREYER, W., & SEIFERT, F., 1969. Compatibility relations of aluminium silicates in the systems $MgO-Al_2O_3-SiO_2-H_2O$ and $K_2O-MgO-Al_2O_3-SiO_2-H_2O$ at high pressures. Am. J. Sci. 267, 373-88.

SCHREYER, W., & YODER, H.S., 1961. Petrographic guides to the experimental petrology of cordierite. Yb. Carnegie-Instn. Wash. 60, 147-52.

SCHREYER, W., & YODER, H.S., 1964. The system Mg-cordierite plus water. Neues. Jb. Miner. 7, 272-342.

SCHUILING, R.D., 1960. Le dome gneissique de l'Agout. Mém. Soc. Géol. France, 91, 1-58.

SCHWARTZ, G.M., 1958. Alteration of biotite under mesothermal conditions. Econ. Geol. 53, 164-177.

SEIFERT, F., 1970. Low temperature compatibility relations of cordierite in haplo pelites of the system $K_2O-MgO-Al_2O_3-SiO_2-H_2O$. J. Petrology, 11, 73-99.

SEIFERT, F., & SCHREYER, W., 1970. Lower temperature stability limit of Mg-cordierite in the range 1 - 7 kilobars water pressure. A redetermination. Contr. Miner. Petrol. 27, 225-38.

SEKI, Y., & YAMASAKI, M., 1957. Aluminian ferro-anthophyllite from the Kitakami mountain land, north-eastern Japan. Am. Miner. 42, 506-20.

SEN, S.K., & CHAKRABORTY, K.R., 1968. Magnesium-iron exchange equilibrium in garnet-biotite and metamorphic grade. Neues. Jb. Miner. Abh. 108, 181-207.

SHACKLETON, R.M., 1948. Overturned rhythmic banding in the Huntly gabbro of Aberdeenshire. Geol. Mag. 85, 358-360.

SHACKLETON, R.M., 1958. Downward-facing structures of the Highland Border. Q. Jl. geol. Soc. Lond. 113, 361-392.

SHAW, D.M., 1956. Geochemistry of pelitic rocks. Part III: major elements and general geochemistry. Bull. geol. Soc. Am. 67, 919-34.

SHIDO, F., 1958. Plutonic and metamorphic rocks of the Nakoso and Iritono districts in the central Abukumo Plateau. J. Fac. Sci. Univ. Tokyo, Section II, 11, 131-217.

SIMONEN, A., 1960. Pre-quaternary rocks in Finland. Bull. geol. Finlande, 191, 1-49.

SMITH, J.V., 1968. The crystal structure of staurolite. Am. Miner. 53, 1139-55.

SNELLING, N.J., 1957. Notes on the mineralogy and petrology of Barrow's zones. Geol. Mag. 94, 297- 304

SOBOLEV, V.S., DOBRETSOV, N.L., REVERDATTO, V.V., SOBOLEV, N.V., USHRAKOVA, E.N., & KHLESTOV, V.V., 1967. Metamorphic facies and series of facies in the U.S.S.R. Meddr. Dansk. Geol. For. 17, 458-472.

SPRY, A., 1969. Metamorphic textures. Pergamon Press, London.

STEWART, F.H., 1946. The gabbroic complex of Belhelvie in Aberdeenshire. Q. Jl. geol. Soc. Lond. 102, 465-498.

STEWART, F.H., & JOHNSON, M.R.W., 1961. The structural problem of the younger gabbros of north east Scotland. Trans. Edinb. geol. Soc. 18, 104-112.

STRECKEISEN, A., 1928. Geologie und petrographie der Fluelagruppe (Graubunden). Schweiz. miner. petrogr. Mitt. 7, 124-129.

STURT, B.A., 1961. The geological structure of the area south of Loch Tummel. Q. Jl. geol. Soc. Lond. 117, 131-56.

STURT, B.A., & HARRIS, A.L., 1961. The metamorphic history of the Loch Tummel area, central Perthshire, Scotland. Lpool and Manchr geol Jl. 2, 689-711.

SUK, M., 1964. Material characteristics of the metamorphism and migmatization of Moldanubian paragneisses in central Bohemia. Krystalinikum, 2, 71-105.

SUTTON, J., & WATSON, J.V., 1955. The deposition of the Upper Dalradian rocks of the Banffshire Coast. Proc. Geol. Ass. Lond. 66, 101-133.

SUTTON, J., & WATSON, J.V., 1956. The Boyndie Bay Syncline of the Dalradian of the Banffshire Coast. Q. Jl. geol. Soc. Lond. 112 (for 1955) 103-128.

SUZUKI, J., 1930. Uber die staurolit-andalusit paragenesis im glimmergneis von Piodina bei Brissago (Tessin). Schweiz. miner. petrogr. Mitt. 10, 117-132.

SWEATMAN, T.R., & LONG, J.V.P., 1969. Quantitative electron-probe micro analysis of rock forming minerals. J. Petrology, 10, 332-79.

TAGIRI, M., 1971. Metamorphic rocks of the Hitachi district southern Abukuma Plateau. J. Jap. Assoc. Mineral. Petrol. econ. Geol. 65, 77-103.

TEX, E.den., 1965. Metamorphic lineages of orogenic plutonism. Geol. en Mijnb. 44, 105-132.

THOMPSON, J.B., Jnr., 1955. The thermodynamic basis for the mineral facies concept. Am. J. Sci. 253, 65-103.

THOMPSON, J.B., Jnr., 1957. The graphical analysis of mineral assemblages in pelitic schists. Am. Miner. 42, 842-58.

THOMPSON, J.B.Jnr., 1961. Mineral facies in pelitic schists (Eng. summ.) Moscow Akad. Nauk. S.S.S.R., Korzinskii festschr. 313-325.

THOMPSON J.B. Jnr., & NORTON, S.A., 1968. Palaeozoic regional metamorphism in New England and adjacent areas. In Studies in Appalachian Geology, Northern and Maritime, Zen et. al. (Eds). John Wiley, New York.

TILLEY, C.E., 1924. The facies classification of metamorphic rocks. Geol. Mag. 61, 167-171.

TILLEY, C.E., 1925. A preliminary survey of metamorphic zones in the Southern Highlands of Scotland. Q. Jl. geol. Soc. Lond. 81, 100-12.

TILLEY, C.E., 1926. Some mineralogical transformations in crystalline schists. Mineralog. Mag. 21, 34-46.

TILLEY, C.E., 1937. Anthophyllite-cordierite granulites from the Lizard. Geol. Mag. 74, 300.

TOBSCHALL, H.J., 1969. A sequence of sub facies of the greenschist facies in the Cévennes Medianes with pyrophyllite-bearing parageneses. (German-Engl. abstract). Contr. Mineral. Petrol. 24, 76-91.

TOUMINEN, H.V., & MIKKOLA, T., 1950. Metamorphic Mg-Fe enrichment in the Orijarvi area as related to folding. Bull. Comm. geol. Finlande 150, 67-92.

TREAGUS, J.E., 1964. Notes on the structure of the Ben Lawers Synform. Geol. Mag. 101, 260-270.

TROGER, W.E., 1963. Der geothermische gradient im pt-Feld der metamorphen Facies. Beitr. Miner. und Petrogr., 9, 1-12.

TURNER, F.J., 1968. Metamorphic petrology, mineralogical and field aspects. McGraw-Hill, New York.

TURNOCK, A.C., 1960. The stability of iron chlorites. Yb. Carnegie Instn. Wash. 59, 98-103

VALLANCE, T.G., 1967. Mafic rock alteration and isochemical development of some cordierite-anthophyllite rocks. J. Petrology, 8, 84-96.

VELDE, B., 1965. Phengite micas: synthesis, stability and natural occurrence. Am. J. Sci. 263, 886-913.

VELDE, B., 1966. Upper limits of stability of muscovite. Am. Miner. 51, 924-9.

VELDE, B., 1967. Si^{+4} content of natural phengites. Contr. Miner. Petrol. 14, 250-8.

WALLS, R., 1937. Andalusite-schists and associated rocks of N.E. Scotland. Unpublished PhD. Thesis University of Liverpool.

WHITE, A.J.R., 1966. Genesis of migmatites from the Palmer region of South Australia. Chem. Geol. I, 165-200.

WILLIAMSON, D.H., 1953. Petrology of chloritoid and staurolite rocks north of Stonehaven, Kincardineshire. Geol. Mag. 90, 353-61.

WILSON, A.D., 1955. A new method for the determination of ferrous iron in rocks and minerals. Bull. Geol. Surv. Gt. Britain 9, 56-58.

WILSON, J.S.G., 1882. Mem. Geol. Surv. Scot. for sheet 97.

WILSON, J.S.G., 1886. Mem. Geol. Surv. Scot. for sheet 87.

WIMMENAUER, W., 1950. Cordierit führende Gesteine im Grundgebirge des Schauinsland gebeites. Neues. Jb. Min. Geol. Pal. 80, 375-436.

WINKLER, H.G.F., 1967. Petrogenesis of metamorphic rocks. 2nd Ed. Springer-Verlag.

WINKLER, H.G.F., 1970. Abolition of metamorphic facies, introduction of the four divisions of metamorphic stage, and of a classification of isograds in common rocks. Neues. Jb. Miner. 5, 189-248.

WINKLER, H.G.F., 1974. Petrogenesis of metamorphic rocks. 3rd Ed. Springer-Verlag.

WISEMAN, J.D.H., 1934. The central and south-west Highland epidiorites. Q. Jl. geol. Soc. Lond. 90, 354-417.

WONES, D., & EUGSTER, H.P., 1965. Stability of biotite: experiment, theory and application. Am. Miner. 50, 1228-72.

YODER, H.S., & EUGSTER, H.P., 1955. Synthetic and natural muscovites. Geochim. cosmochim. Acta. 8, 225-80.

ZEN, E-AN., 1966. Construction of pressure-temperature diagrams for multi component systems after the method of Schreinemakers - A geometric approach. U.S. geol. Surv. Bull. 1225, 56.

ZWART, J.J., 1958. Regional metamorphism and related granitization in the Valle de Aran. Geol. Mijnbow, 20, 18-30.

ZWART, H.J., 1962. On the determination of polymetamorphic mineral associations and its application to the Bosost area (Central Pyrenees). Geol. Rundschau 52, 38-65.

ZWART, H.J., 1963. The structural evolution of the paleozoic of the Pyrenees. Geol. Rundschau, 53, 170-205.

ZWART, H.J., 1967. The duality of orogenic belts. Geol. Mijnbouw, 46, 283-309.

Plate 1 (a) : Alternating sandstone and shale units in the biotite zone. Howe of Tarlair.

Plate 1 (b) : Laminations and fine scale crossbeds preserved in silty unit.
Howe of Tarlair.

Plate 2 (a) : Slumped horizon. Howe of Tarlair.

Plate 2 (b) : Photomicrograph of biotite free slate (specimen 43851) showing large chlorite lenses aligned in the cleavage.
Bar represents 2 mm p.p.l.
Old Haven

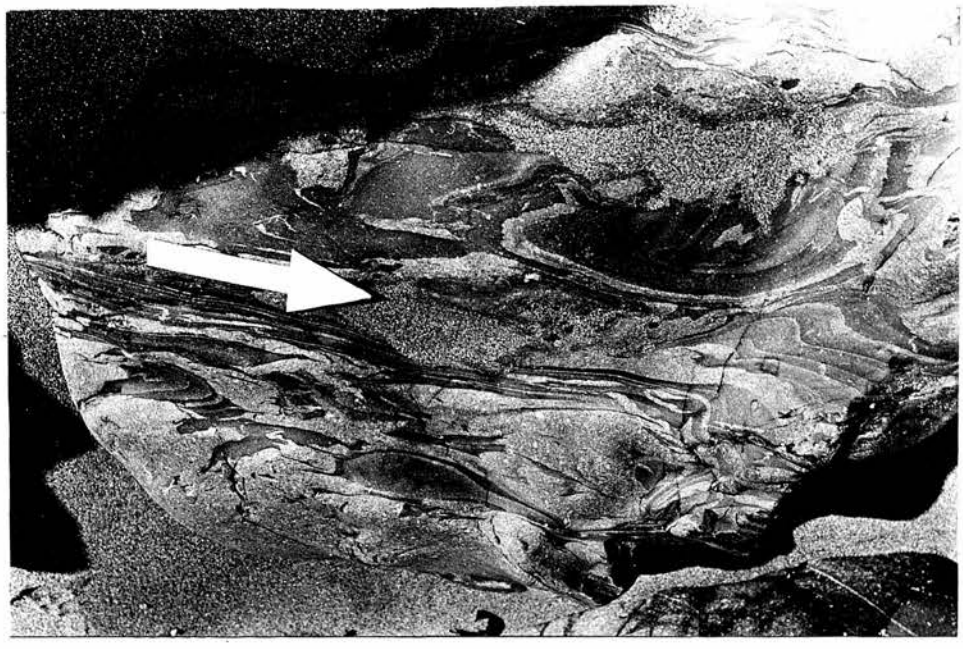

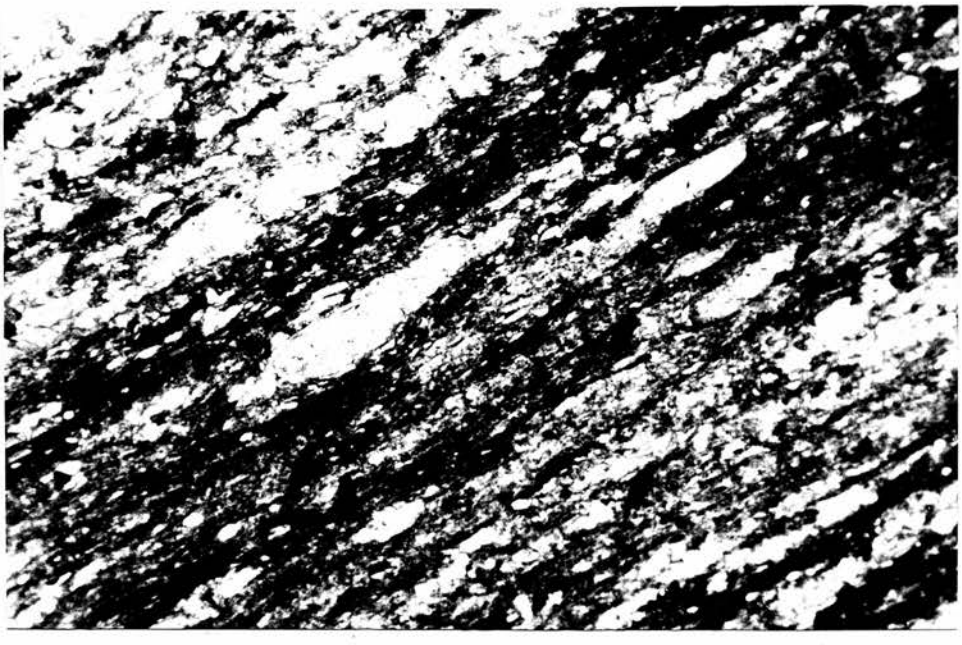

Plate 3 (a) : Photomicrograph of biotite bearing slate (specimen 43860) showing small biotite porphyroblasts.
Bar represents 2 mm p.p.l.
Macduff.

Plate 3 (b) : 'Spots' in a slump horizon.
Banff.

Plate 4 (a) : 'Spots' showing growth across silt laminations. The 'spots' are $\sim$ 5 mm in diameter.
Banff.

Plate 4 (b) : Enlargement of the top right corner of Plate 4 (a) showing the continuity of the silty laminations through the 'spots'.

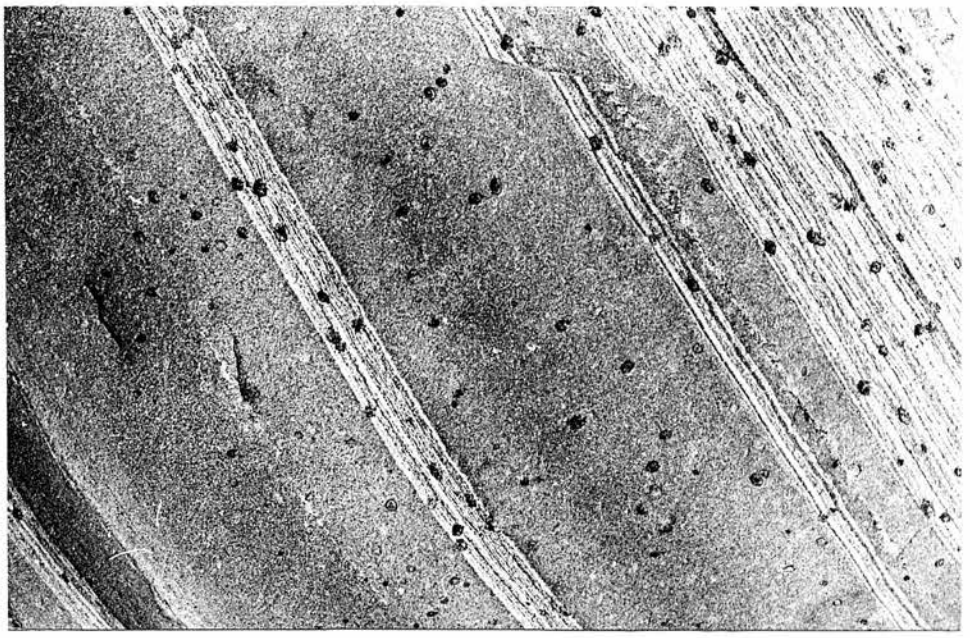

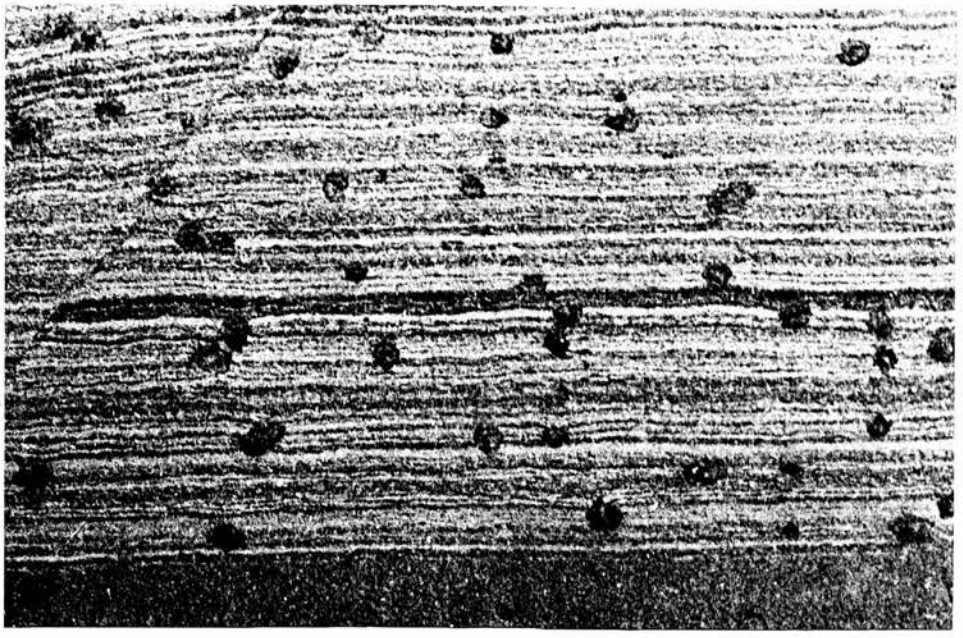

Plate 5 (a) : Photomicrograph of a 'spot' from the cordierite isograd (specimen 43867). Bar represents 1 mm. p.p.l. Boat Hythe, Banff.

Plate 5 (b) : As Plate 5 (a). Crossed Nicols.

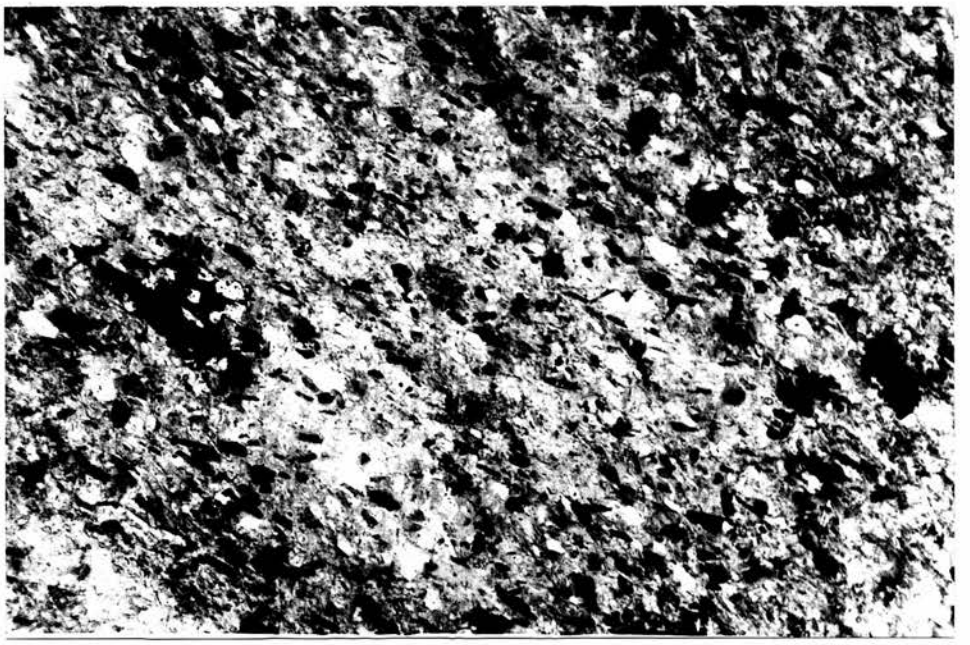

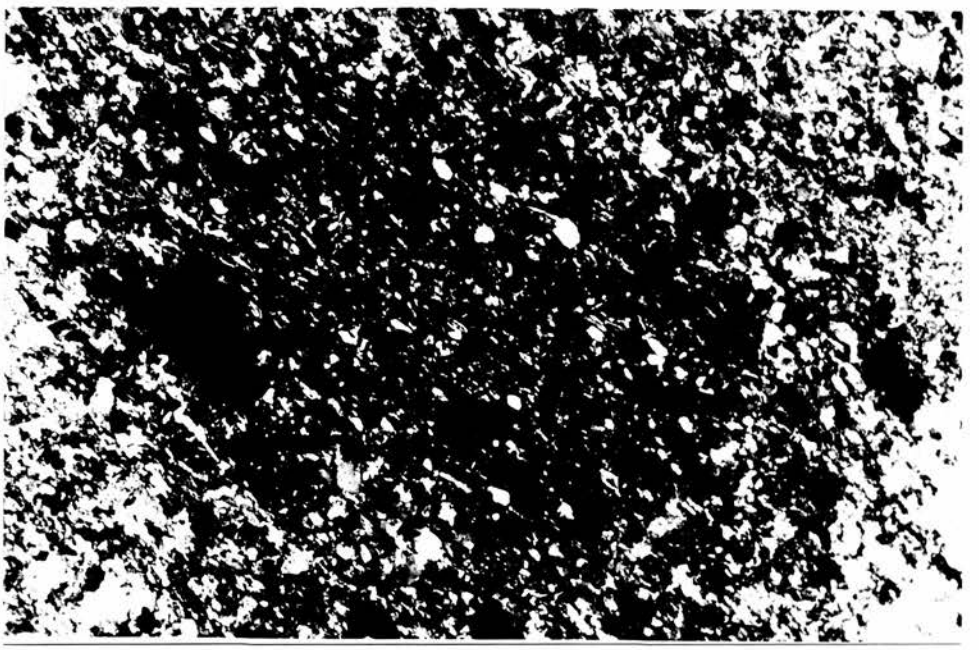

Plate 6 (a) : Cordierite porphyroblasts near the andalusite isograd.
Scotstown shore, Banff.

Plate 6 (b) : Photomicrograph showing partial sector twins and pinite margin in large cordierite porphyroblast (specimen 43873). Bar represents 1.5 mm. Crossed Nicols.
Scotstown shore, Banff.

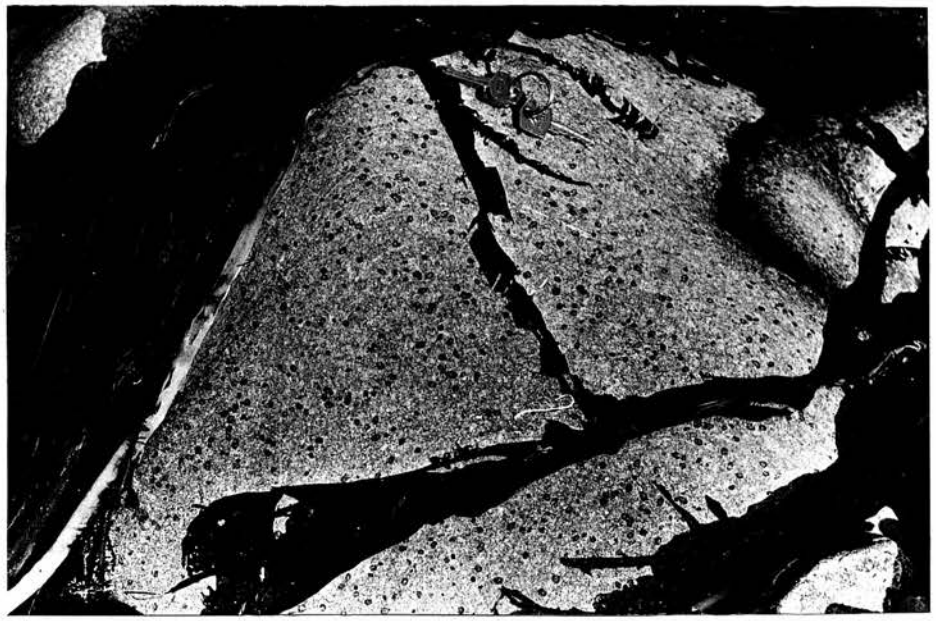

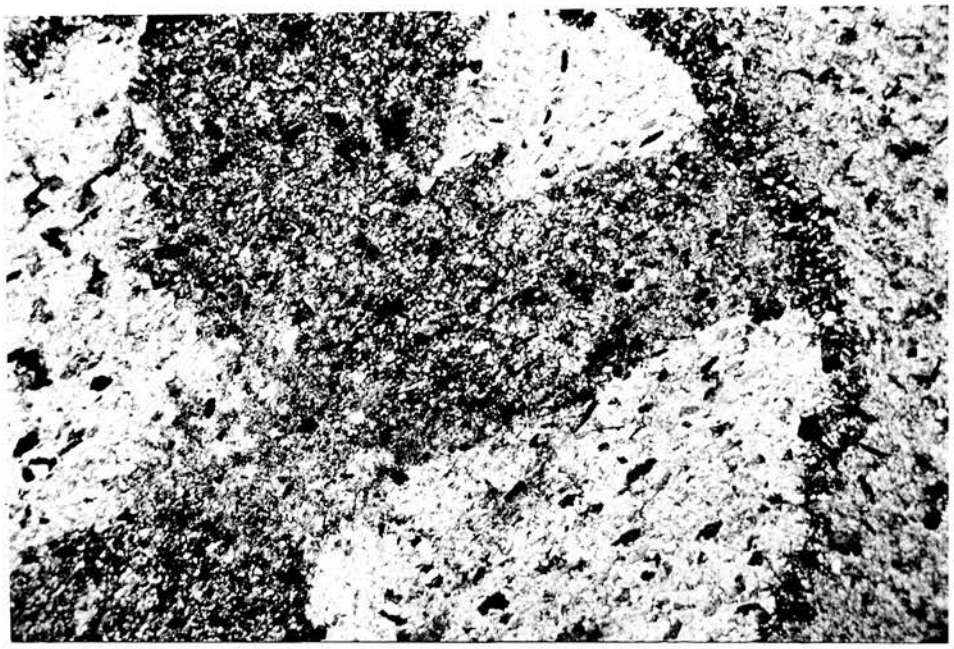

Plate 7 (a) : Enlarger photograph showing large cordierite and andalusite porphyroblasts in weakly schistose matrix (specimen 43876).
Bar represents 2 mm. Ordinary light.
Andalusite isograd, Scotstown shore, Banff.

Plate 7 (b) : Photomicrograph showing preferred orientation in biotite passing without deflection across the edge of a cordierite porphyroblast.
Same specimen as Plate 7 (a).
The bar represents 0.5 mm. p.p.l.

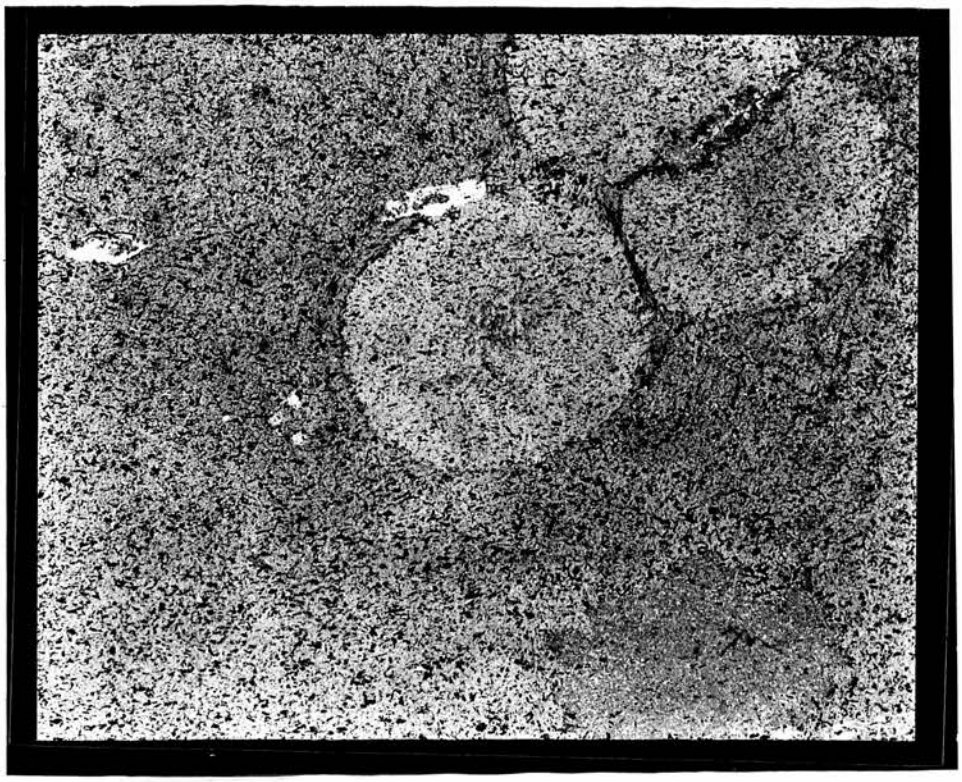

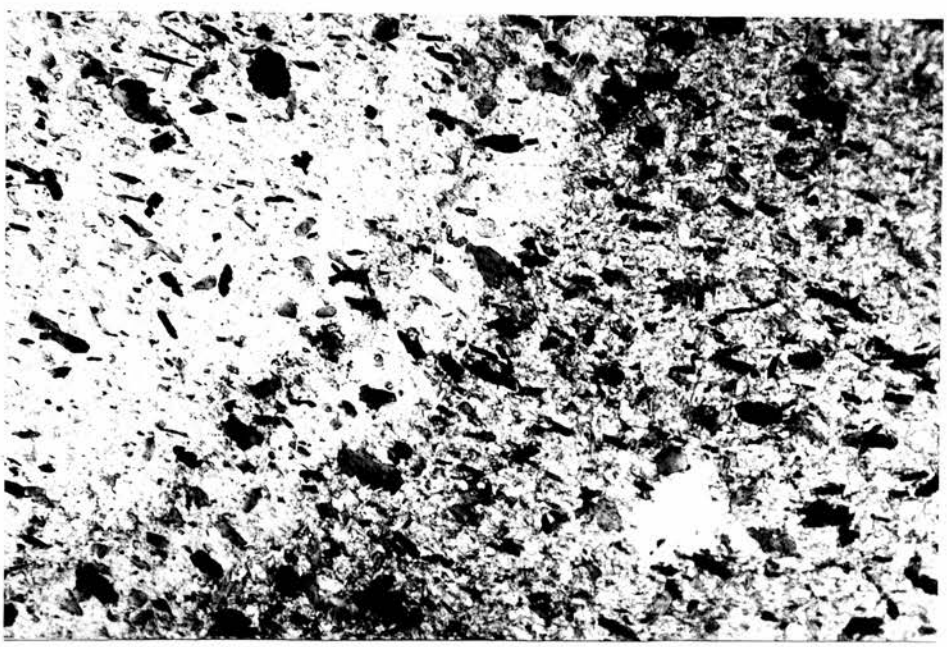

Plate 8 (a) : High power photomicrograph showing the random orientation of white mica and the granoblastic nature of quartz and feldspar in the matrix of specimen 43876 (see also Plate 7).
The bar represents 0.2 mm. p.p.l.

Plate 8 (b) : Enlarger photograph showing a highly schistose rock from the andalusite zone. (specimen 43882) (c.f. Plate 7 (a)).
Bar represents 2 mm. Ordinary light.
Tumblers, East side of Boyndie Bay.

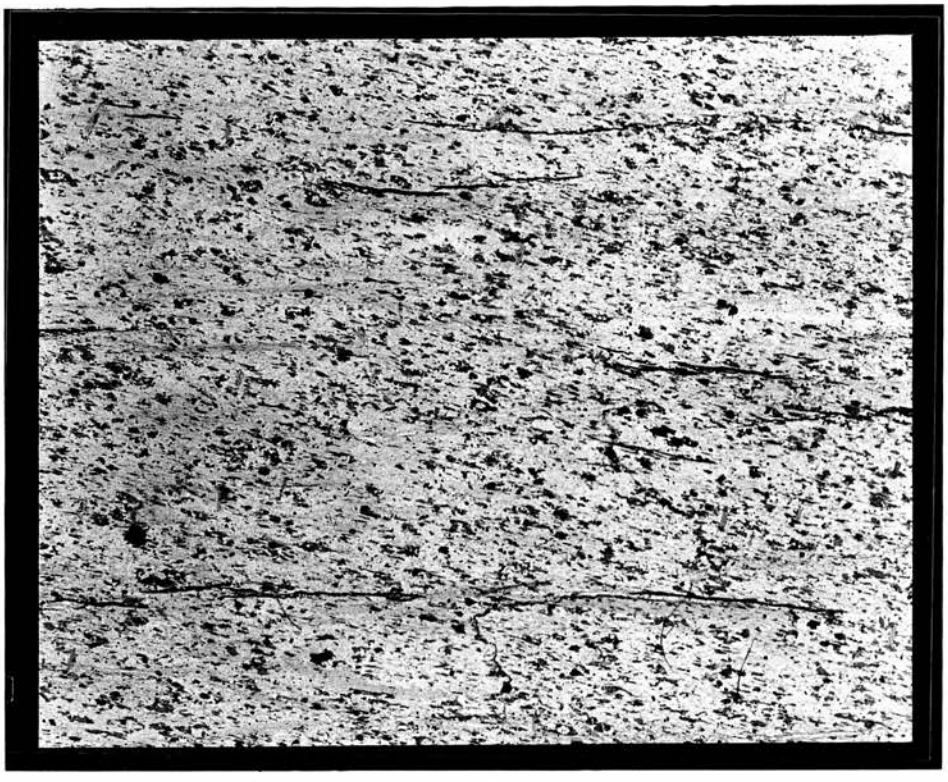

Plate 9 (a) : Enlarger photograph showing andalusite growing between (altered) cordierite porphyroblasts. Specimen 44010. Bar represents 3 mm. Ordinary light. Braes of Gight, Ythan Valley.

Plate 9 (b) : As plate 9 (a) (Specimen 44012). Bar represents 3 mm. Ordinary light.

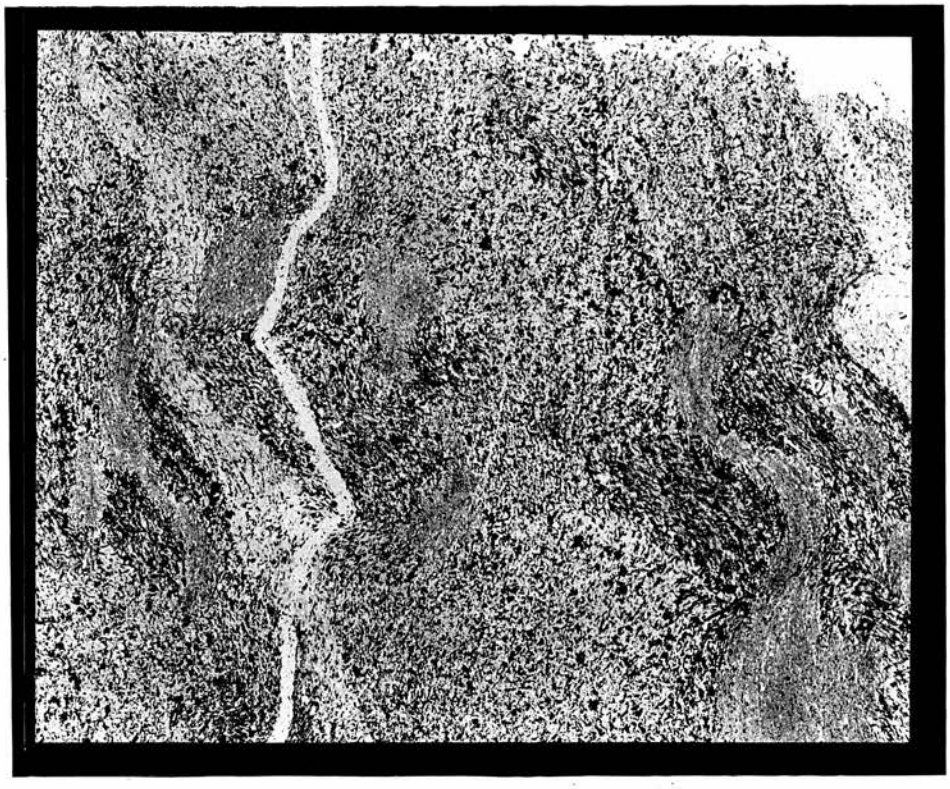

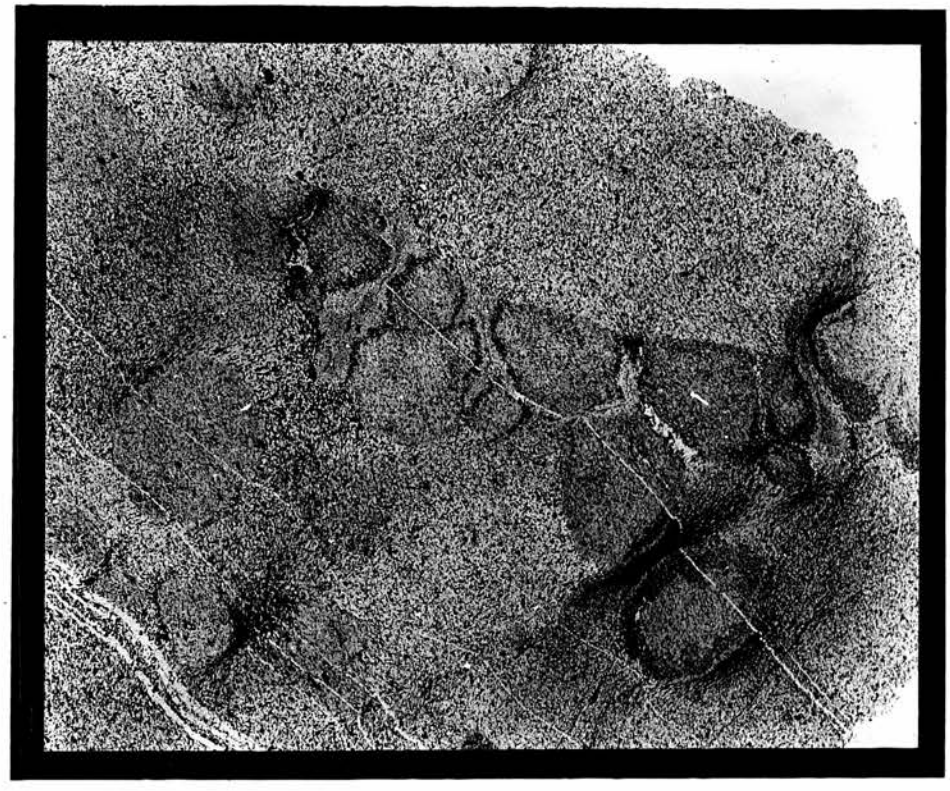

Plate 10 (a) : Enlarger photograph showing enclaves in andalusite porphyroblasts where these border on cordierite (Specimen 44013). Bar represents 3 mm. Ordinary light. Braes of Gight, Ythan Valley.

Plate 10 (b) : Photomicrograph showing granoblastic material filling enclaves between andalusite and cordierite. Same specimen as Plate 10 (a).
Bar represents 0.2 mm. p.p.l.

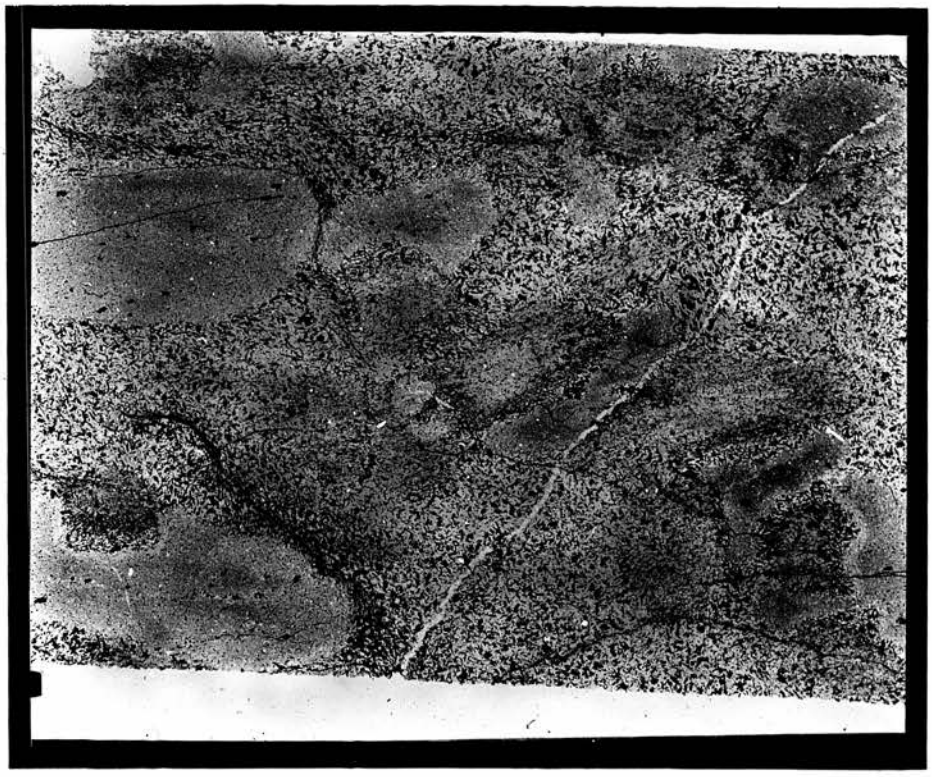

Plate 11 (a) : Pelite and coarse psammite horizons.
Staurolite Zone.
Upper Whitehills group, Knock Head.

Plate 11 (b) : Pelites with thin sandstone units.
Staurolite Zone.
West side of Boyndie Bay.

Plate 12 (a) : Large andalusite porphyroblasts on weathered surface of pelite unit. W. Boyndie Bay.

Plate 12 (b) : Enlarger photograph (specimen 43904 from exposure figure in Plate 12 (a)). Note strong schistosity and trails in andalusite and cordierite porphyroblasts. Crenulations developed near two altered cordierite porphyroblasts (middle right) are absent from surrounding ground mass. Staurolite is also present.
Bar represents 7 mm. Ordinary light.


SCOTTISH
BLUEBELL
MATCHES

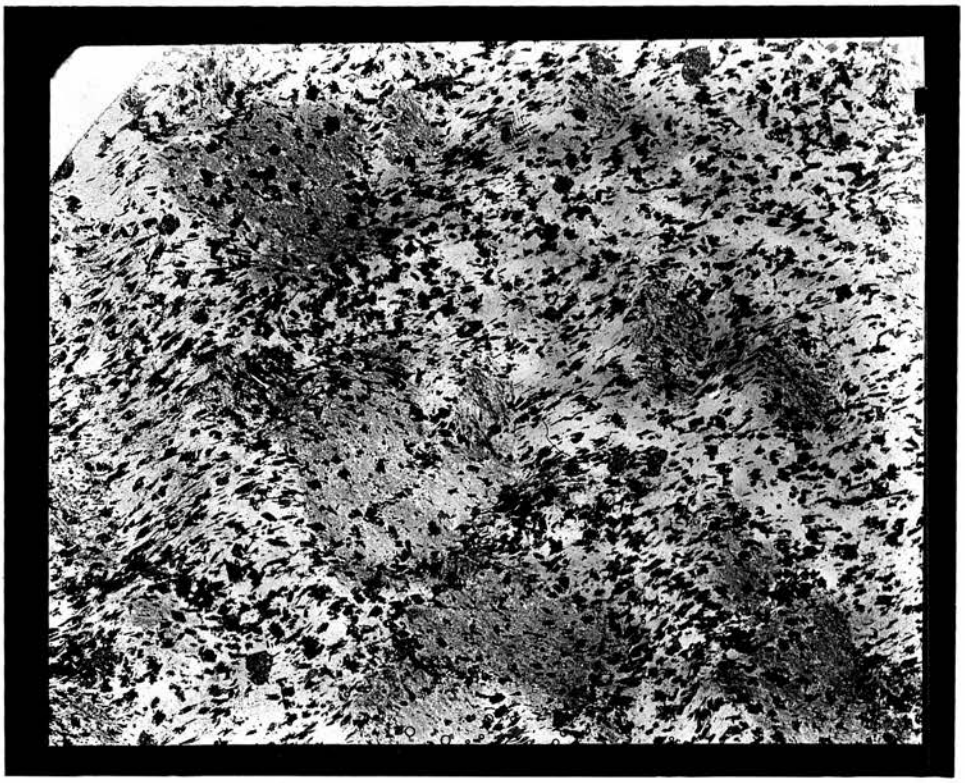

Plate 13 (a) : Enlarger photograph showing large andalusite and smaller staurolite porphyroblasts in a dominantly granoblastic ground mass. Crenulations have developed adjacent to the two lower andalusites which include the schistosity. Specimen 43912.
Bar represents 3 mm. Ordinary light.
W. Boyndie Bay.

Plate 13 (b) : Photomicrograph showing random orientation of biotite and granoblastic nature of quartz and feldspar in the ground mass of specimen 43912. The area figures lies below and between the two upper andalusite porphyroblasts of Plate 13 (a).
Bar represents 0.2 mm. p.p.l.

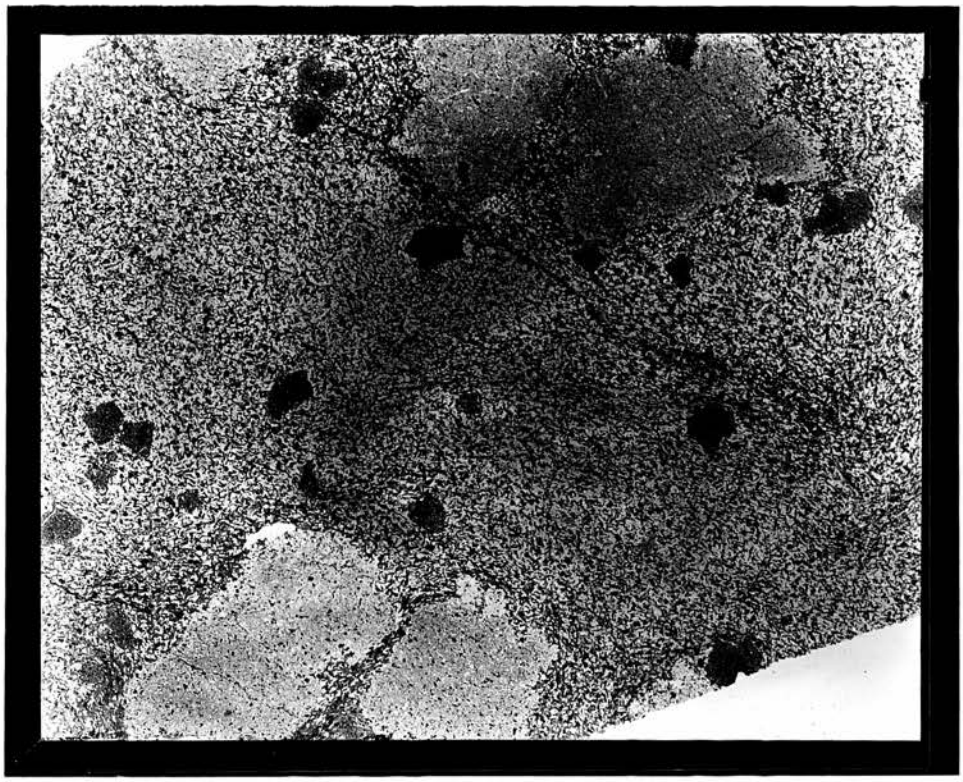

Plate 14 (a) : Enlarger photograph (specimen 43945) showing granoblastic ground mass quartz and plagioclase carrying oriented mica. Large andalusite, smaller staurolite and very small garnet porphyroblasts are present.
Bar represents 3 mm. Ordinary light.
Kinnairdy.

Plate 14 (b) : Photomicrograph showing garnet near andalusite and staurolite. Same specimen as Plate 14 (a).
Bar represents 1.5 mm. p.p.l.

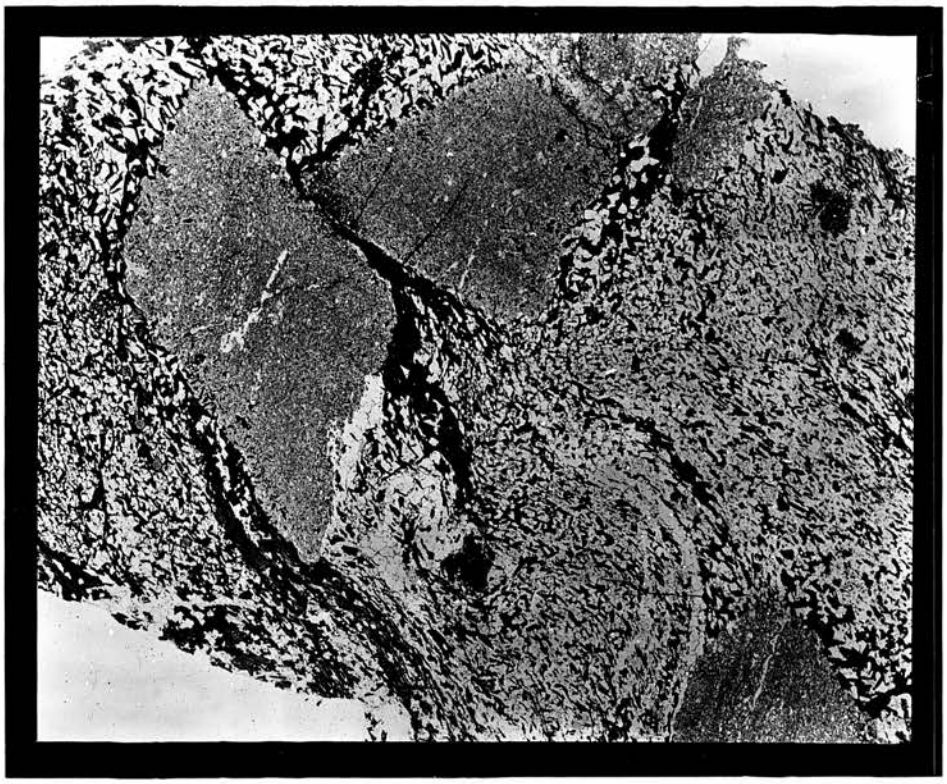

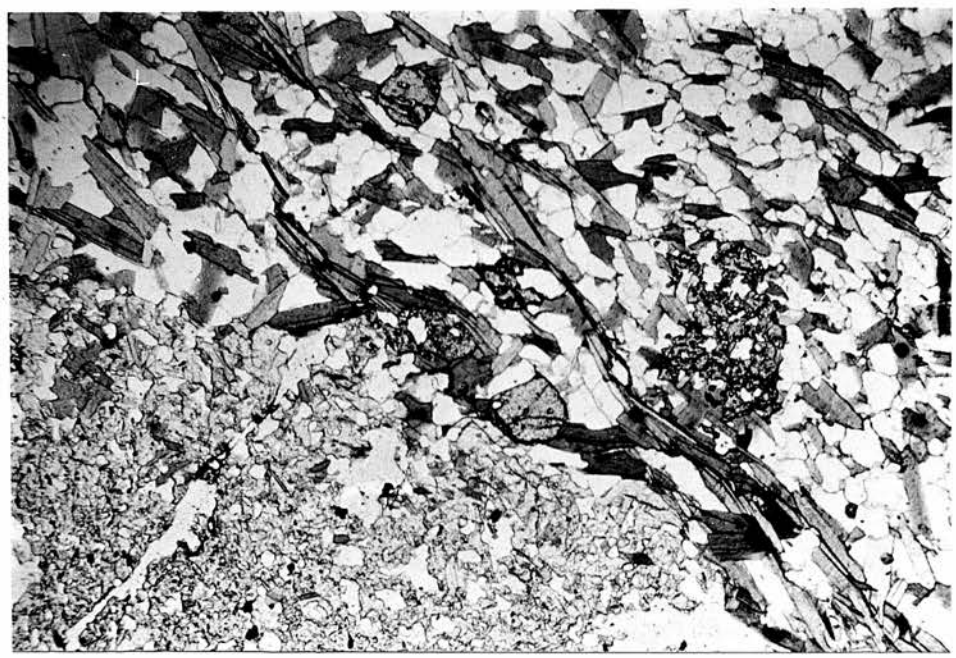

Plate 15 (a) : Enlarger photograph showing enclaves in large andalusite porphyroblasts (Specimen 43943).
Bar represents 4 mm. Ordinary light.
Kinnairdy.

Plate 15 (b) : Photomicrograph of material filling enclave. Same specimen as Plate 15 (a).
Bar represents 1 mm. p.p.l.

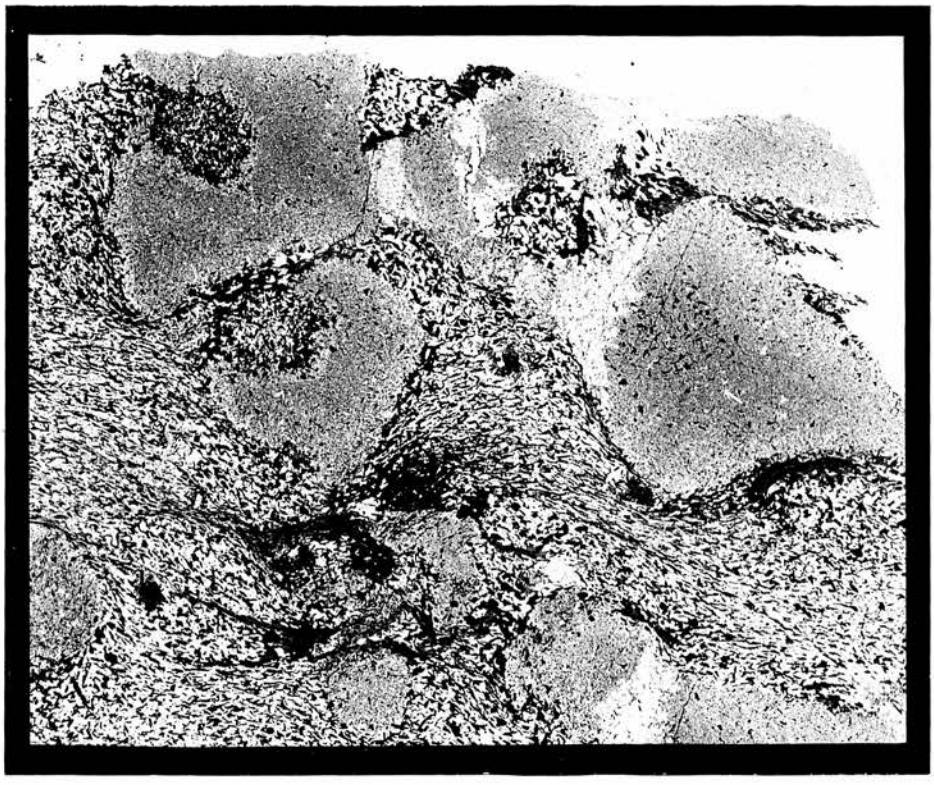

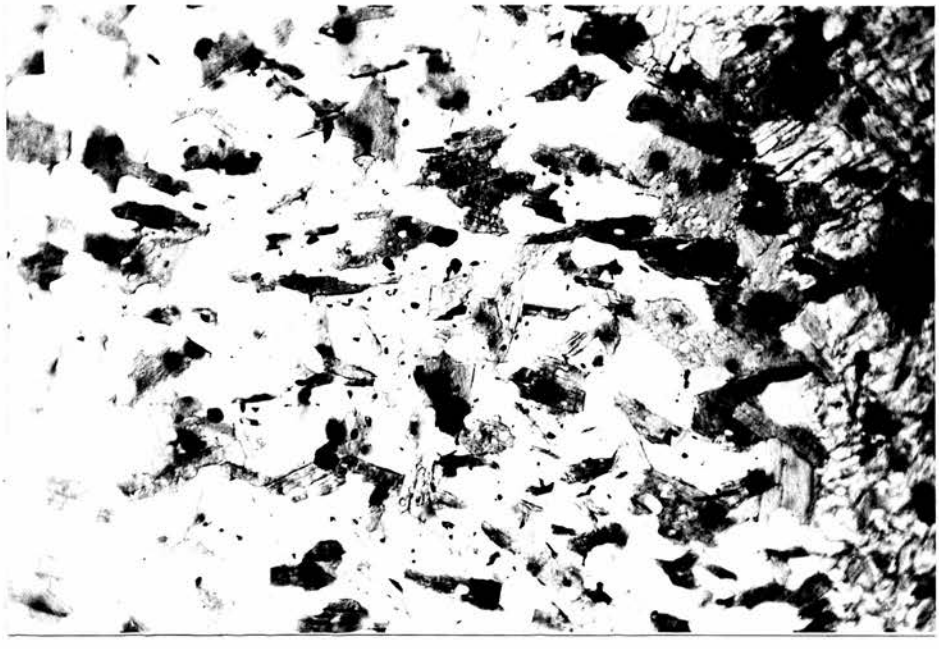

Plate 16 (a) : Enlarger photograph of specimen 43918, showing inclusion trails in andalusite and staurolite and F_3 crenulations. Bar represents 3 mm. Ordinary light. Whitehills.

Plate 16 (b) : Photomicrograph showing a large chiastolite cross structure developed in an apatite rich unit. Specimen 43910. Bar represents 1 mm. p.p.l. West Boyndie Bay.

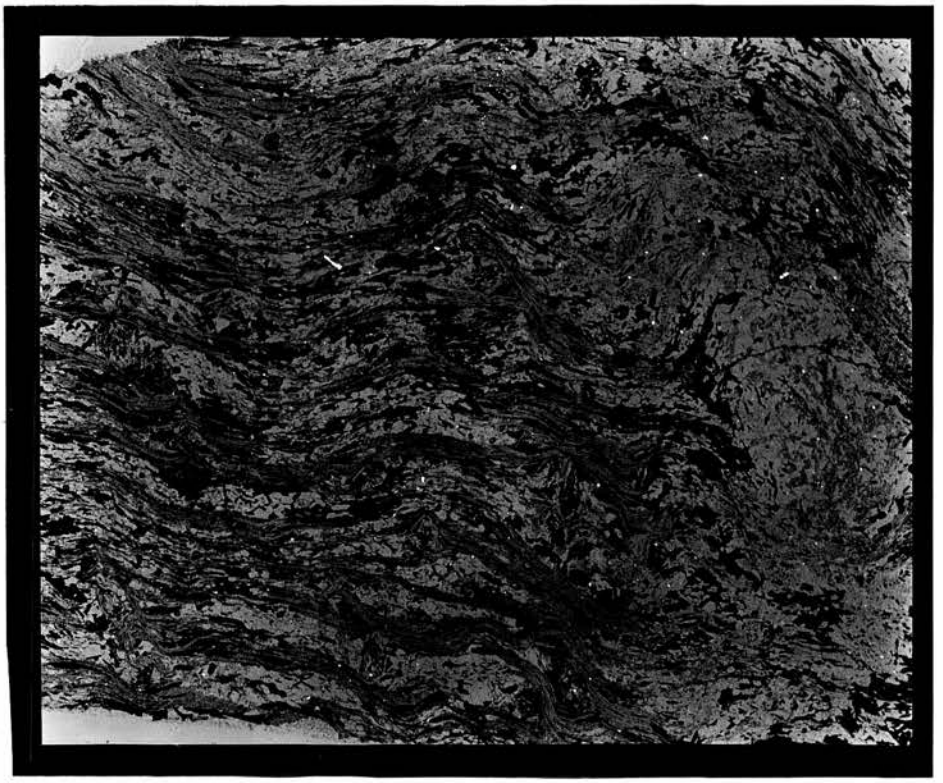

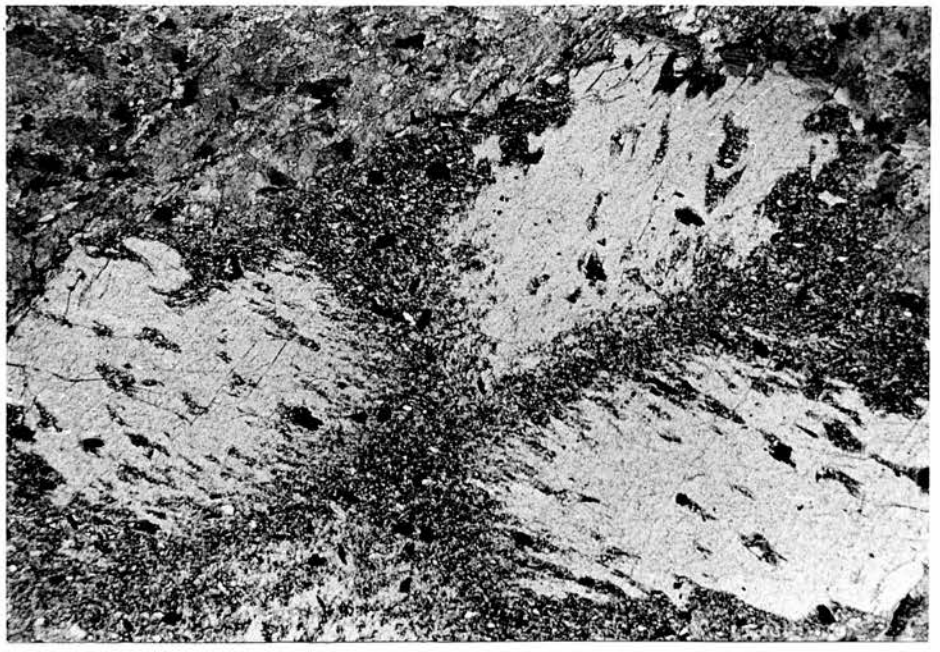

Plate 17 (a) : Graded greywacke unit. The silty top unit of this bed contains staurolite, cordierite, andalusite, garnet and biotite but no muscovite.
West Boyndie Bay.

Plate 17 (b) : Enlarger photograph of muscovite free greywacke siltstone (Specimen 43942). Bar represents 3 mm. p.p.l.
Maunderlea Quarry.

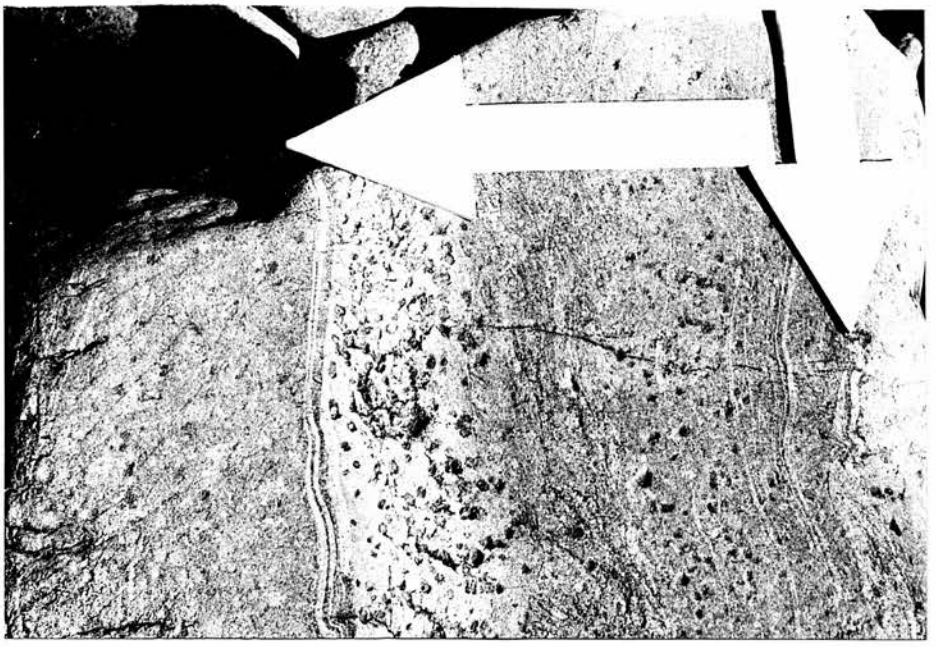

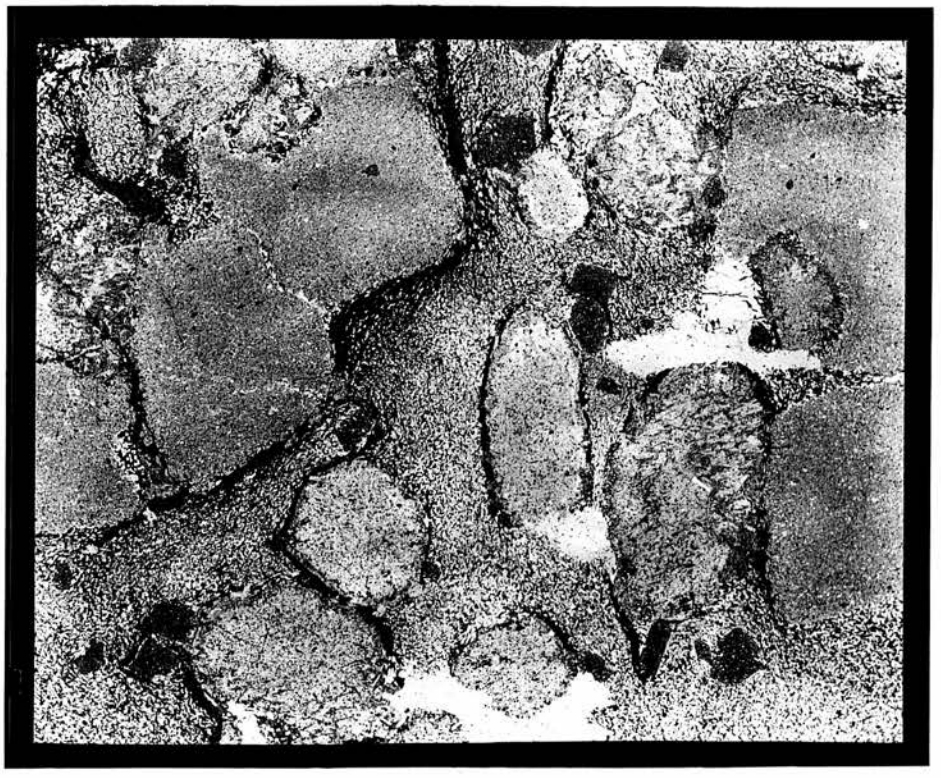

Plate 18 (a) : Garnet rich layer in specimen 43939.
Bar represents 1·5 mm p.p.l.
Maunderlea Quarry.

Plate 18 (b) : Strain slip cleavages (S_3?) interupted by cordierite porphyroblast.
(Specimen 43933).
Bar represents 2 mm. Ordinary light.
Castlebrae Quarry.

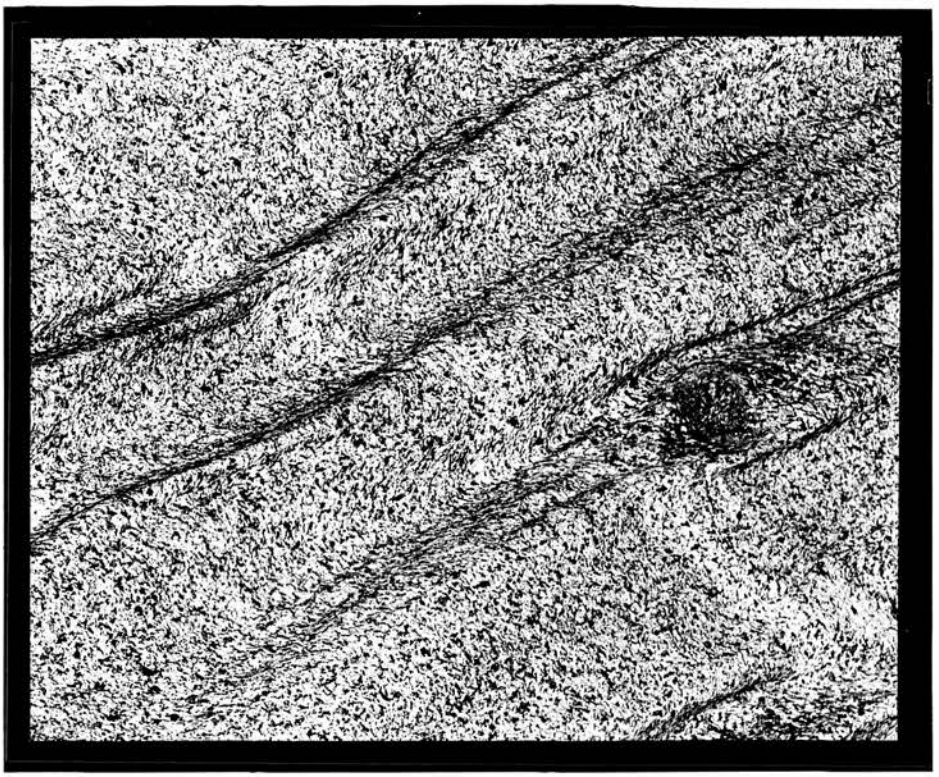

Plate 19 (a) : Radiating gedrite crystals in granoblastic matrix of specimen 43923. Bar represents 2 mm. Ordinary light. Near Whyntie Head.

Plate 19 (b) : Prismatic sillimanite and fibrolite in potash feldspar gneiss. Bar represents 4 mm. Ordinary light. East of Methlick, Ythan Valley.

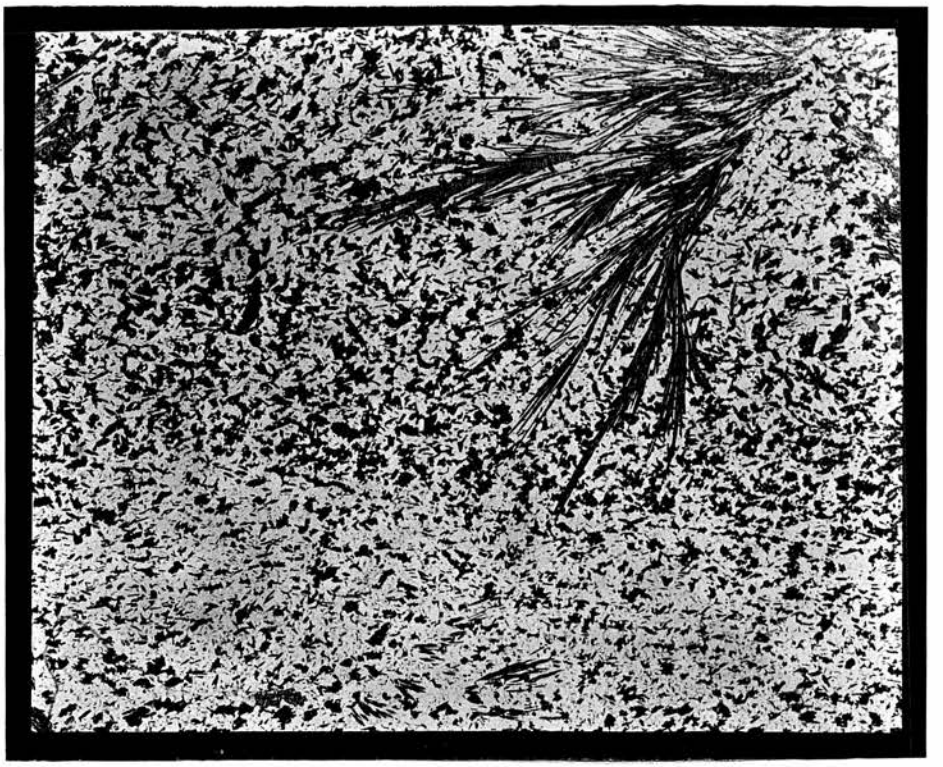

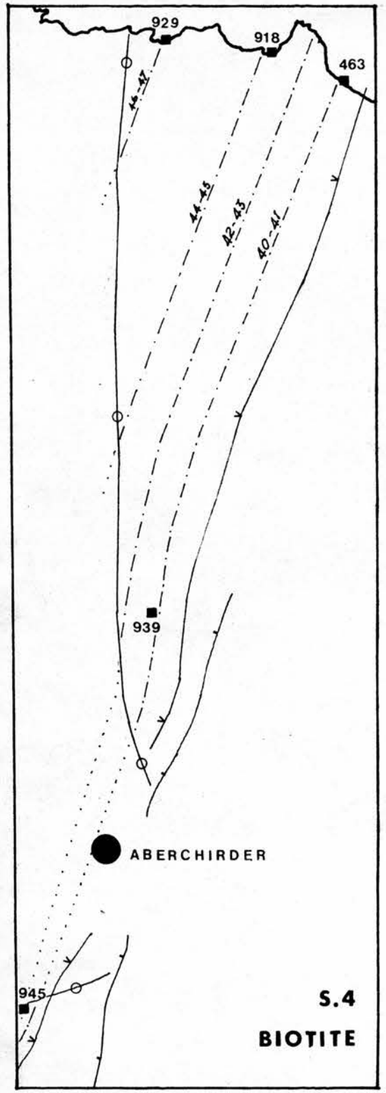

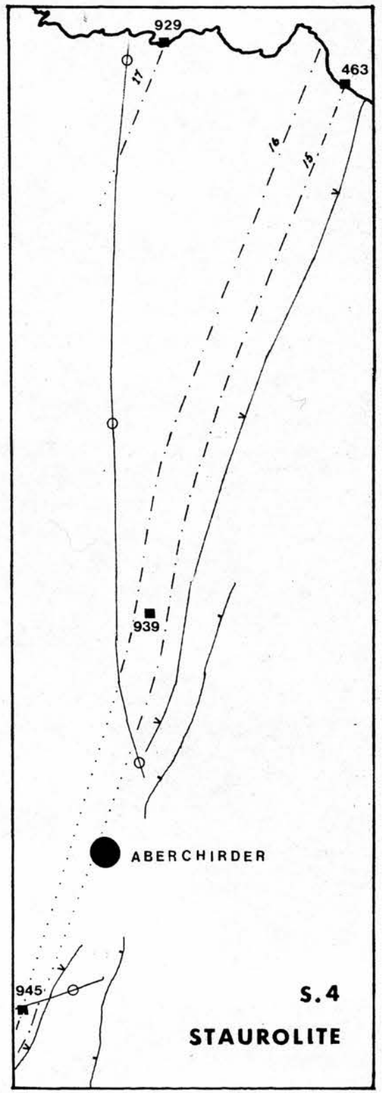

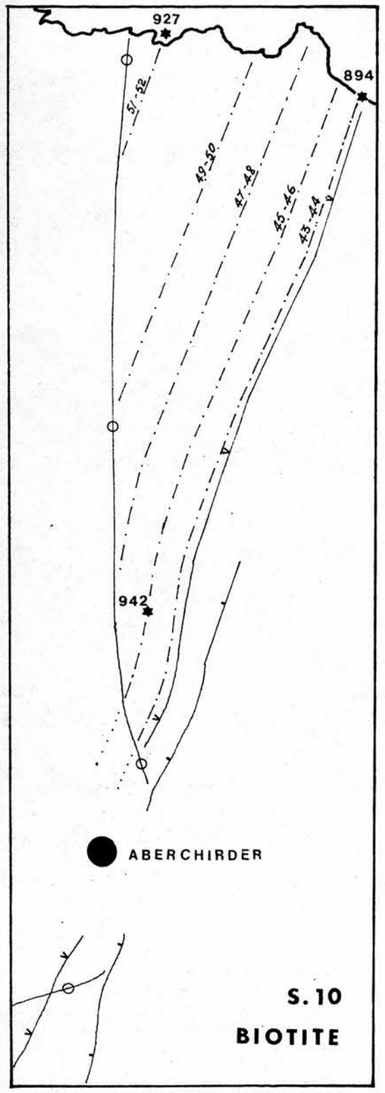

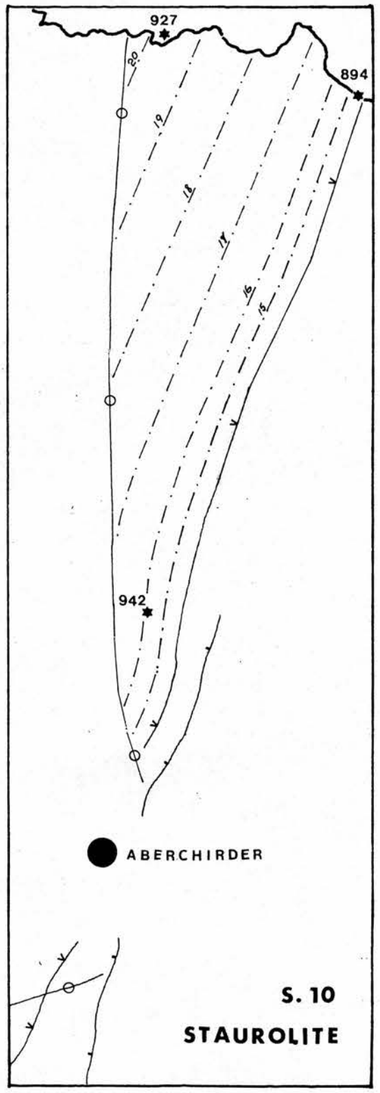

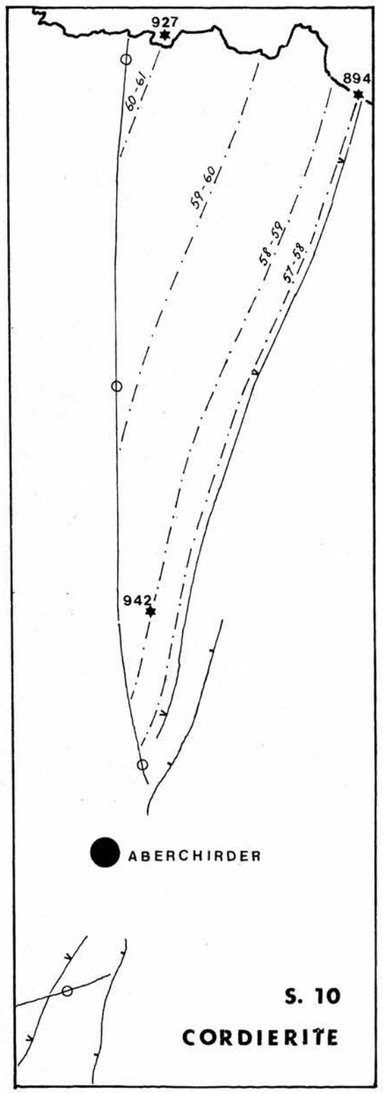

MAP 6.

Estimated Contours for Staurolite Zone Mineral Compositions in Banffshire..

■ and - staur - biot - musc - qz ± gt (S.4)

✱ and - staur - biot - cord - qz (S.10)

939 Specimen No.

15 100 MgO / MgO + FeO of mineral

Composition contour.

Isograds. (See Map 4)

Cordierite.

Staurolite.

Sillimanite.

4 Km